AdS/CFT
and
condensed matter

Reviews:

arXiv:0907.0008

arXiv:0901.4103

arXiv:0810.3005 (with Markus Mueller)

Talk online: sachdev.physics.harvard.edu

PHYSICS
HARVARD

Lars Fritz, Harvard
Victor Galitski, Maryland
Max Metlitski, Harvard
Eun Gook Moon, Harvard
Markus Mueller, Trieste
Yang Qi, Harvard
Joerg Schmalian, Iowa
Cenke Xu, Harvard

Frederik Denef, Harvard
Sean Hartnoll, Harvard
Christopher Herzog, Princeton
Pavel Kovtun, Victoria
Dam Son, Washington

PHYSICS
HARVARD

Outline

A. "Relativistic" field theories of quantum phase transitions

1. Coupled dimer antiferromagnets
2. Triangular lattice antiferromagnets
3. Graphene
4. AdS/CFT and quantum critical transport

Outline

B. Finite density quantum matter

1. Graphene

   Fermi surfaces and Fermi liquids

2. Quantum phase transitions of Fermi liquids

   Pomeranchuk instability and spin density waves;
   Fermi surfaces and "non-Fermi liquids"

3. AdS_2 theory

4. Cuprate superconductivity

Outline

A. "Relativistic" field theories of quantum phase transitions

Outline

A. “Relativistic” field theories of quantum phase transitions

1. Coupled dimer antiferromagnets
2. Triangular lattice antiferromagnets
3. Graphene
4. AdS/CFT and quantum critical transport

$TlCuCl_3$

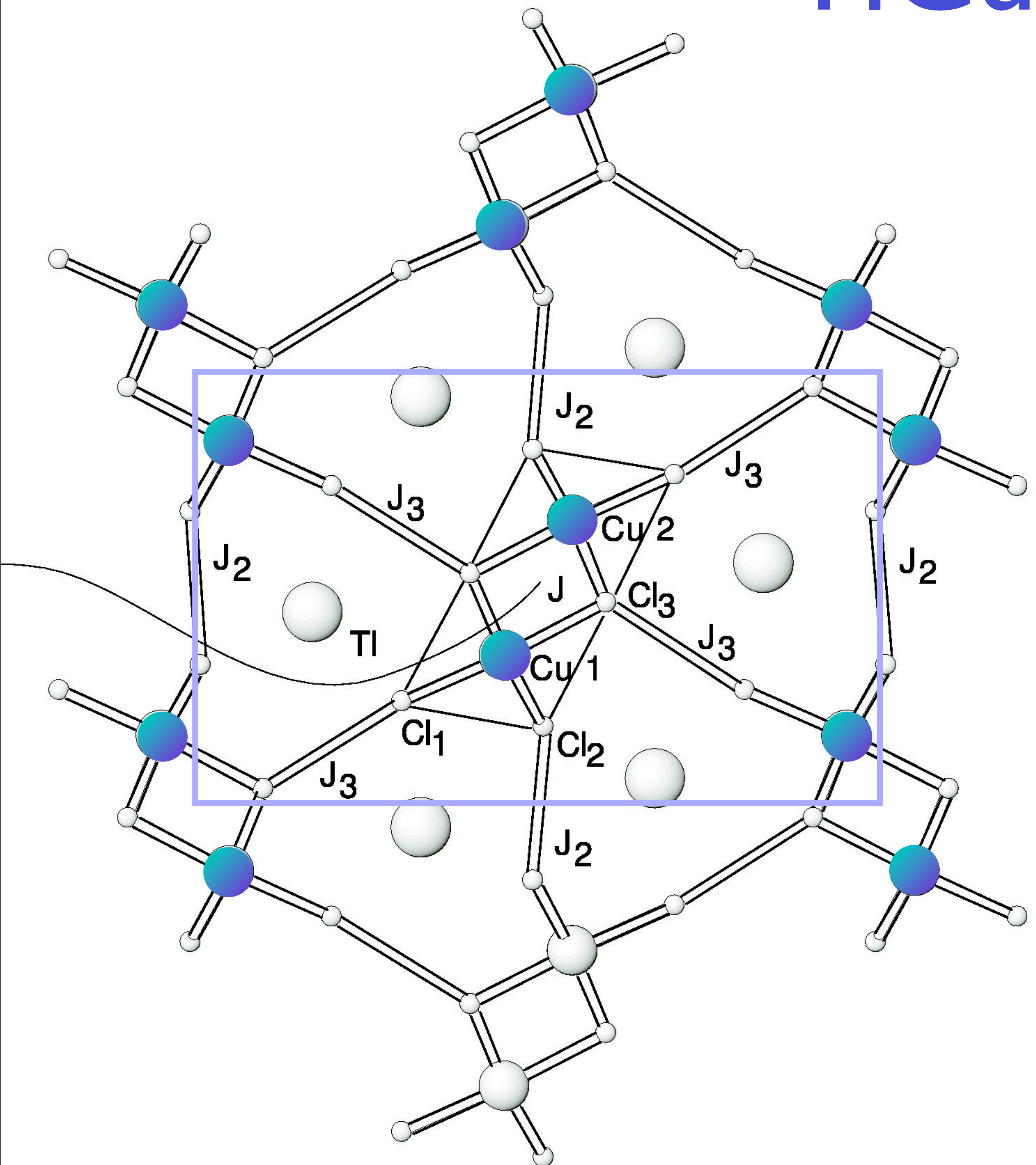

J2
J3
J2
J3
Cu 2
J
Cl3
Tl
Cu 1
J3
J2
Cl1
Cl2
J3
J2

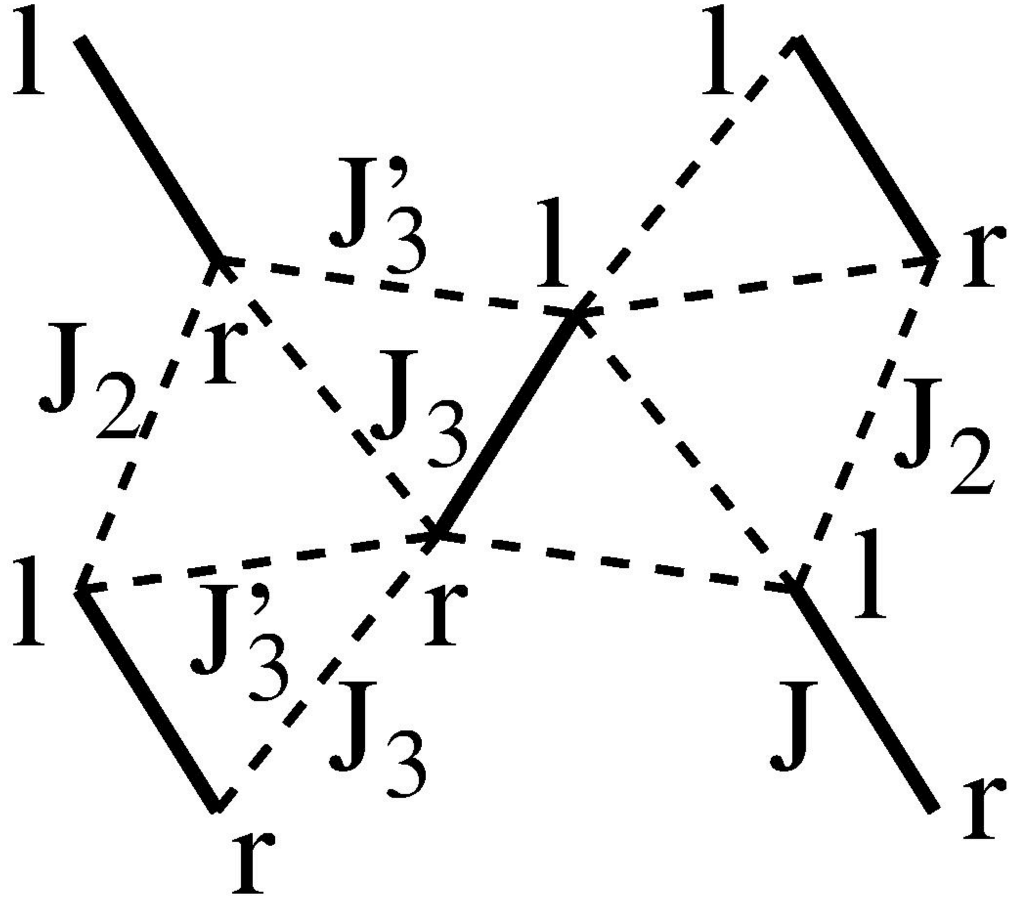

l
l
J'3
l
r
r
J2
J3
J2
l
r
l
J'3
J3
J
r
r

$TlCuCl_3$

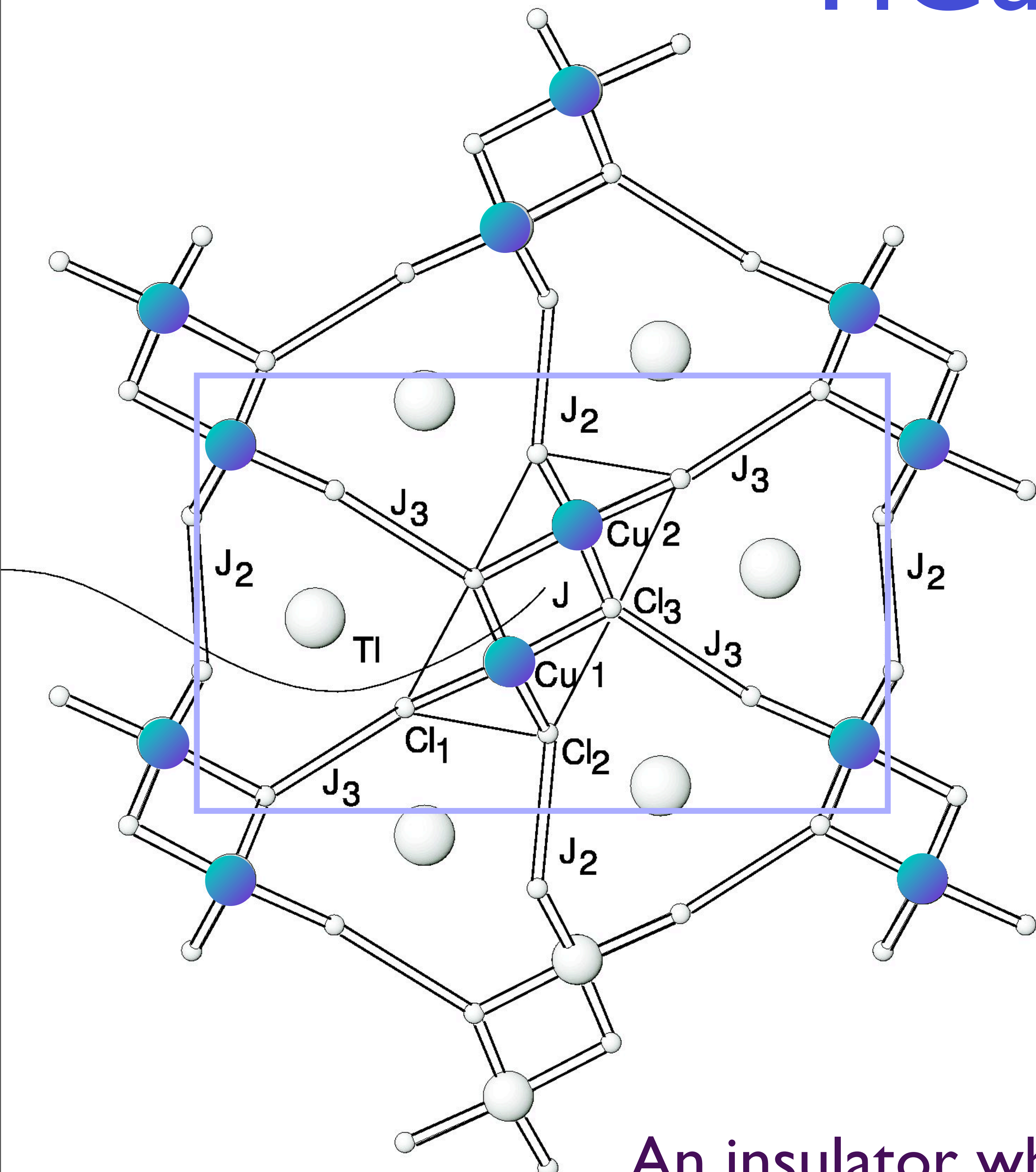

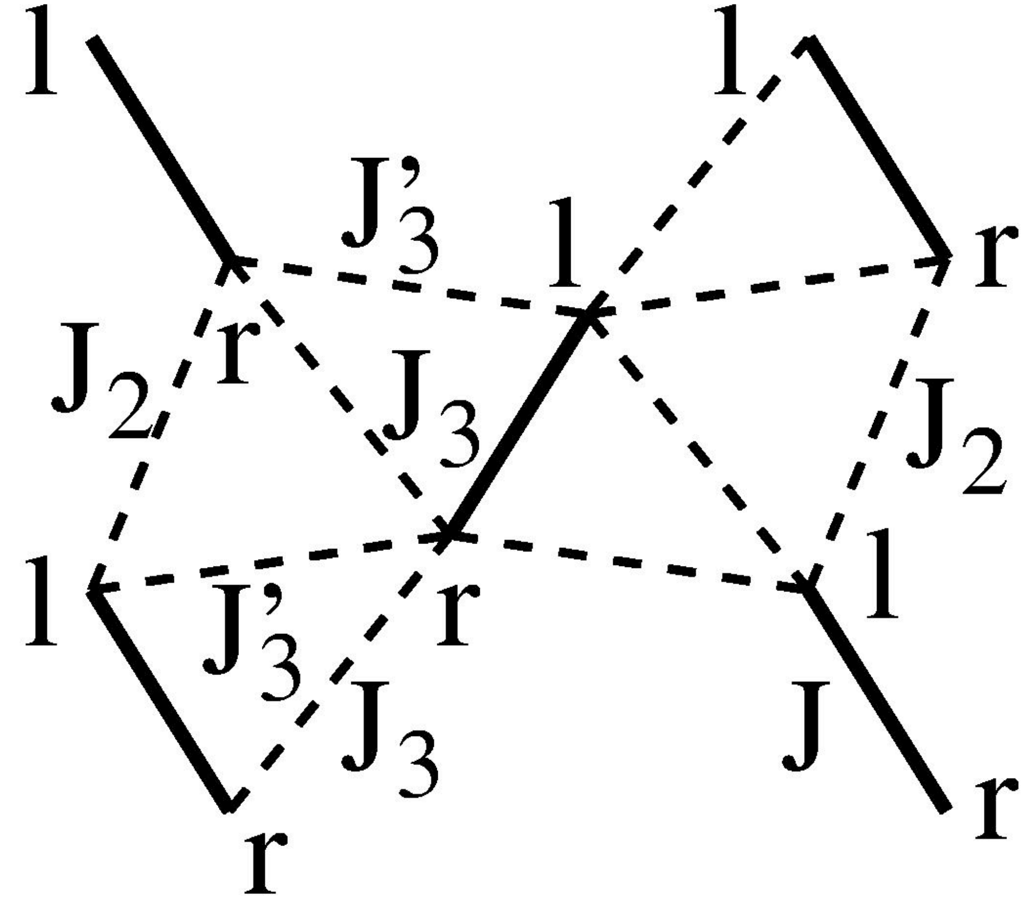

An insulator whose spin susceptibility vanishes exponentially as the temperature T tends to zero.

Square lattice antiferromagnet

$$H = \sum_{\langle ij \rangle} J_{ij} \vec{S}_i \cdot \vec{S}_j$$

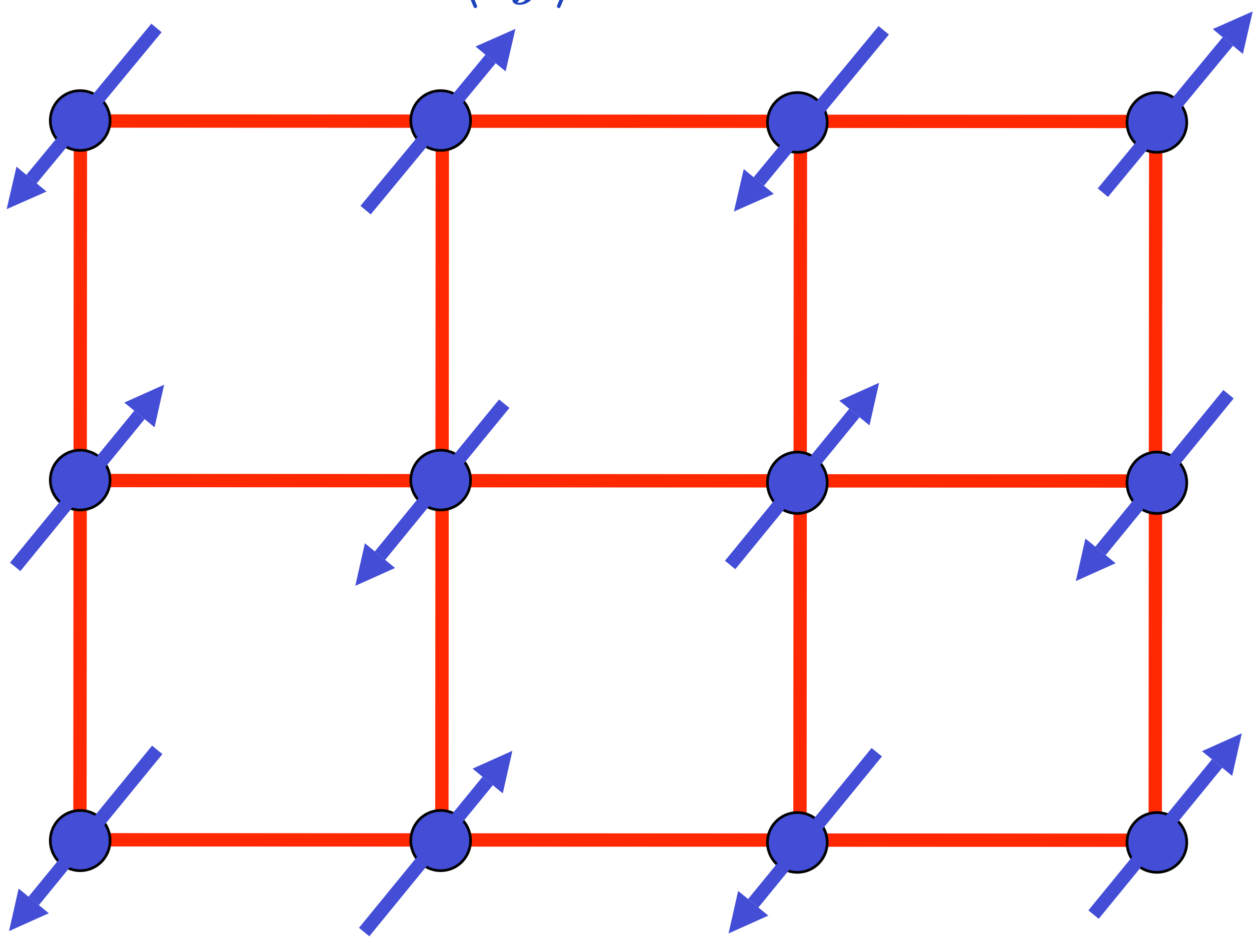

Ground state has long-range Néel order

Order parameter is a single vector field $\vec{\varphi} = \eta_i \vec{S}_i$

$\eta_i = \pm 1$ on two sublattices

$\langle \vec{\varphi} \rangle \neq 0$ in Néel state.

Square lattice antiferromagnet

$$H = \sum_{\langle ij \rangle} J_{ij} \vec{S}_i \cdot \vec{S}_j$$

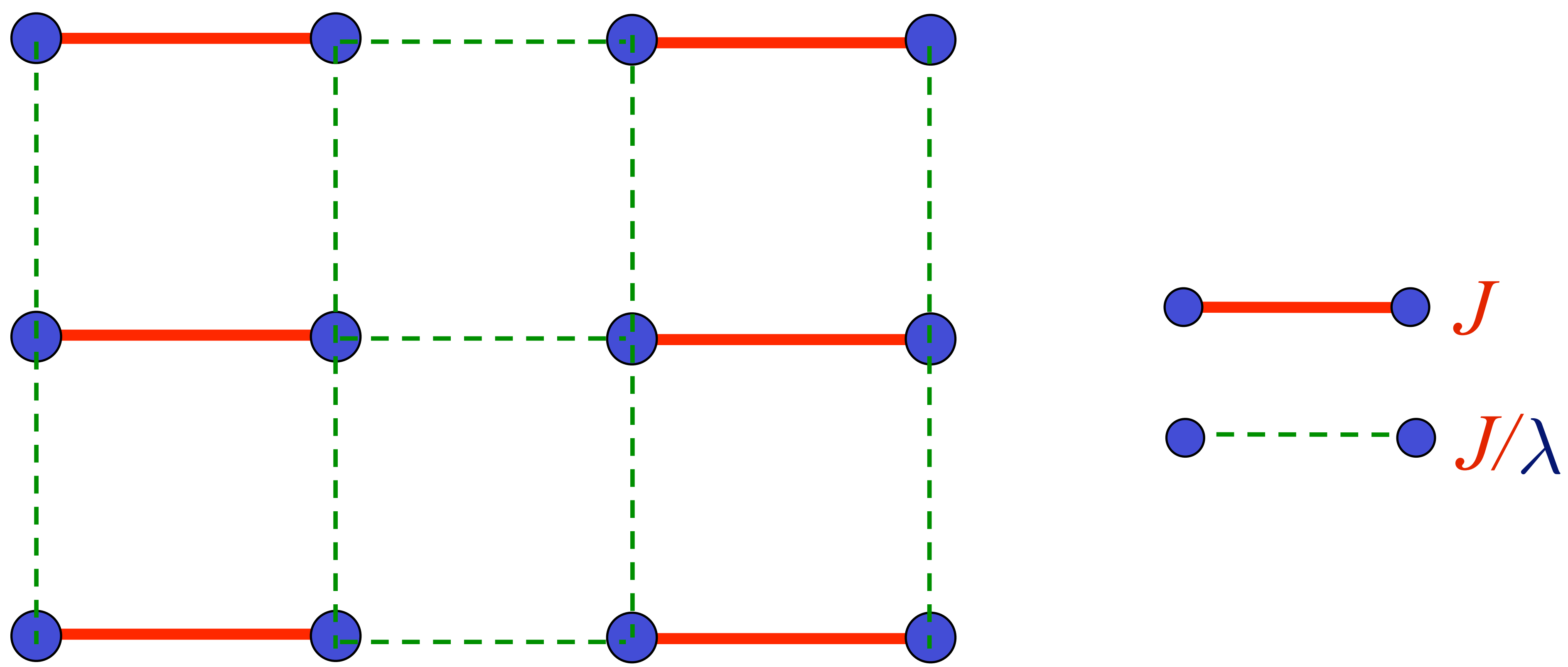

Weaken some bonds to induce spin entanglement in a new quantum phase

Square lattice antiferromagnet

$$H = \sum_{\langle ij \rangle} J_{ij} \vec{S}_i \cdot \vec{S}_j$$

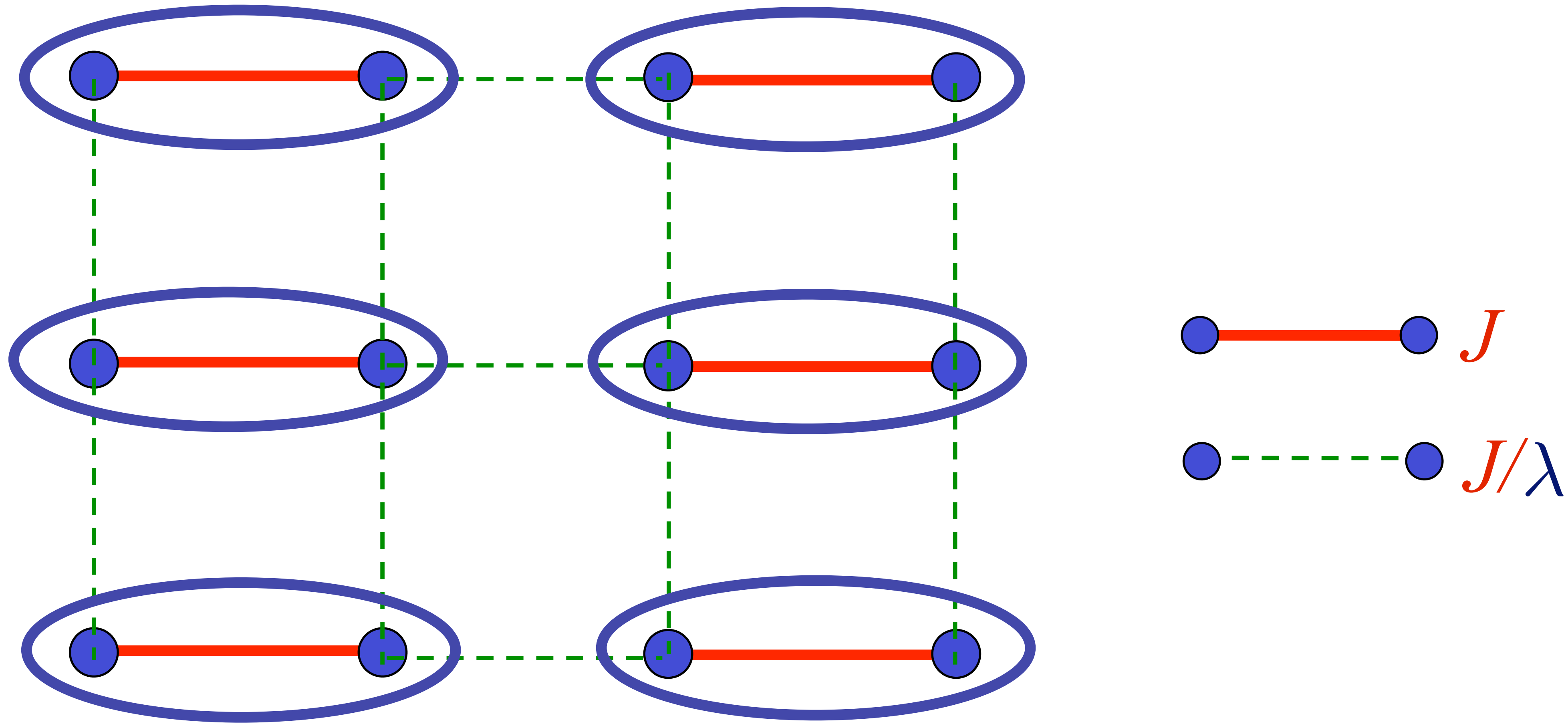

Ground state is a "quantum paramagnet" with spins locked in valence bond singlets

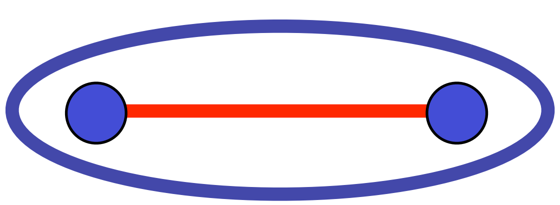

$$= \frac{1}{\sqrt{2}} \Big(\big| \uparrow \downarrow \big\rangle - \big| \downarrow \uparrow \big\rangle \Big)$$

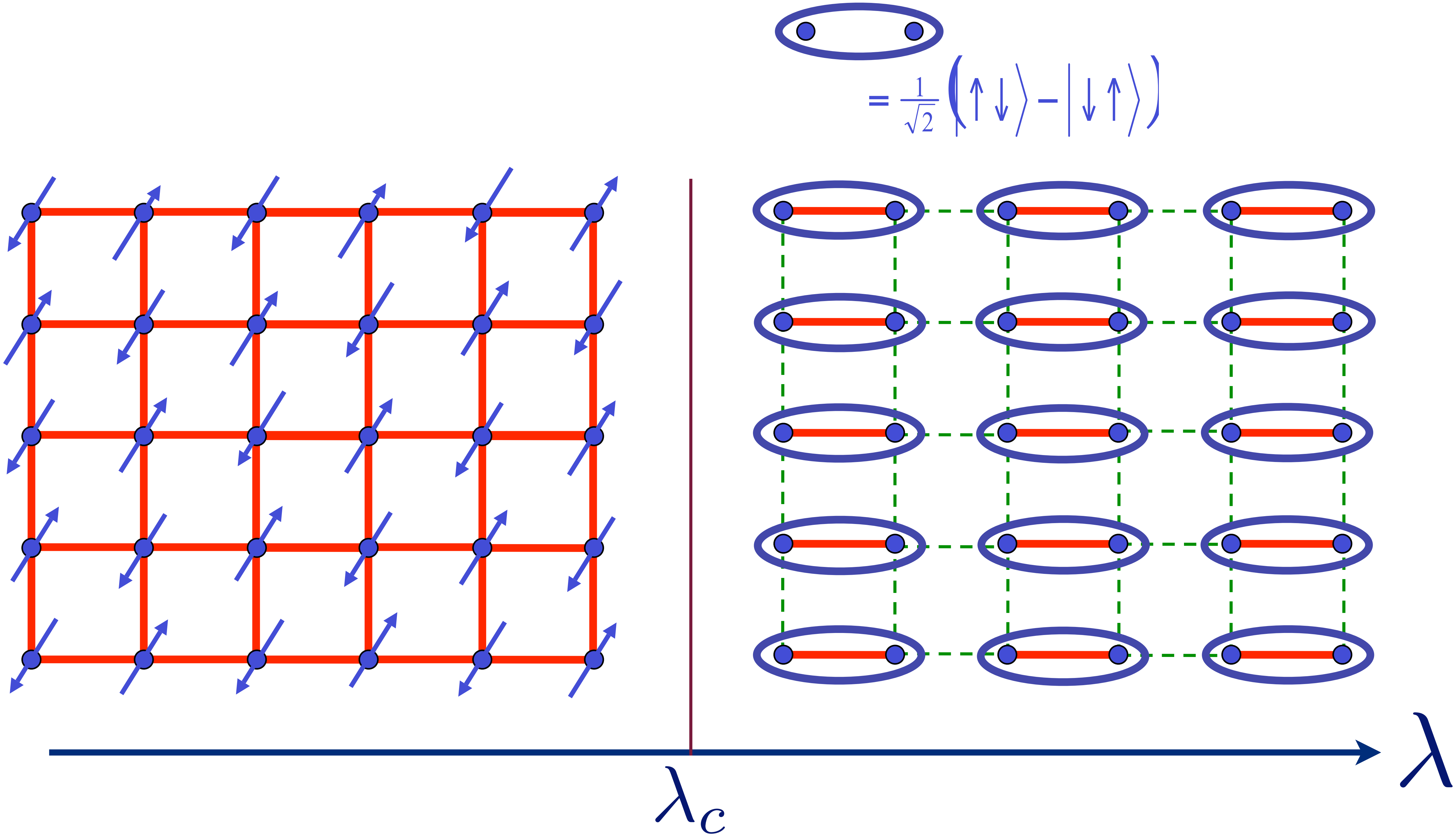

Pressure in $TlCuCl_3$

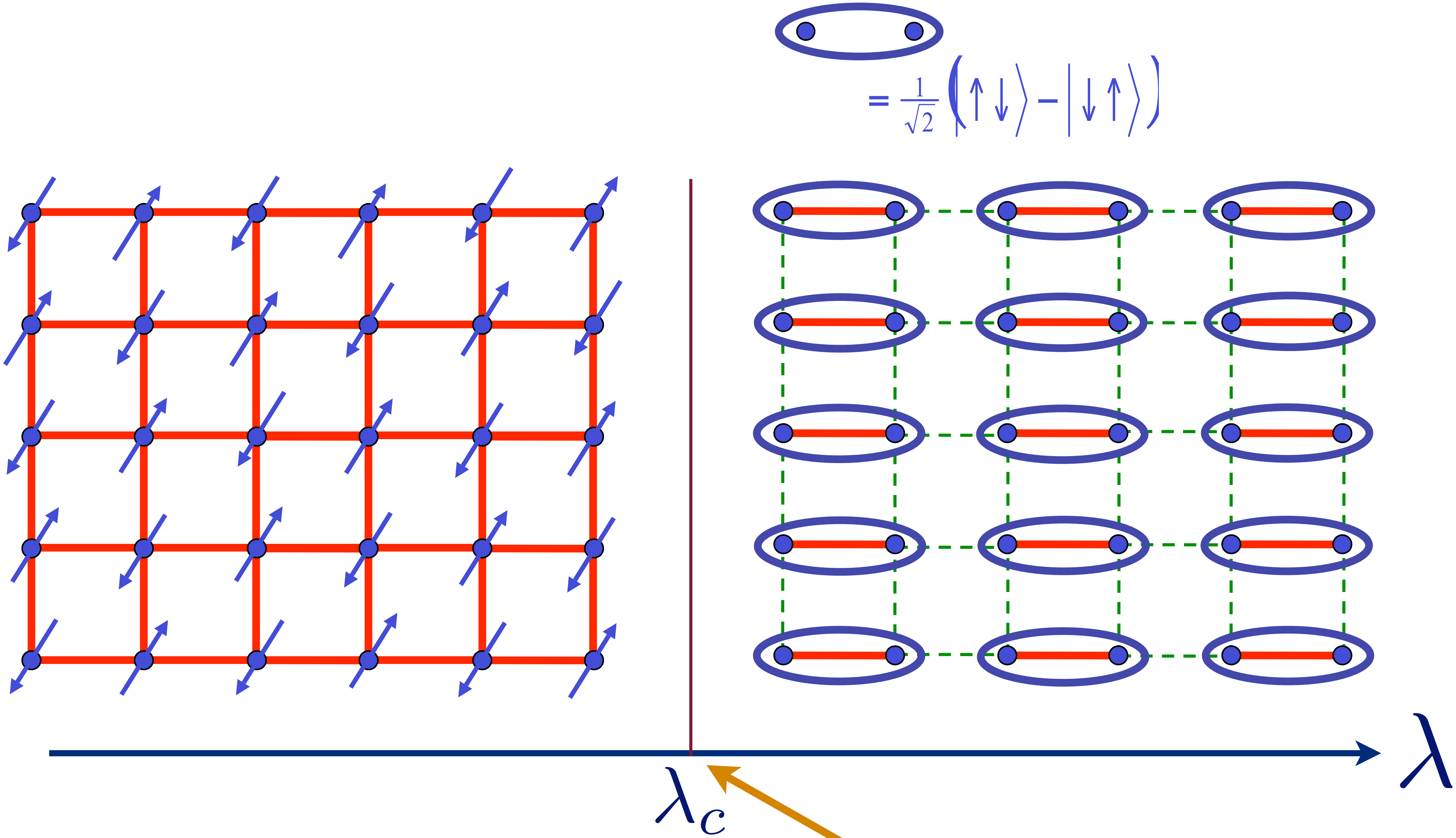

Quantum critical point with non-local entanglement in spin wavefunction

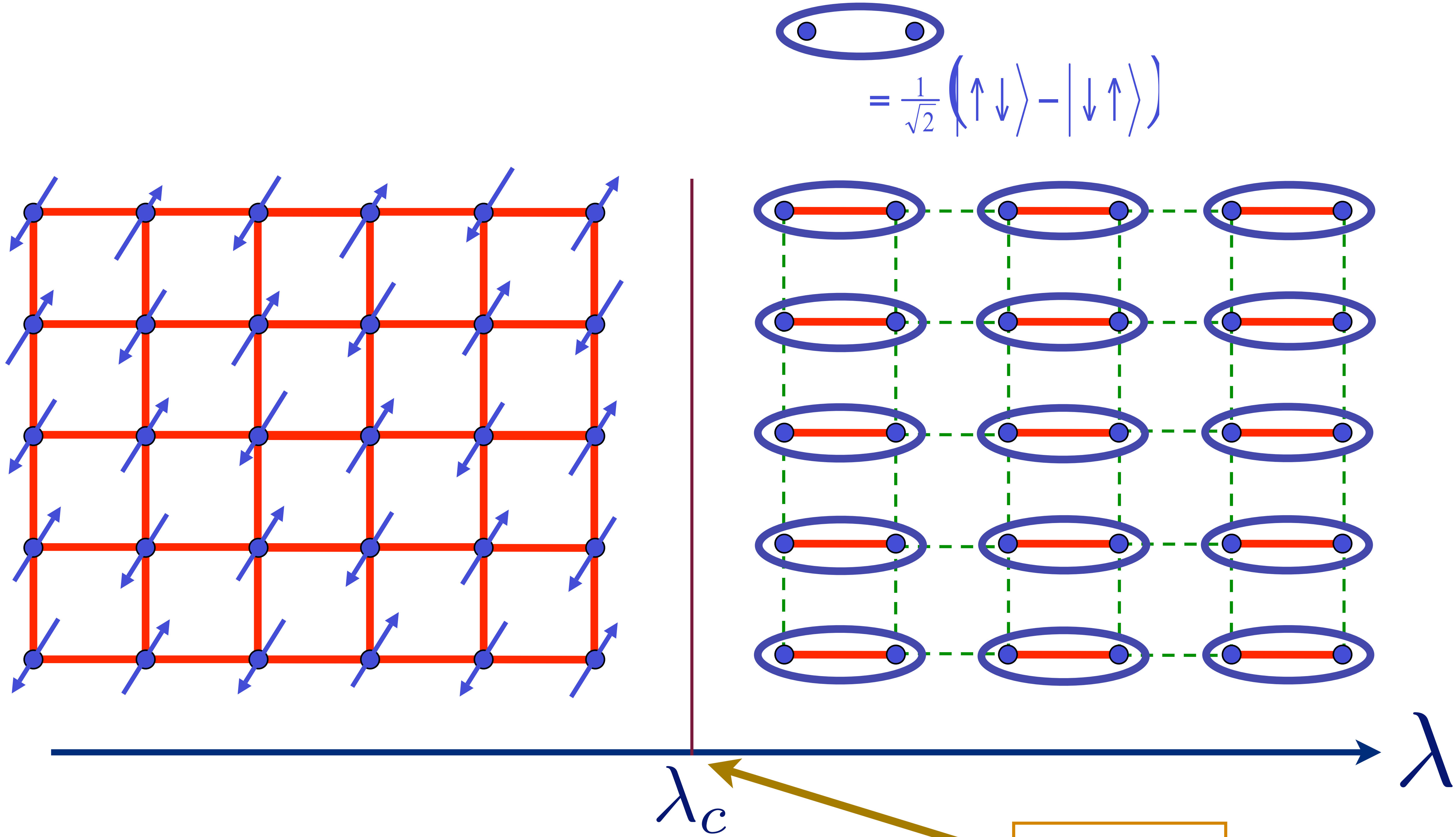

O(3) order parameter $\vec{\varphi}$

$$\mathcal{S} = \int d^2 r d\tau \left[(\partial_\tau \vec{\varphi})^2 + c^2 (\nabla_r \vec{\varphi})^2 + (\lambda - \lambda_c)\vec{\varphi}^2 + u \left(\vec{\varphi}^2\right)^2 \right]$$

Excitation spectrum in the paramagnetic phase

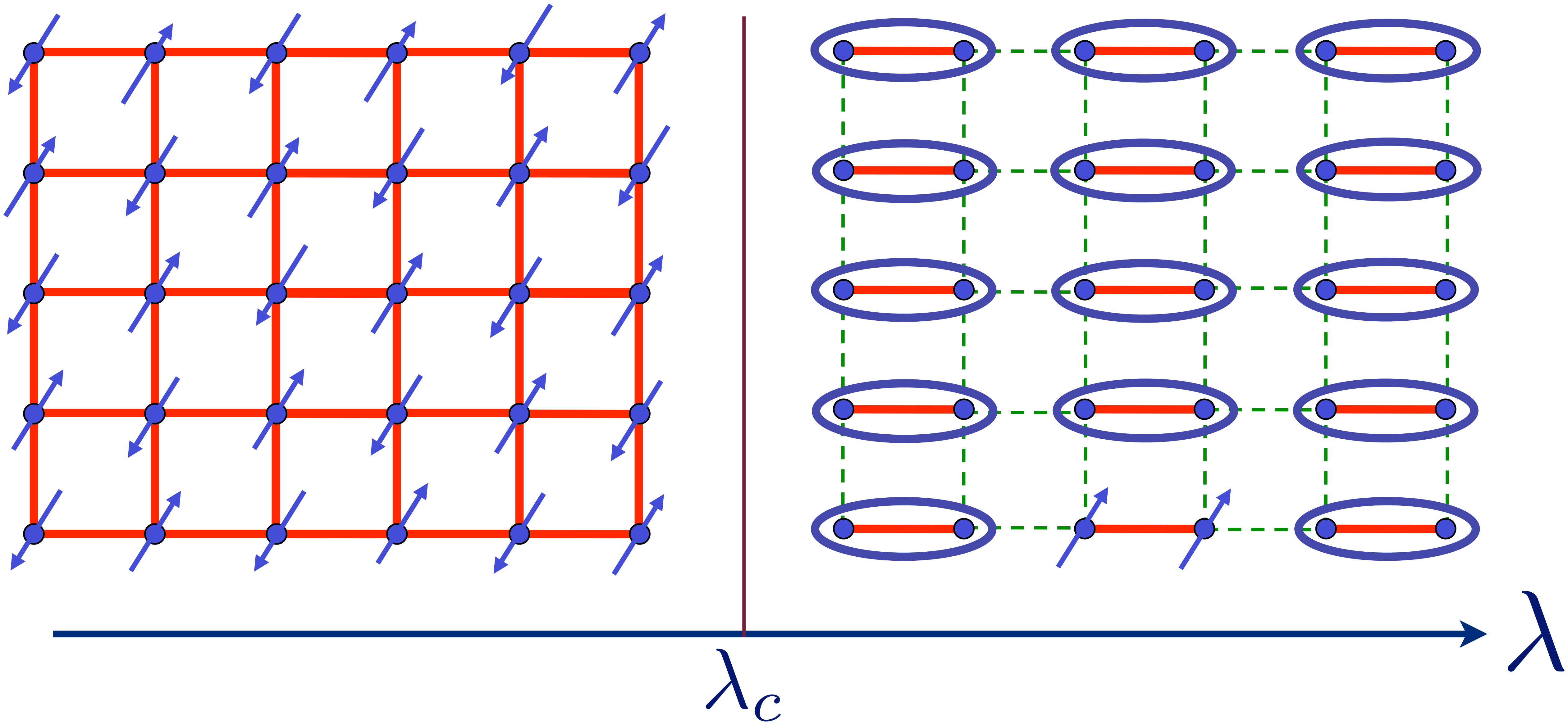

$$V(\vec{\varphi}) = (\lambda - \lambda_c)\vec{\varphi}^2 + u\left(\vec{\varphi}^2\right)^2$$

$$\lambda > \lambda_c$$

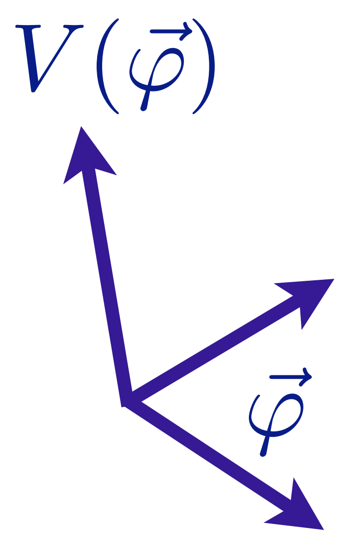

Spin $S = 1$
"triplon"

Excitation spectrum in the paramagnetic phase

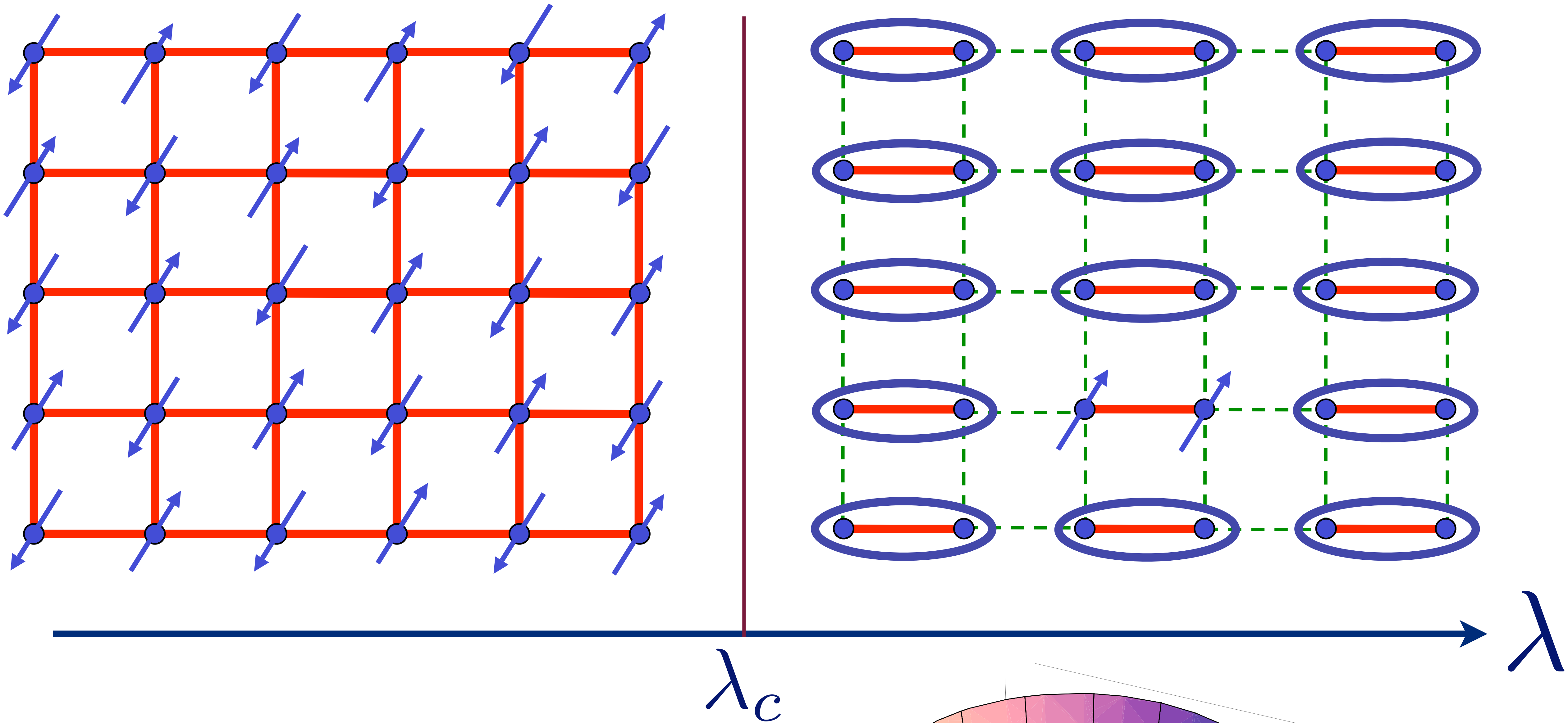

$$V(\vec{\varphi}) = (\lambda - \lambda_c)\vec{\varphi}^2 + u\left(\vec{\varphi}^2\right)^2$$

$$\lambda > \lambda_c$$

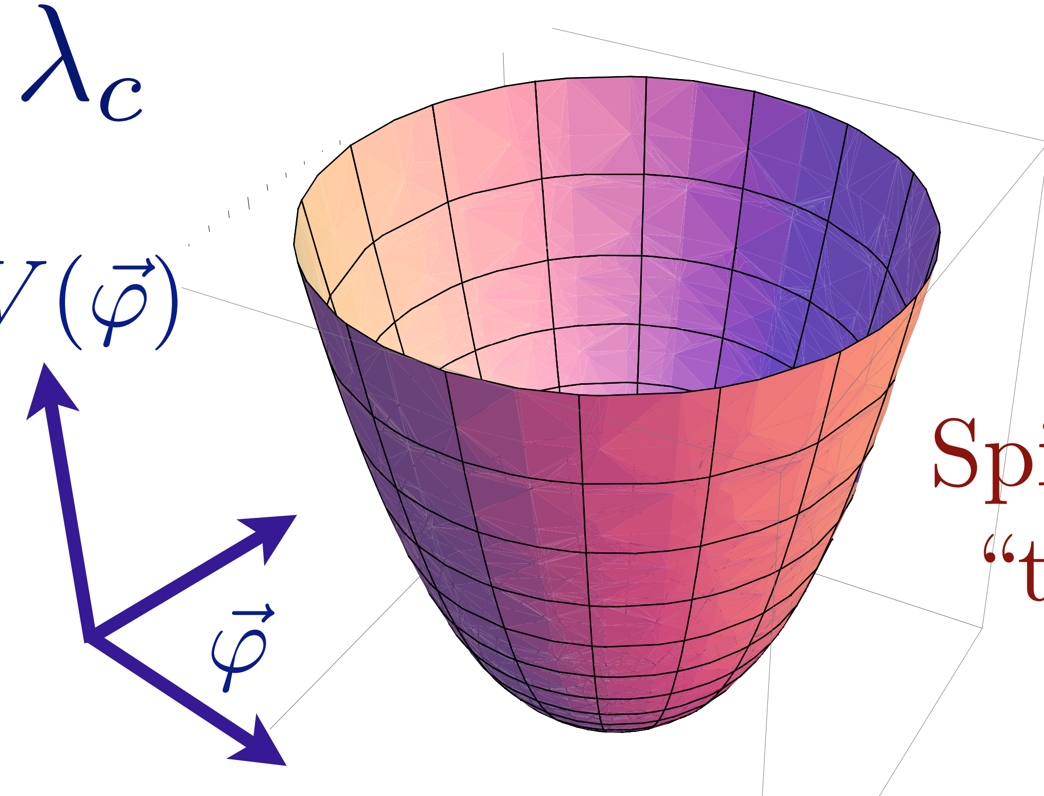

Spin $S = 1$
"triplon"

Excitation spectrum in the paramagnetic phase

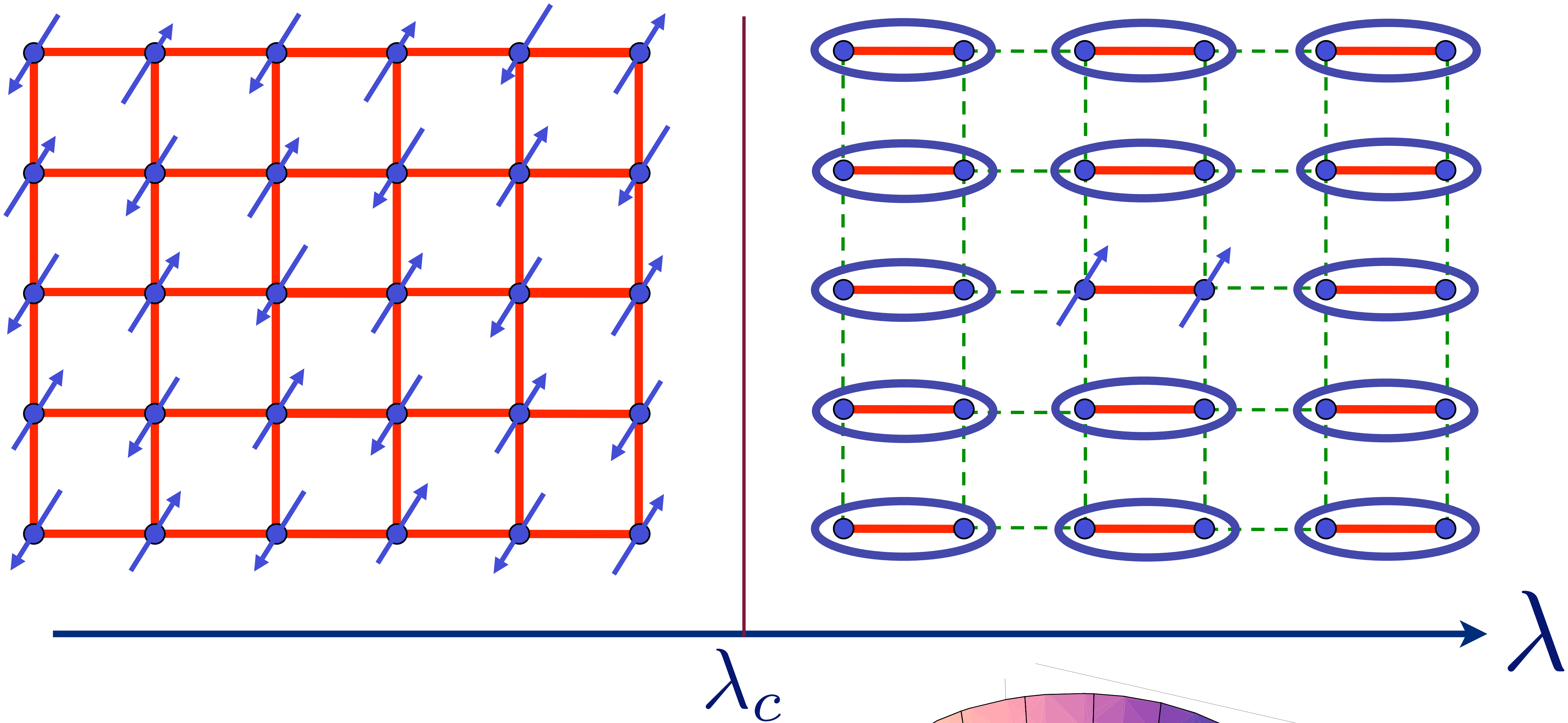

$$V(\vec{\varphi}) = (\lambda - \lambda_c)\vec{\varphi}^2 + u\left(\vec{\varphi}^2\right)^2$$

$$\lambda > \lambda_c$$

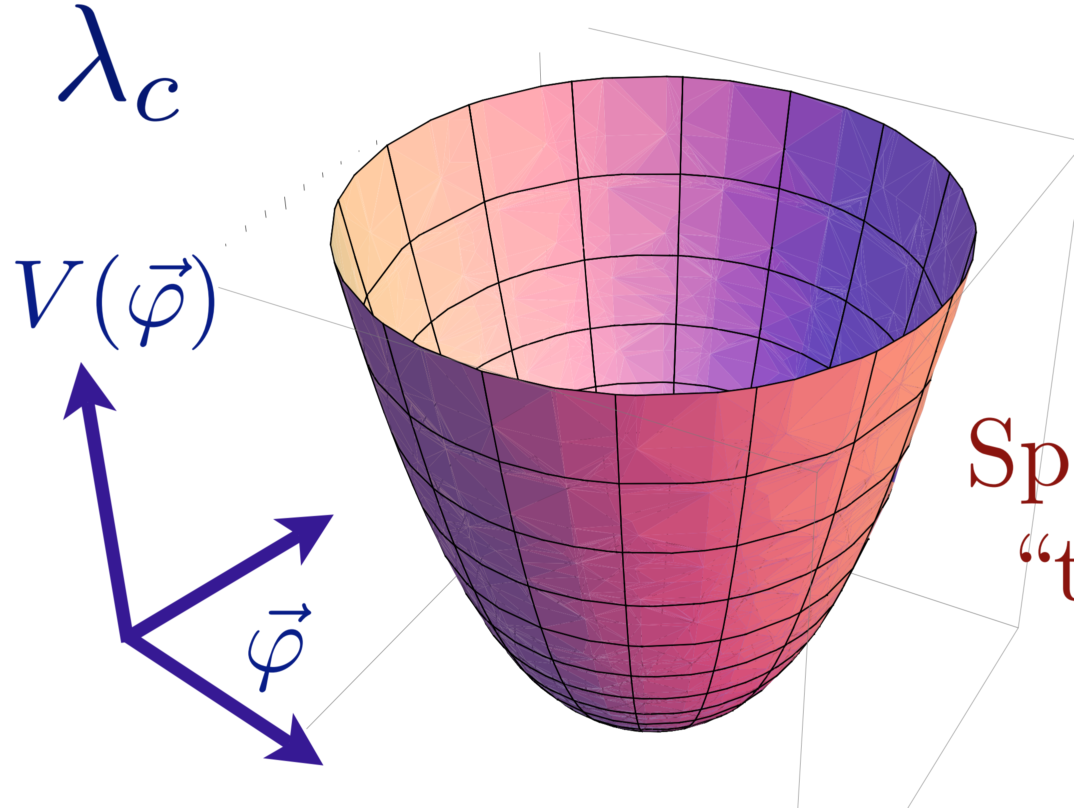

Spin $S = 1$
"triplon"

Excitation spectrum in the paramagnetic phase

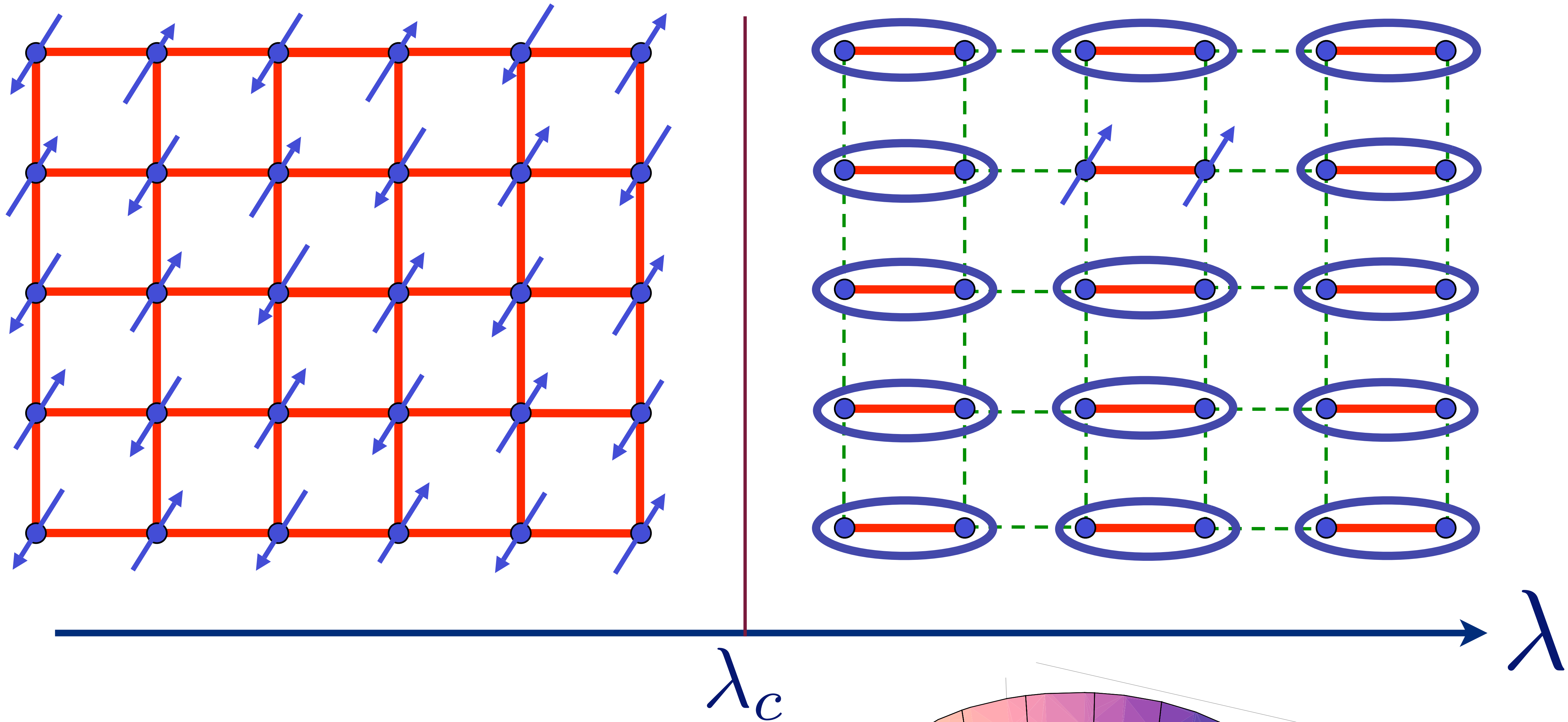

$$V(\vec{\varphi}) = (\lambda - \lambda_c)\vec{\varphi}^2 + u\left(\vec{\varphi}^2\right)^2$$

$$\lambda > \lambda_c$$

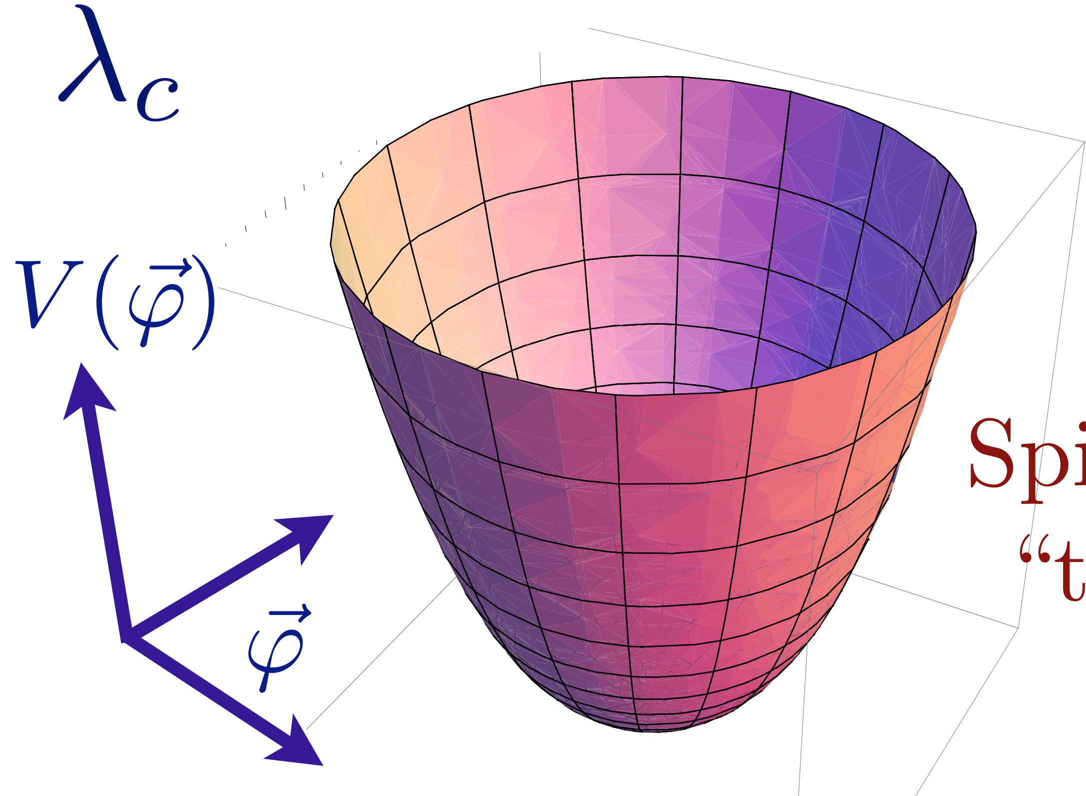

Spin $S = 1$
"triplon"

Excitation spectrum in the paramagnetic phase

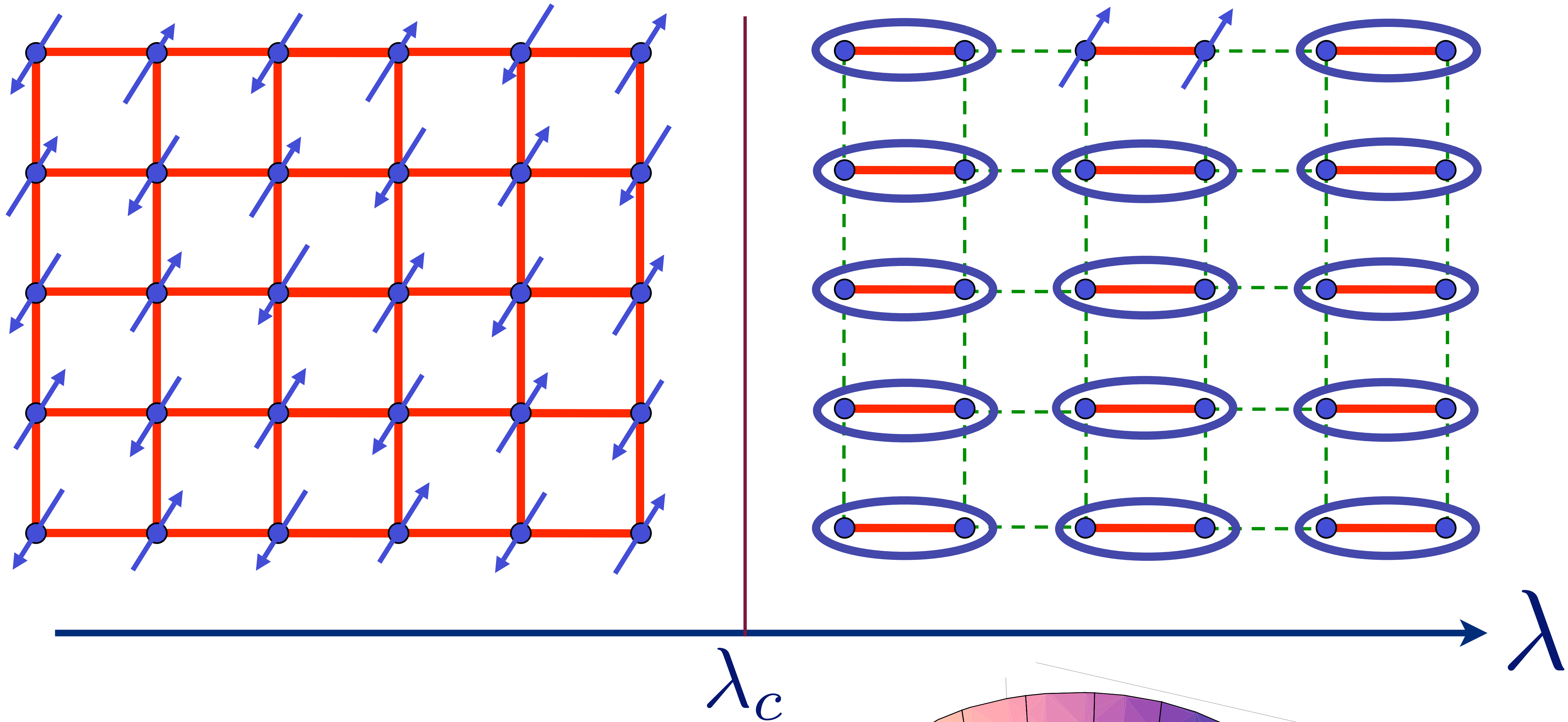

$$V(\vec{\varphi}) = (\lambda - \lambda_c)\vec{\varphi}^2 + u\left(\vec{\varphi}^2\right)^2$$

$$\lambda > \lambda_c$$

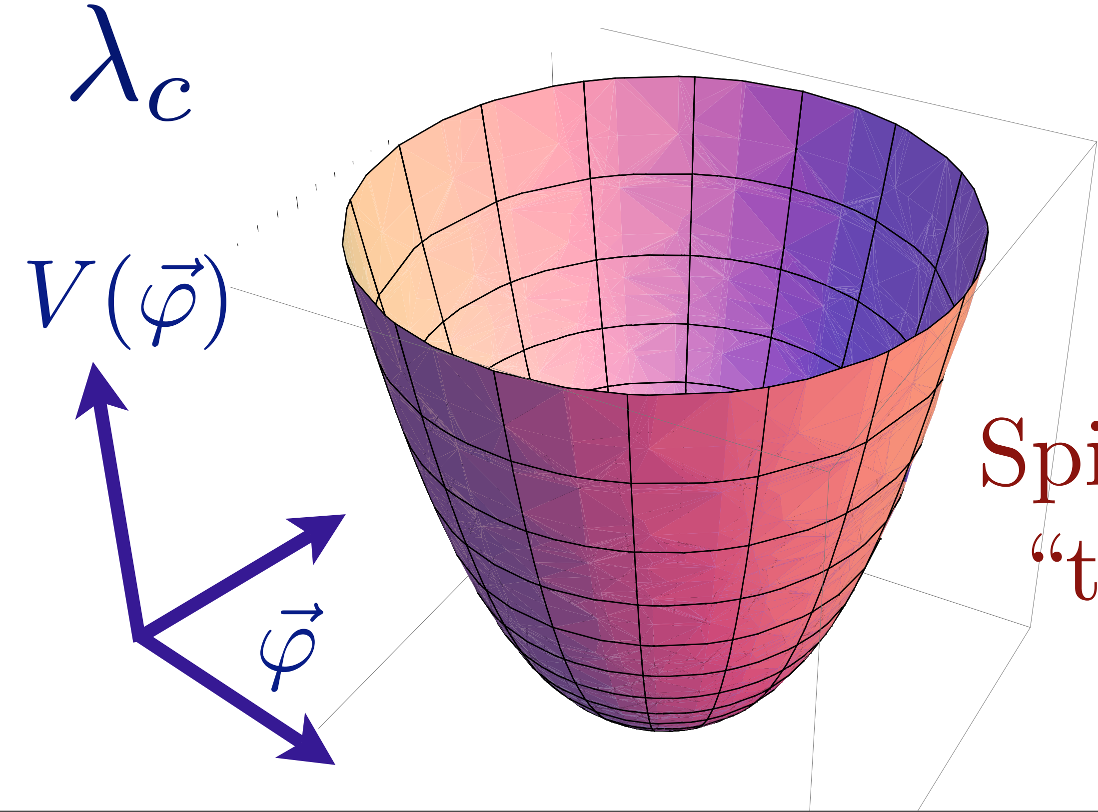

Spin $S = 1$
"triplon"

$TlCuCl_3$ at ambient pressure

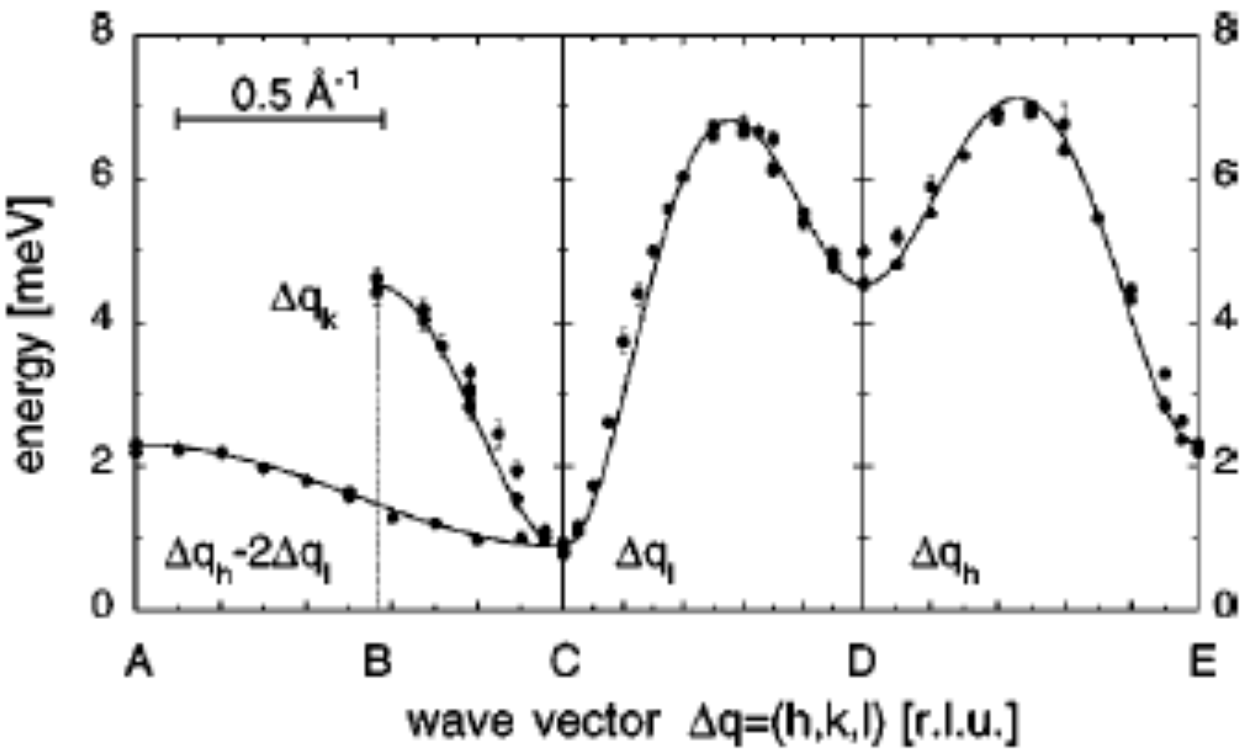

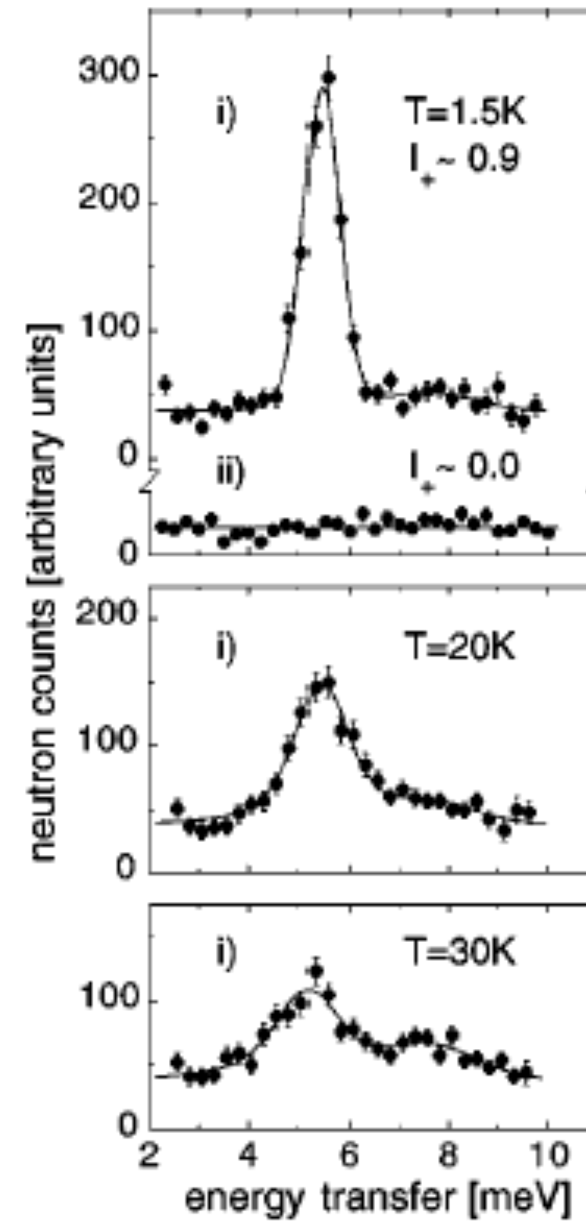

FIG. 1. Measured neutron profiles in the a^*c^* plane of $TlCuCl_3$ for $i=(1.35,0,0)$, $ii=(0,0,3.15)$ [r.l.u]. The spectrum at $T=1.5$ K

N. Cavadini, G. Heigold, W. Henggeler, A. Furrer, H.-U. Güdel, K. Krämer and H. Mutka, *Phys. Rev.* B 63 172414 (2001).

$TlCuCl_3$ at ambient pressure

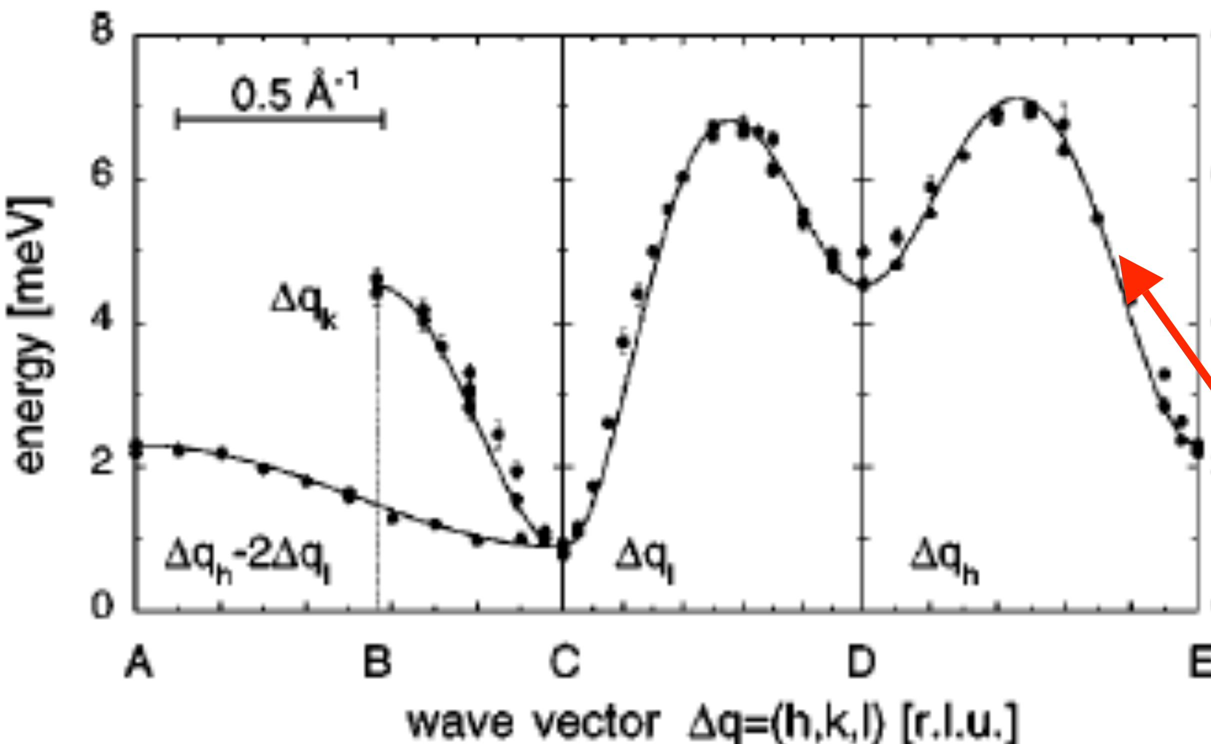

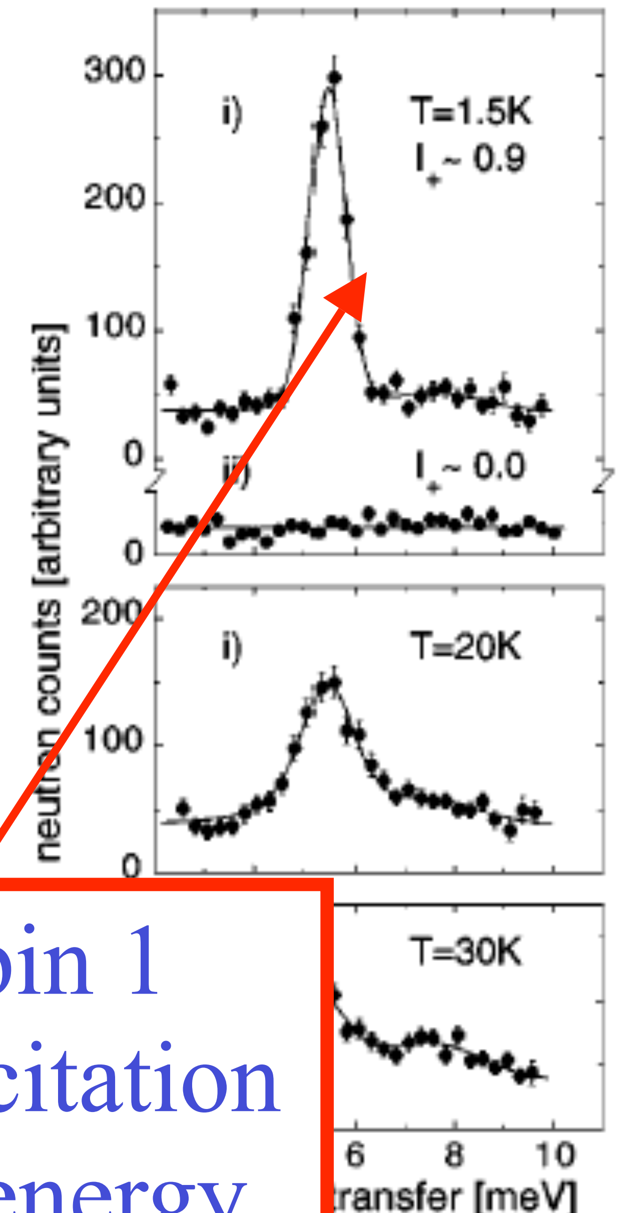

Sharp spin 1 particle excitation above an energy gap (spin gap)

les in the a^*c^* plane of $TlCuCl_3$
[r.l.u]. The spectrum at T= 1.5 K

N. Cavadini, G. Heigold, W. Henggeler, A. Furrer, H.-U. Güdel, K. Krämer and H. Mutka, *Phys. Rev.* B 63 172414 (2001).

Excitation spectrum in the Néel phase

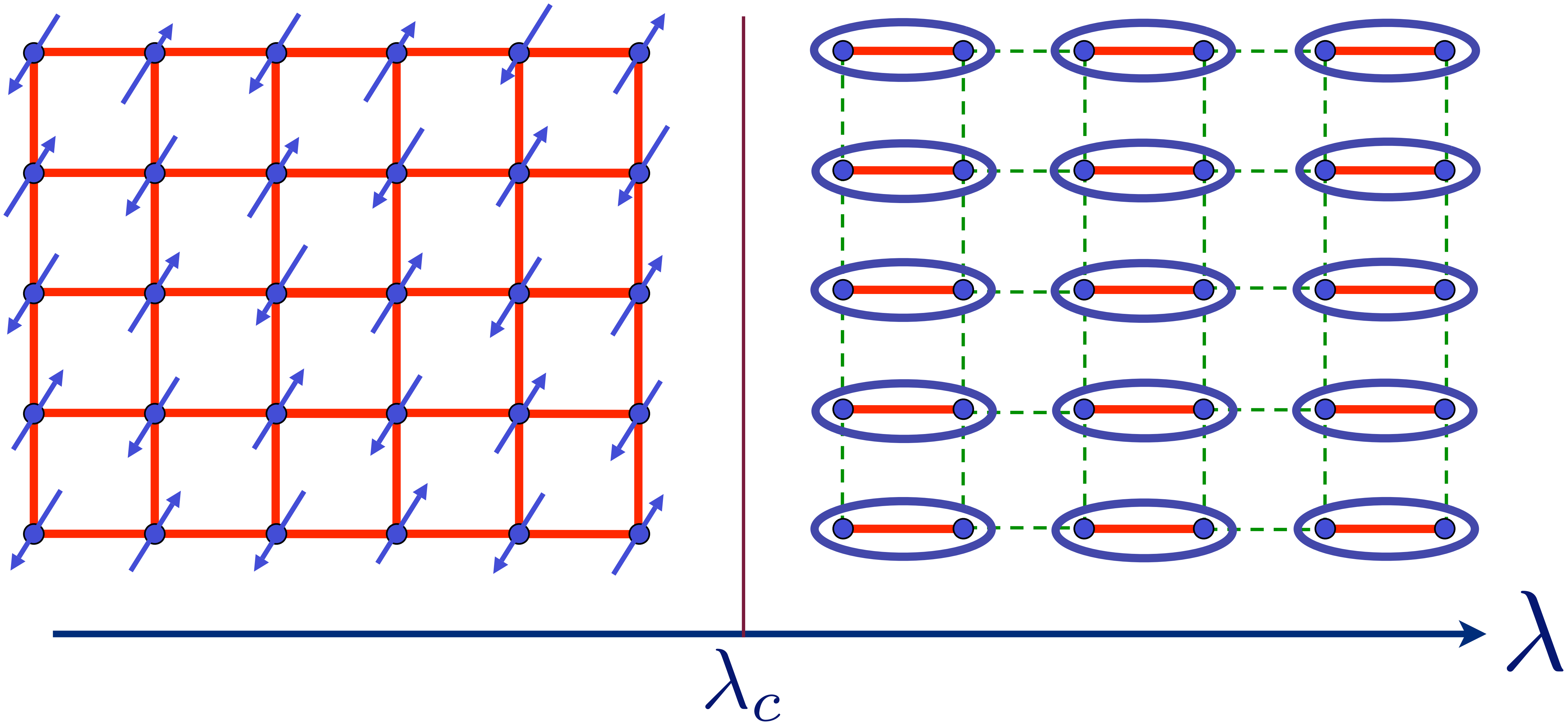

Excitation spectrum in the Néel phase

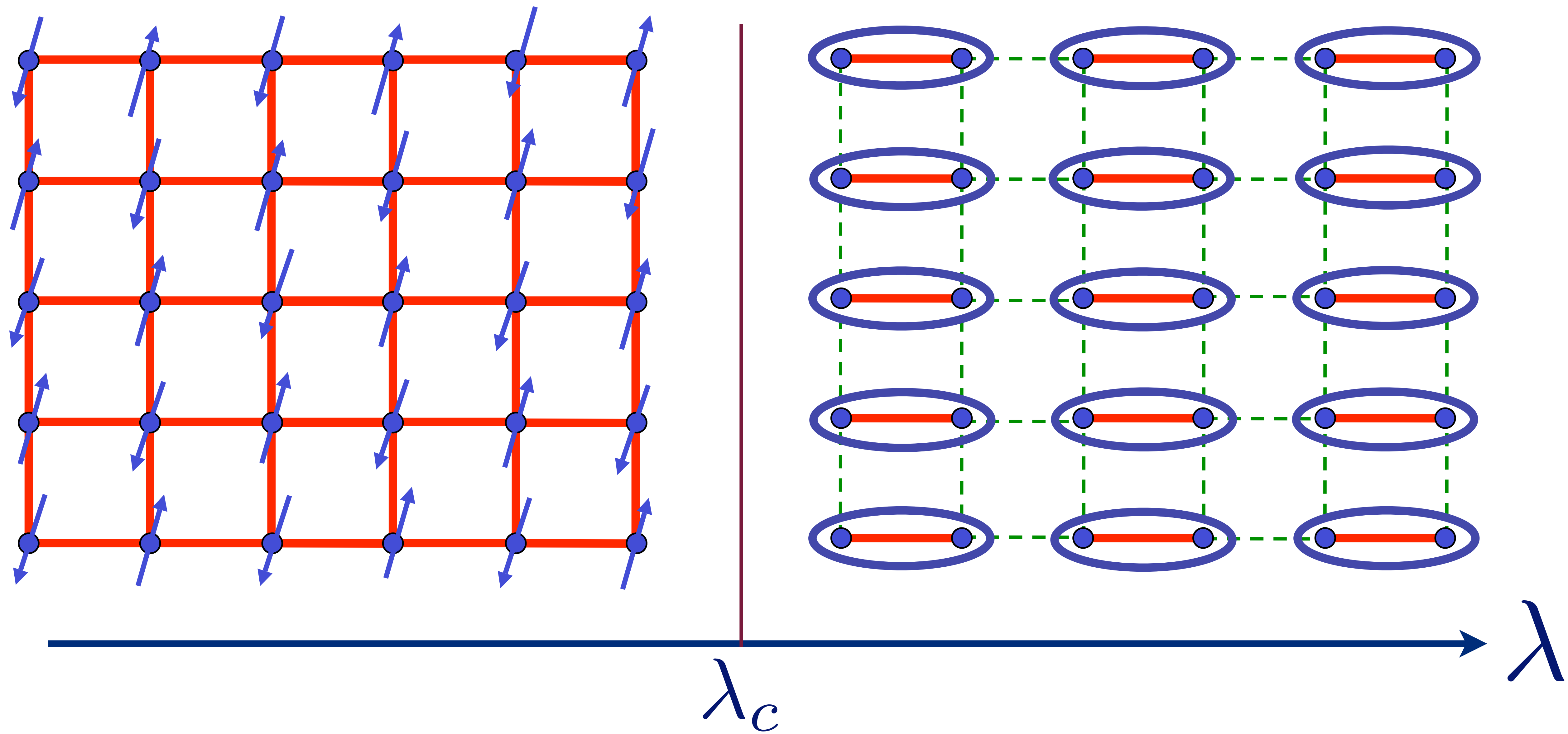

Spin waves

Excitation spectrum in the Néel phase

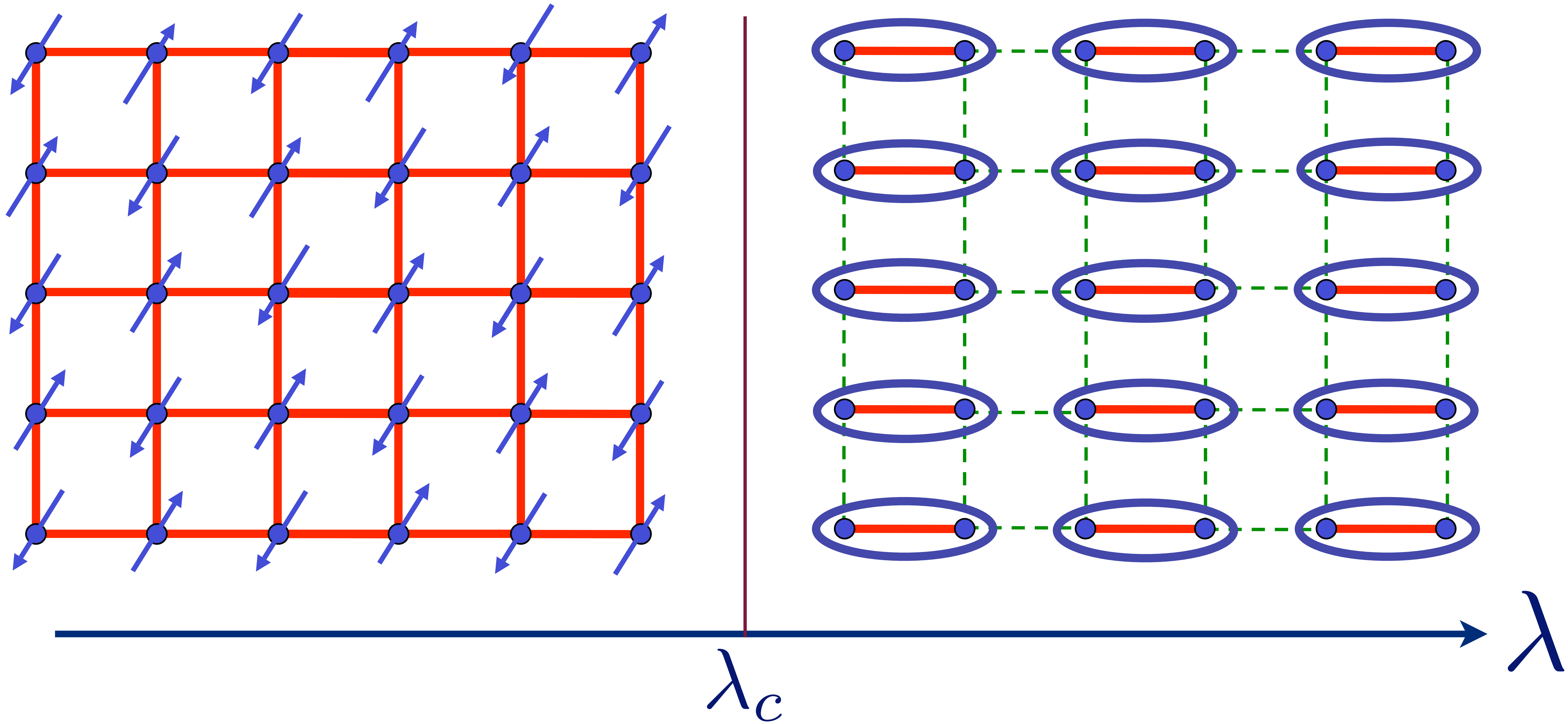

Spin waves

Excitation spectrum in the Néel phase

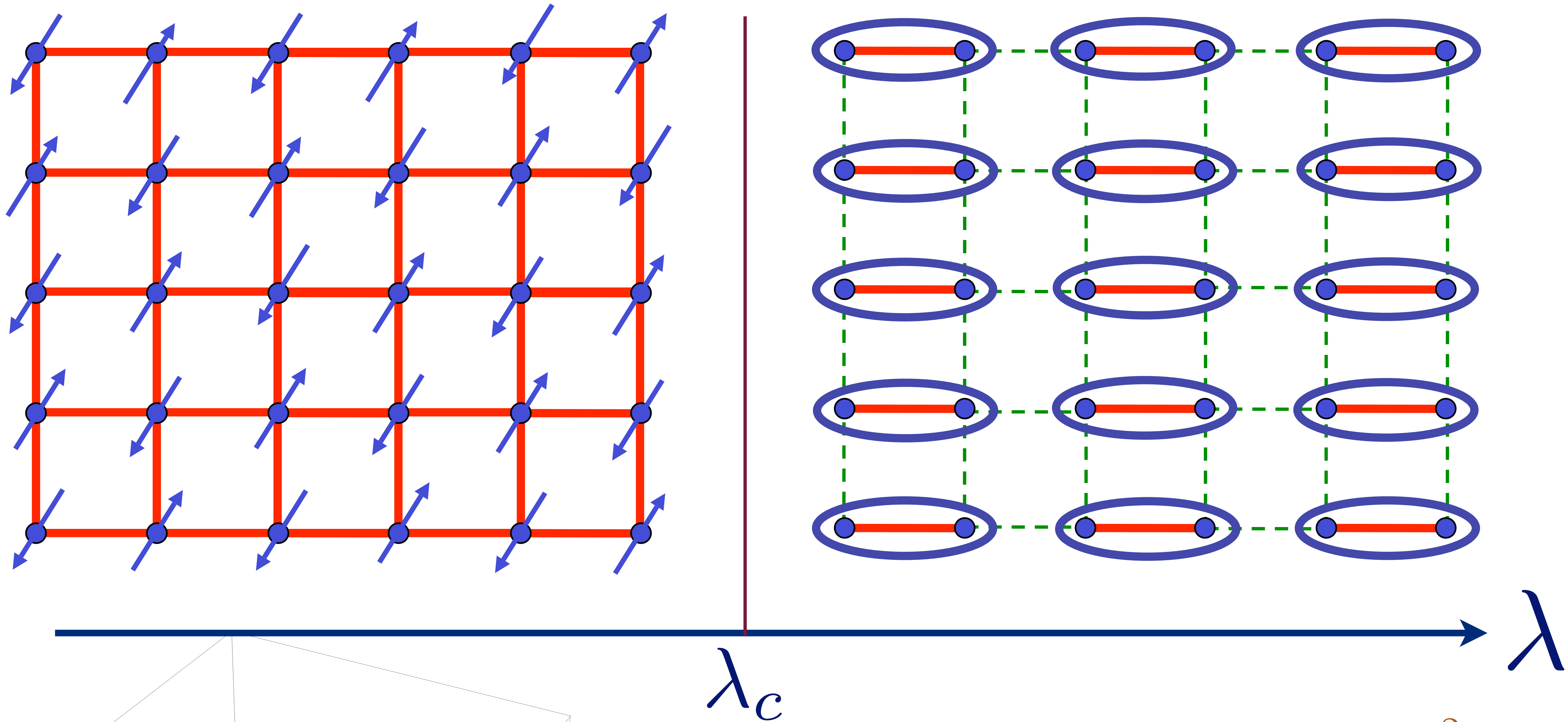

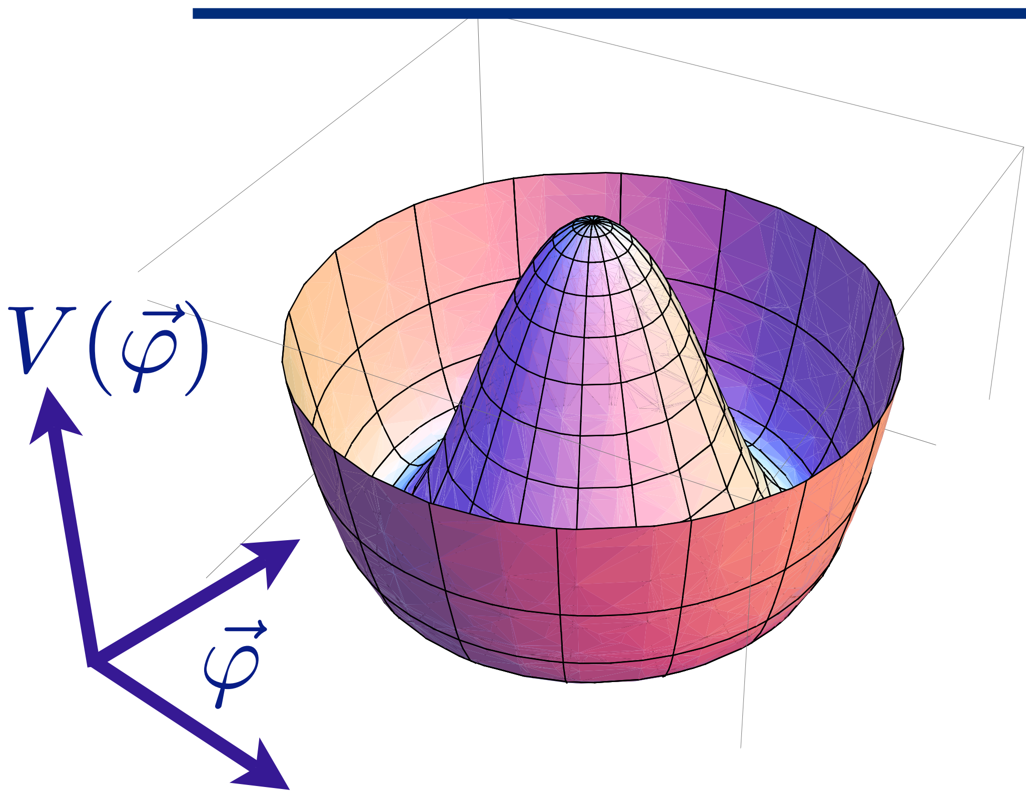

$$V(\vec{\varphi}) = (\lambda - \lambda_c)\vec{\varphi}^2 + u\left(\vec{\varphi}^2\right)^2$$

$$\lambda < \lambda_c$$

Excitation spectrum in the Néel phase

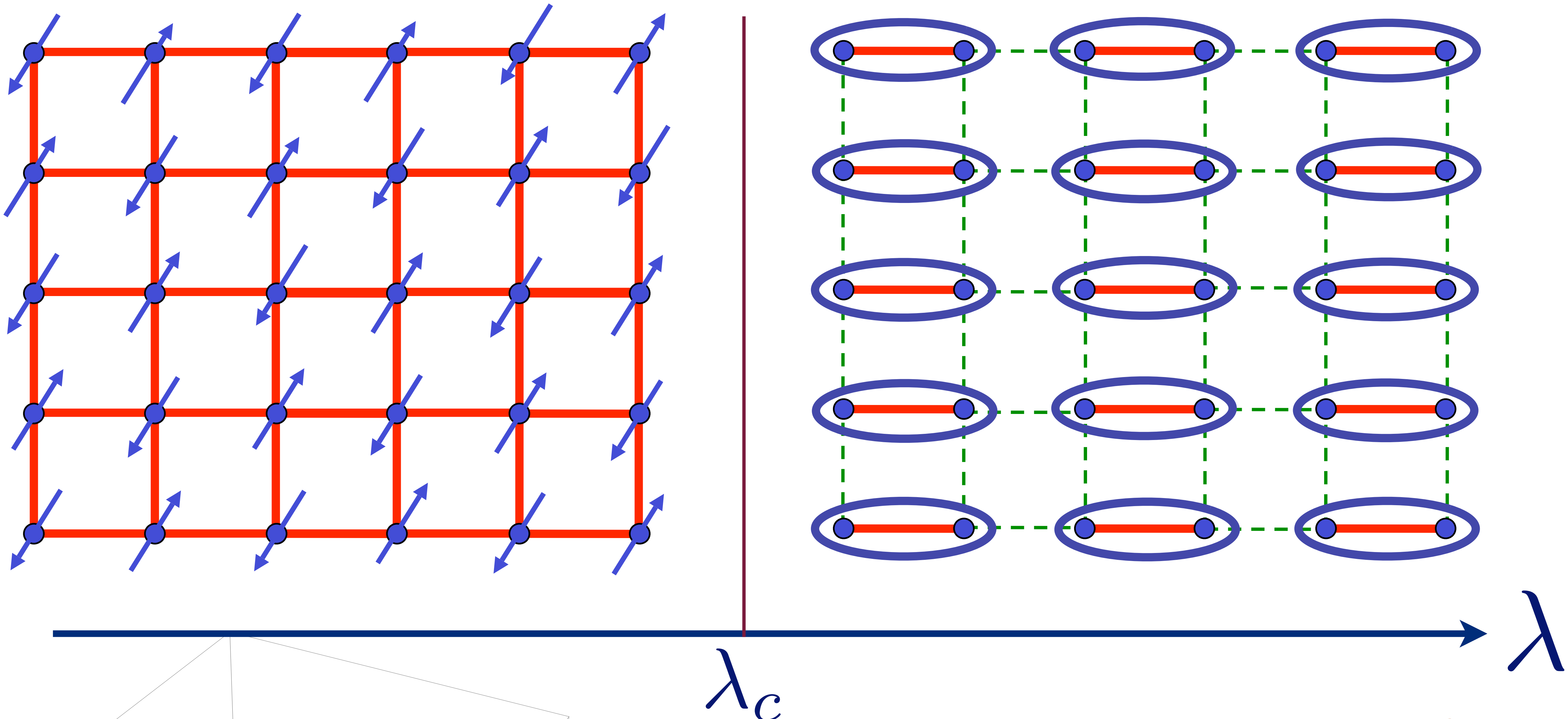

$$V(\vec{\varphi}) = (\lambda - \lambda_c)\vec{\varphi}^2 + u\left(\vec{\varphi}^2\right)^2$$

$$\lambda < \lambda_c$$

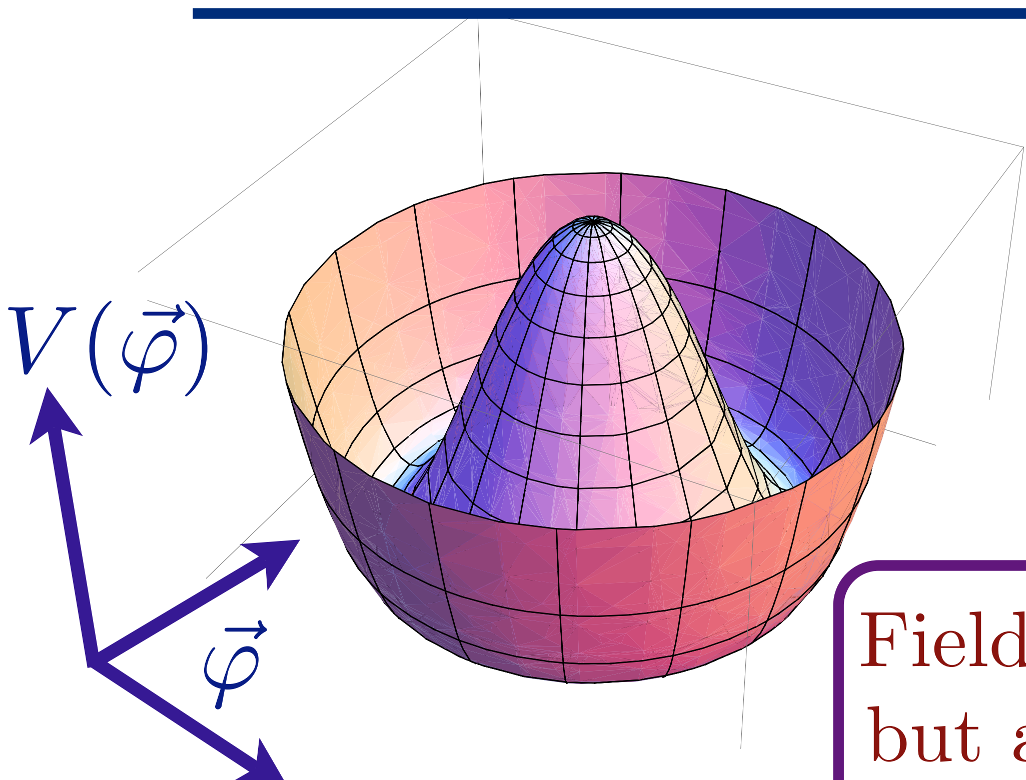

Field theory yields spin waves ("Goldstone" modes) but also an additional longitudinal "Higgs" particle

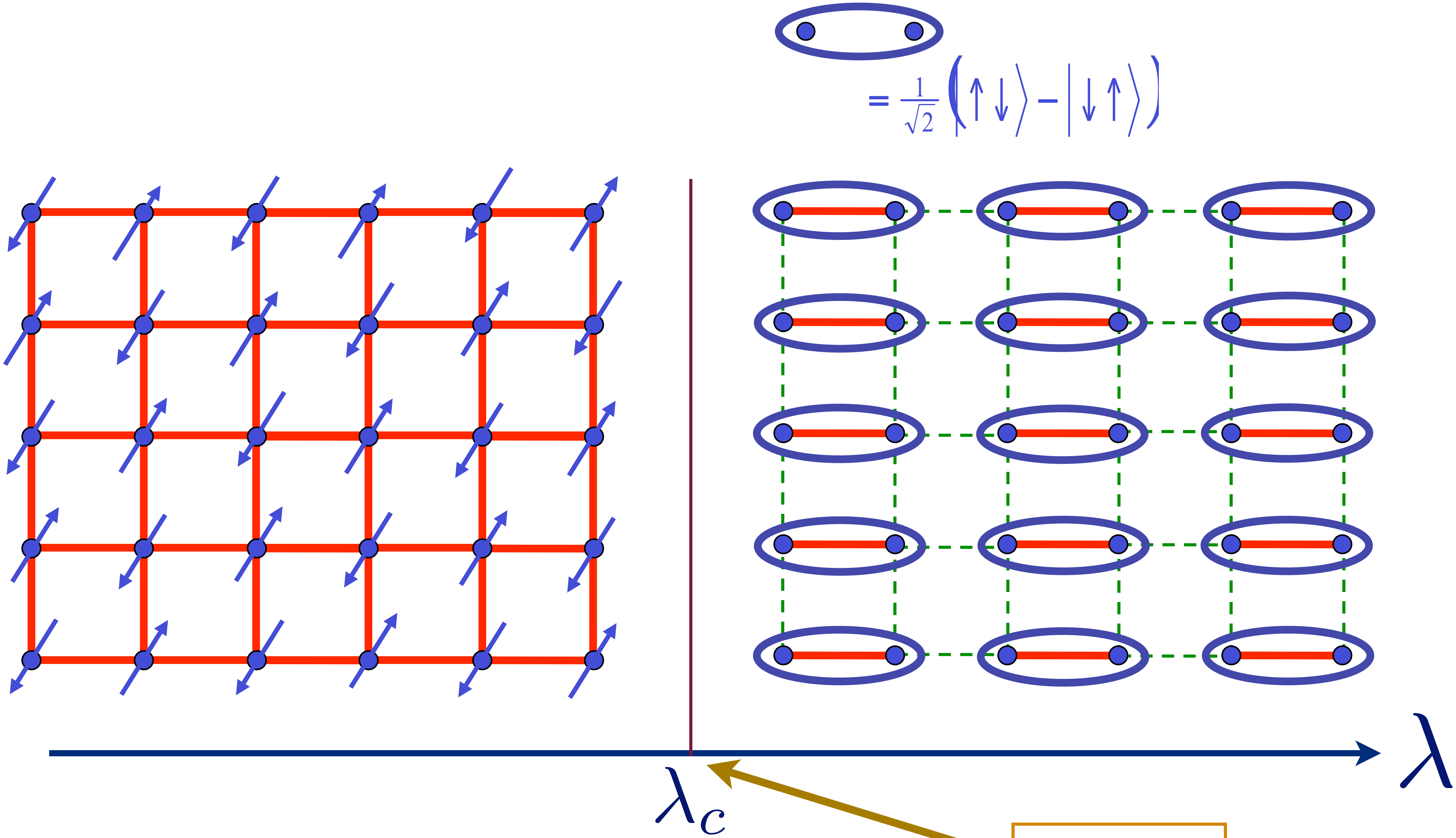

O(3) order parameter $\vec{\varphi}$

$$\mathcal{S} = \int d^2r d\tau \left[(\partial_\tau \vec{\varphi})^2 + c^2 (\nabla_r \vec{\varphi})^2 + (\lambda - \lambda_c)\vec{\varphi}^2 + u\left(\vec{\varphi}^2\right)^2 \right]$$

Quantum Monte Carlo - critical exponents

Table IV: Fit results for the critical exponents ν, β/ν, and η. We summarize results including a variation of the critical point within its error bar. For the ladder model (top group of values) fit results and quality of fits are also given at the previous best estimate of α_c. The bottom group are results for the plaquette model. Numbers in [...] brackets denote the χ^2/d.o.f. For comparison relevant reference values for the 3D $O(3)$ universality class are given in the last line.

α_c	ν^a	β/ν^b	η^c
$1.9096-\sigma$	0.712(4) [1.8]	0.516(2) [0.5]	0.026(2) [0.2]
1.9096	0.711(4) [1.8]	0.518(2) [1.1]	0.029(5) [0.8]
$1.9096+\sigma$	0.710(4) [1.8]	0.519(3) [2.5]	0.032(7) [1.4]
1.9107^d	0.709(3) [1.7]	0.525(8) [15.3]	0.051(10) [12]
$1.8230-\sigma$	0.708(4) [0.99]	0.515(2) [0.84]	0.025(4) [0.15]
1.8230	0.706(4) [1.04]	0.516(2) [0.40]	0.028(3) [0.31]
$1.8230+\sigma$	0.706(4) [1.10]	0.517(2) [1.6]	0.031(5) [0.80]
Ref. 49	0.7112(5)	0.518(1)	0.0375(5)

$^a L > 12$.
$^b L > 16$.
$^c L > 20$.
^{d}Previous best estimate of Ref. 19.

S. Wenzel and W. Janke, arXiv:0808.1418
M. Troyer, M. Imada, and K. Ueda, *J. Phys. Soc. Japan* (1997)

Quantum Monte Carlo - critical exponents

Table IV: Fit results for the critical exponents ν, β/ν, and η. We summarize results including a variation of the critical point within its error bar. For the ladder model (top group of values) fit results and quality of fits are also given at the previous best estimate of α_c. The bottom group are results for the plaquette model. Numbers in [...] brackets denote the χ^2/d.o.f. For comparison relevant reference values for the 3D $O(3)$ universality class are given in the last line.

α_c	ν^a	β/ν^b	η^c
$1.9096-\sigma$	0.712(4) [1.8]	0.516(2) [0.5]	0.026(2) [0.2]
1.9096	0.711(4) [1.8]	0.518(2) [1.1]	0.029(5) [0.8]
$1.9096+\sigma$	0.710(4) [1.8]	0.519(3) [2.5]	0.032(7) [1.4]
1.9107^d	0.709(3) [1.7]	0.525(8) [15.3]	0.051(10) [12]
$1.8230-\sigma$	0.708(4) [0.99]	0.515(2) [0.84]	0.025(4) [0.15]
1.8230	0.706(4) [1.04]	0.516(2) [0.40]	0.028(3) [0.31]
$1.8230+\sigma$	0.706(4) [1.10]	0.517(2) [1.6]	0.031(5) [0.80]
Ref. 49	0.7112(5)	0.518(1)	0.0375(5)

[a] $L > 12$.
[b] $L > 16$.
[c] $L > 20$.
[d] Previous best estimate of Ref. 19.

Field-theoretic RG of CFT3 E. Vicari *et al.*

S. Wenzel and W. Janke, arXiv:0808.1418
M. Troyer, M. Imada, and K. Ueda, *J. Phys. Soc. Japan* (1997)

$TlCuCl_3$ with varying pressure

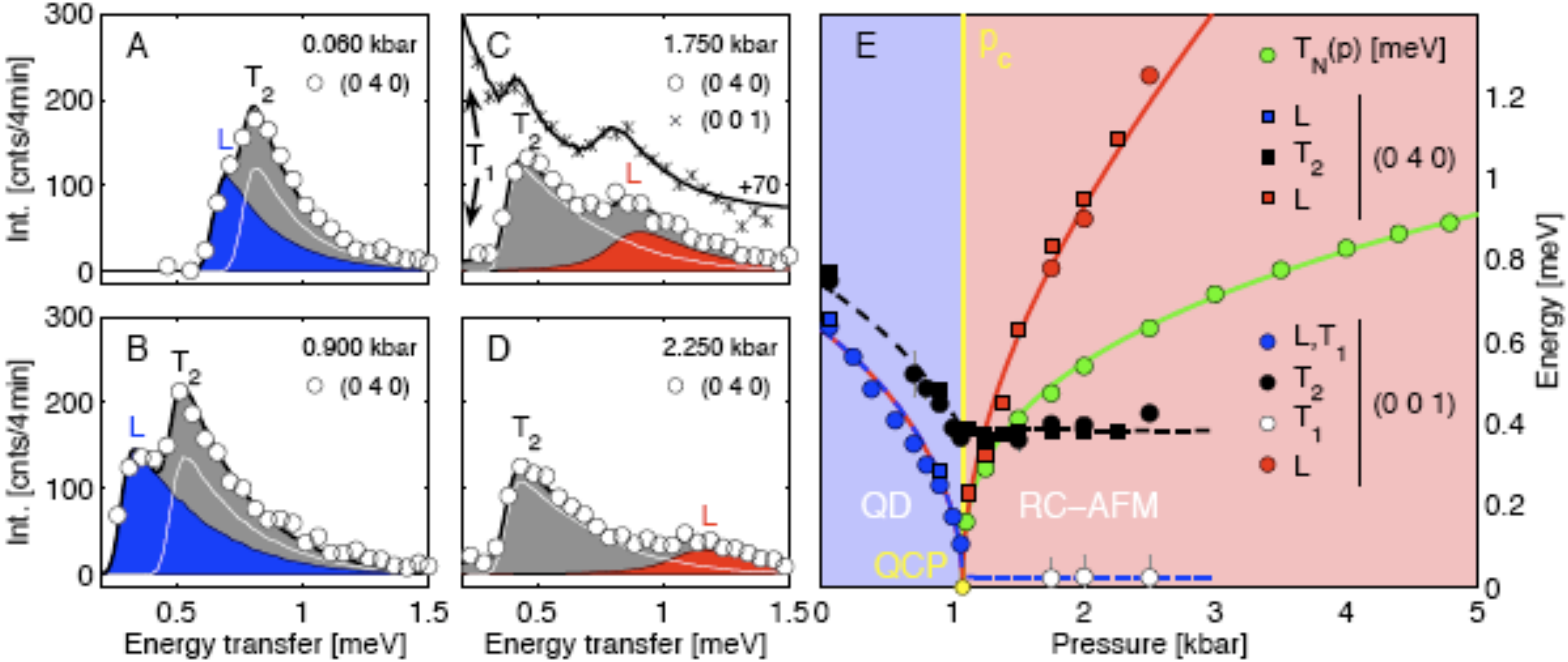

Observation of $3 \rightarrow 2$ low energy modes,
emergence of new Higgs particle in the Néel phase,
and vanishing of Néel temperature at the quantum critical point

Christian Ruegg, Bruce Normand, Masashige Matsumoto, Albert Furrer, Desmond McMorrow, Karl Kramer, Hans–Ulrich Gudel, Severian Gvasaliya, Hannu Mutka, and Martin Boehm, *Phys. Rev. Lett.* **100**, 205701 (2008)

Prediction of quantum field theory

Potential for $\vec{\varphi}$ fluctuations: $V(\vec{\varphi}) = (\lambda - \lambda_c)\vec{\varphi}^2 + u\left(\vec{\varphi}^2\right)^2$

Paramagnetic phase, $\lambda > \lambda_c$

Expand about $\vec{\varphi} = 0$:

$$V(\vec{\varphi}) \approx (\lambda - \lambda_c)\vec{\varphi}^2$$

Yields 3 particles with energy gap $\sim \sqrt{(\lambda - \lambda_c)}$

Néel phase, $\lambda < \lambda_c$

Expand $\vec{\varphi} = \left(0, 0, \sqrt{(\lambda_c - \lambda)/(2u)}\right) + \vec{\varphi}_1$:

$$V(\vec{\varphi}) \approx 2(\lambda_c - \lambda)\varphi_{1z}^2$$

Yields 2 gapless spin waves and one Higgs particle
with energy gap $\sim \sqrt{2(\lambda_c - \lambda)}$

Prediction of quantum field theory

$$\frac{\text{Energy of "Higgs" particle}}{\text{Energy of triplon}} = \sqrt{2}$$

$$V(\vec{\varphi}) = (\lambda - \lambda_c)\vec{\varphi}^2 + u\left(\vec{\varphi}^2\right)^2$$

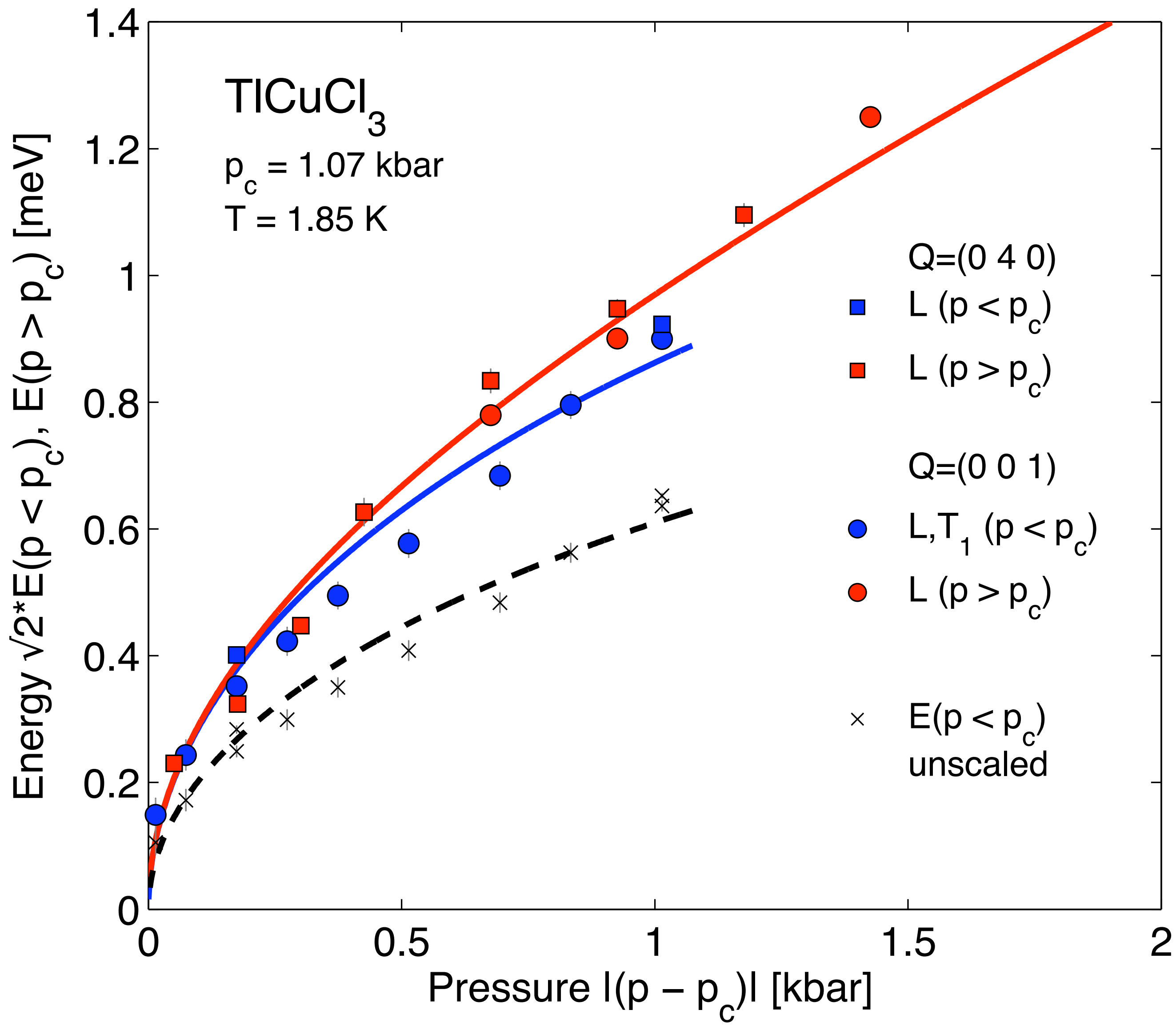

Christian Ruegg, Bruce Normand, Masashige Matsumoto, Albert Furrer, Desmond McMorrow, Karl Kramer, Hans-Ulrich Gudel, Severian Gvasaliya, Hannu Mutka, and Martin Boehm, *Phys. Rev. Lett.* **100**, 205701 (2008)

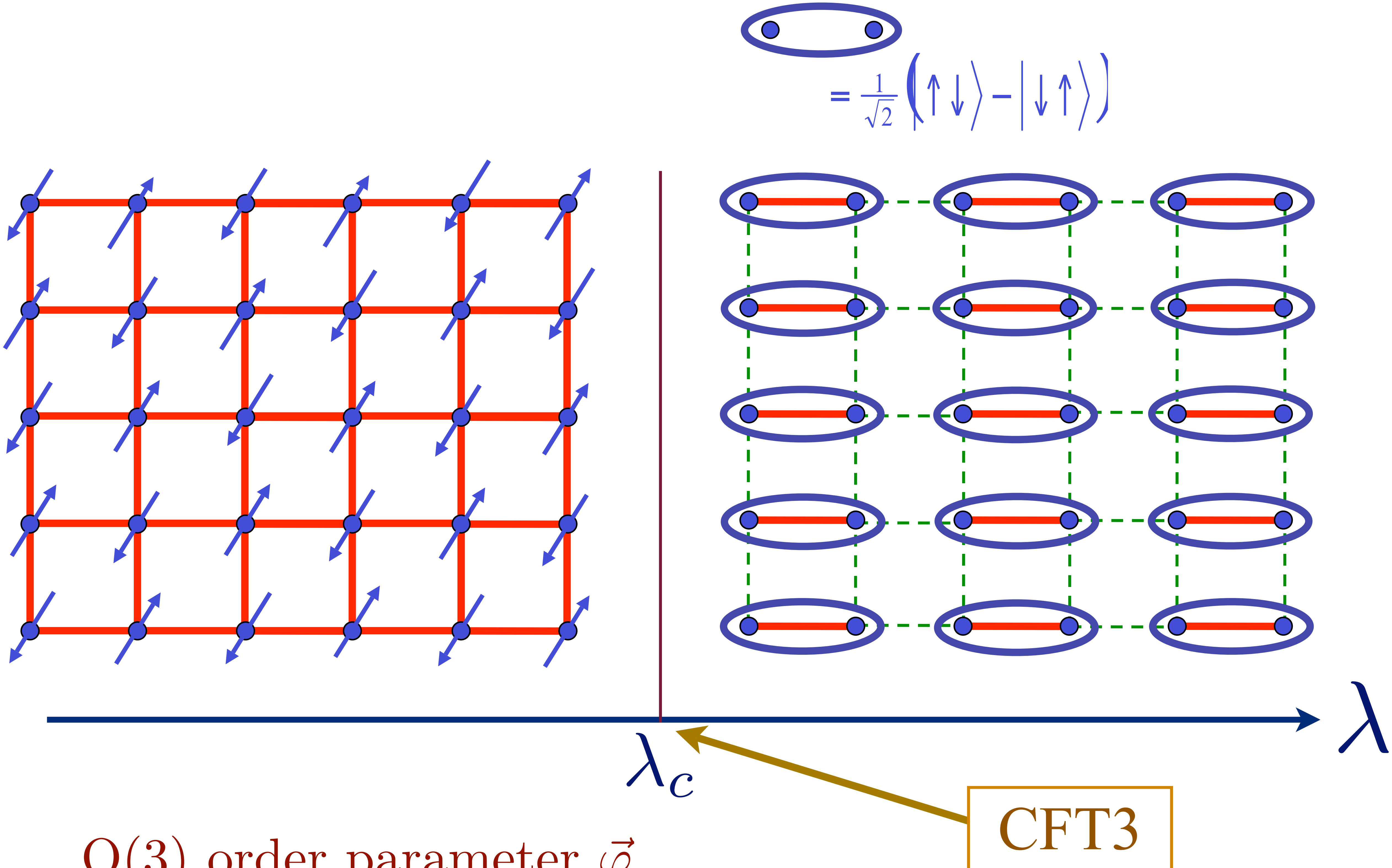

O(3) order parameter $\vec{\varphi}$

$$\mathcal{S} = \int d^2 r d\tau \left[(\partial_\tau \varphi)^2 + c^2 (\nabla_r \vec{\varphi})^2 + s\vec{\varphi}^2 + u \left(\vec{\varphi}^2\right)^2 \right]$$

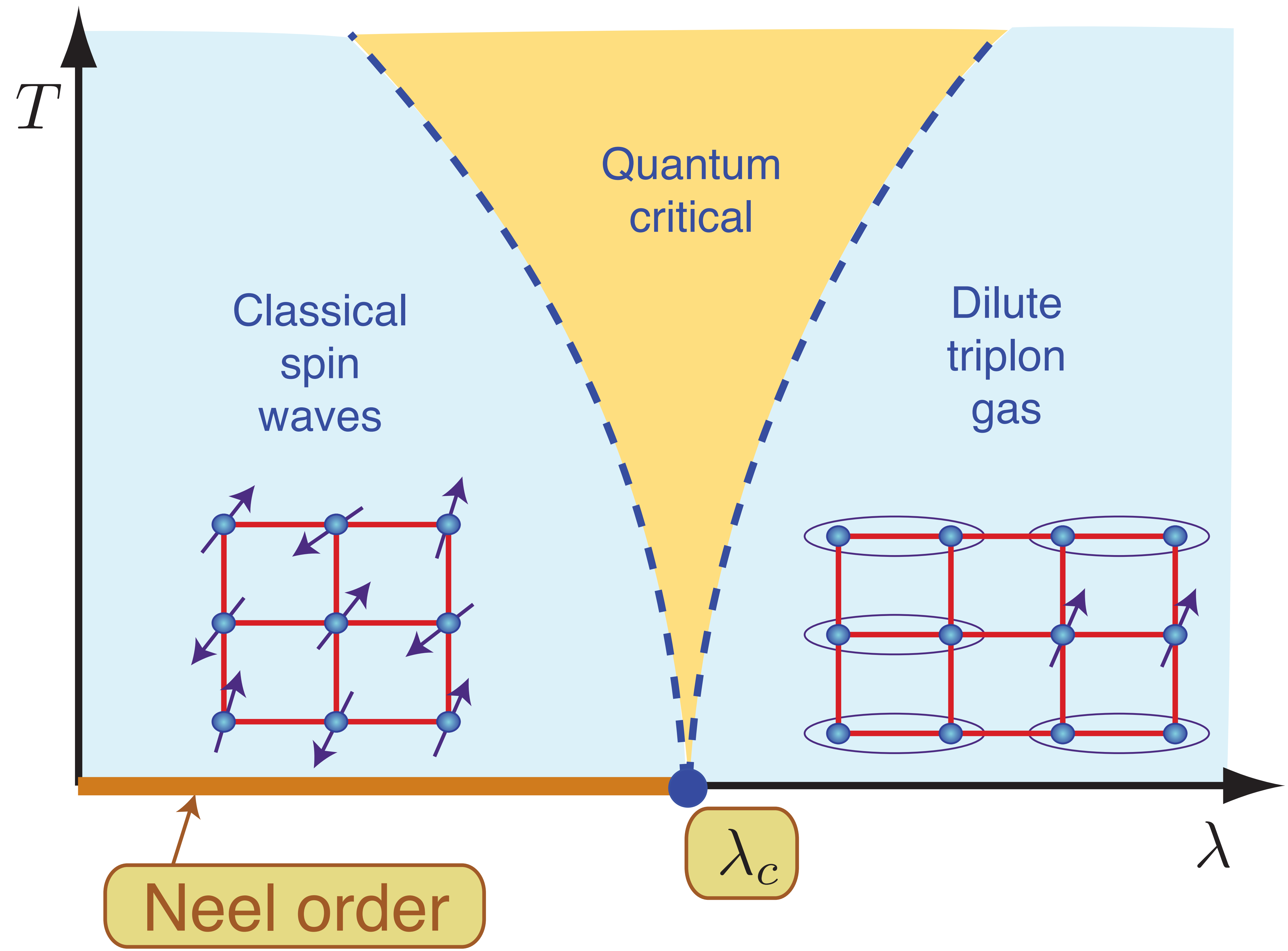

T
Quantum critical
Classical spin waves
Dilute triplon gas
Neel order
λ_c
λ

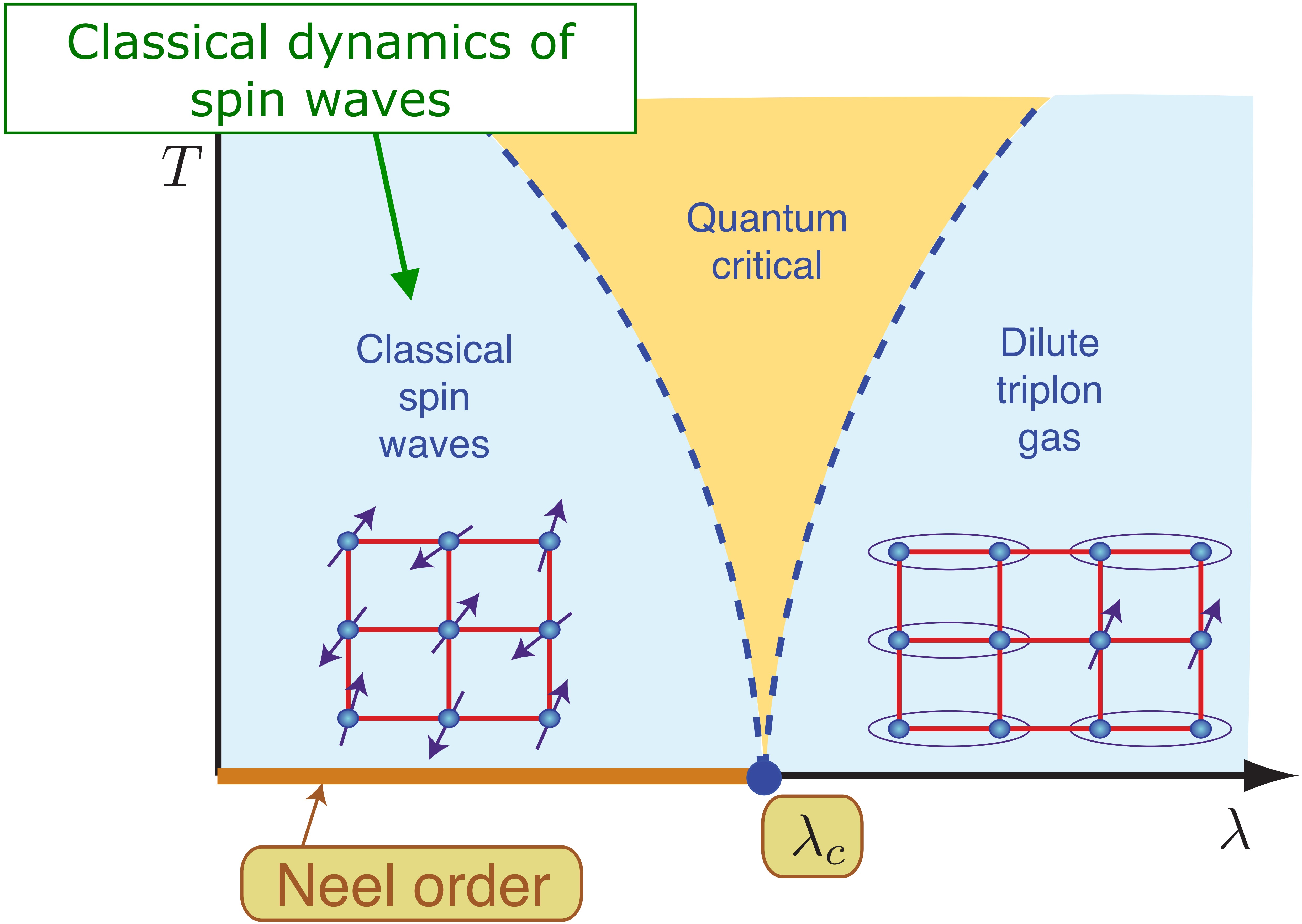
Classical dynamics of spin waves
T
Quantum critical
Classical spin waves
Dilute triplon gas
Neel order
λ_c
λ

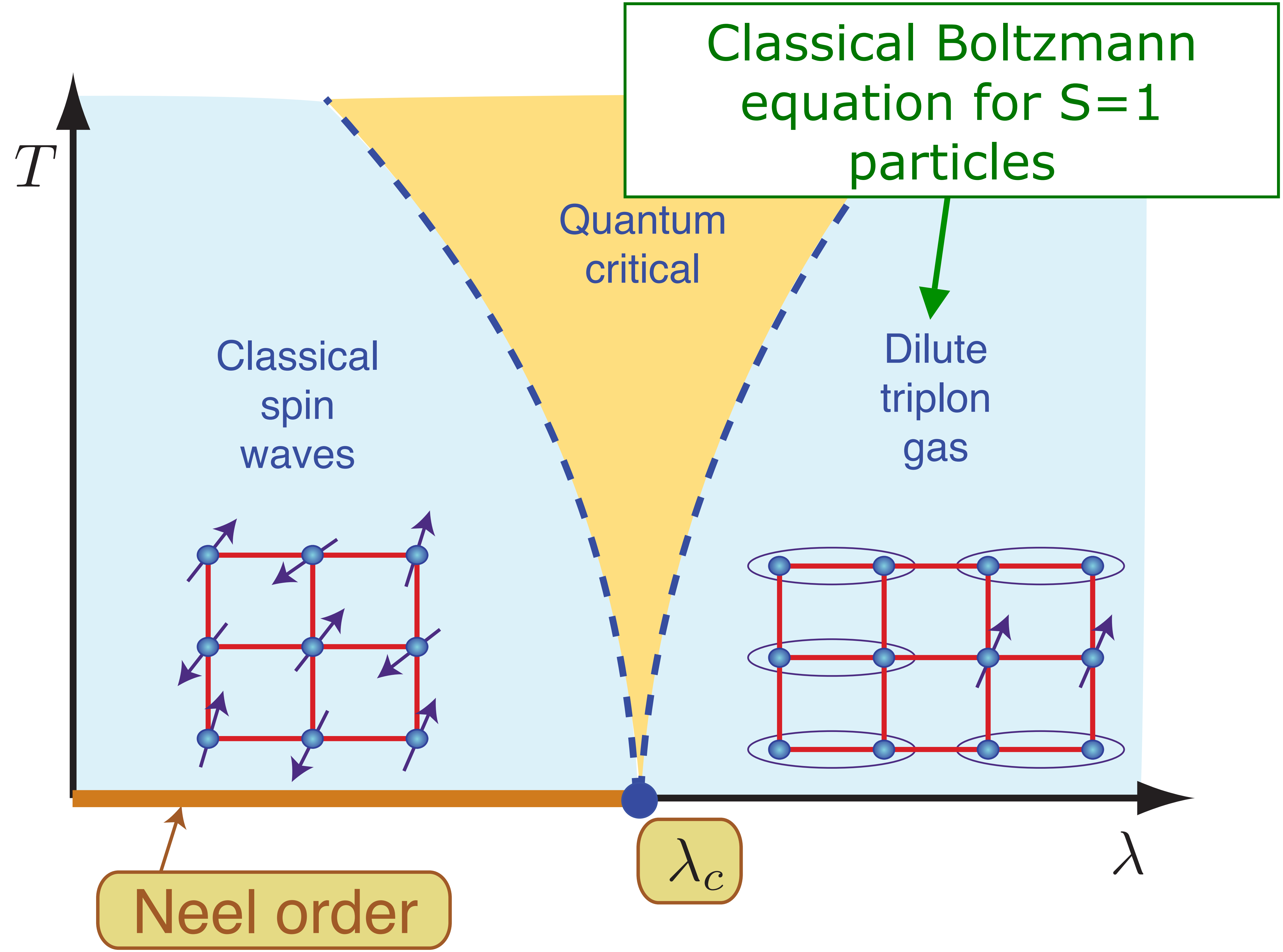

Classical Boltzmann equation for S=1 particles
T
Quantum critical
Classical spin waves
Dilute triplon gas
Neel order
λ_c
λ

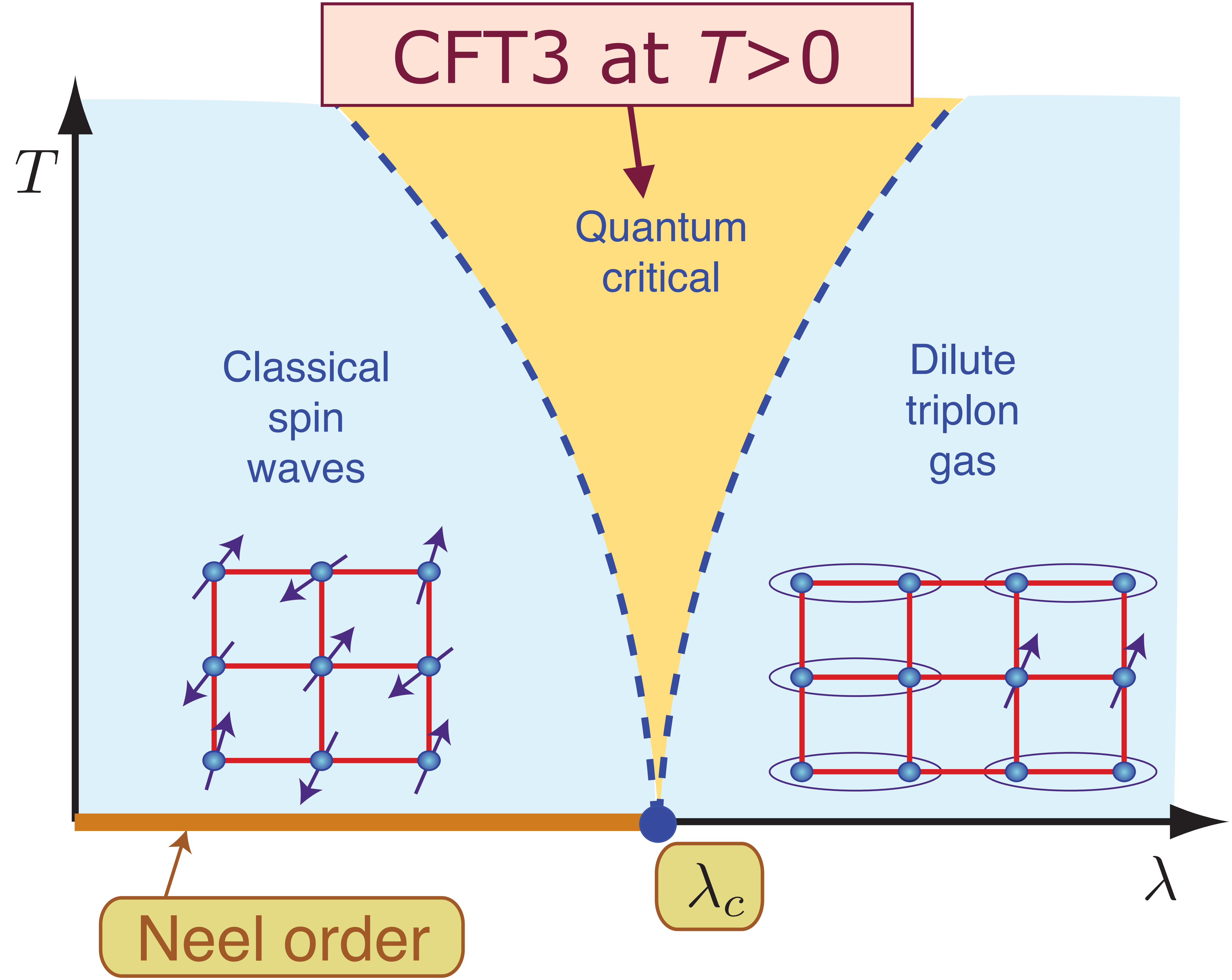
CFT3 at $T>0$
T
Quantum
critical
Classical
spin
waves
Dilute
triplon
gas
λ_c
λ
Neel order

Outline

A. "Relativistic" field theories of quantum phase transitions

1. Coupled dimer antiferromagnets
2. Triangular lattice antiferromagnets
3. Graphene
4. AdS/CFT and quantum critical transport

Outline

A. "Relativistic" field theories of quantum phase transitions

1. Coupled dimer antiferromagnets

2. Triangular lattice antiferromagnets

3. Graphene

4. AdS/CFT and quantum critical transport

X[Pd(dmit)$_2$]$_2$

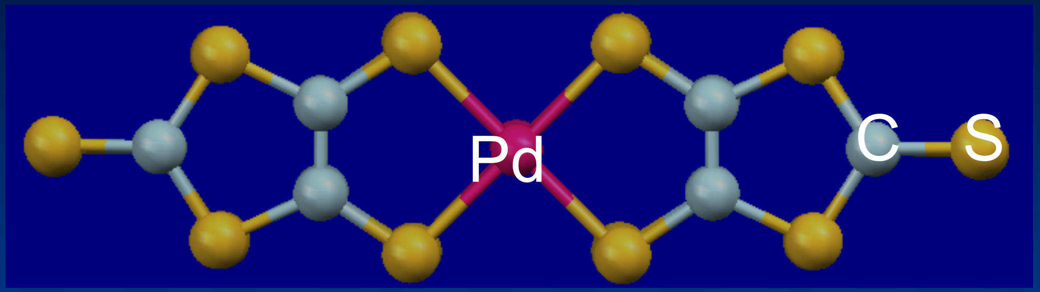

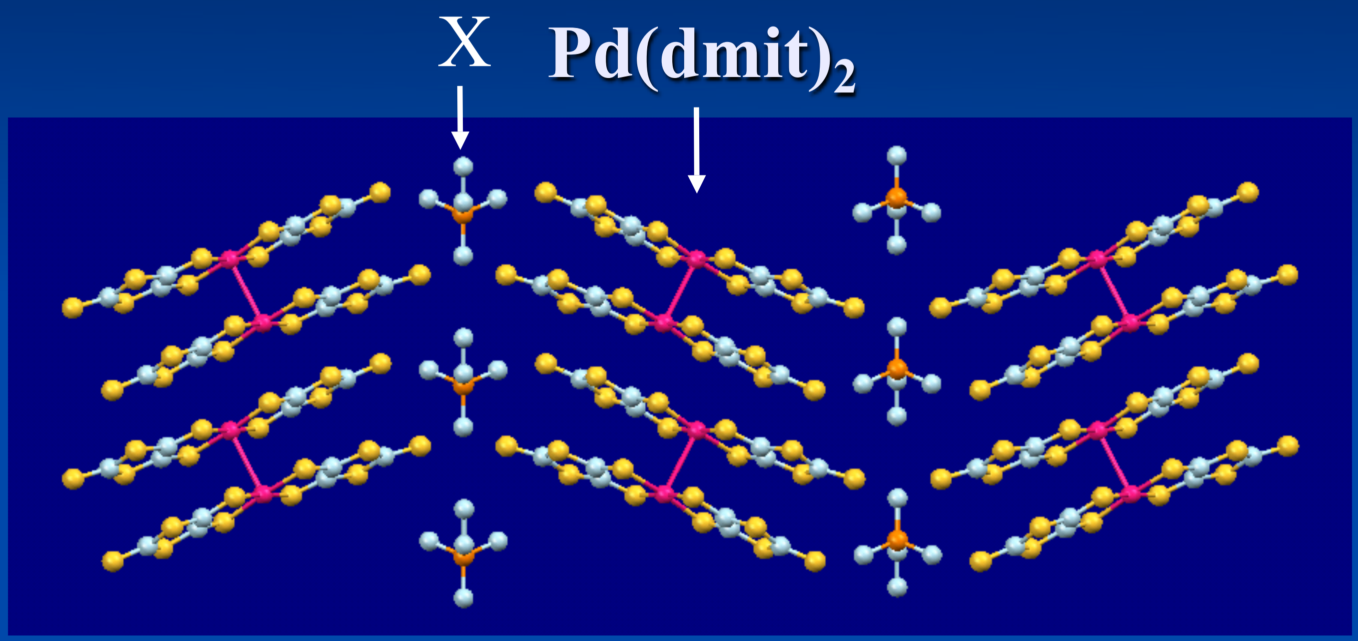

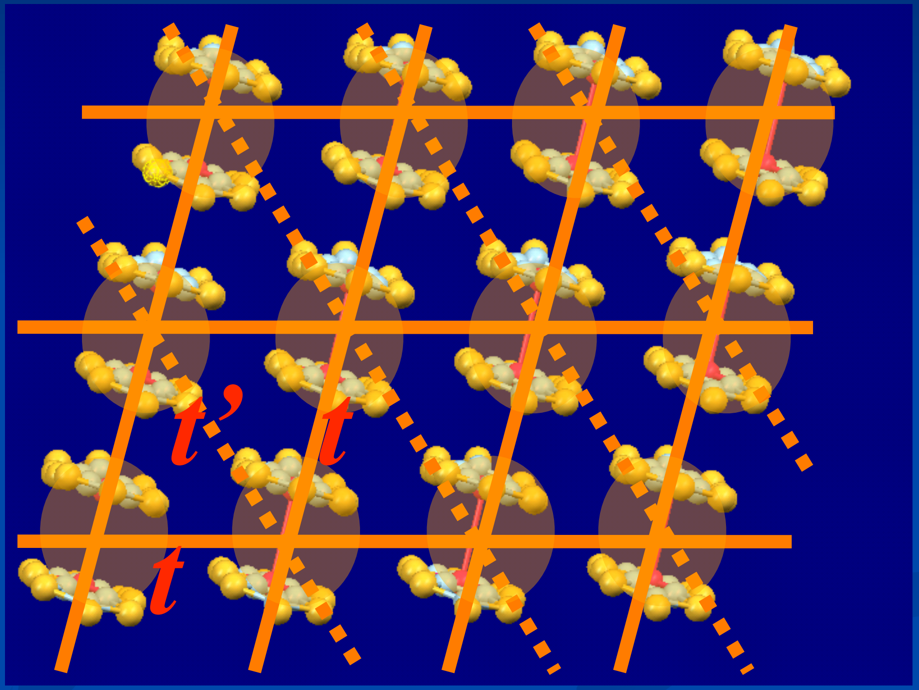

Half-filled band → Mott insulator with spin S = 1/2

Triangular lattice of [Pd(dmit)$_2$]$_2$
→ frustrated quantum spin system

Y. Shimizu, H. Akimoto, H. Tsujii, A. Tajima, and R. Kato, *J. Phys.: Condens. Matter* **19**, 145240 (2007)

$$H = \sum_{\langle ij \rangle} J_{ij} \vec{S}_i \cdot \vec{S}_j + \dots$$

$\vec{S}_i \;\Rightarrow\;$ spin operator with $S = 1/2$

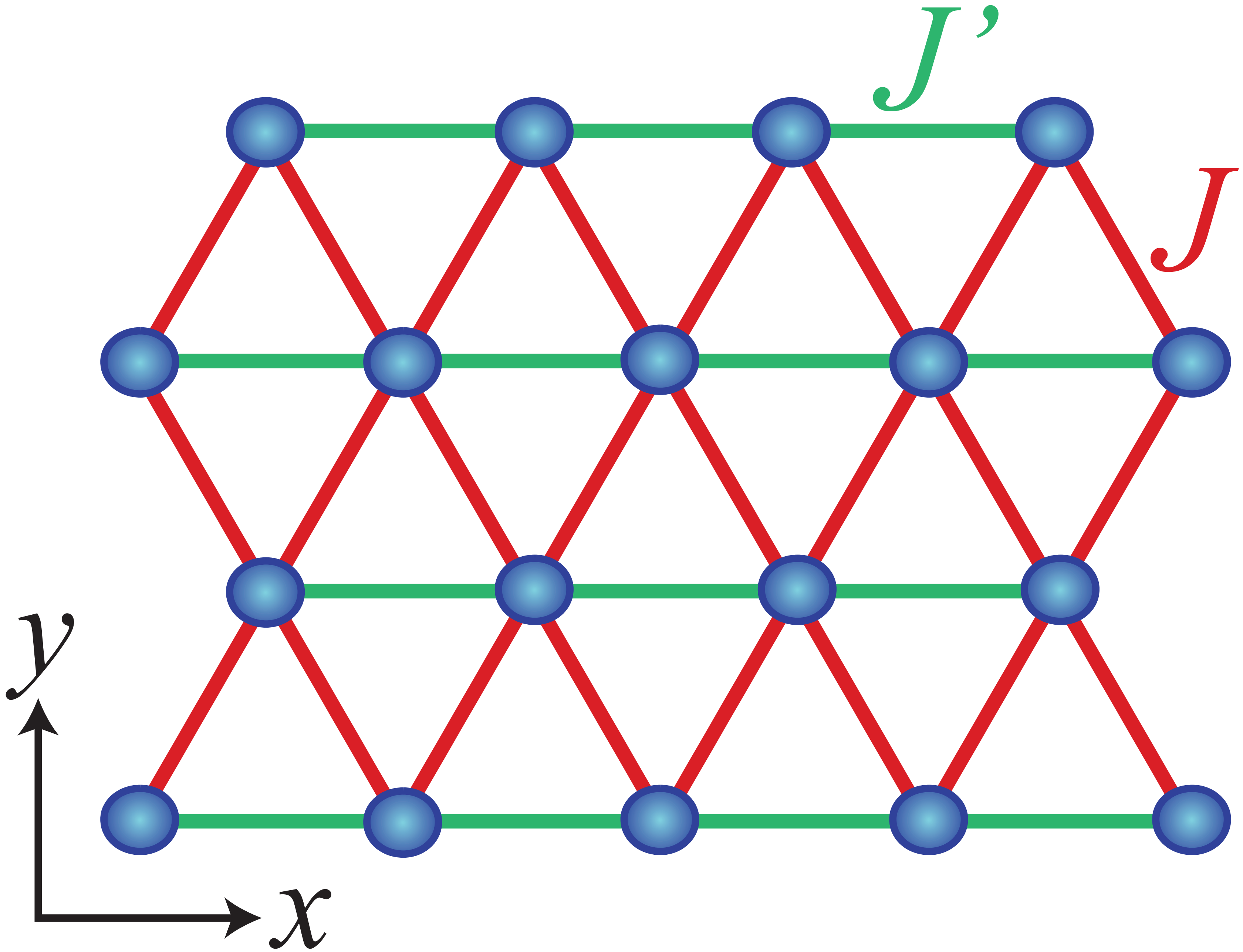

$$H = \sum_{\langle ij \rangle} J_{ij} \vec{S}_i \cdot \vec{S}_j + \ldots$$

$\vec{S}_i \;\Rightarrow\;$ spin operator with $S = 1/2$

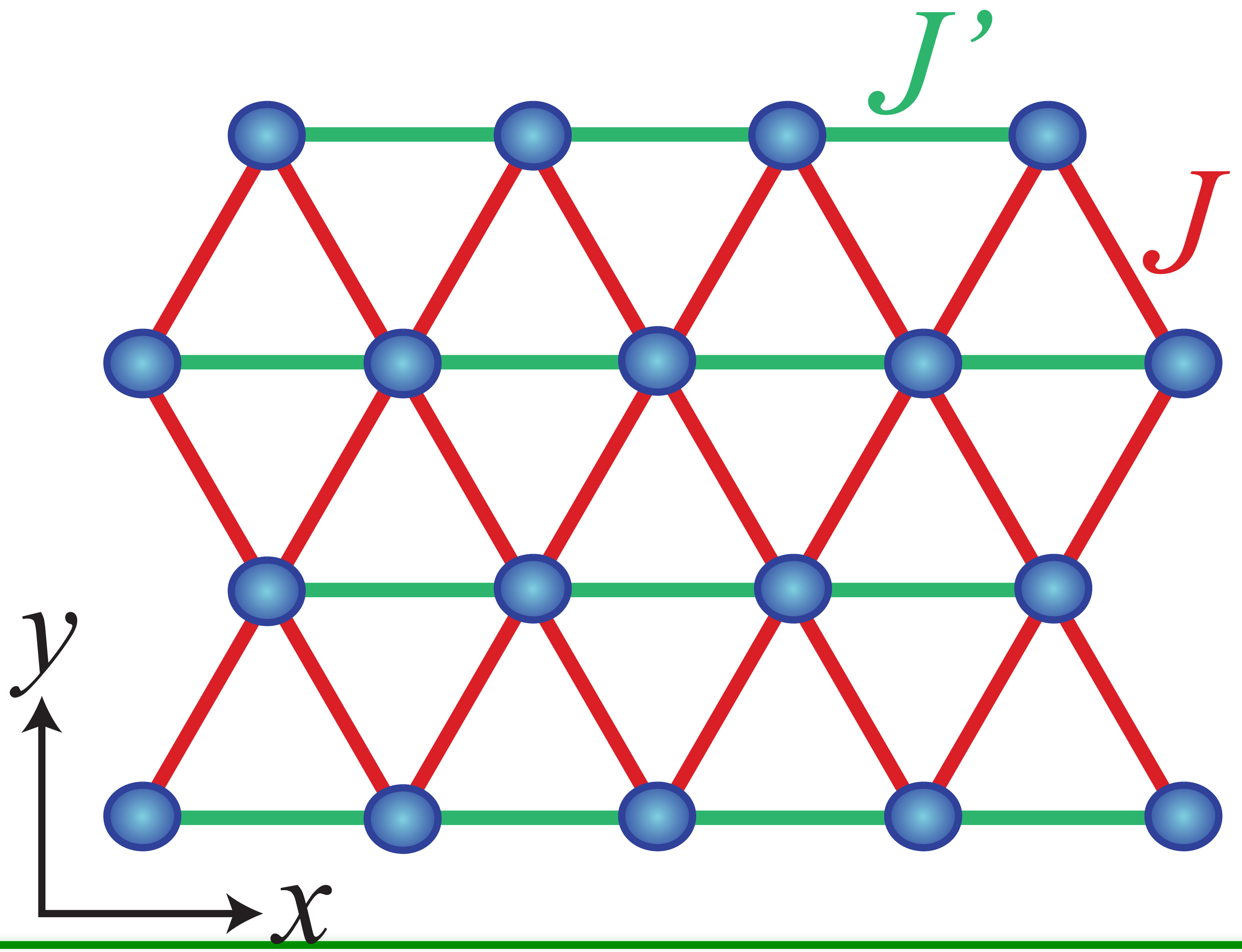

What is the ground state as a function of J'/J ?

Anisotropic triangular lattice antiferromagnet

Broken spin rotation symmetry

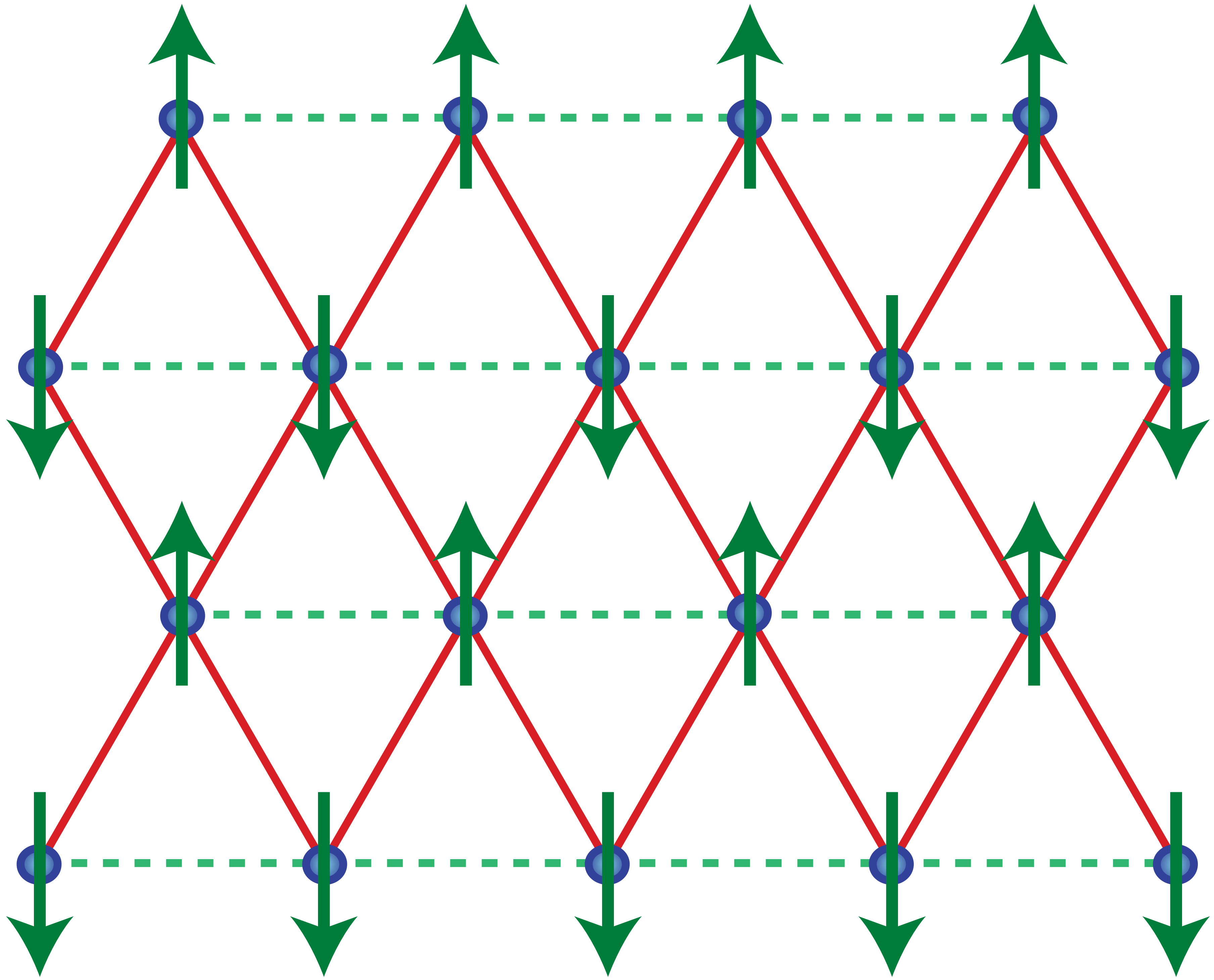

Neel ground state for small J'/J

Anisotropic triangular lattice antiferromagnet

Possible ground states as a function of J'/J

- Néel antiferromagnetic LRO

Magnetic Criticality

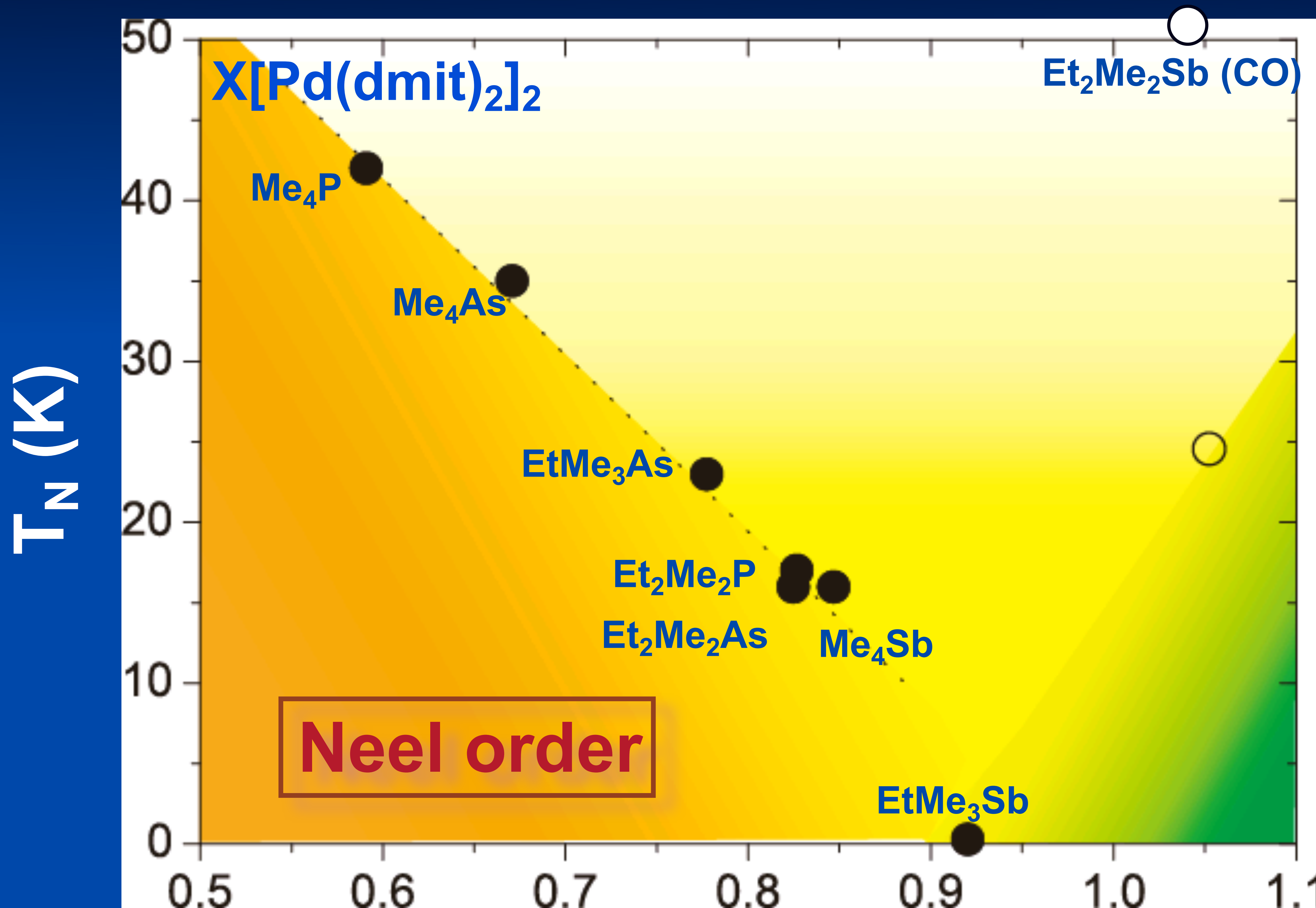

$\sqrt{J'/J}$

Y. Shimizu, H. Akimoto, H. Tsujii, A. Tajima, and R. Kato, *J. Phys.: Condens. Matter* **19**, 145240 (2007)

Anisotropic triangular lattice antiferromagnet

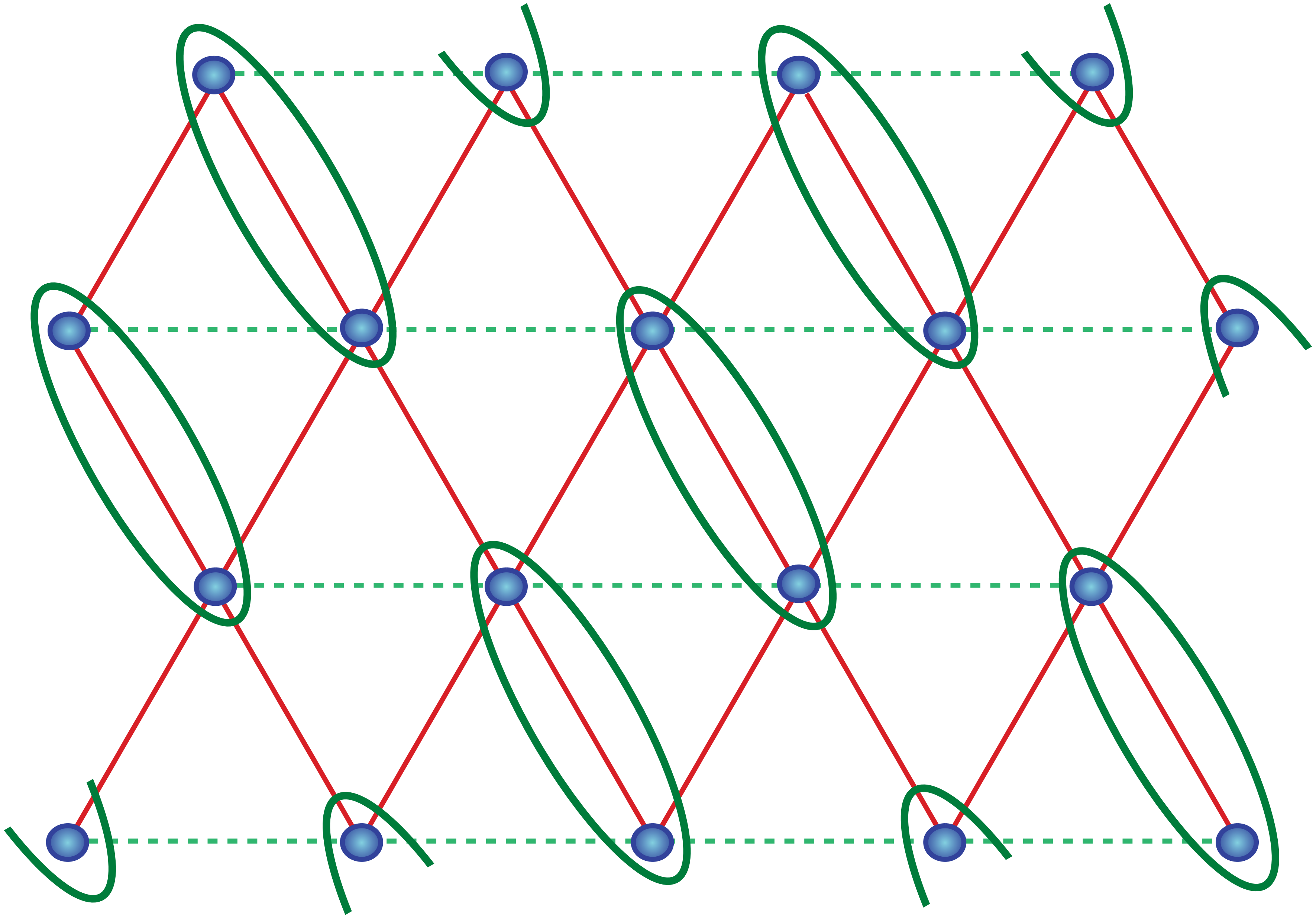

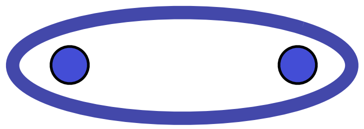

$$= \frac{(|\uparrow\downarrow\rangle - |\downarrow\uparrow\rangle)}{\sqrt{2}}$$

Possible ground state for intermediate J'/J

N. Read and S. Sachdev, *Phys. Rev. Lett.* **62**, 1694 (1989)

Anisotropic triangular lattice antiferromagnet

Broken lattice space group symmetry

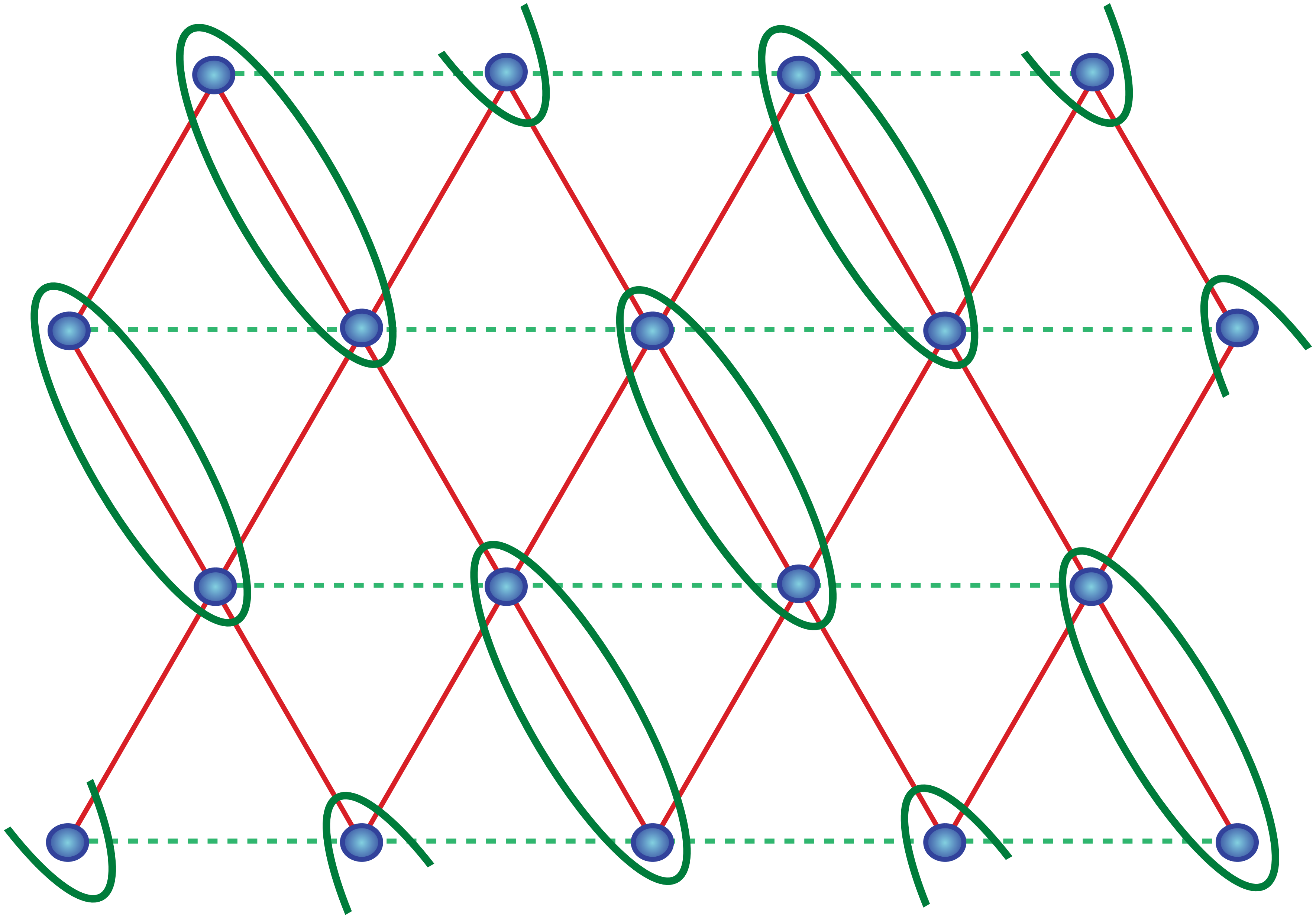

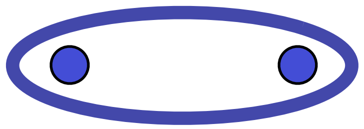

$$= \frac{(|\uparrow\downarrow\rangle - |\downarrow\uparrow\rangle)}{\sqrt{2}}$$

Valence bond solid (VBS)

Possible ground state for intermediate J'/J

N. Read and S. Sachdev, *Phys. Rev. Lett.* **62**, 1694 (1989)

Anisotropic triangular lattice antiferromagnet

Broken lattice space group symmetry

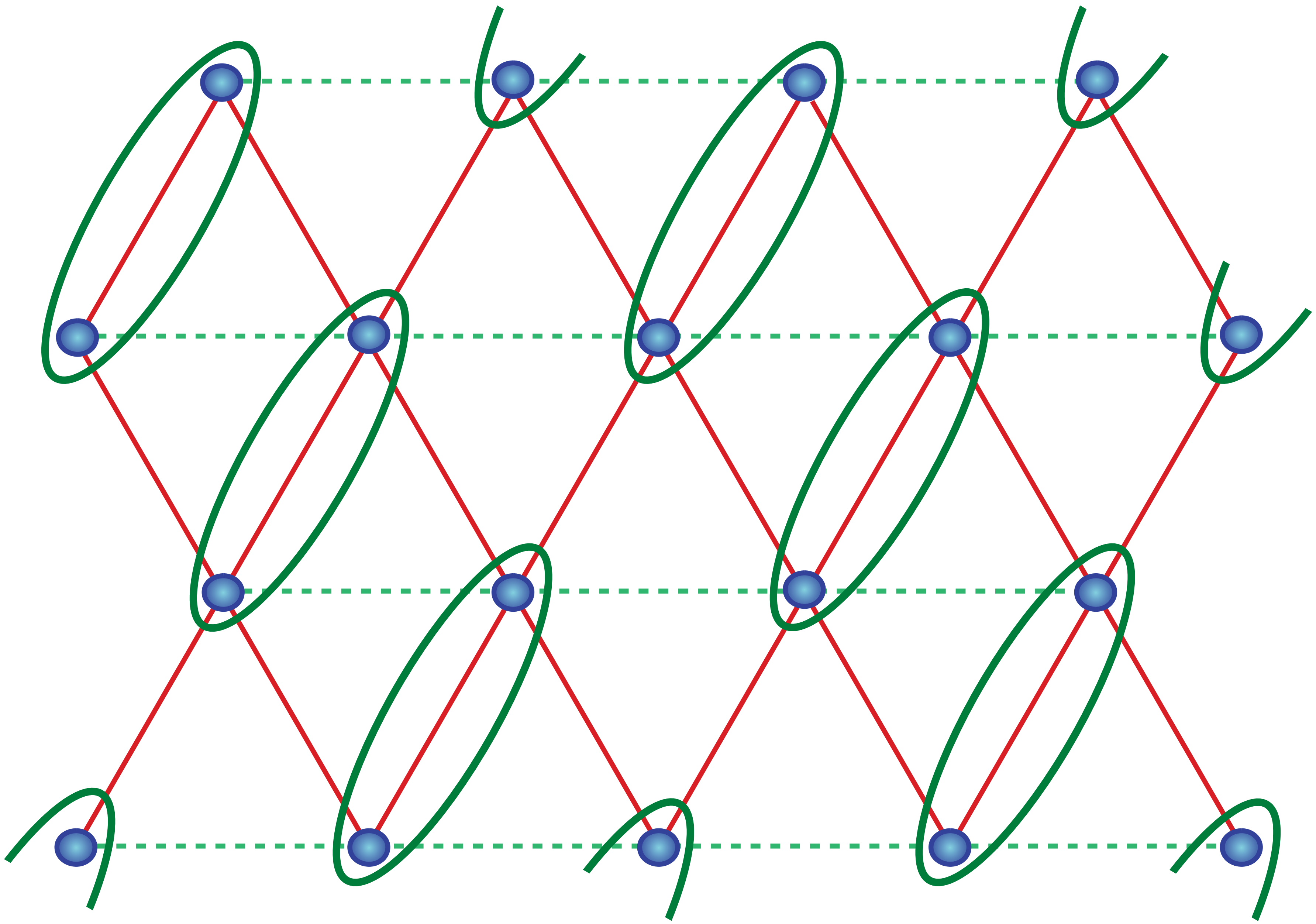

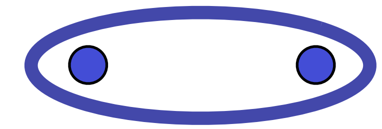

$$= \frac{\left(|\uparrow\downarrow\rangle - |\downarrow\uparrow\rangle\right)}{\sqrt{2}}$$

Valence bond solid (VBS)

Possible ground state for intermediate J'/J

N. Read and S. Sachdev, *Phys. Rev. Lett.* **62**, 1694 (1989)

Anisotropic triangular lattice antiferromagnet

Broken lattice space group symmetry

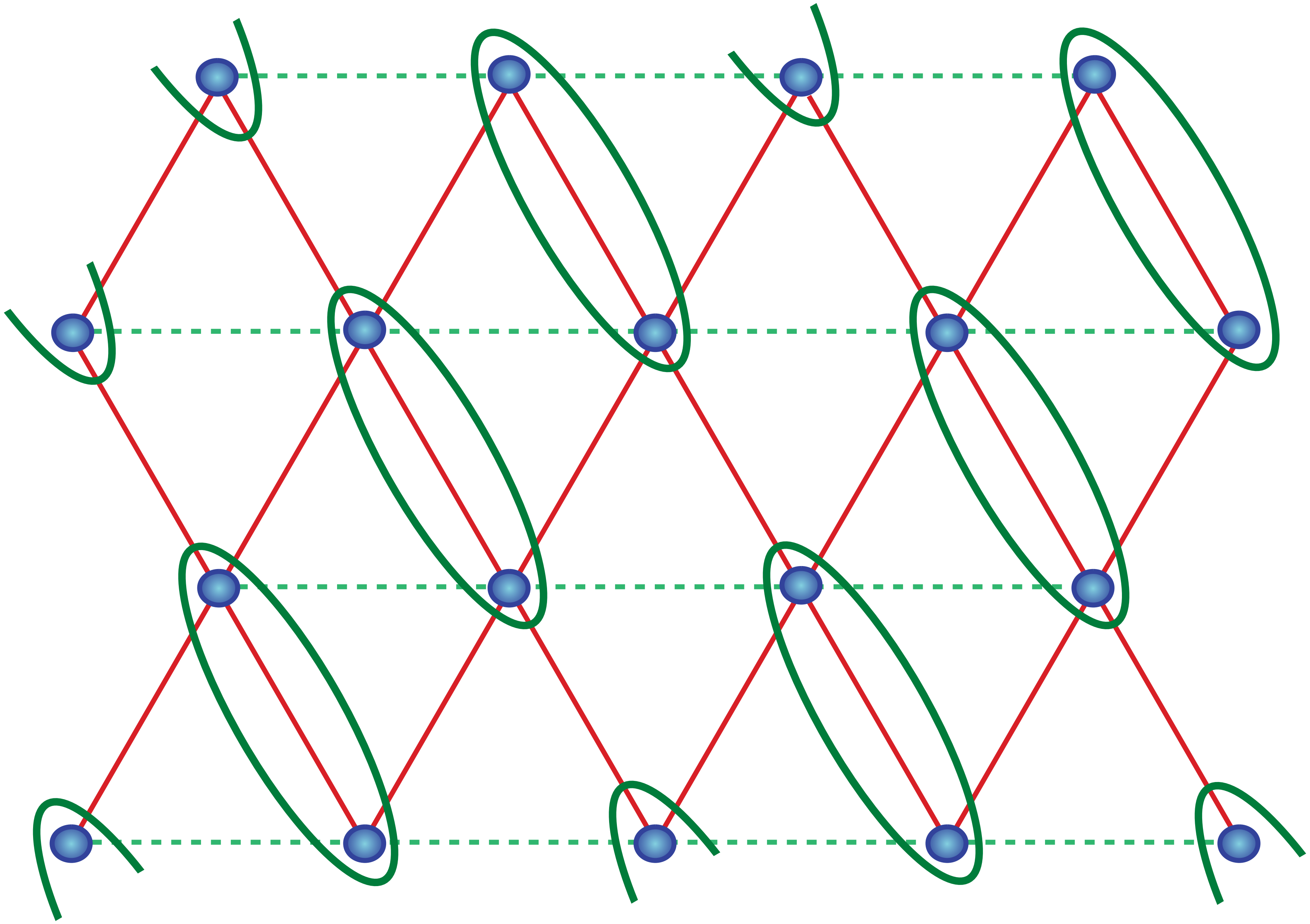

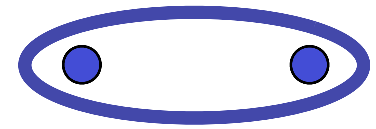

$$= \frac{(|\uparrow\downarrow\rangle - |\downarrow\uparrow\rangle)}{\sqrt{2}}$$

Valence bond solid (VBS)

Possible ground state for intermediate J'/J

N. Read and S. Sachdev, *Phys. Rev. Lett.* **62**, 1694 (1989)

Anisotropic triangular lattice antiferromagnet

Broken lattice space group symmetry

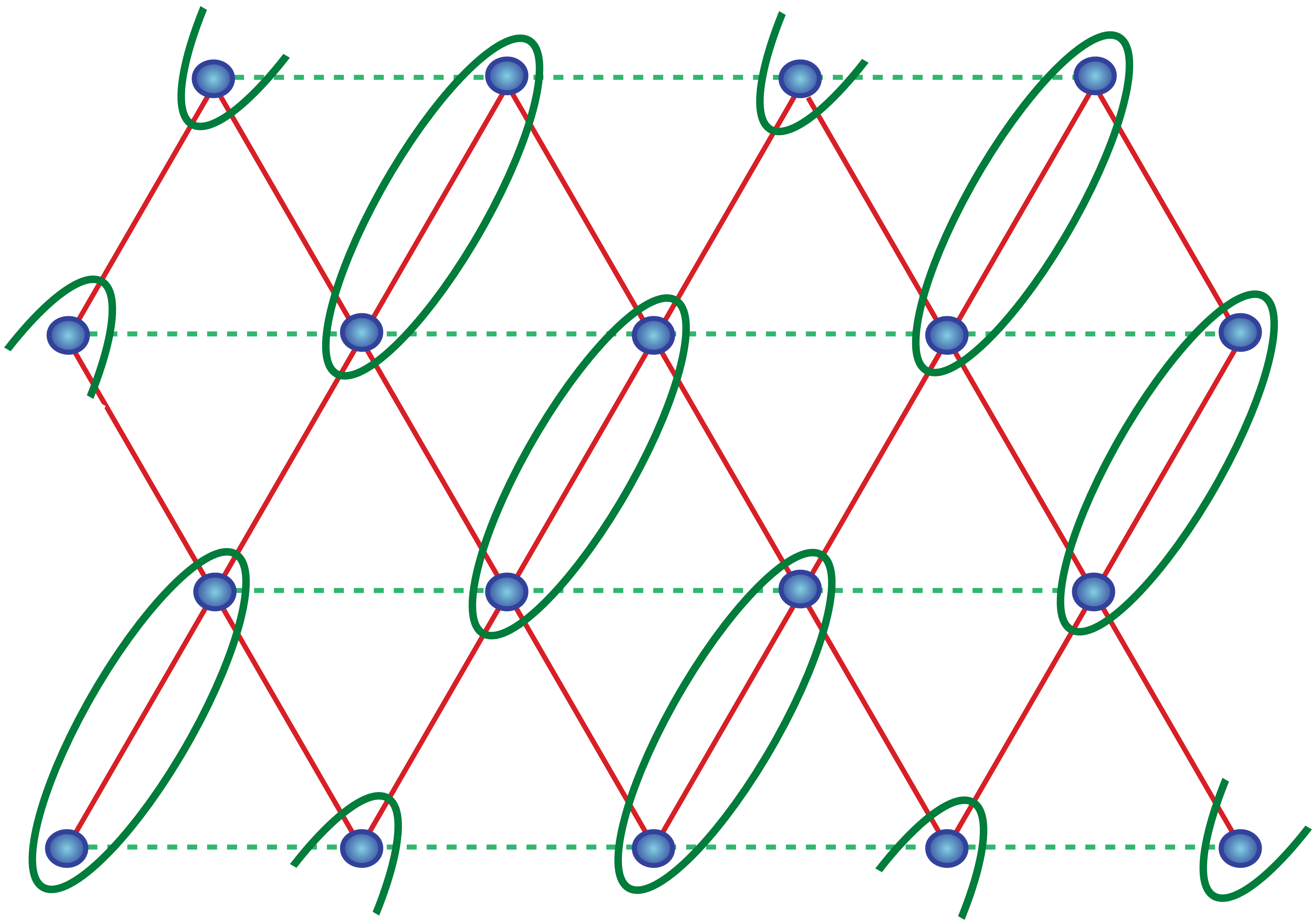

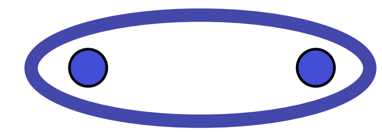

$$= \frac{(|\uparrow\downarrow\rangle - |\downarrow\uparrow\rangle)}{\sqrt{2}}$$

Valence bond solid (VBS)

Possible ground state for intermediate *J'/J*

N. Read and S. Sachdev, *Phys. Rev. Lett.* **62**, 1694 (1989)

Anisotropic triangular lattice antiferromagnet

Possible ground states as a function of J'/J

- Néel antiferromagnetic LRO

- Valence bond solid

Magnetic Criticality

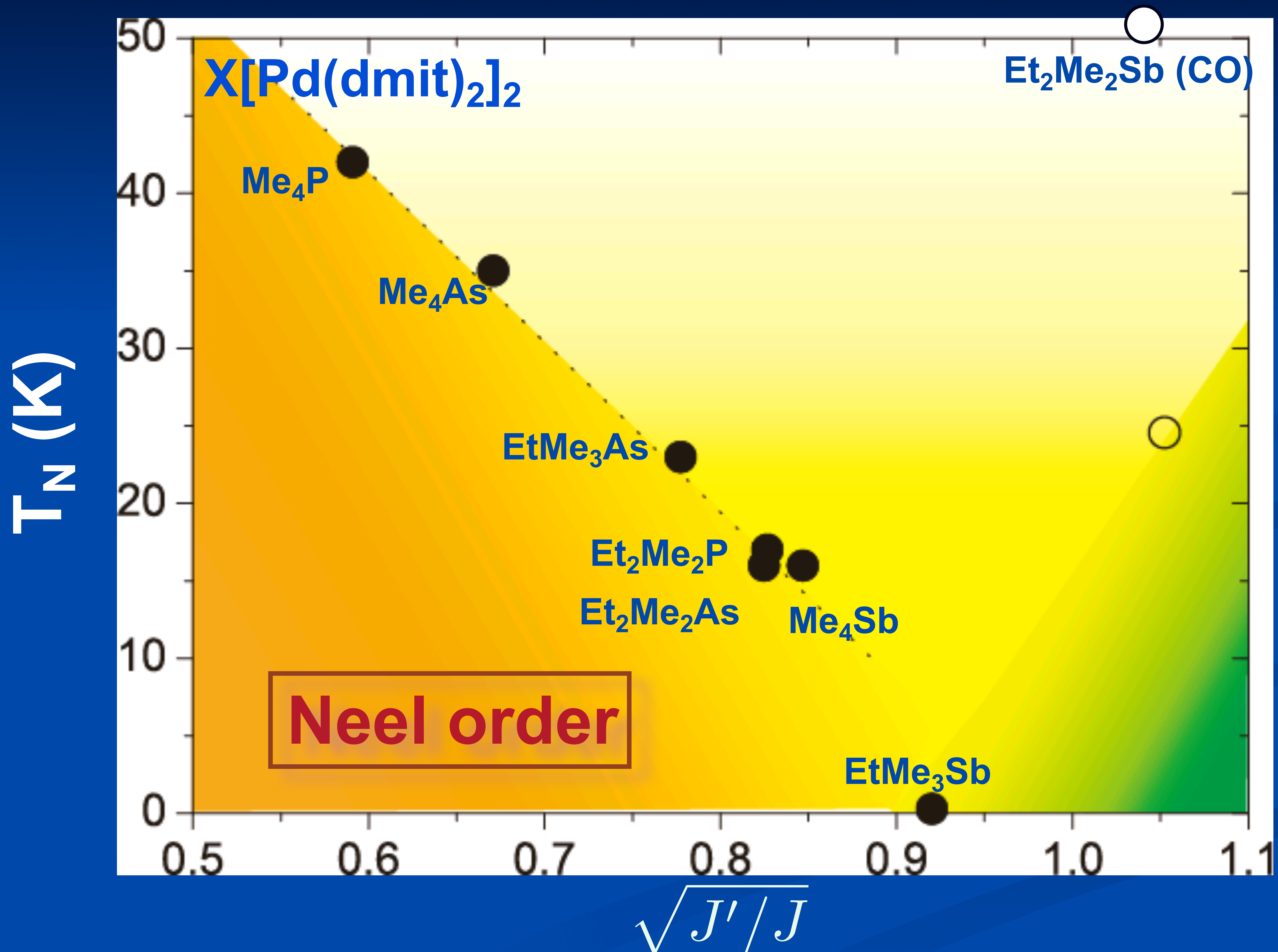

Y. Shimizu, H. Akimoto, H. Tsujii, A. Tajima, and R. Kato, *J. Phys.: Condens. Matter* **19**, 145240 (2007)

Magnetic Criticality

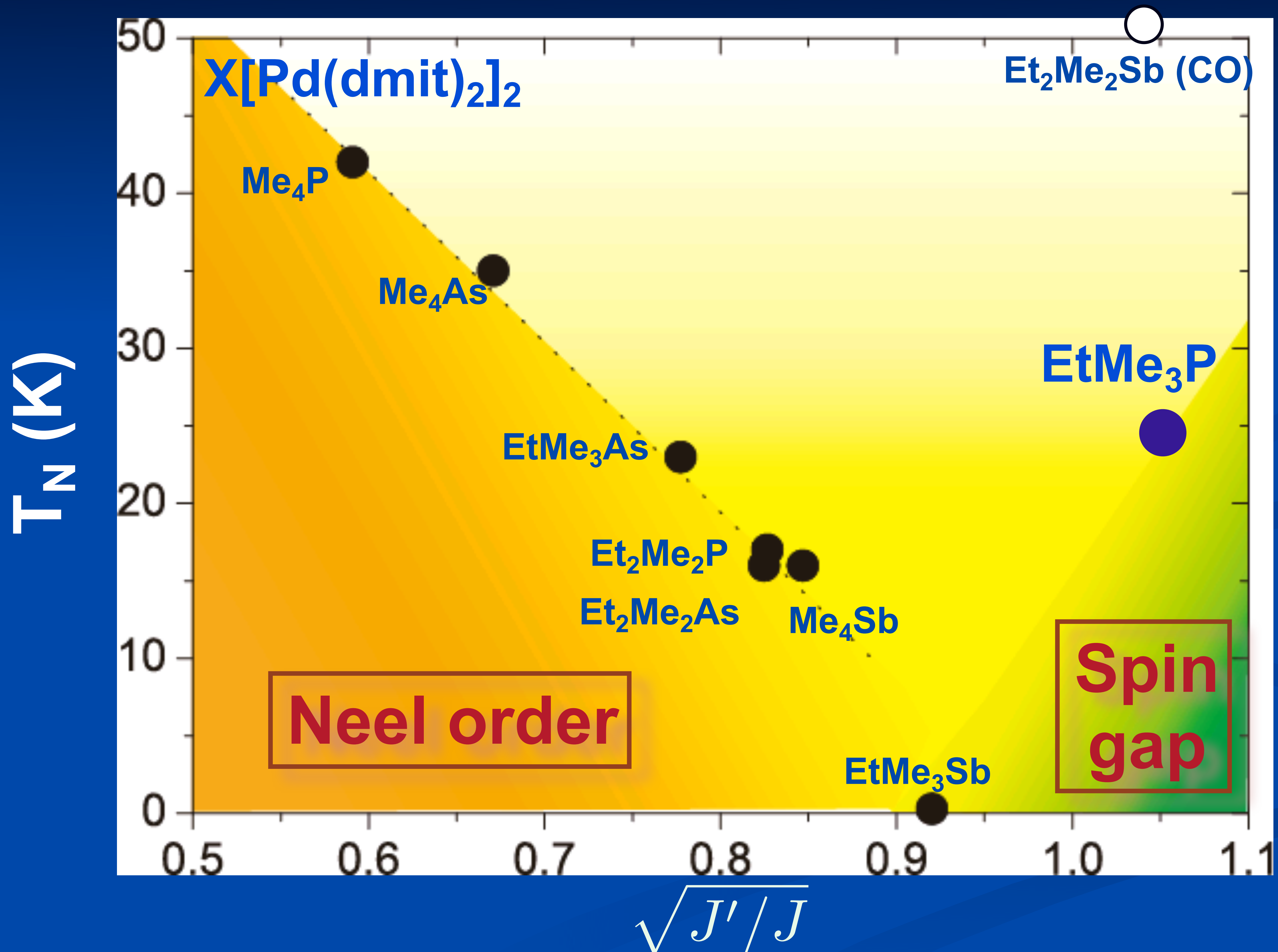

Y. Shimizu, H. Akimoto, H. Tsujii, A. Tajima, and R. Kato, *J. Phys.: Condens. Matter* **19**, 145240 (2007)

Magnetic Criticality

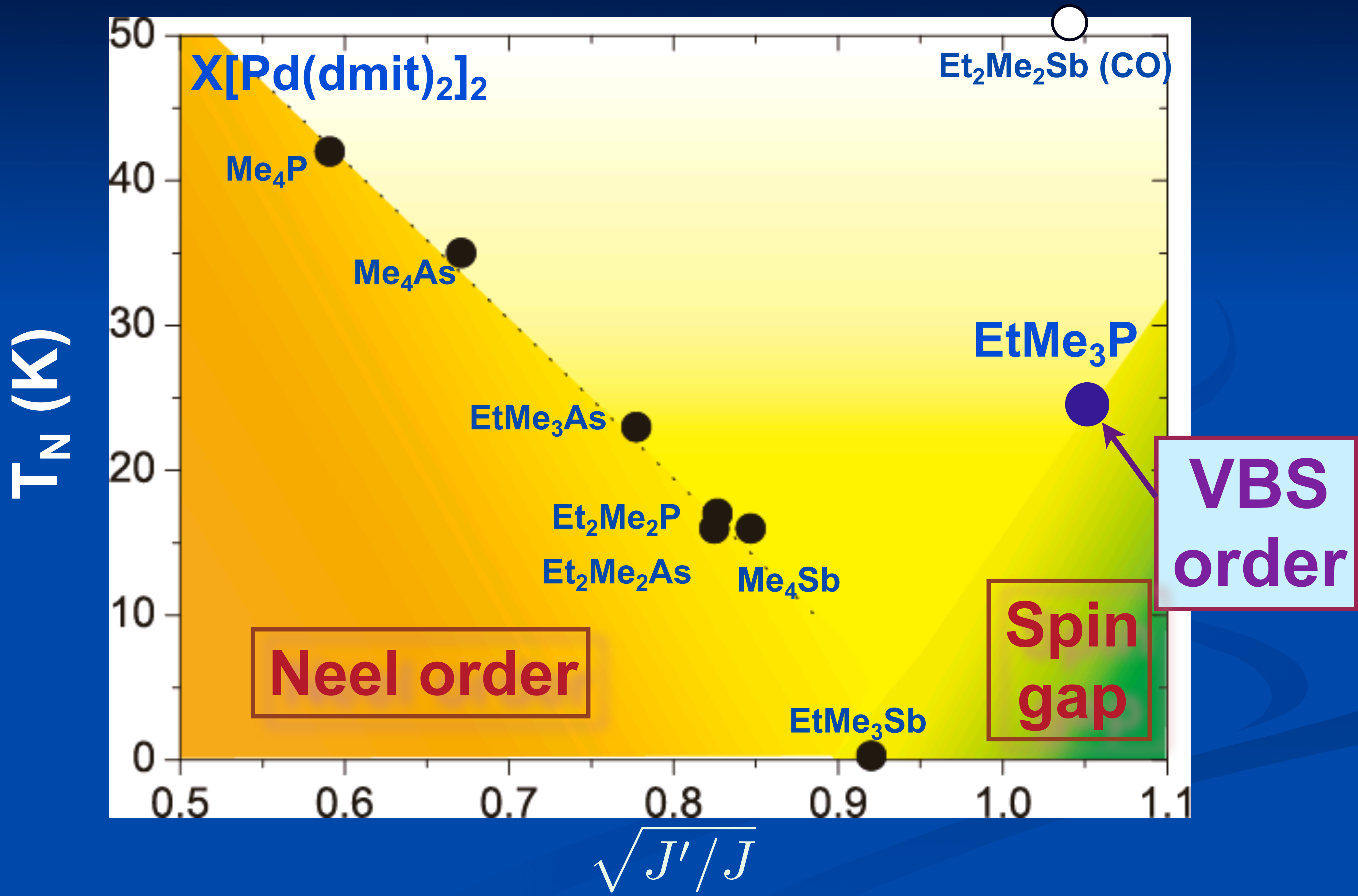

Y. Shimizu, H. Akimoto, H. Tsujii, A. Tajima, and R. Kato, *J. Phys.: Condens. Matter* **19**, 145240 (2007)

Observation of a valence bond solid (VBS) in $ETMe_3P[Pd(dmit)_2]_2$

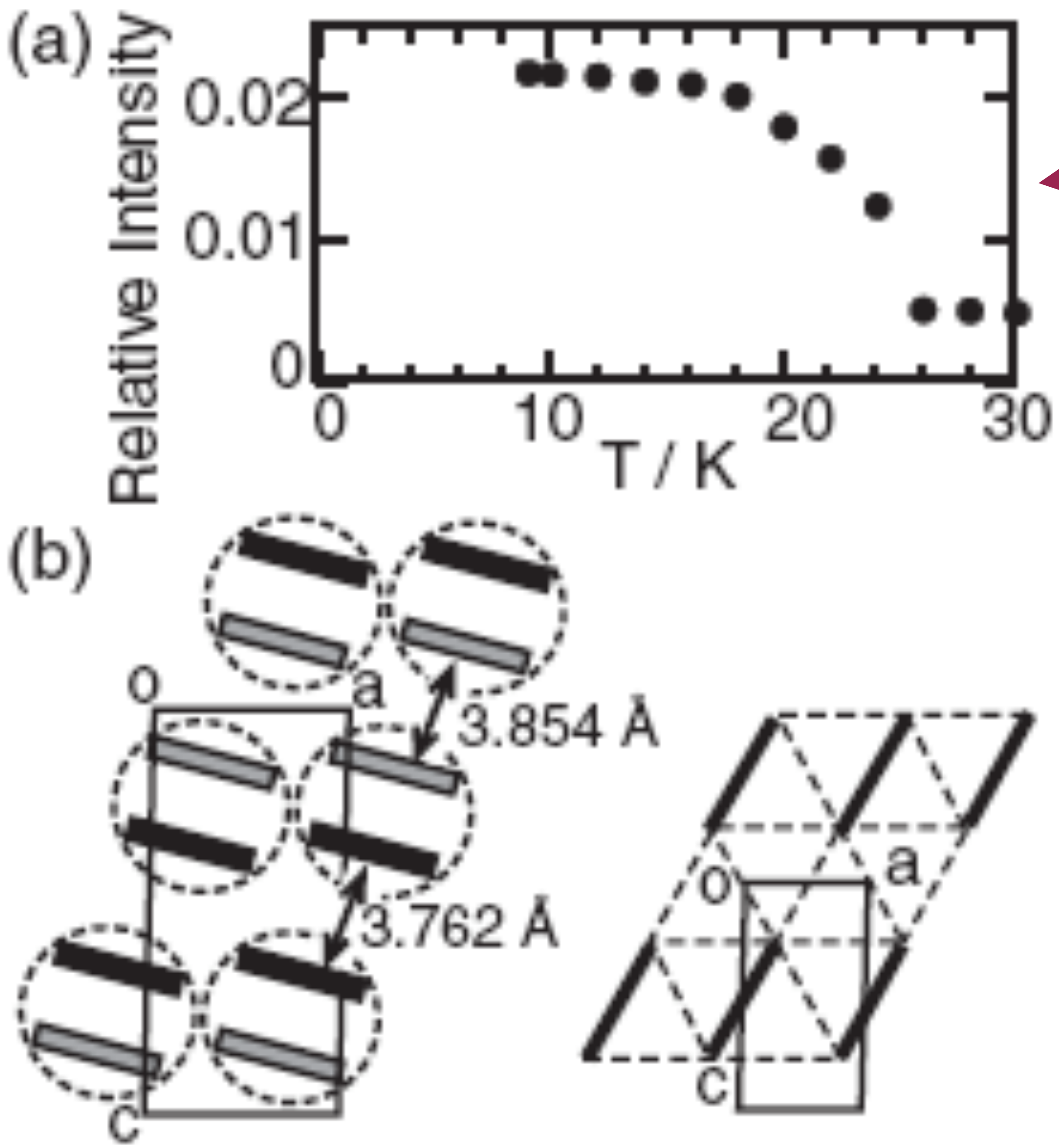

X-ray scattering

Spin gap ~ 40 K
J ~ 250 K

M. Tamura, A. Nakao and R. Kato, *J. Phys. Soc. Japan* **75**, 093701 (2006)
Y. Shimizu, H. Akimoto, H. Tsujii, A. Tajima, and R. Kato, *Phys. Rev. Lett.* **99**, 256403 (2007)

Magnetic Criticality

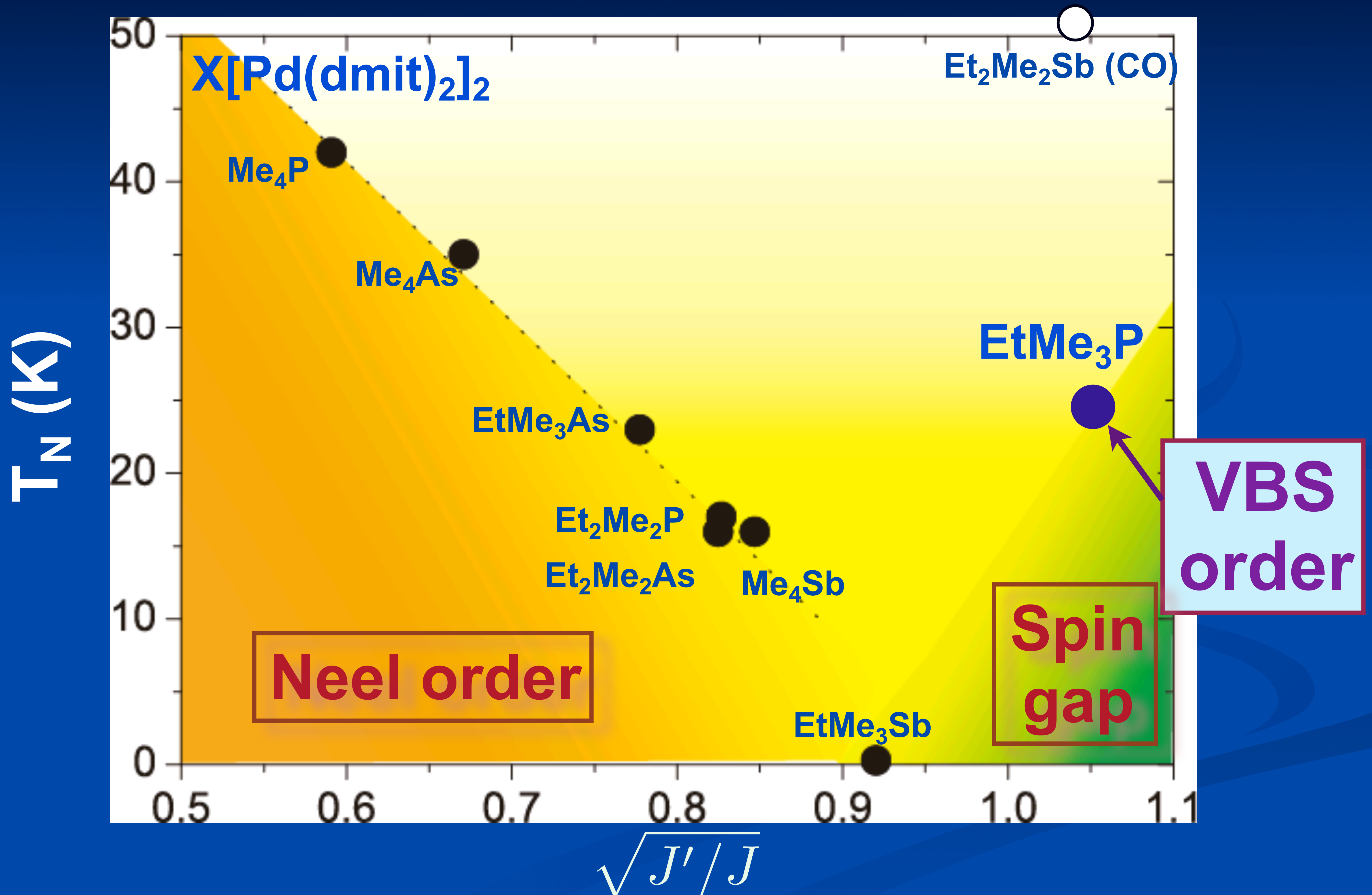

Y. Shimizu, H. Akimoto, H. Tsujii, A. Tajima, and R. Kato, *J. Phys.: Condens. Matter* **19**, 145240 (2007)

Anisotropic triangular lattice antiferromagnet

Possible ground states as a function of J'/J

- Néel antiferromagnetic LRO
- Valence bond solid

Anisotropic triangular lattice antiferromagnet

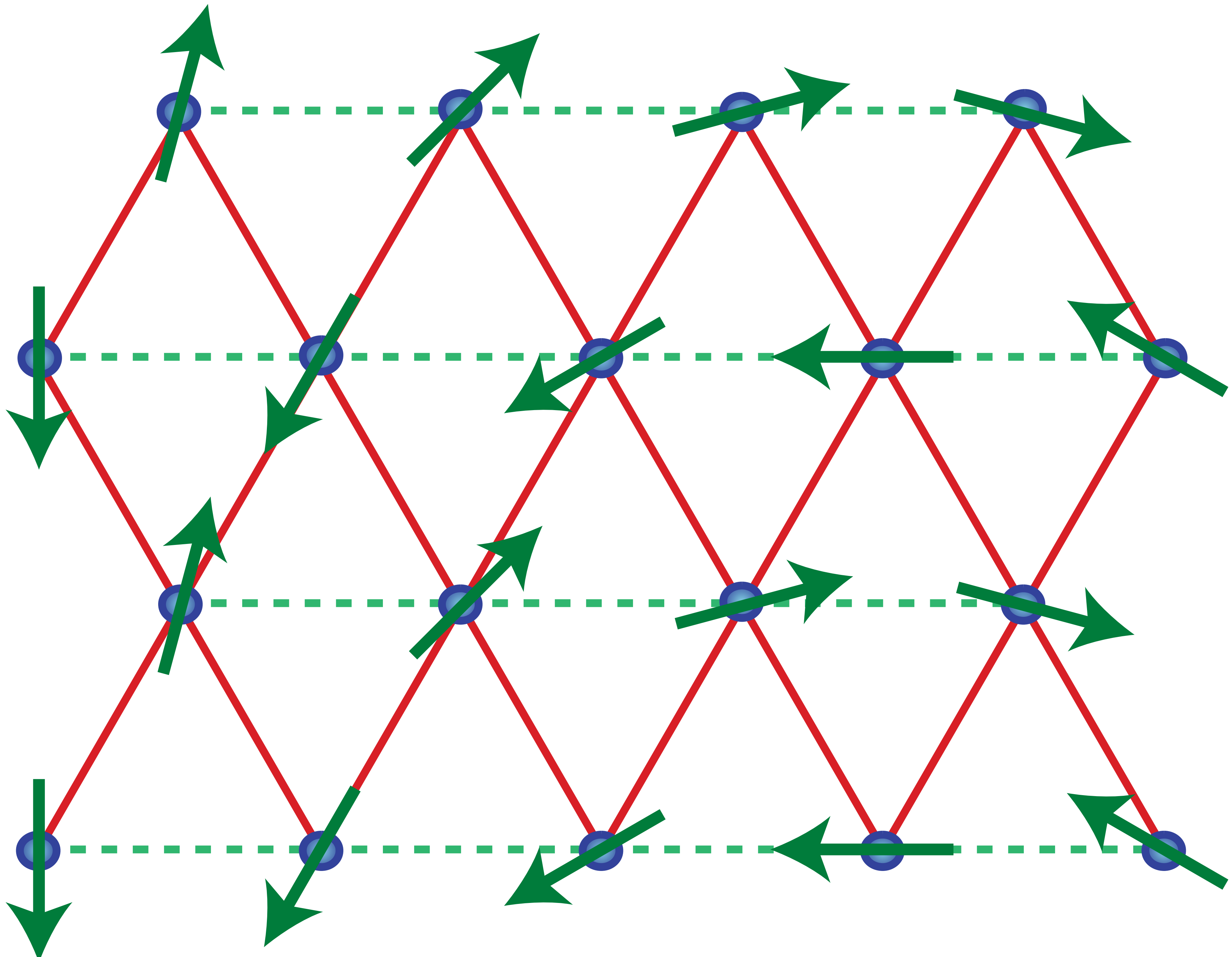

Classical ground state for large J'/J

Found in Cs_2CuCl_4

Anisotropic triangular lattice antiferromagnet

Possible ground states as a function of J'/J

- Néel antiferromagnetic LRO
- Valence bond solid
- Spiral LRO

Anisotropic triangular lattice antiferromagnet

Possible ground states as a function of J'/J

- Néel antiferromagnetic LRO
- Valence bond solid
- Spiral LRO
- Z_2 spin liquid: preserves all symmetries of Hamiltonian

Triangular lattice antiferromagnet

Spin liquid obtained in a generalized spin model with *S*=1/2 per unit cell

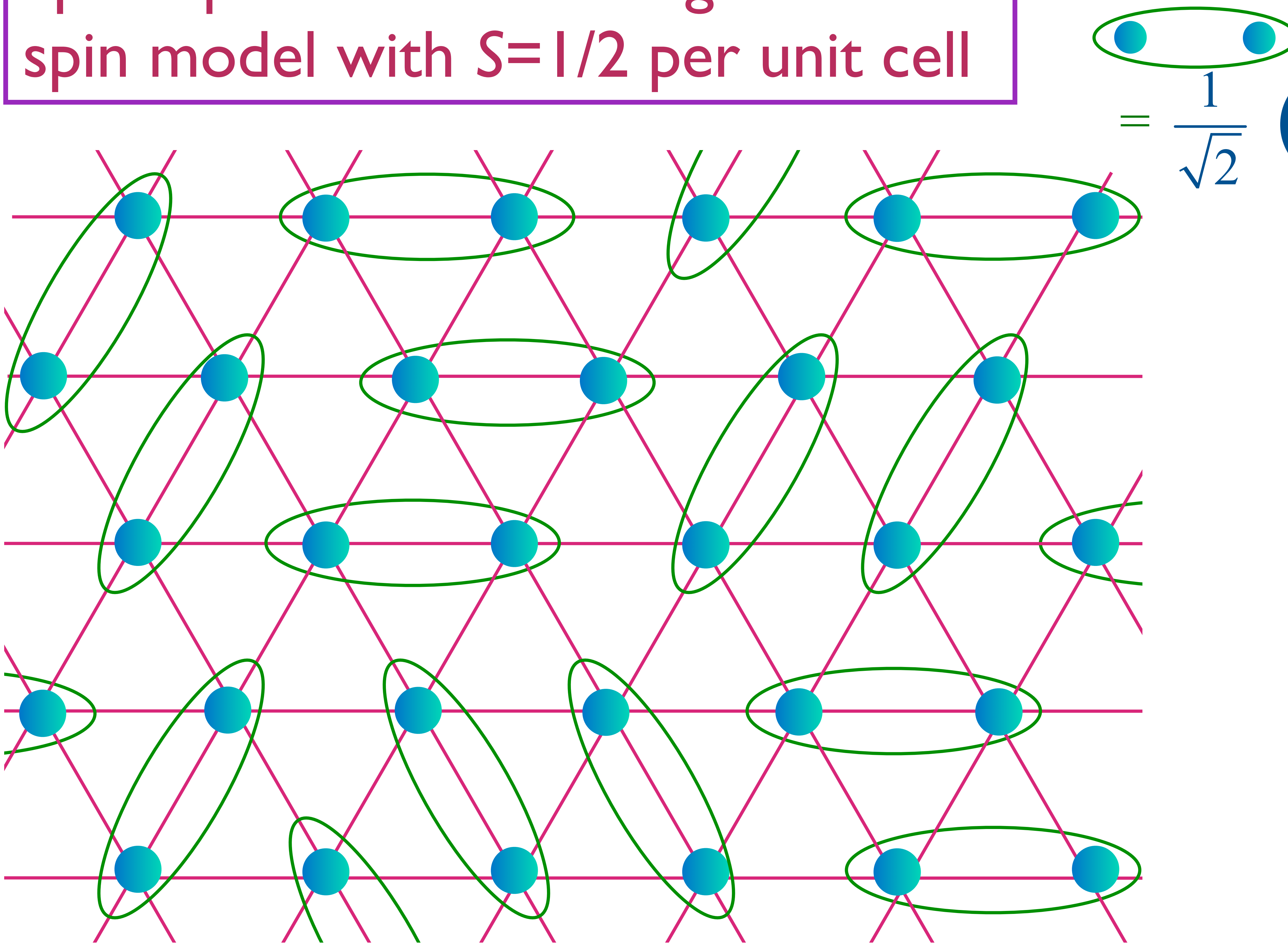

$$= \frac{1}{\sqrt{2}}\Big(|\uparrow\downarrow\rangle - |\downarrow\uparrow\rangle \Big)$$

P. Fazekas and P. W. Anderson, *Philos. Mag.* **30**, 23 (1974).

Triangular lattice antiferromagnet

Spin liquid obtained in a generalized spin model with S=1/2 per unit cell

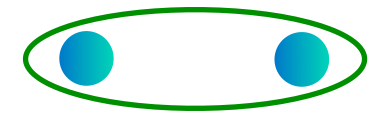

$$= \frac{1}{\sqrt{2}} \Big(|\uparrow\downarrow\rangle - |\downarrow\uparrow\rangle \Big)$$

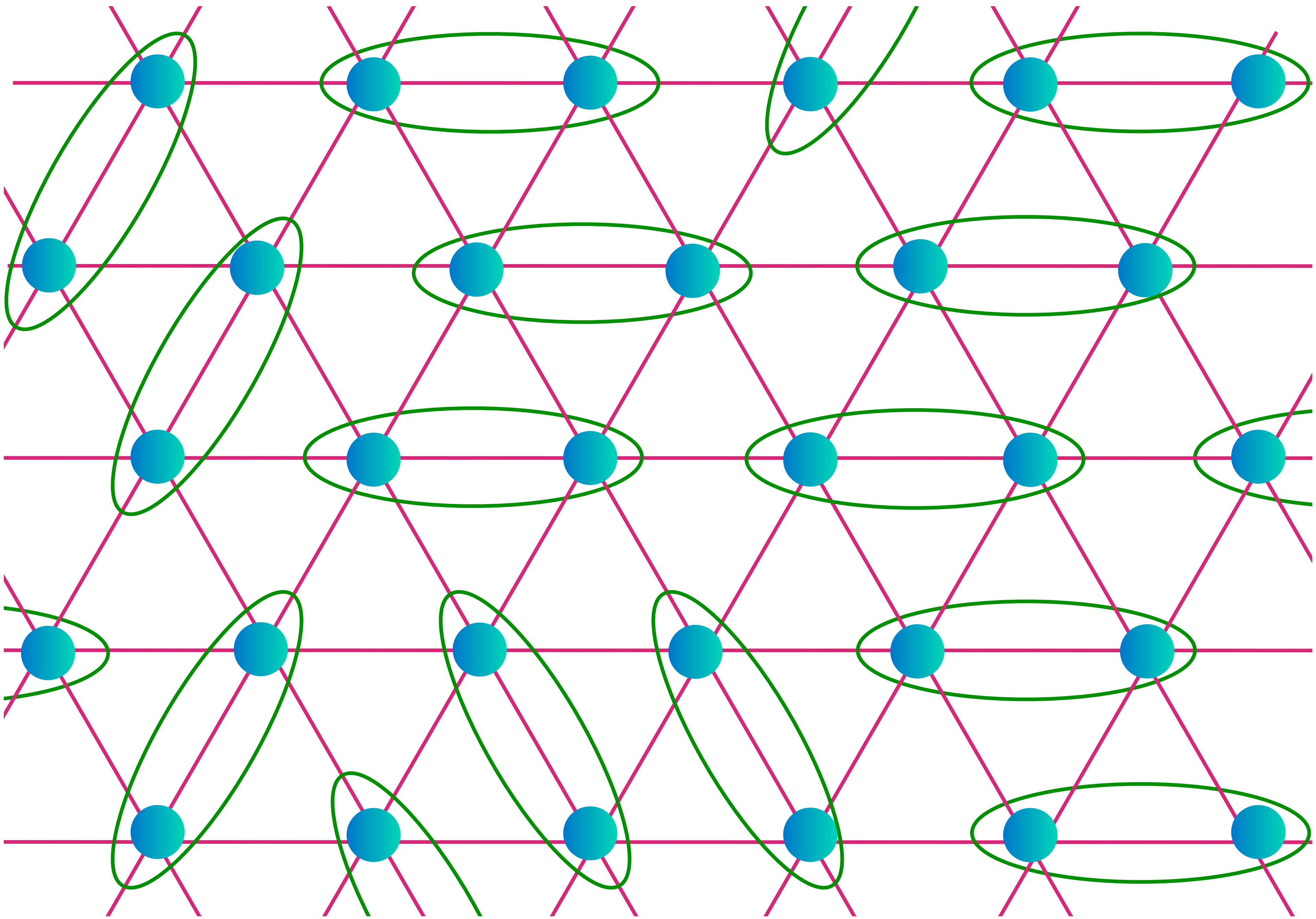

P. Fazekas and P. W. Anderson, *Philos. Mag.* **30**, 23 (1974).

Triangular lattice antiferromagnet

Spin liquid obtained in a generalized spin model with S=1/2 per unit cell

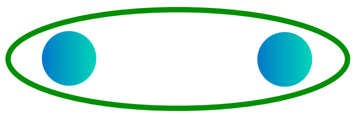

$$= \frac{1}{\sqrt{2}} \Big(\left| \uparrow \downarrow \right\rangle - \left| \downarrow \uparrow \right\rangle \Big)$$

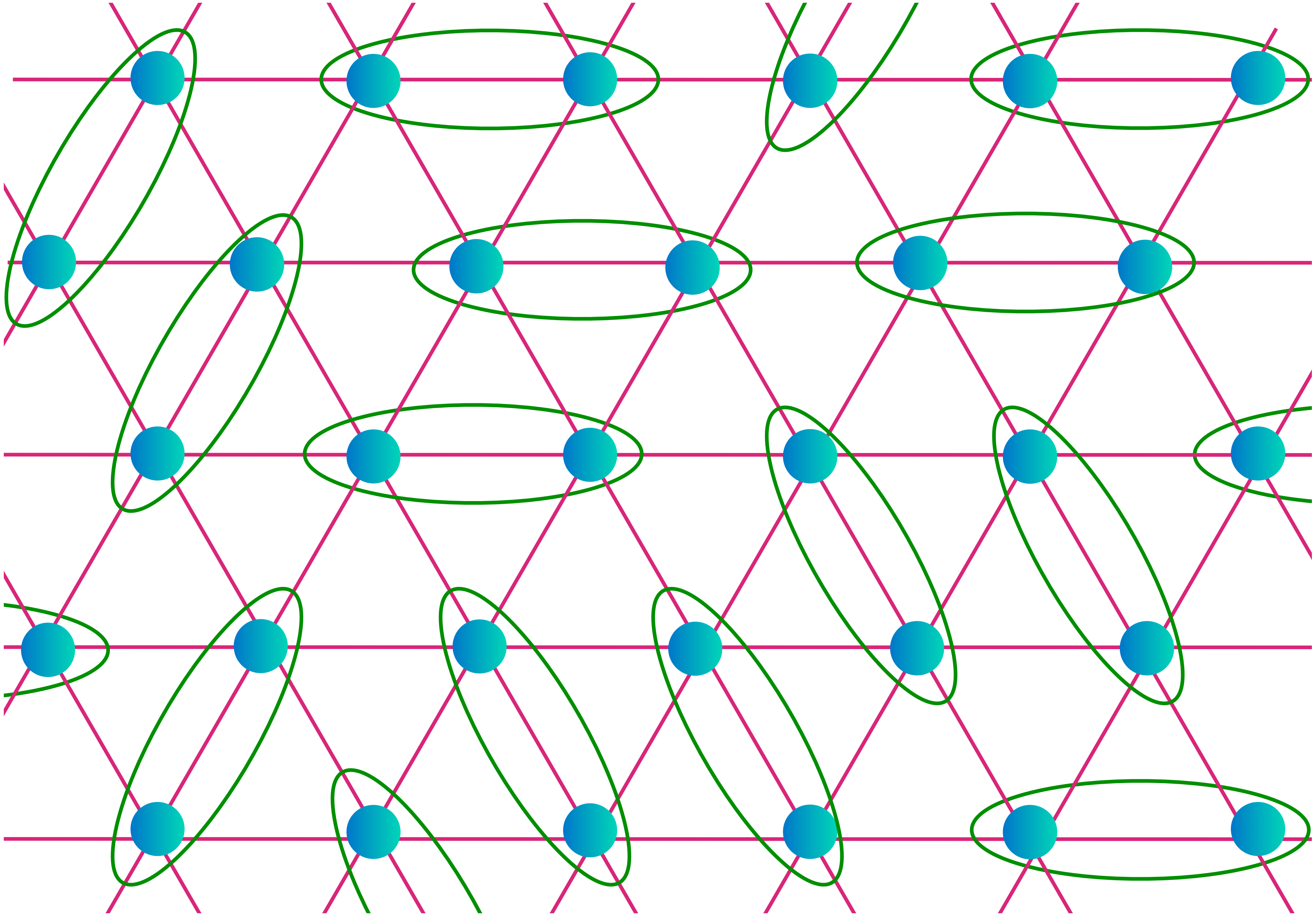

P. Fazekas and P. W. Anderson, *Philos. Mag.* **30**, 23 (1974).

Triangular lattice antiferromagnet

Spin liquid obtained in a generalized spin model with S=1/2 per unit cell

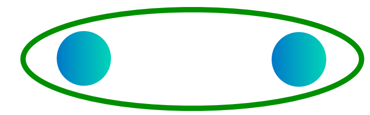

$$= \frac{1}{\sqrt{2}} \left(\left| \uparrow \downarrow \right\rangle - \left| \downarrow \uparrow \right\rangle \right)$$

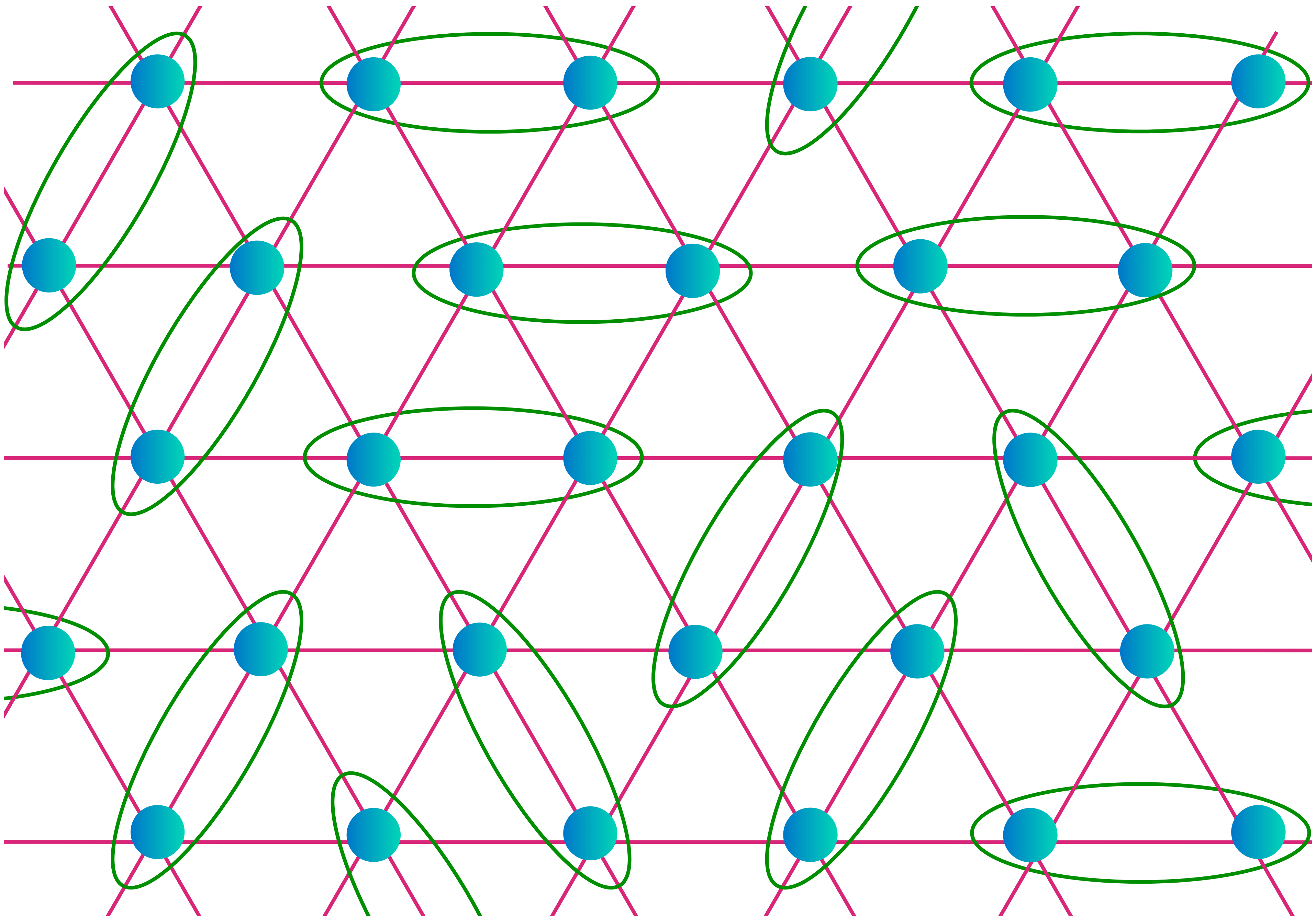

P. Fazekas and P. W. Anderson, *Philos. Mag.* **30**, 23 (1974).

Triangular lattice antiferromagnet

Spin liquid obtained in a generalized spin model with S=1/2 per unit cell

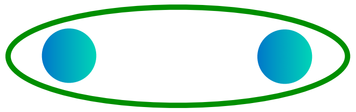

$$= \frac{1}{\sqrt{2}}\left(\left|\uparrow\downarrow\right\rangle - \left|\downarrow\uparrow\right\rangle\right)$$

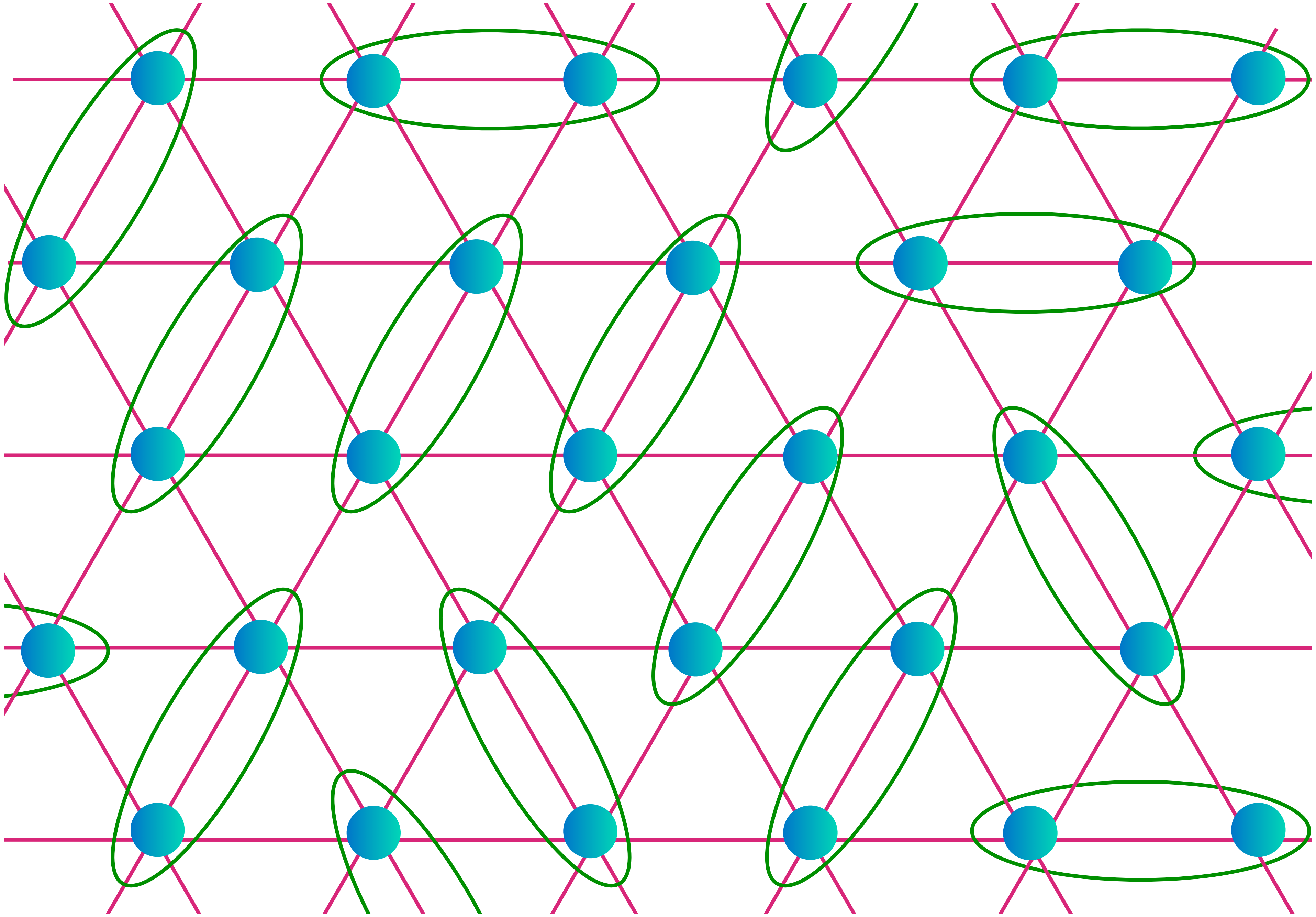

P. Fazekas and P. W. Anderson, *Philos. Mag.* **30**, 23 (1974).

Triangular lattice antiferromagnet

Spin liquid obtained in a generalized spin model with S=1/2 per unit cell

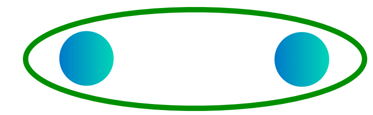

$$= \frac{1}{\sqrt{2}}\Big(\left|\uparrow\downarrow\right\rangle - \left|\downarrow\uparrow\right\rangle\Big)$$

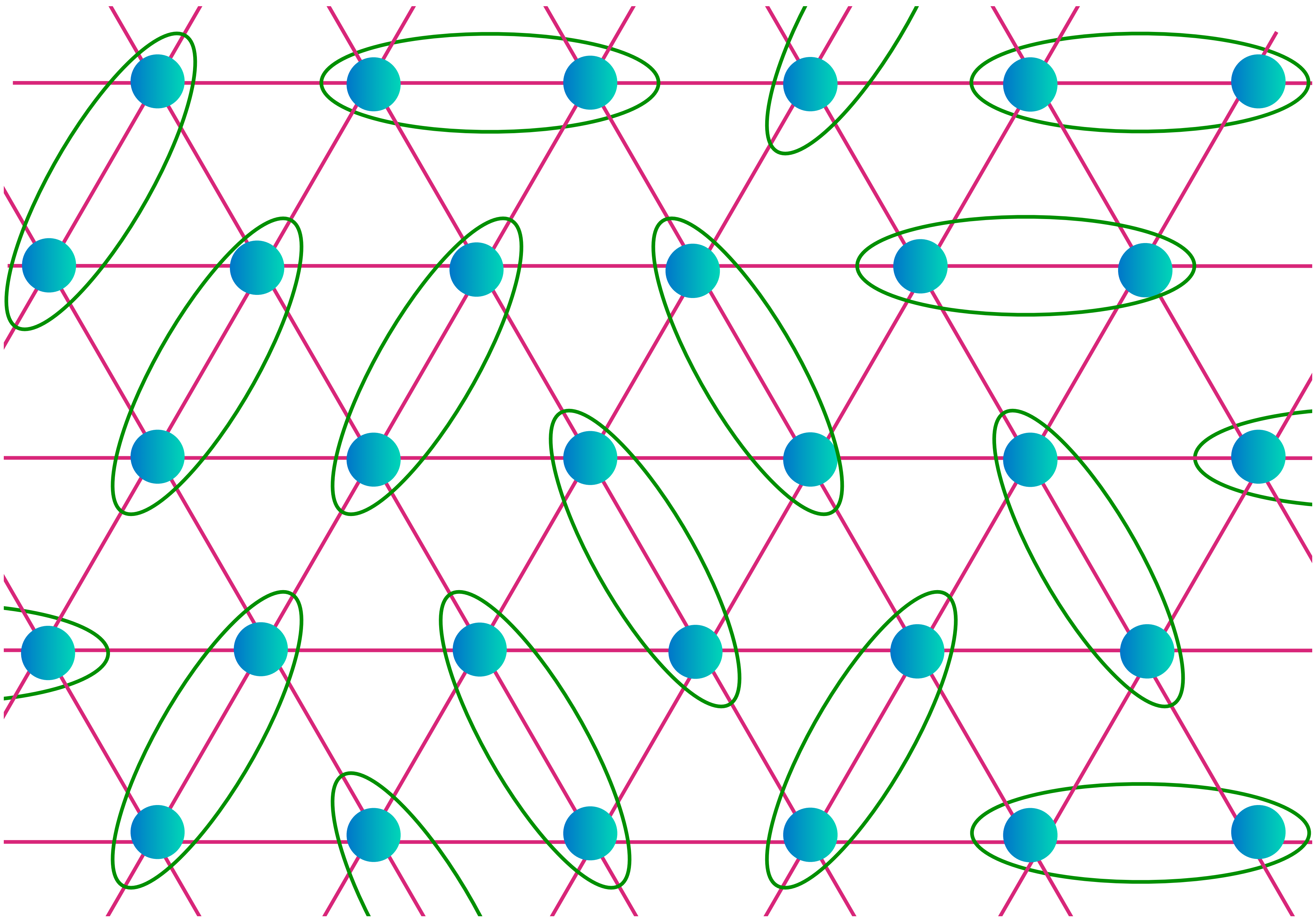

P. Fazekas and P. W. Anderson, *Philos. Mag.* **30**, 23 (1974).

Excitations of the Z_2 Spin liquid

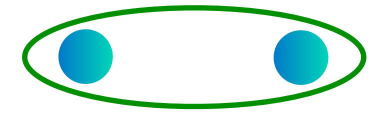

$$= \frac{1}{\sqrt{2}} \left(|\uparrow\downarrow\rangle - |\downarrow\uparrow\rangle \right)$$

A spinon

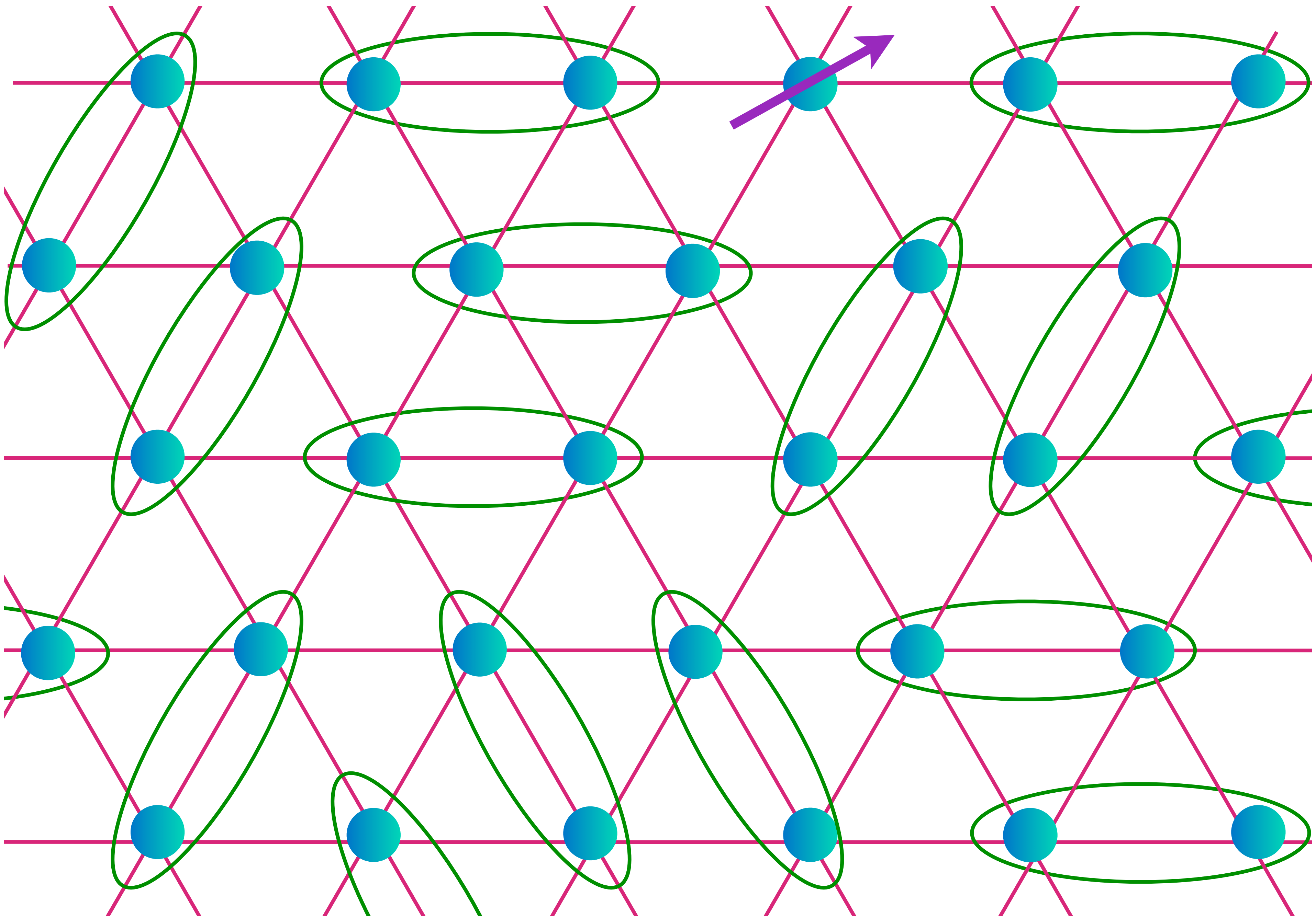

Excitations of the Z_2 Spin liquid

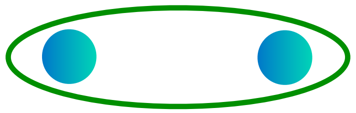

$$= \frac{1}{\sqrt{2}} \left(|\uparrow\downarrow\rangle - |\downarrow\uparrow\rangle \right)$$

A spinon

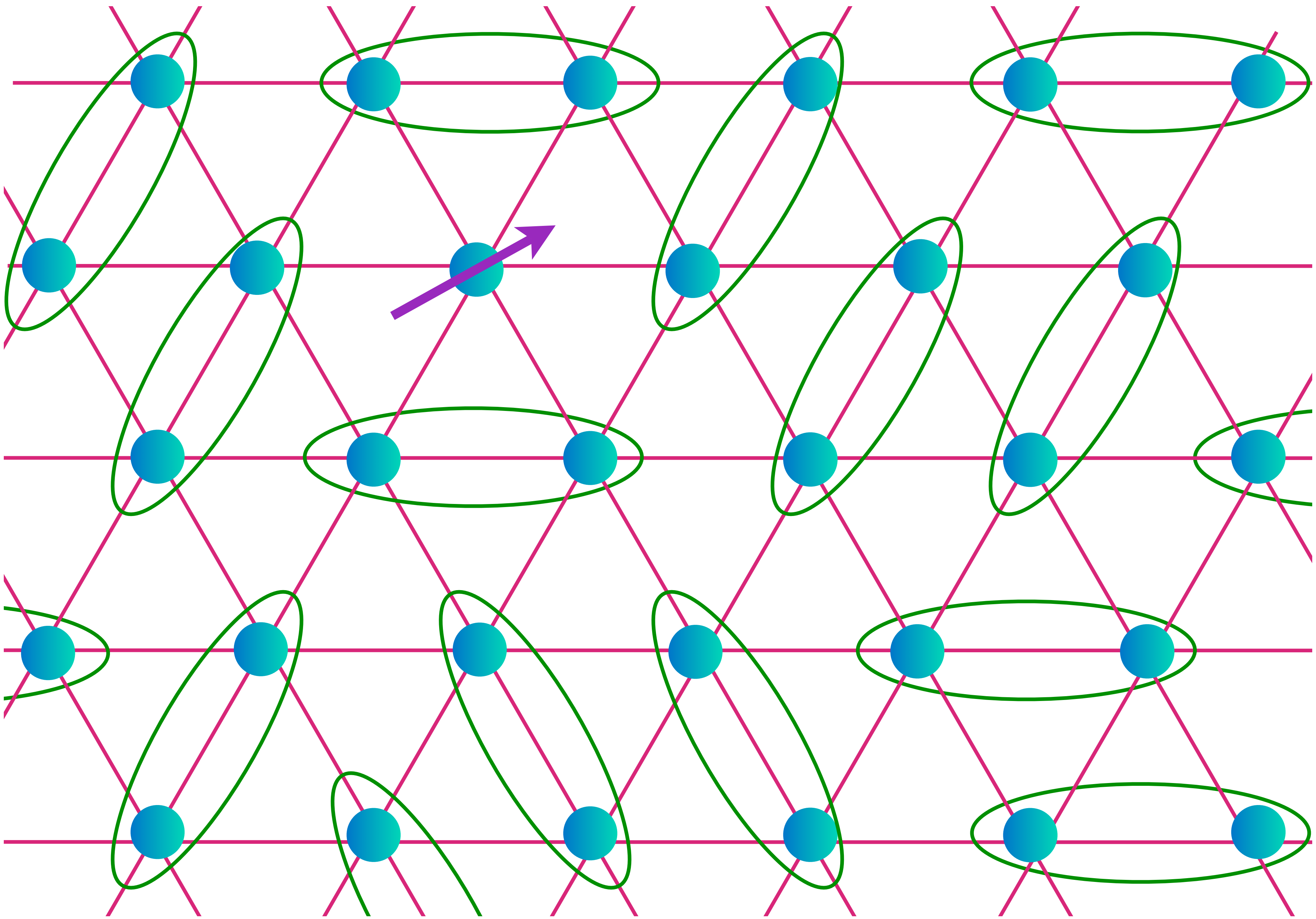

Excitations of the Z_2 Spin liquid

A spinon

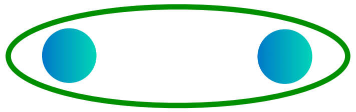

$$= \frac{1}{\sqrt{2}} \left(|\uparrow\downarrow\rangle - |\downarrow\uparrow\rangle \right)$$

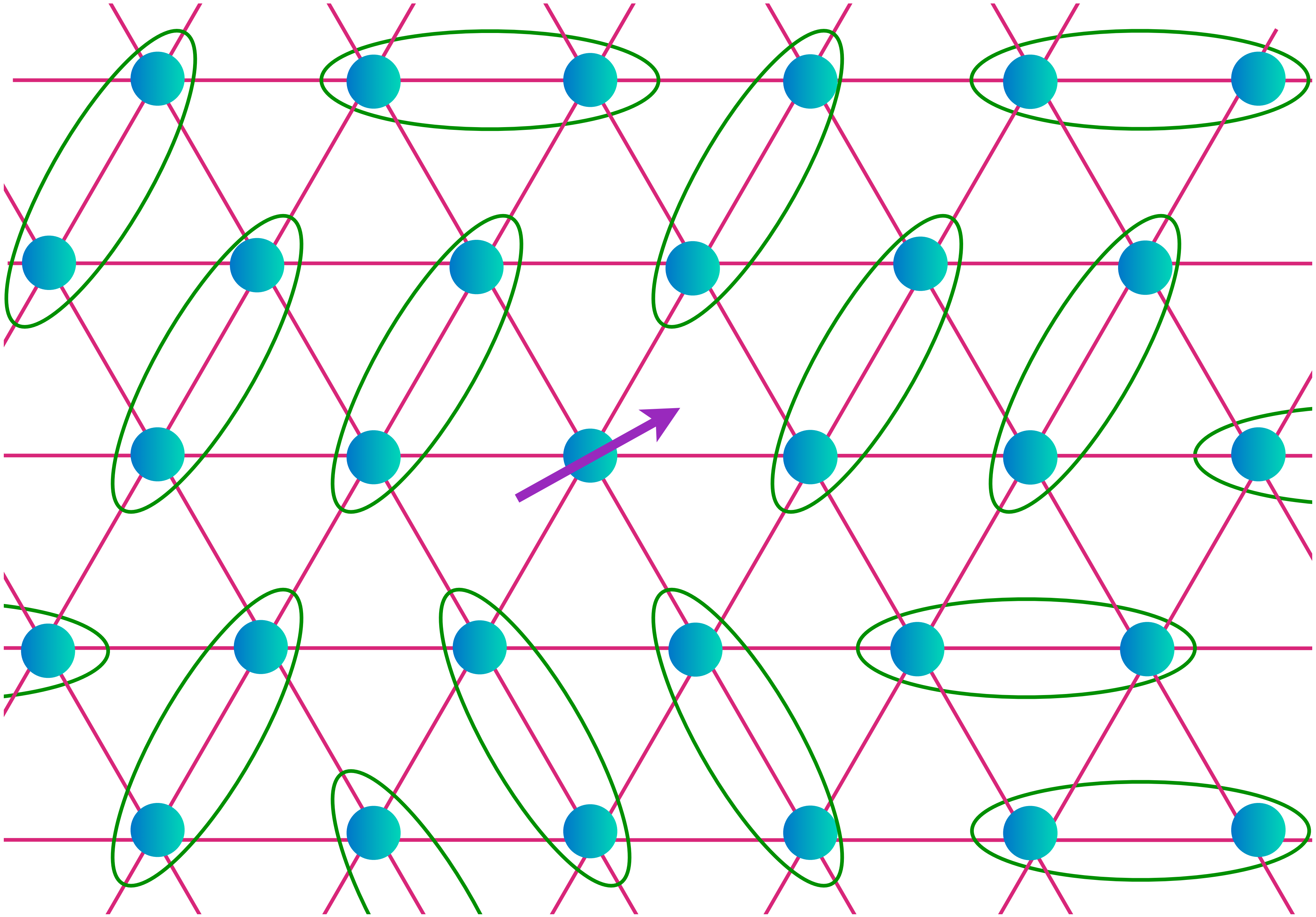

Excitations of the Z_2 Spin liquid

A spinon

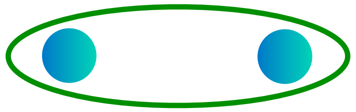

$$= \frac{1}{\sqrt{2}} \left(|\uparrow\downarrow\rangle - |\downarrow\uparrow\rangle \right)$$

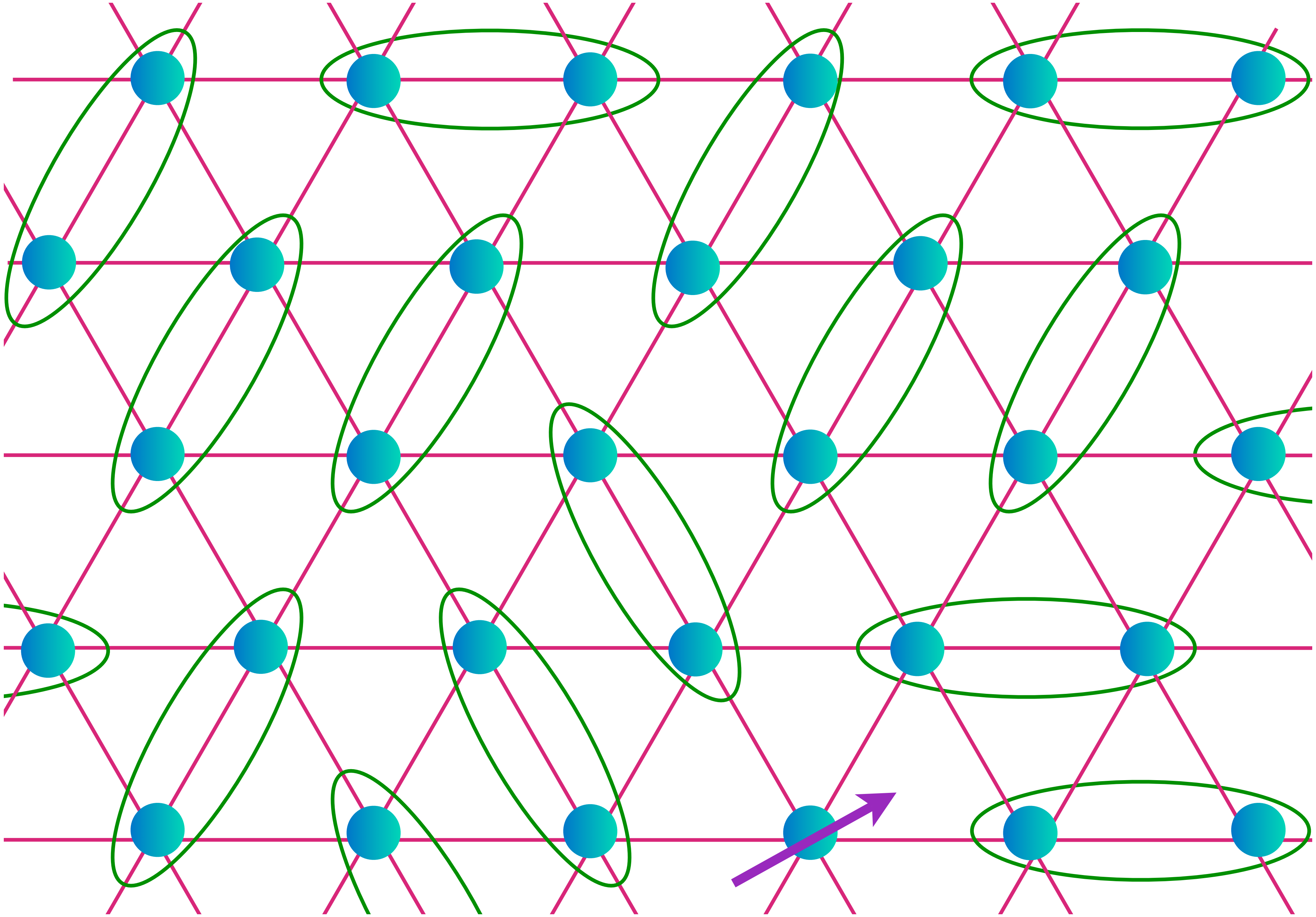

Excitations of the Z_2 Spin liquid

A spinon

The spinon annihilation operator is a spinor z_α, where $\alpha = \uparrow, \downarrow$.

The Néel order parameter, $\vec{\varphi}$ is a composite of the spinons:

$$\vec{\varphi} = z_{i\alpha}^\dagger \vec{\sigma}_{\alpha\beta} z_{i\beta}$$

where $\vec{\sigma}$ are Pauli matrices

Excitations of the Z_2 Spin liquid

A spinon

The spinon annihilation operator is a spinor z_α, where $\alpha = \uparrow, \downarrow$.

The Néel order parameter, $\vec{\varphi}$ is a composite of the spinons:

$$\vec{\varphi} = z_{i\alpha}^\dagger \vec{\sigma}_{\alpha\beta} z_{i\beta}$$

where $\vec{\sigma}$ are Pauli matrices

The theory for quantum phase transitions is expressed in terms of fluctuations of z_α, and *not* the order parameter $\vec{\varphi}$.

Effective theory for z_α must be invariant under the U(1) gauge transformation

$$z_{i\alpha} \to e^{i\theta} z_{i\alpha}$$

Excitations of the Z_2 Spin liquid

A vison

- A characteristic property of a Z_2 spin liquid is the presence of a spinon pair condensate
- A vison is an Abrikosov vortex in the pair condensate of spinons
- Visons are are the **dark matter** of spin liquids: they likely carry most of the energy, but are very hard to detect because they do not carry charge or spin.

N. Read and S. Sachdev, *Phys. Rev. Lett.* **66**, 1773 (1991)

Excitations of the Z_2 Spin liquid

A vison

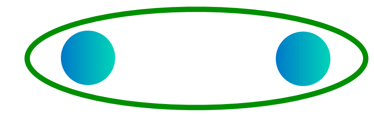

$$= \frac{1}{\sqrt{2}}\Big(|\uparrow\downarrow\rangle - |\downarrow\uparrow\rangle\Big)$$

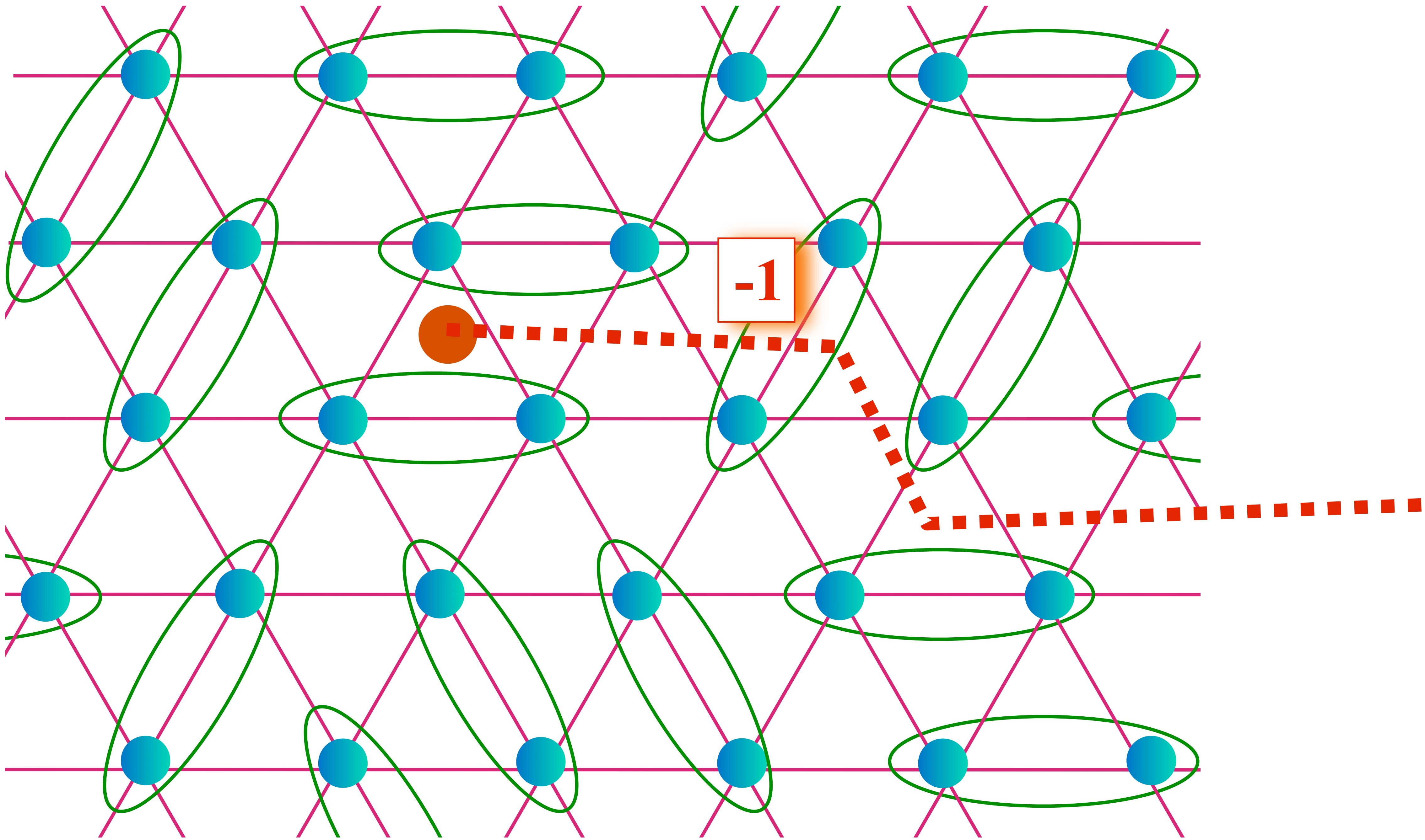

N. Read and S. Sachdev, *Phys. Rev. Lett*. **66**, 1773 (1991)

Excitations of the Z_2 Spin liquid

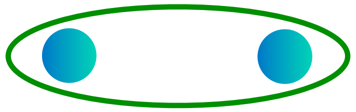

$$= \frac{1}{\sqrt{2}} \Big(\left|\uparrow\downarrow\right\rangle - \left|\downarrow\uparrow\right\rangle \Big)$$

A vison

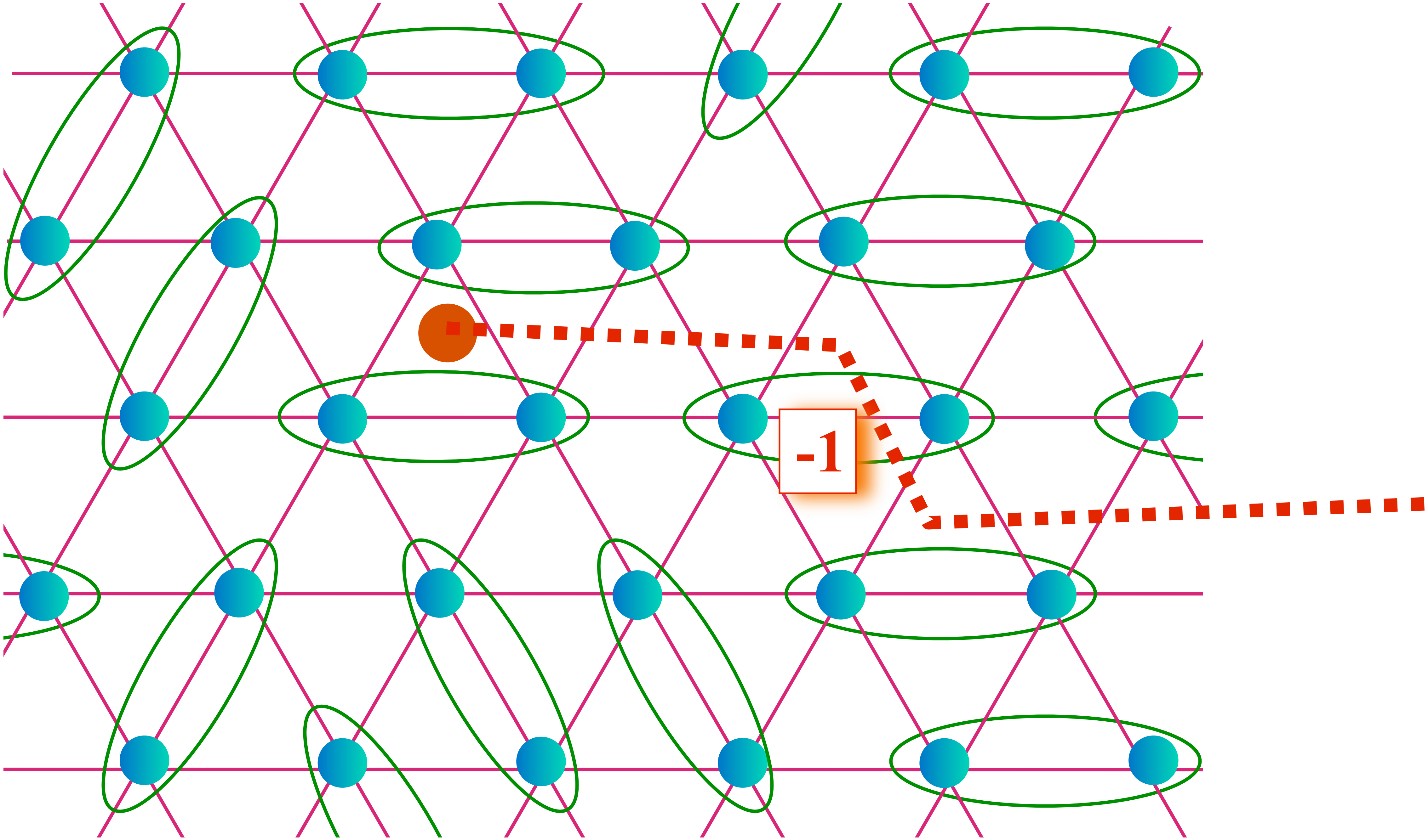

N. Read and S. Sachdev, *Phys. Rev. Lett.* **66**, 1773 (1991)

Excitations of the Z_2 Spin liquid

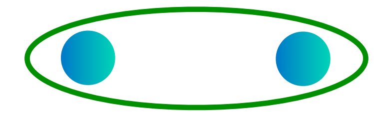

$$= \frac{1}{\sqrt{2}} \left(\left| \uparrow \downarrow \right\rangle - \left| \downarrow \uparrow \right\rangle \right)$$

A vison

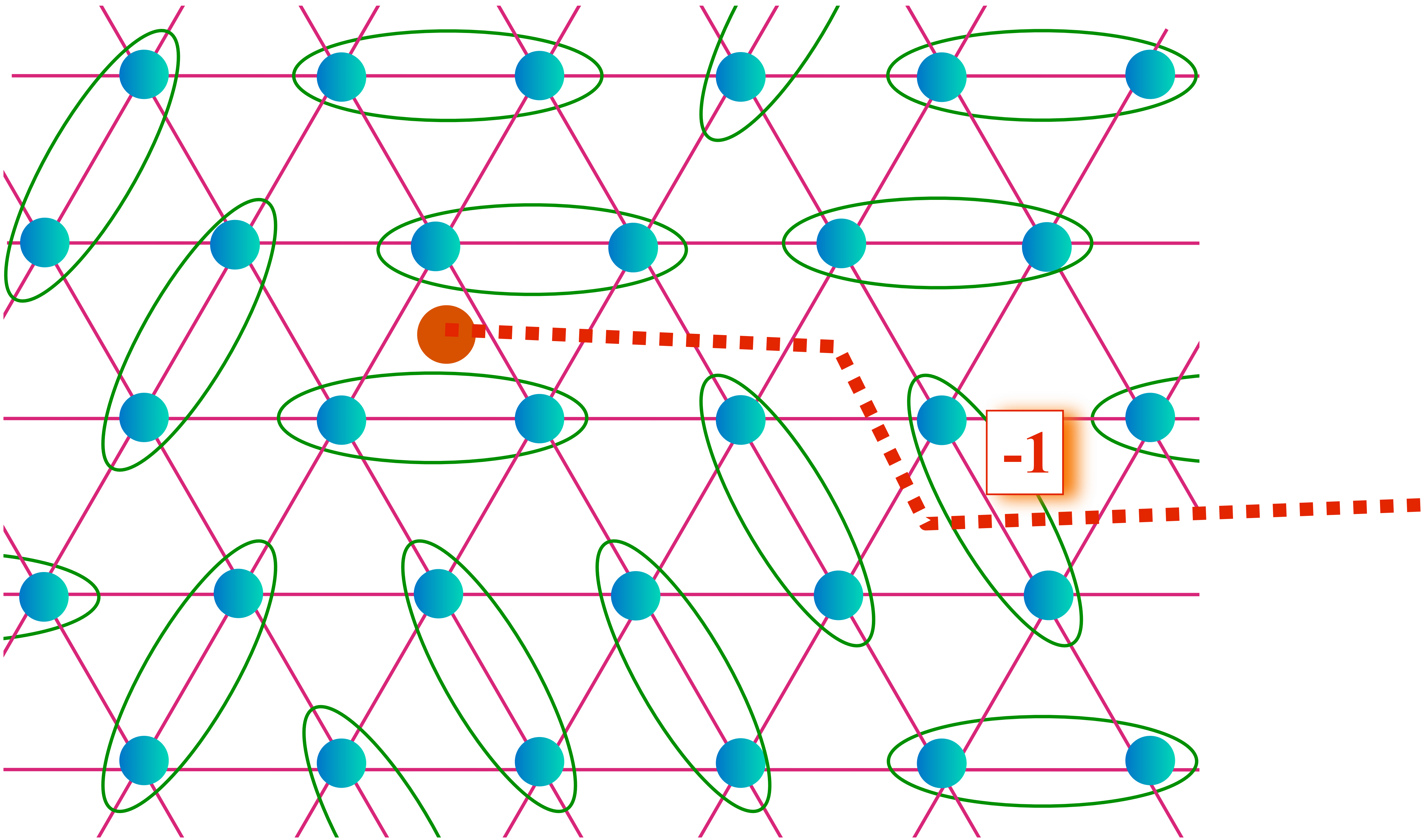

N. Read and S. Sachdev, *Phys. Rev. Lett*. **66**, 1773 (1991)

Excitations of the Z_2 Spin liquid

A vison

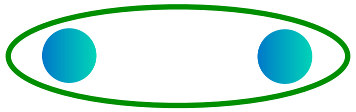

$$= \frac{1}{\sqrt{2}}\left(|\uparrow\downarrow\rangle - |\downarrow\uparrow\rangle \right)$$

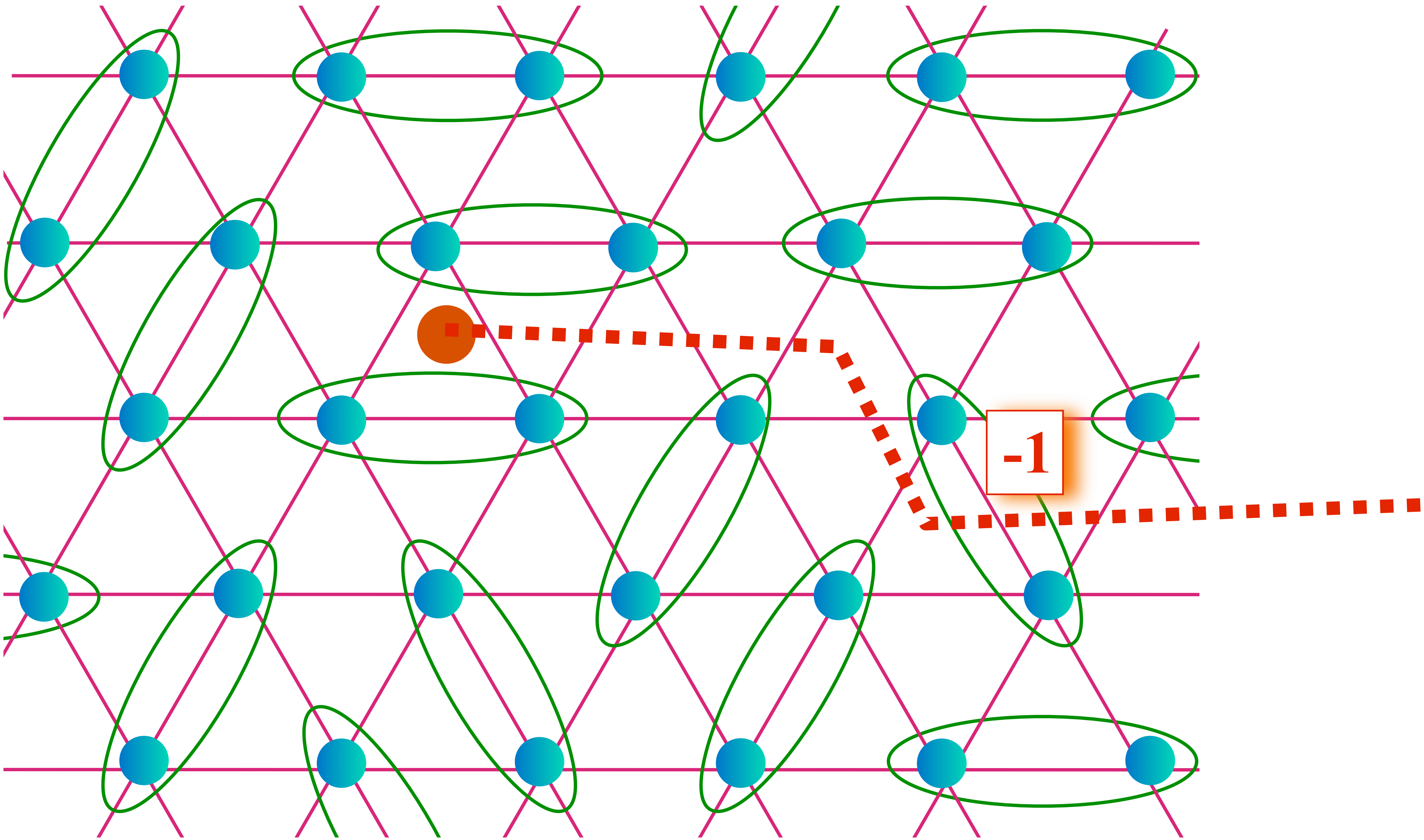

N. Read and S. Sachdev, *Phys. Rev. Lett.* **66**, 1773 (1991)

Excitations of the Z_2 Spin liquid

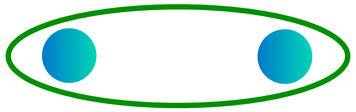

$$= \frac{1}{\sqrt{2}}\left(\left|\uparrow\downarrow\right\rangle - \left|\downarrow\uparrow\right\rangle\right)$$

A vison

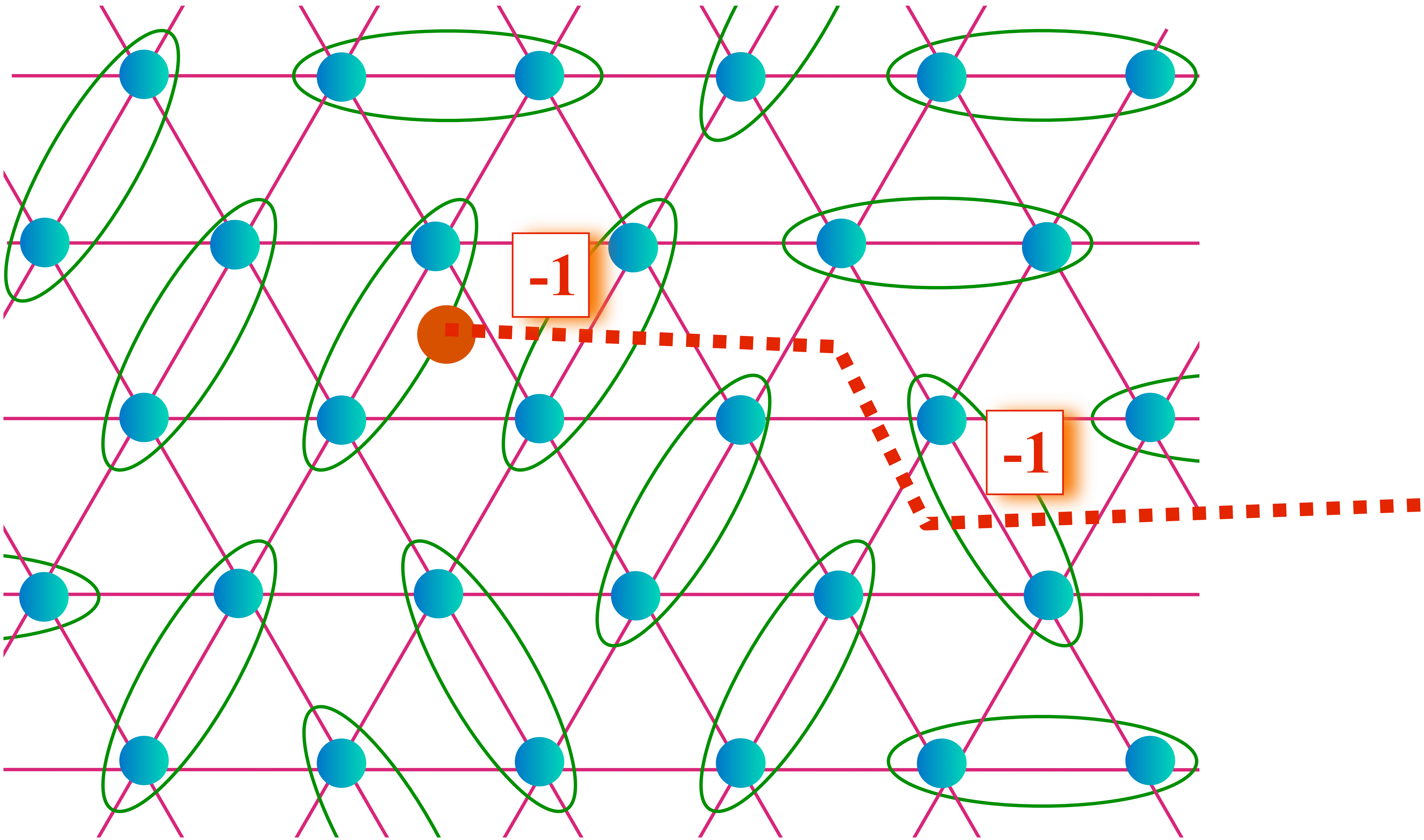

N. Read and S. Sachdev, *Phys. Rev. Lett*. **66**, 1773 (1991)

Excitations of the Z_2 Spin liquid

A vison

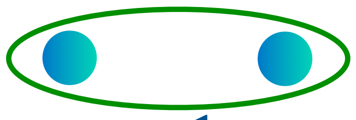

$$= \frac{1}{\sqrt{2}}\left(\left|\uparrow\downarrow\right\rangle - \left|\downarrow\uparrow\right\rangle\right)$$

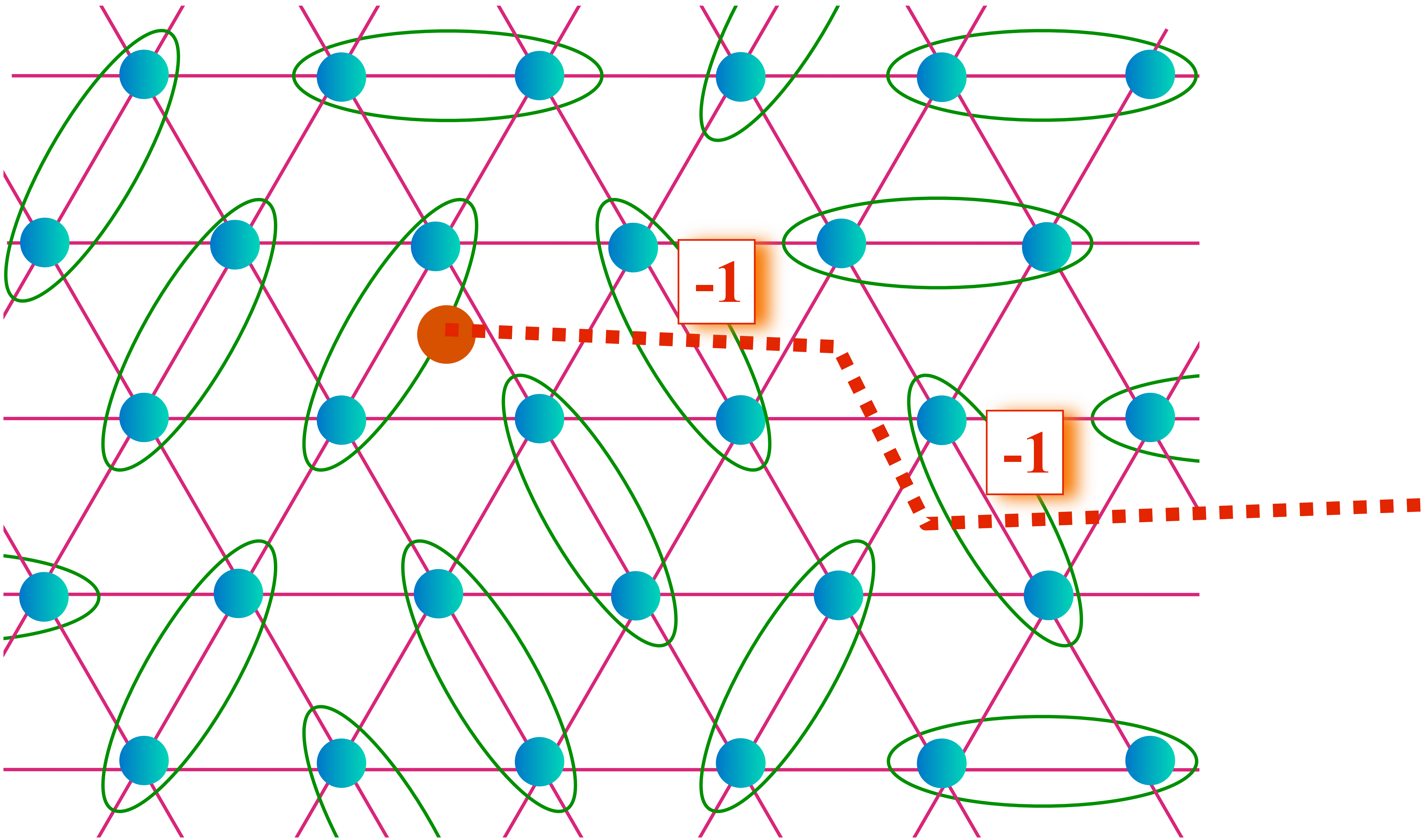

N. Read and S. Sachdev, *Phys. Rev. Lett.* **66**, 1773 (1991)

Mutual Chern-Simons Theory

Express theory in terms of the physical excitations of the Z_2 spin liquid: the spinons, z_α, and the visons. After accounting for Berry phase effects, the visons can be described by complex fields v_a, which transforms non-trivially under the square lattice space group operations.

A related Berry phase is the phase of -1 acquired by a spinon encircling a vortex. This is implemented in the following "mutual Chern-Simons" theory at $k = 2$:

$$
\begin{aligned}
\mathcal{L} &= \sum_{\alpha=1}^{2} \left\{ |(\partial_\mu - i a_\mu) z_\alpha|^2 + s_z |z_\alpha|^2 + u_z (|z_\alpha|^2)^2 \right\} \\
&+ \sum_{a=1}^{N_v} \left\{ |(\partial_\mu - i b_\mu) v_a|^2 + s_v |v_a|^2 + u_v (|v_a|^2)^2 \right\} \\
&+ \frac{ik}{2\pi} \epsilon_{\mu\nu\lambda} a_\mu \partial_\nu b_\lambda + \cdots
\end{aligned}
$$

Cenke Xu and S. Sachdev, arXiv:0811.1220

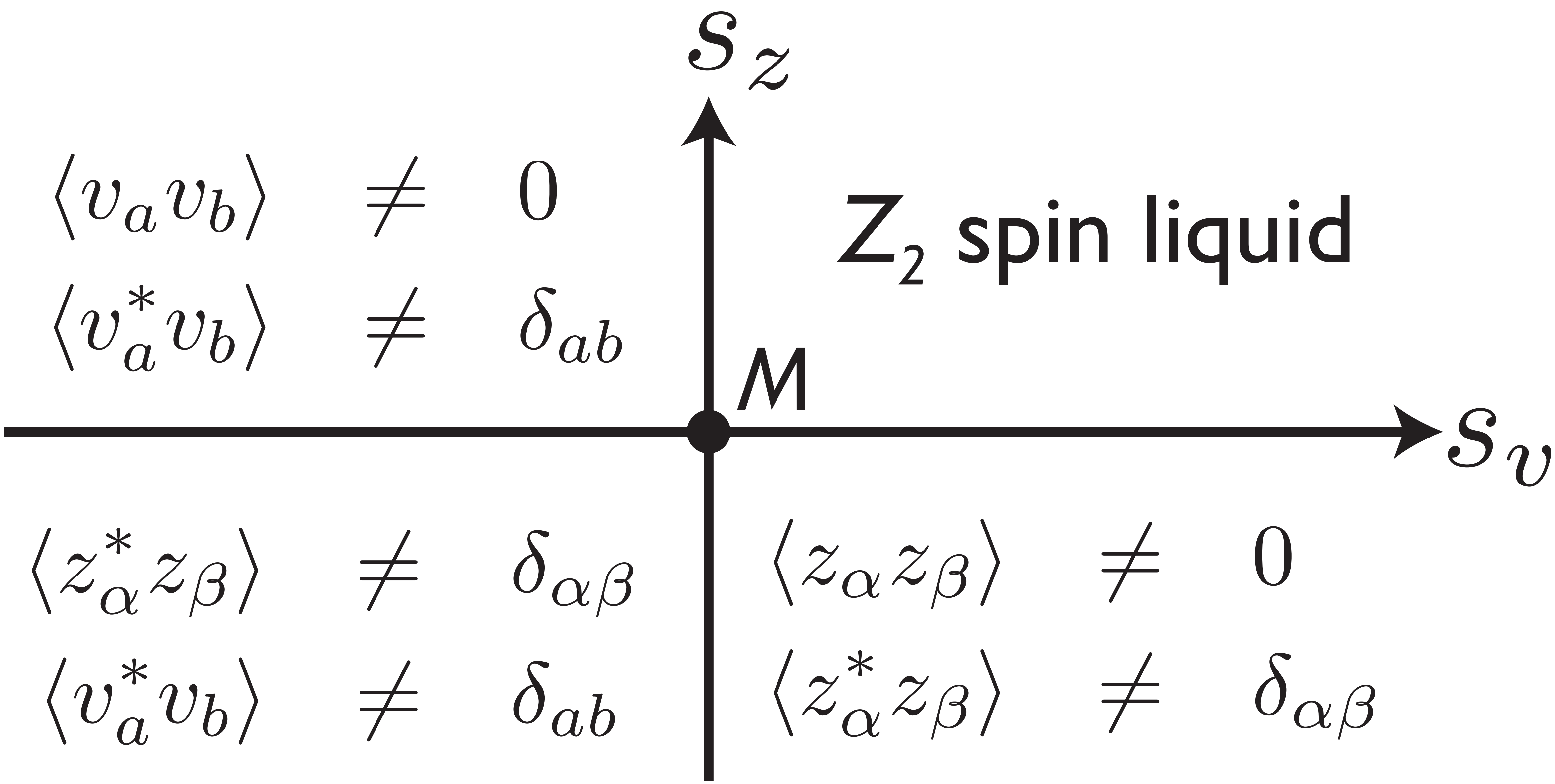

Cenke Xu and S. Sachdev, arXiv:0811.1220

Theoretical global phase diagram

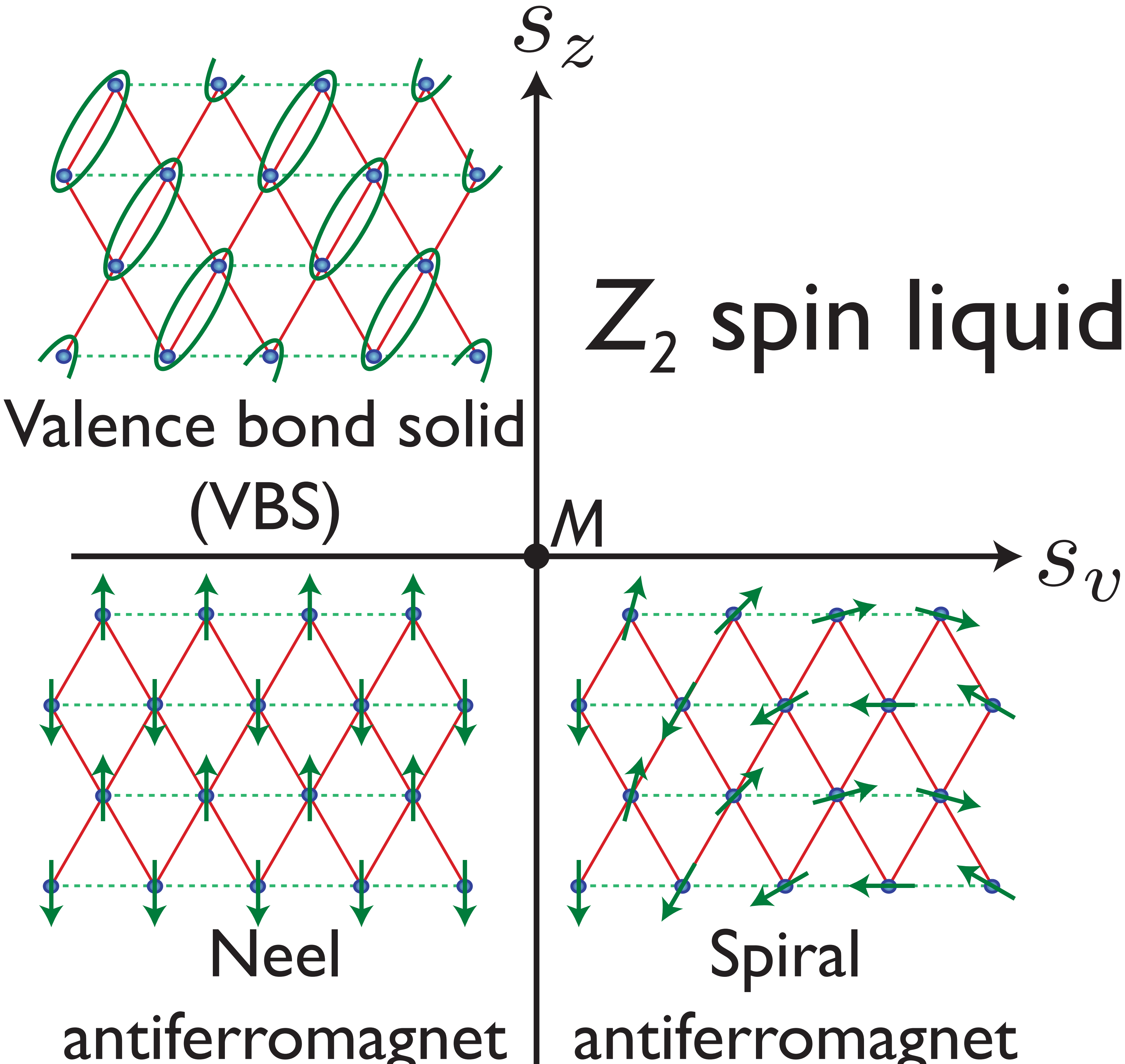

N. Read and S. Sachdev, *Phys. Rev. Lett*. **66**, 1773 (1991)
T. Senthil, A. Vishwanath, L. Balents, S. Sachdev and M.P.A. Fisher, *Science* **303**, 1490 (2004).
Cenke Xu and S. Sachdev, arXiv:0811.1220

Theoretical global phase diagram

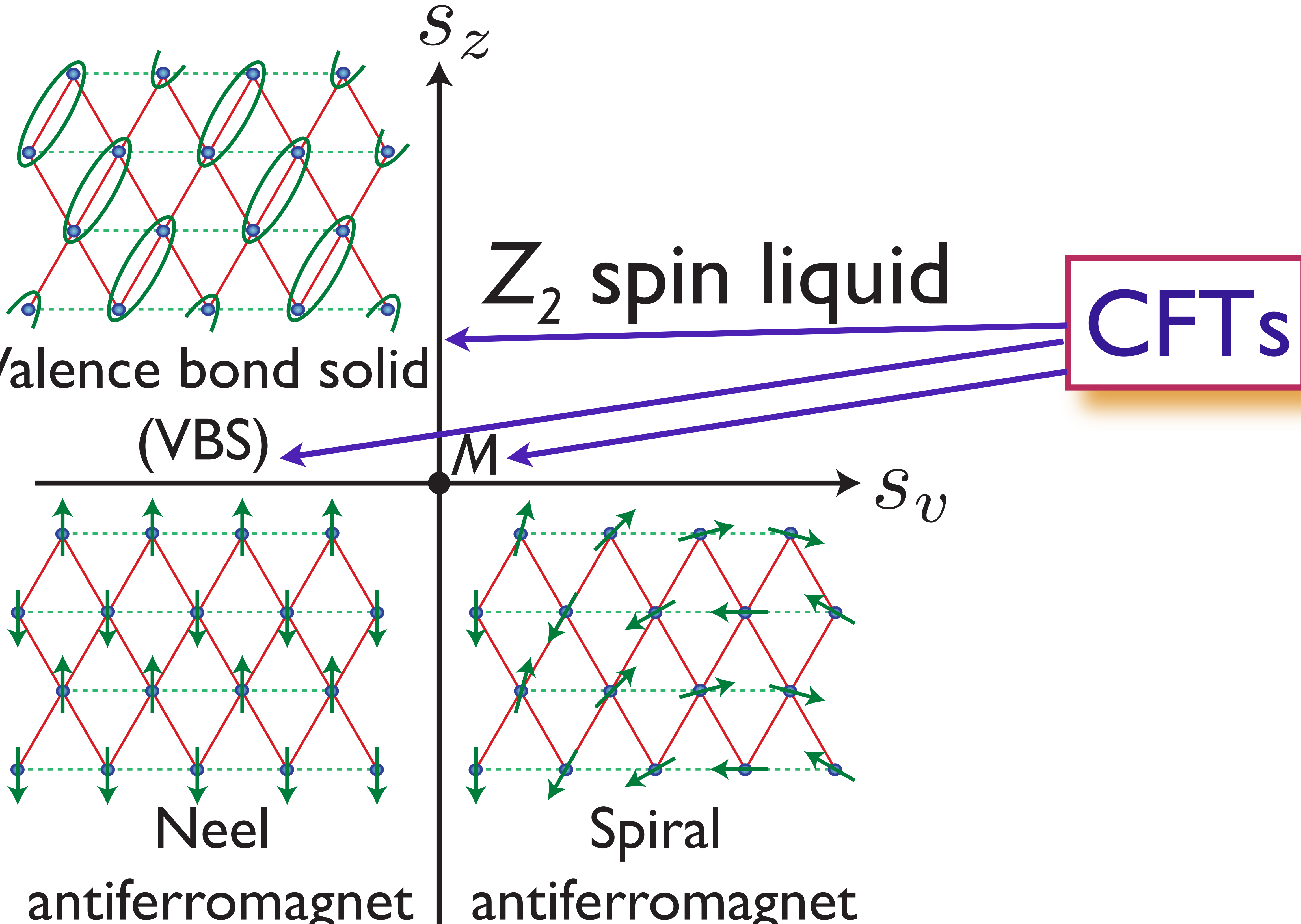

N. Read and S. Sachdev, *Phys. Rev. Lett*. **66**, 1773 (1991)
T. Senthil, A. Vishwanath, L. Balents, S. Sachdev and M.P.A. Fisher, *Science* **303**, 1490 (2004).
Cenke Xu and S. Sachdev, arXiv:0811.1220

From quantum antiferromagnets to string theory

A direct generalization of the CFT of the multicritical point M ($s_z = s_v = 0$) to $\mathcal{N} = 4$ supersymmetry and the U(N) gauge group was shown by O. Aharony, O. Bergman, D. L. Jafferis, J. Maldacena, JHEP **0810**, 091 (2008) to be dual to a theory of quantum gravity (M theory) on $\mathrm{AdS}_4 \times \mathrm{S}_7 / Z_k$.

$$
\begin{aligned}
\mathcal{L} &= \sum_{\alpha=1}^{2} \left\{ |(\partial_\mu - i a_\mu) z_\alpha|^2 + s_z |z_\alpha|^2 + u_z (|z_\alpha|^2)^2 \right\} \\
&+ \sum_{a=1}^{N_v} \left\{ |(\partial_\mu - i b_\mu) v_a|^2 + s_v |v_a|^2 + u_v (|v_a|^2)^2 \right\} \\
&+ \frac{ik}{2\pi} \epsilon_{\mu\nu\lambda} a_\mu \partial_\nu b_\lambda + \cdots
\end{aligned}
$$

Magnetic Criticality

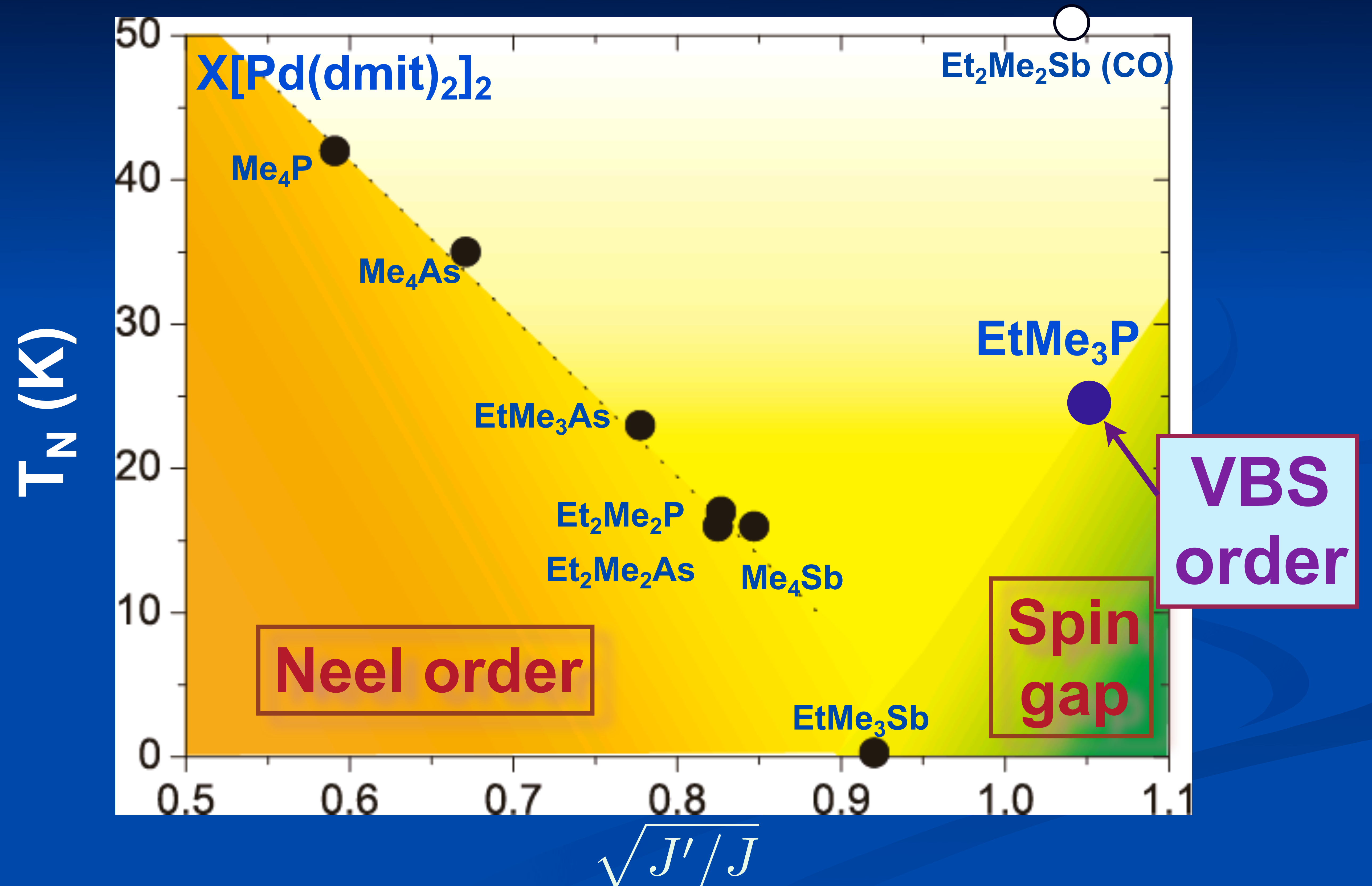

Y. Shimizu, H. Akimoto, H. Tsujii, A. Tajima, and R. Kato, *J. Phys.: Condens. Matter* **19**, 145240 (2007)

Magnetic Criticality

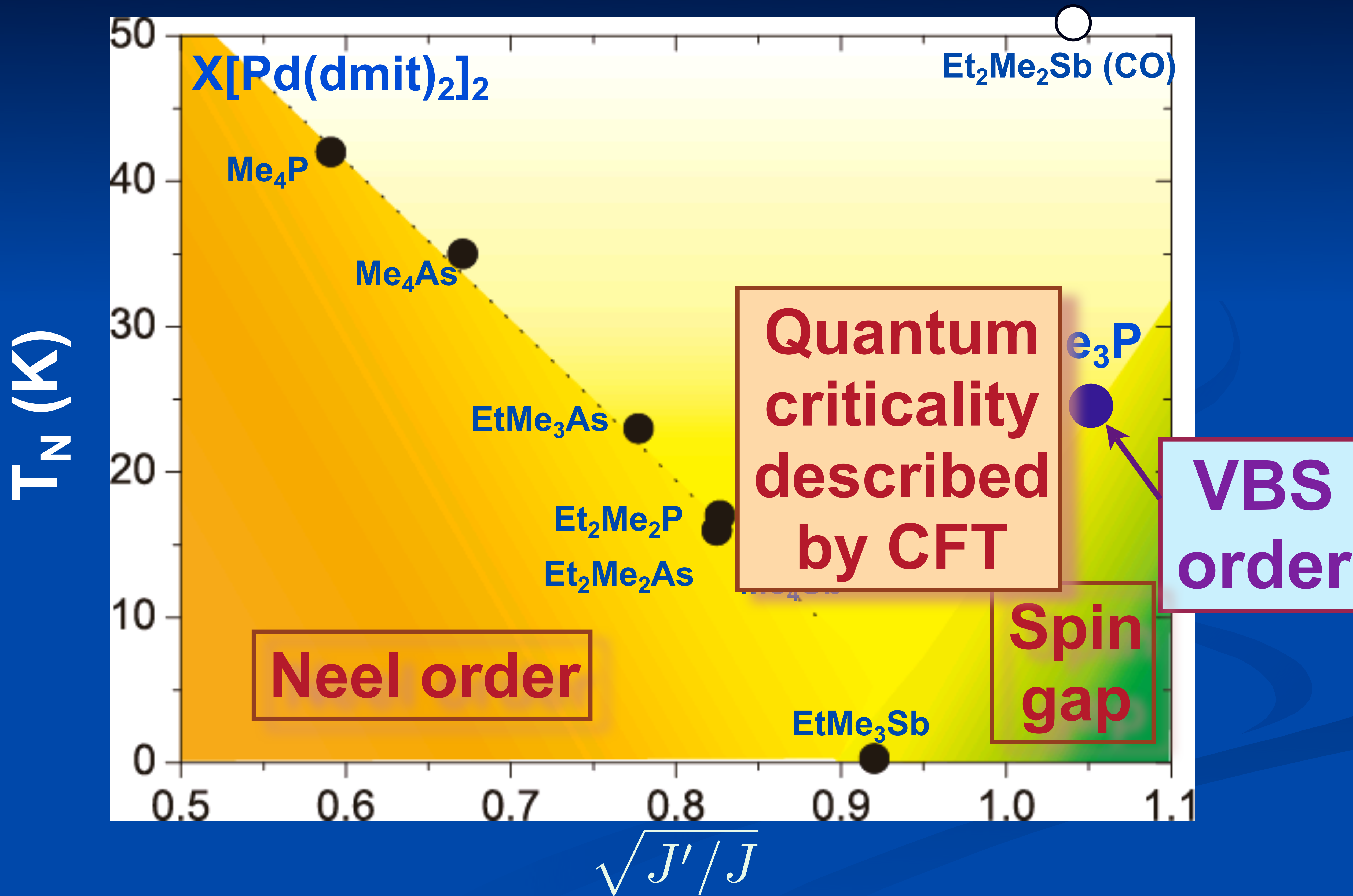

Y. Shimizu, H. Akimoto, H. Tsujii, A. Tajima, and R. Kato, *J. Phys.: Condens. Matter* **19**, 145240 (2007)

Outline

A. "Relativistic" field theories of quantum phase transitions

1. Coupled dimer antiferromagnets

2. Triangular lattice antiferromagnets

3. Graphene

4. AdS/CFT and quantum critical transport

Outline

A. “Relativistic” field theories of quantum phase transitions

1. Coupled dimer antiferromagnets

2. Triangular lattice antiferromagnets

3. Graphene

4. AdS/CFT and quantum critical transport

Graphene

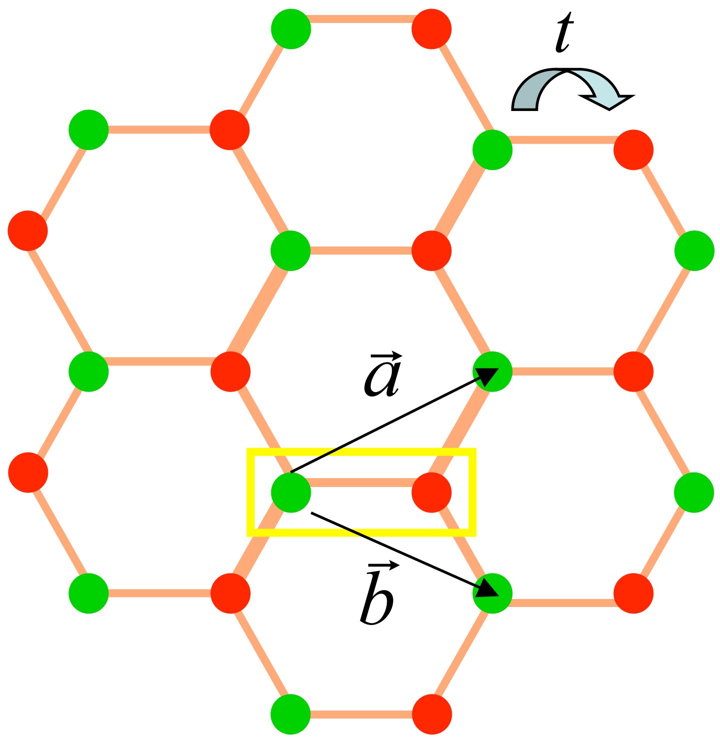

Graphene

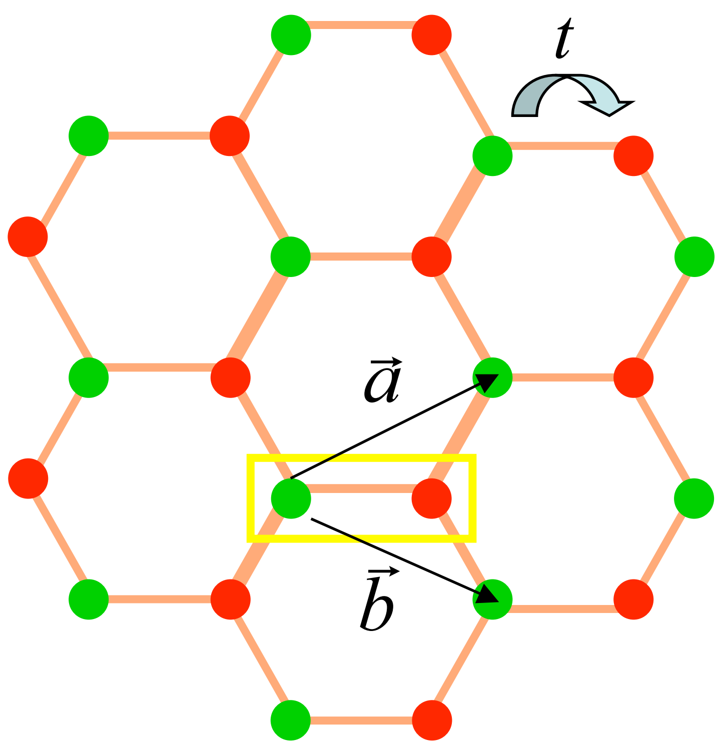

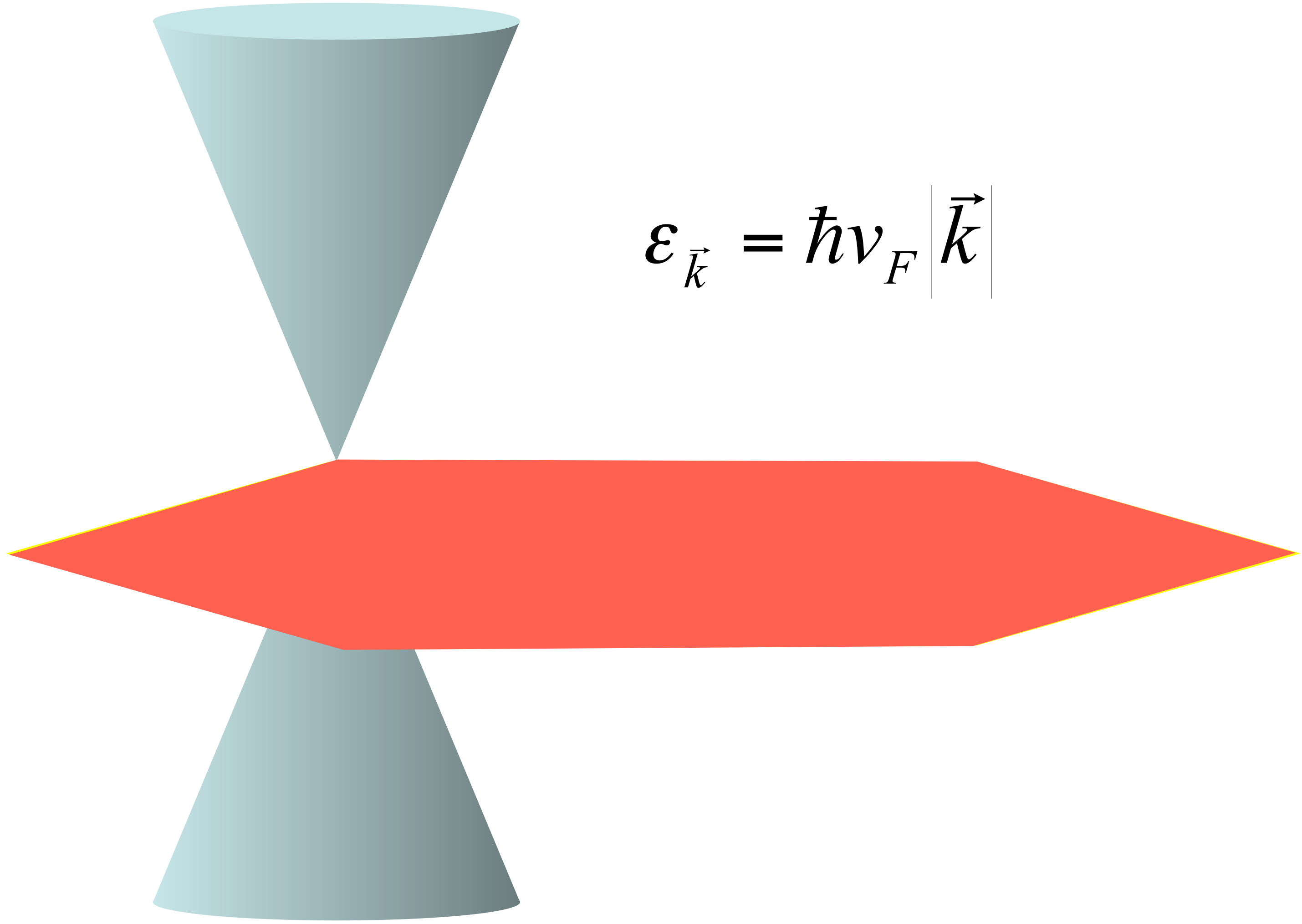

$$\varepsilon_{\vec{k}} = \hbar v_F \left|\vec{k}\right|$$

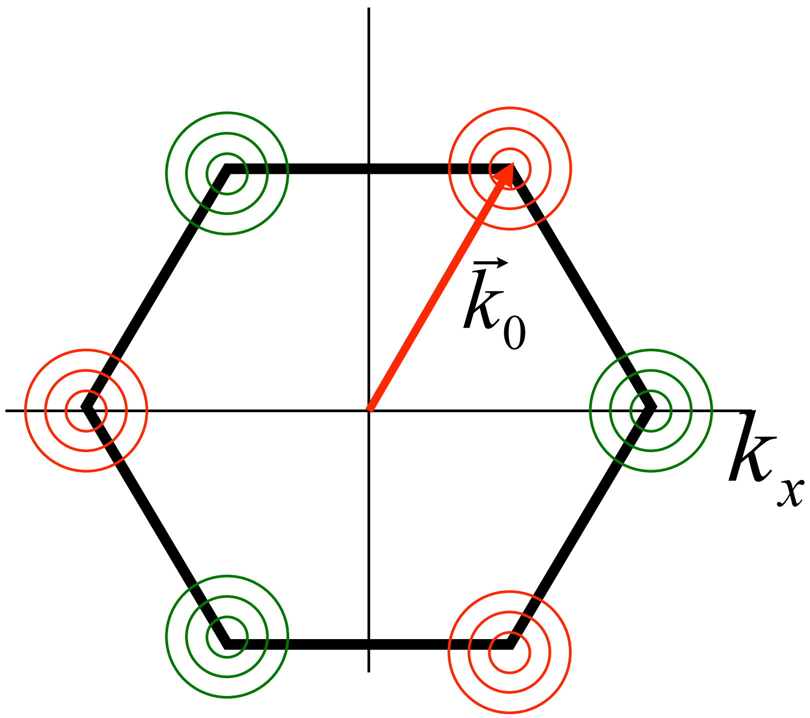

Conical Dirac dispersion

Quantum phase transition in graphene tuned by a bias voltage

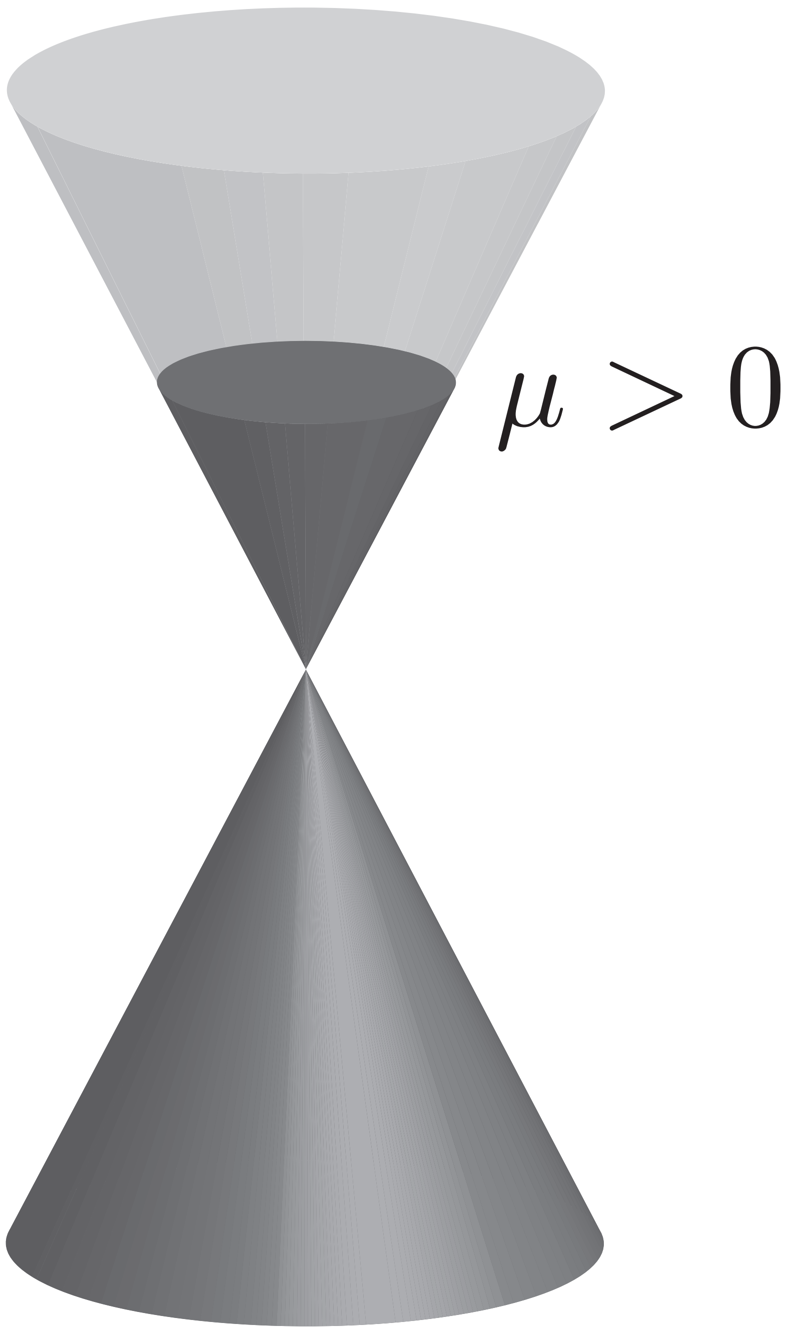

Electron
Fermi surface

Quantum phase transition in graphene tuned by a bias voltage

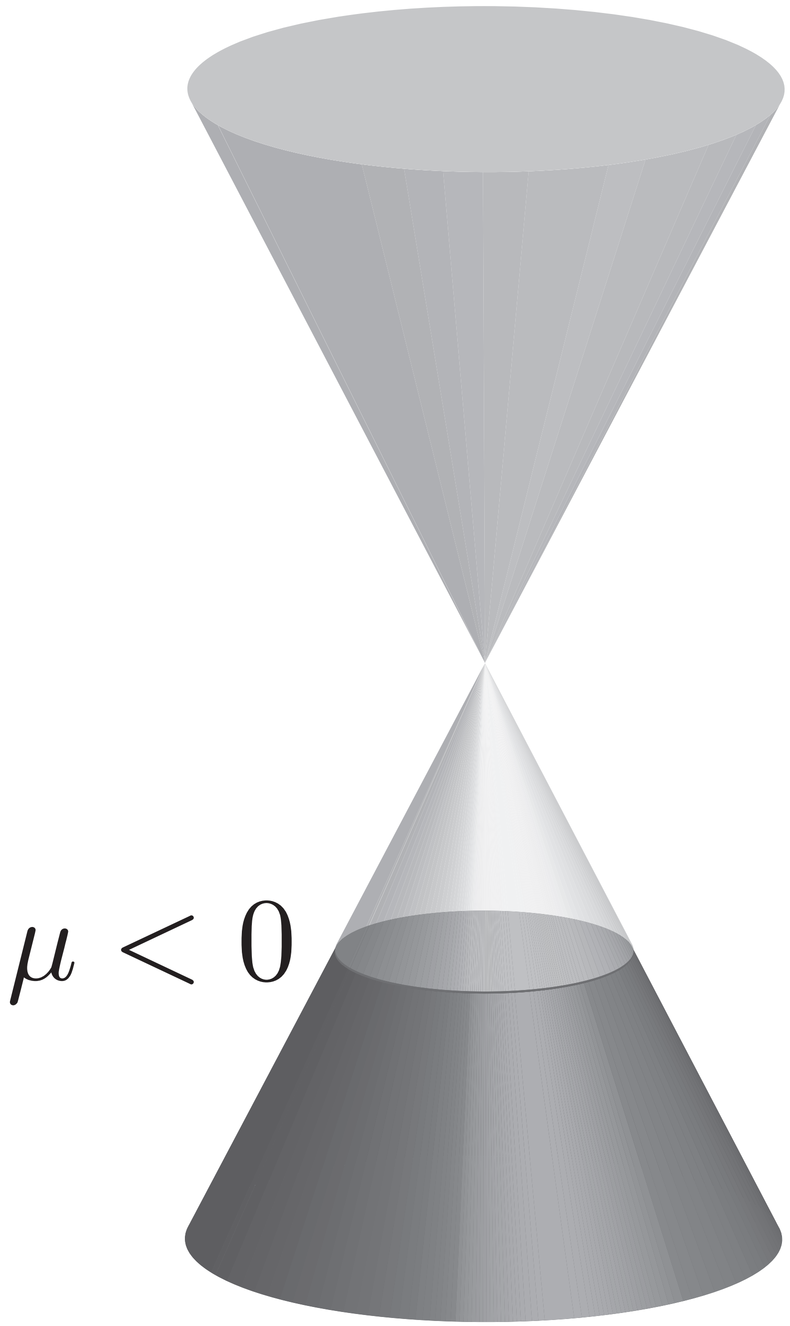

Hole
Fermi surface

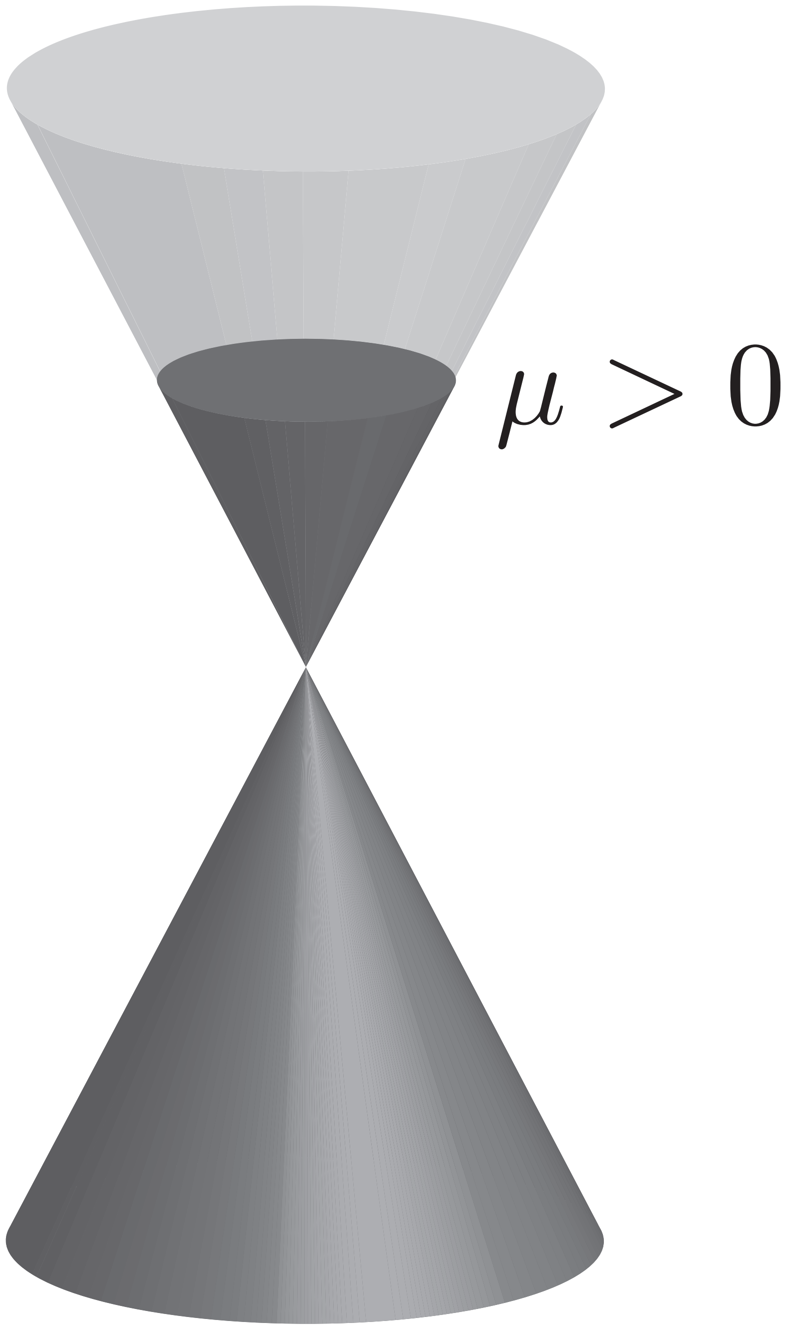

Electron
Fermi surface

Quantum phase transition in graphene tuned by a bias voltage

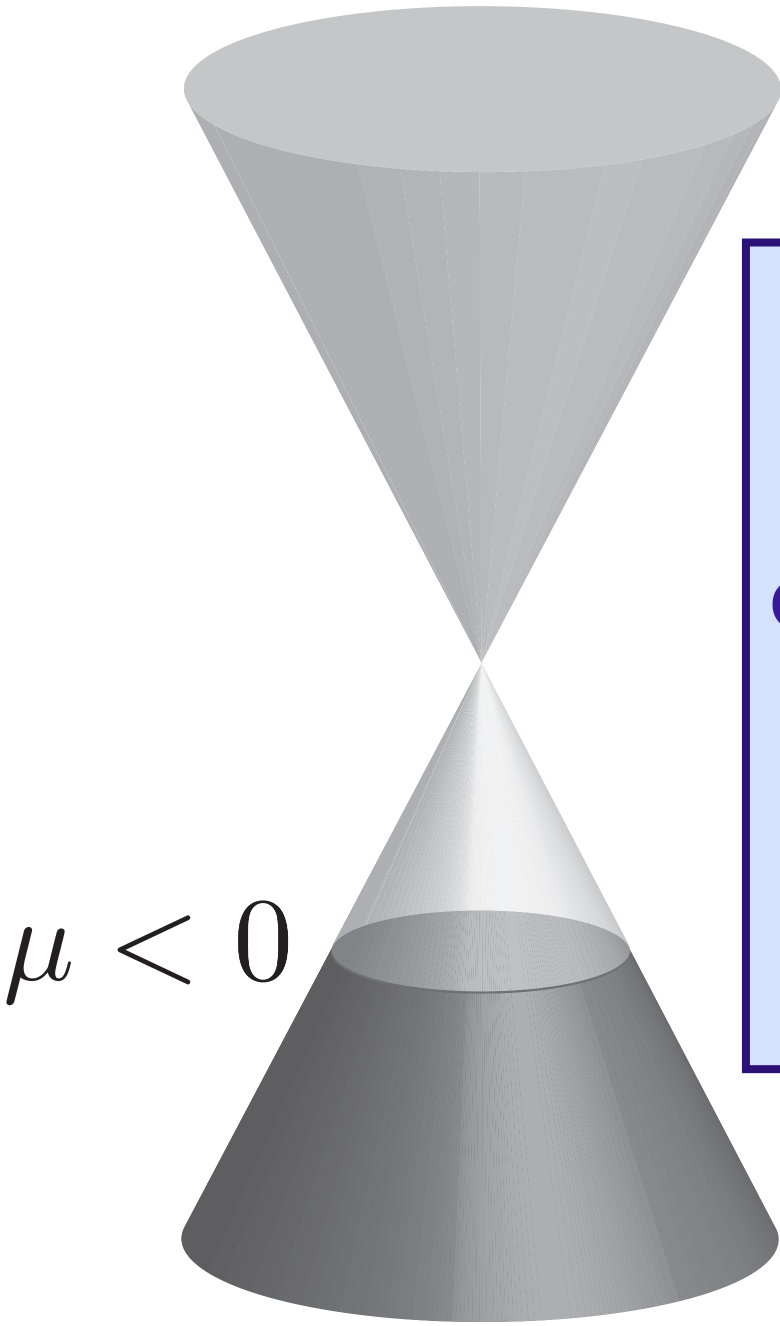

Hole
Fermi surface

There must be an intermediate quantum critical point where the Fermi surfaces reduce to a Dirac point

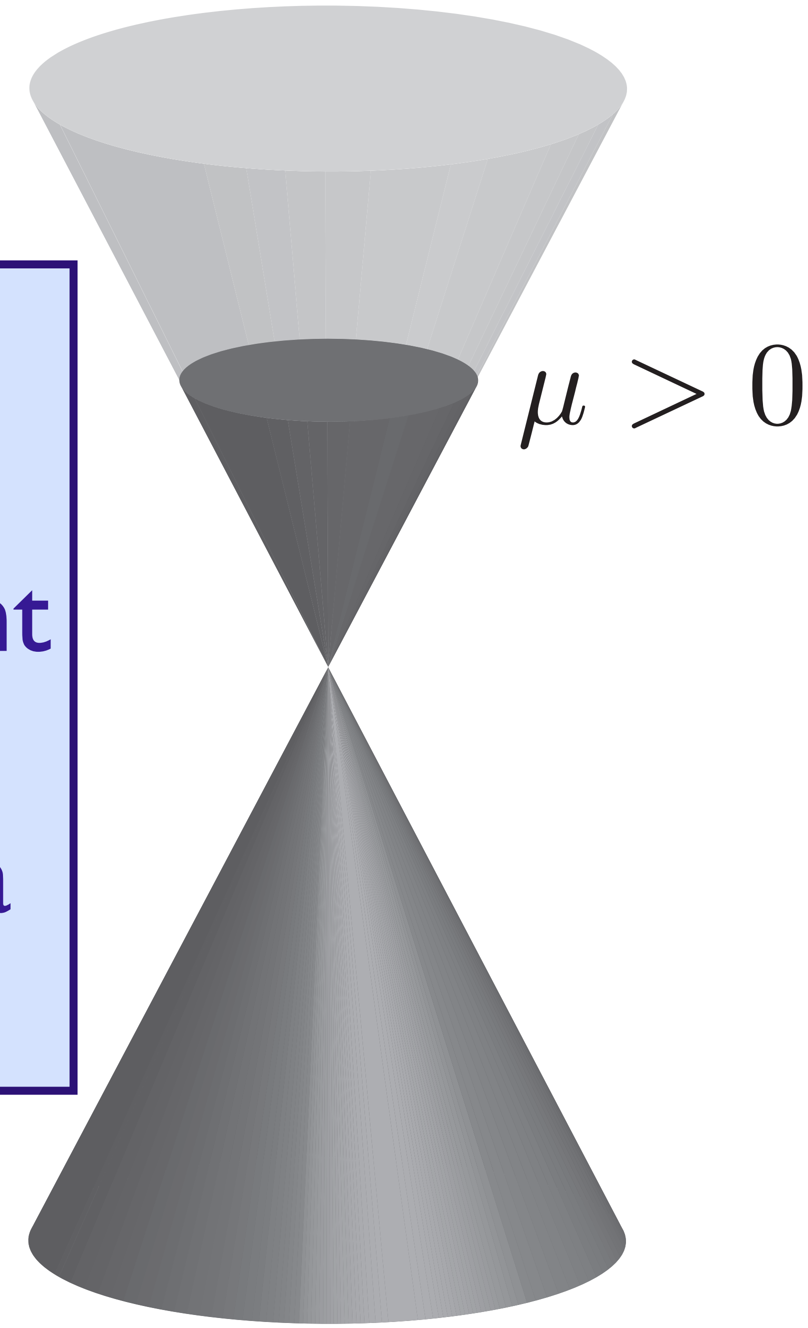

Electron
Fermi surface

Quantum critical graphene

Low energy theory has 4 two-component Dirac fermions, ψ_σ, $\sigma = 1 \ldots 4$, interacting with a $1/r$ Coulomb interaction

$$\begin{aligned} \mathcal{S} &= \int d^2 r d\tau \psi_\sigma^\dagger \left(\partial_\tau - i v_F \vec{\sigma} \cdot \vec{\nabla} \right) \psi_\sigma \\ &\quad + \frac{e^2}{2} \int d^2 r d^2 r' d\tau \psi_\sigma^\dagger \psi_\sigma(r) \frac{1}{|r - r'|} \psi_{\sigma'}^\dagger \psi_{\sigma'}(r') \end{aligned}$$

Quantum critical graphene

Low energy theory has 4 two-component Dirac fermions, ψ_σ, $\sigma = 1 \ldots 4$, interacting with a $1/r$ Coulomb interaction

$$\mathcal{S} = \int d^2 r d\tau \psi_\sigma^\dagger \left(\partial_\tau - i v_F \vec{\sigma} \cdot \vec{\nabla} \right) \psi_\sigma + \frac{e^2}{2} \int d^2 r d^2 r' d\tau \psi_\sigma^\dagger \psi_\sigma(r) \frac{1}{|r - r'|} \psi_{\sigma'}^\dagger \psi_{\sigma'}(r')$$

Dimensionless "fine-structure" constant $\alpha = e^2/(\hbar v_F)$.
RG flow of α:

$$\frac{d\alpha}{d\ell} = -\alpha^2 + \ldots$$

Behavior is similar to a conformal field theory (CFT) in 2+1 dimensions with $\alpha \sim 1/\ln(\text{scale})$

Quantum phase transition in graphene

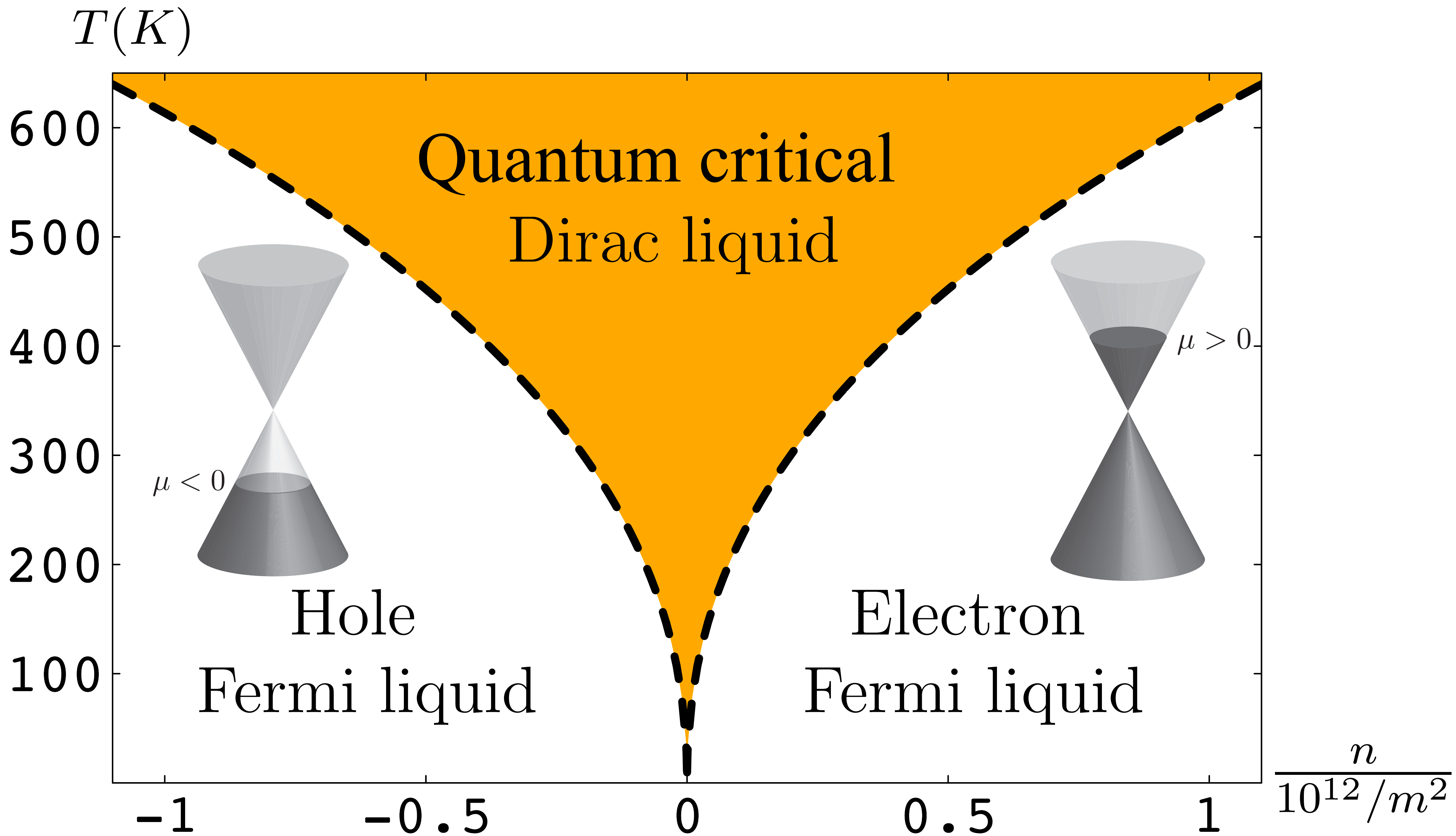

Outline

A. “Relativistic” field theories of quantum phase transitions

1. Coupled dimer antiferromagnets

2. Triangular lattice antiferromagnets

3. Graphene

4. AdS/CFT and quantum critical transport

Outline

A. "Relativistic" field theories of quantum phase transitions

1. Coupled dimer antiferromagnets
2. Triangular lattice antiferromagnets
3. Graphene
4. AdS/CFT and quantum critical transport

Quantum critical transport

Quantum *"perfect fluid"*
with shortest possible
relaxation time, τ_R

$$\boxed{\tau_R \gtrsim \frac{\hbar}{k_B T}}$$

S. Sachdev, *Quantum Phase Transitions,* Cambridge (1999).

Quantum critical transport

Transport co-oefficients not determined by collision rate, but by universal constants of nature

Electrical conductivity

$$\boxed{\sigma = \frac{e^2}{h} \times [\text{Universal constant } \mathcal{O}(1)\ ]}$$

K. Damle and S. Sachdev, *Phys. Rev. B* **56**, 8714 (1997).

Quantum critical transport

Transport co-oefficients not determined by collision rate, but by universal constants of nature

Momentum transport

$$\frac{\eta}{s} \equiv \frac{\text{viscosity}}{\text{entropy density}}$$
$$= \frac{\hbar}{k_B} \times [\text{Universal constant } \mathcal{O}(1)\ ]$$

P. Kovtun, D. T. Son, and A. Starinets, *Phys. Rev. Lett.* **94,** 11601 (2005)

Density correlations in CFTs at $T > 0$

Two-point density correlator, $\chi(k,\omega)$

Kubo formula for conductivity $\sigma(\omega) = \lim_{k\to 0} \dfrac{-i\omega}{k^2}\chi(k,\omega)$

For *all* CFT2s, at all $\hbar\omega/k_BT$

$$\chi(k,\omega) \quad = \quad \frac{4e^2}{h} K \frac{vk^2}{v^2k^2-\omega^2} \quad ; \quad \sigma(\omega) = \frac{4e^2}{h}\frac{Kv}{-i\omega}$$

where K is a universal number characterizing the CFT2 (the level number), and v is the velocity of "light".

This follows from the conformal mapping of the plane to the cylinder, which relates correlators at $T = 0$ to those at $T > 0$.

Density correlations in CFTs at $T > 0$

Two-point density correlator, $\chi(k, \omega)$

Kubo formula for conductivity $\sigma(\omega) = \lim_{k \to 0} \dfrac{-i\omega}{k^2} \chi(k, \omega)$

For *all* CFT2s, at all $\hbar\omega / k_B T$

$$\chi(k, \omega) = \frac{4e^2}{h} K \frac{v k^2}{v^2 k^2 - \omega^2} \quad ; \quad \sigma(\omega) = \frac{4e^2}{h} \frac{K v}{-i\omega}$$

where K is a universal number characterizing the CFT2 (the level number), and v is the velocity of "light".

This follows from the conformal mapping of the plane to the cylinder, which relates correlators at $T = 0$ to those at $T > 0$.

No hydrodynamics in CFT2s.

Density correlations in CFTs at $T > 0$

Two-point density correlator, $\chi(k,\omega)$

Kubo formula for conductivity $\sigma(\omega) = \lim_{k\to 0} \frac{-i\omega}{k^2}\chi(k,\omega)$

For *all* CFT3s, at $\underline{\hbar\omega \gg k_B T}$

$$\chi(k,\omega) = \frac{4e^2}{h} K \frac{k^2}{\sqrt{v^2k^2-\omega^2}} \quad ; \quad \sigma(\omega) = \frac{4e^2}{h} K$$

where K is a universal number characterizing the CFT3, and v is the velocity of "light".

Density correlations in CFTs at $T > 0$

Two-point density correlator, $\chi(k,\omega)$

Kubo formula for conductivity $\sigma(\omega) = \lim_{k\to 0} \dfrac{-i\omega}{k^2}\chi(k,\omega)$

However, for *all* CFT3s, at $\underline{\hbar\omega \ll k_B T}$, we have the Einstein relation

$$\chi(k,\omega) \quad = \quad 4e^2\chi_c \frac{Dk^2}{Dk^2 - i\omega} \quad ; \quad \sigma(\omega) = 4e^2 D\chi_c = \frac{4e^2}{h}\Theta_1\Theta_2$$

where the **compressibility**, χ_c, and the **diffusion constant** D obey

$$\chi = \frac{k_B T}{(hv)^2}\Theta_1 \quad ; \quad D = \frac{hv^2}{k_B T}\Theta_2$$

with Θ_1 and Θ_2 universal numbers characteristic of the CFT3

K. Damle and S. Sachdev, *Phys. Rev. B* **56**, 8714 (1997).

Density correlations in CFTs at $T > 0$

In CFT3s collisions are "phase" randomizing, and lead to relaxation to local thermodynamic equilibrium. So there is a crossover from collisionless behavior for $\hbar\omega \gg k_B T$, to hydrodynamic behavior for $\hbar\omega \ll k_B T$.

$$\sigma(\omega) = \begin{cases} \dfrac{4e^2}{h} K & , \quad \hbar\omega \gg k_B T \\[2ex] \dfrac{4e^2}{h} \Theta_1 \Theta_2 \equiv \sigma_Q & , \quad \hbar\omega \ll k_B T \end{cases}$$

and in general we expect $K \neq \Theta_1 \Theta_2$ (verified for Wilson-Fisher fixed point).

K. Damle and S. Sachdev, *Phys. Rev. B* **56**, 8714 (1997).

SU(N) SYM3 with $\mathcal{N} = 8$ supersymmetry

- Has a single dimensionful coupling constant, e_0, which flows to a strong-coupling fixed point $e_0 = e_0^*$ in the infrared.

- The CFT3 describing this fixed point resembles "critical spin liquid" theories.

- This CFT3 is the low energy limit of string theory on an M2 brane. The AdS/CFT correspondence provides a dual description using 11-dimensional supergravity on $\mathrm{AdS}_4 \times S_7$.

- The CFT3 has a global SO(8) R symmetry, and correlators of the SO(8) charge density can be computed exactly in the large N limit, even at $T > 0$.

SU(N) SYM3 with $\mathcal{N} = 8$ supersymmetry

- The SO(8) charge correlators of the CFT3 are given by the usual AdS/CFT prescription applied to the following gauge theory on AdS4:

$$\mathcal{S} = -\frac{1}{4g_{4D}^2}\int d^4x\sqrt{-g}g^{MA}g^{NB}F^a_{MN}F^a_{AB}$$

where $a = 1\ldots 28$ labels the generators of SO(8). Note that in large N theory, this looks like 28 copies of an Abelian gauge theory.

Collisionless to hydrodynamic crossover of SYM3

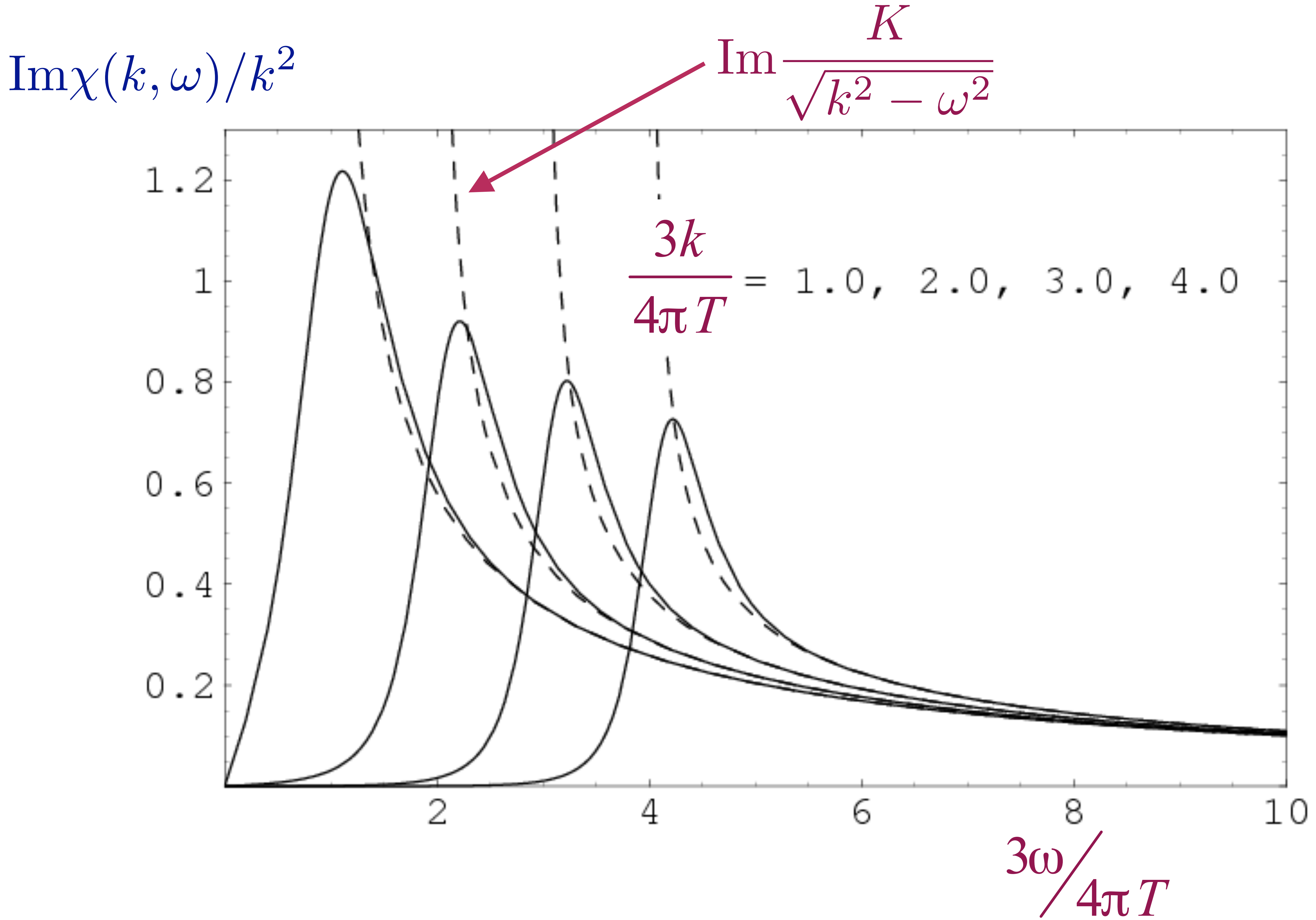

P. Kovtun, C. Herzog, S. Sachdev, and D.T. Son, Phys. Rev. D **75**, 085020 (2007)

Collisionless to hydrodynamic crossover of SYM3

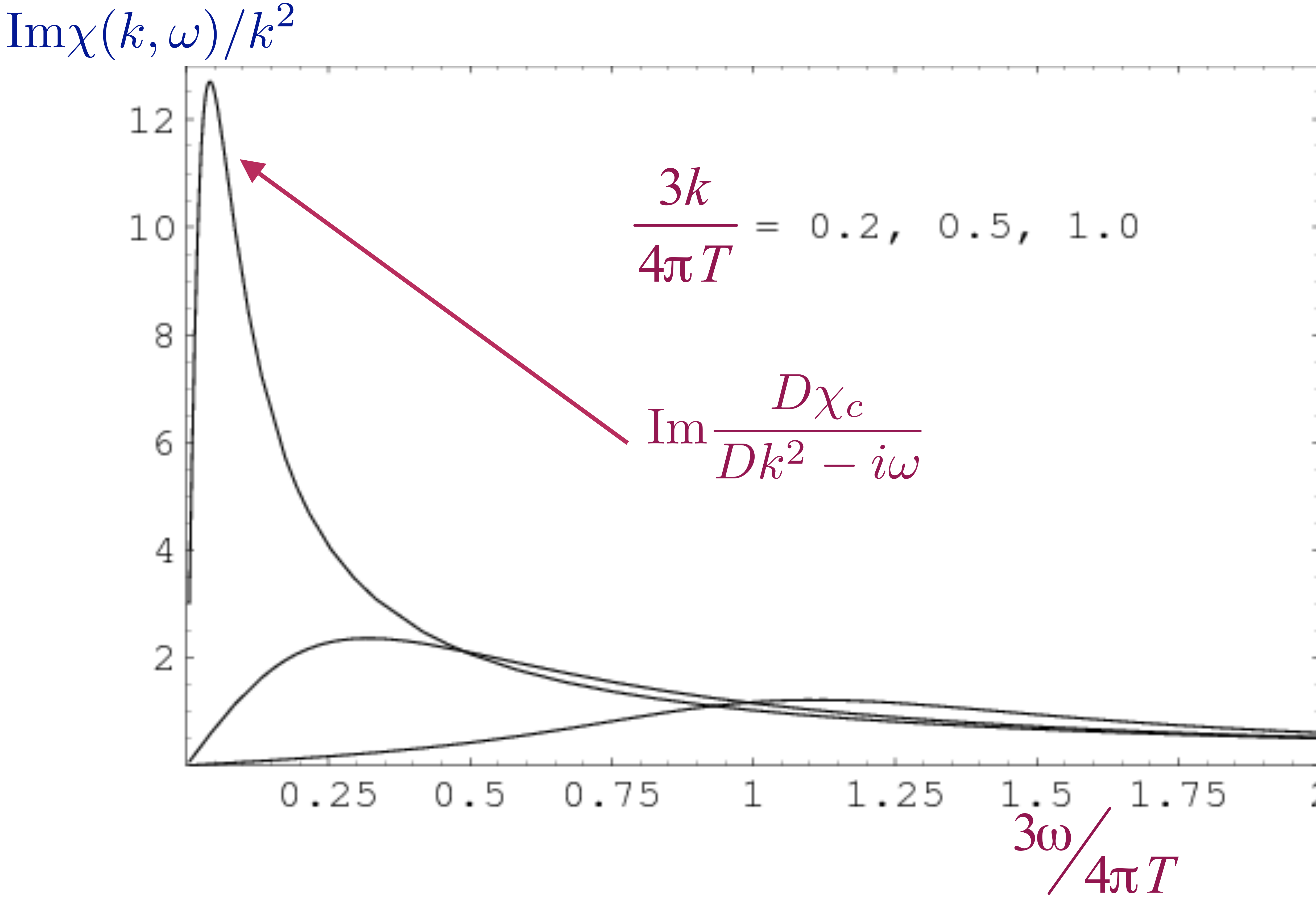

P. Kovtun, C. Herzog, S. Sachdev, and D.T. Son, Phys. Rev. D **75**, 085020 (2007)

Universal constants of SYM3

$$\chi_c = \frac{k_B T}{(hv)^2}\Theta_1$$

$$D = \frac{hv^2}{k_B T}\Theta_2$$

$$\sigma(\omega) = \begin{cases} \dfrac{4e^2}{h}K & , \quad \hbar\omega \gg k_B T \\ \dfrac{4e^2}{h}\Theta_1\Theta_2 & , \quad \hbar\omega \ll k_B T \end{cases}$$

$$\boxed{\begin{aligned} K &= \frac{\sqrt{2}N^{3/2}}{3} \\ \Theta_1 &= \frac{8\pi^2\sqrt{2}N^{3/2}}{9} \\ \Theta_2 &= \frac{3}{8\pi^2} \end{aligned}}$$

C. Herzog, JHEP **0212**, 026 (2002)

P. Kovtun, C. Herzog, S. Sachdev, and D.T. Son, Phys. Rev. D **75**, 085020 (2007)

Electromagnetic self-duality

- Unexpected result, $K = \Theta_1 \Theta_2$. Actually, a stronger result holds: $\sigma(\omega)$ is independent of ω for all $\hbar\omega/(k_B T)$.

Electromagnetic self-duality

- Unexpected result, $K = \Theta_1 \Theta_2$. Actually, a stronger result holds: $\sigma(\omega)$ is independent of ω for all $\hbar\omega/(k_B T)$.

- This is traced to a *four*-dimensional electromagnetic self-duality of the theory on AdS_4. In the large N limit, the SO(8) currents decouple into 28 U(1) currents with a Maxwell action for the U(1) gauge fields on AdS_4.

Electromagnetic self-duality

- Unexpected result, $K = \Theta_1 \Theta_2$. Actually, a stronger result holds: $\sigma(\omega)$ is independent of ω for all $\hbar\omega/(k_B T)$.

- This is traced to a *four*-dimensional electromagnetic self-duality of the theory on AdS_4. In the large N limit, the SO(8) currents decouple into 28 U(1) currents with a Maxwell action for the U(1) gauge fields on AdS_4.

- **Special properties of CFT3s with gravity duals**: $\sigma(\omega)$ is ω-independent and equal to the self-dual value. These results are the analog of $\eta/s = \hbar/(4k_B\pi)$.

Electromagnetic self-duality

- Unexpected result, $K = \Theta_1\Theta_2$. Actually, a stronger result holds: $\sigma(\omega)$ is independent of ω for all $\hbar\omega/(k_B T)$.

- This is traced to a *four*-dimensional electromagnetic self-duality of the theory on AdS_4. In the large N limit, the SO(8) currents decouple into 28 U(1) currents with a Maxwell action for the U(1) gauge fields on AdS_4.

- **Special properties of CFT3s with gravity duals**: $\sigma(\omega)$ is ω-independent and equal to the self-dual value. These results are the analog of $\eta/s = \hbar/(4k_B\pi)$.

- **Curious fact**: Experimental studies show a quantum critical σ close to the self-dual value.

Resistivity of Bi films

Conductivity σ

$$\sigma_{\text{Superconductor}}(T \to 0) = \infty$$

$$\sigma_{\text{Insulator}}(T \to 0) = 0$$

$$\sigma_{\text{Quantum critical point}}(T \to 0) \approx \frac{4e^2}{h}$$

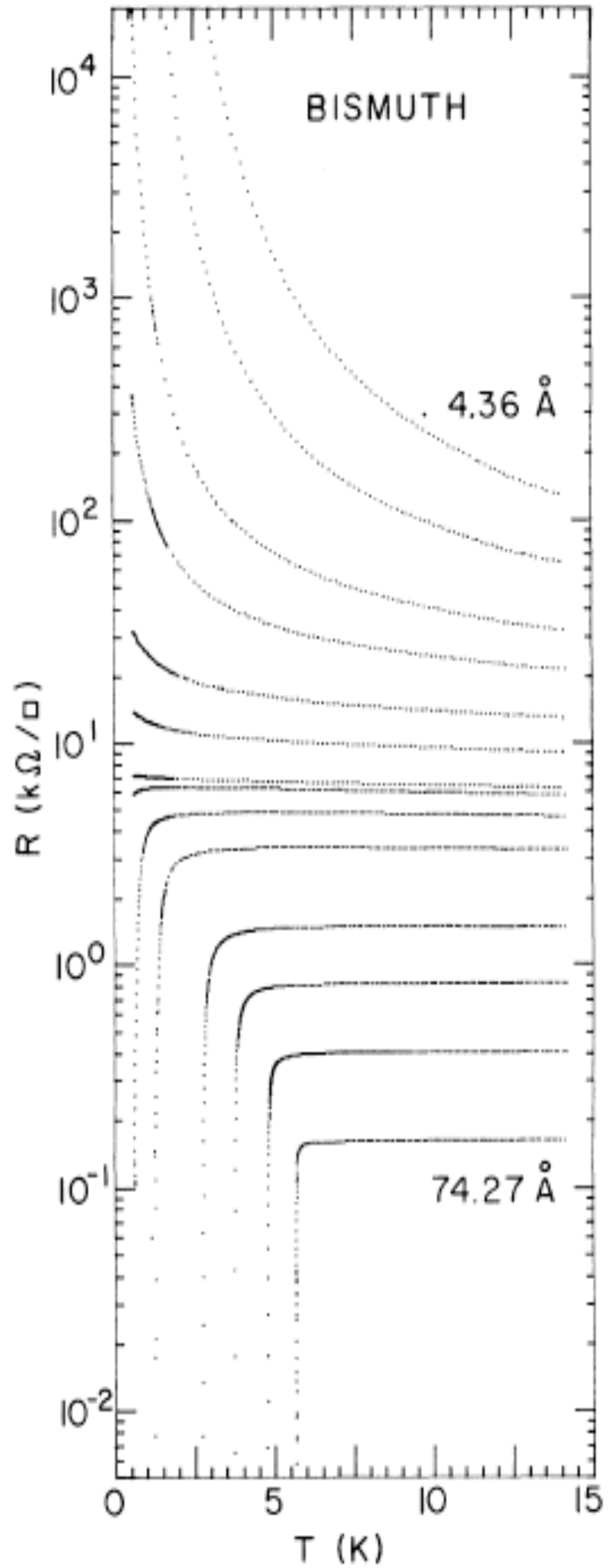

FIG. 1. Evolution of the temperature dependence of the sheet resistance $R(T)$ with thickness for a Bi film deposited onto Ge. Fewer than half of the traces actually acquired are shown. Film thicknesses shown range from 4.36 to 74.27 Å.

D. B. Haviland, Y. Liu, and A. M. Goldman, *Phys. Rev. Lett.* **62**, 2180 (1989)

M. P. A. Fisher, *Phys. Rev. Lett.* **65**, 923 (1990)

Quantum critical transport in graphene

$$\sigma(\omega) = \begin{cases} \dfrac{e^2}{h}\left[\dfrac{\pi}{2} + \mathcal{O}\left(\dfrac{1}{\ln(\Lambda/\omega)}\right)\right] & , \quad \hbar\omega \gg k_B T \\ \dfrac{e^2}{h\alpha^2(T)}\left[0.760 + \mathcal{O}\left(\dfrac{1}{|\ln(\alpha(T))|}\right)\right] & , \quad \hbar\omega \ll k_B T \alpha^2(T) \end{cases}$$

$$\frac{\eta}{s} = \frac{\hbar}{k_B \alpha^2(T)} \times 0.130$$

where the "fine structure constant" is

$$\alpha(T) = \frac{\alpha}{1 + (\alpha/4)\ln(\Lambda/T)} \overset{T\to 0}{\sim} \frac{4}{\ln(\Lambda/T)}$$

L. Fritz, J. Schmalian, M. Müller and S. Sachdev, *Physical Review B* **78**, 085416 (2008)
M. Müller, J. Schmalian, and L. Fritz, *Physical Review Letters* **103**, 025301 (2009)

Outline

A. “Relativistic” field theories of quantum phase transitions

1. Coupled dimer antiferromagnets

2. Triangular lattice antiferromagnets

3. Graphene

4. AdS/CFT and quantum critical transport

B. Finite density quantum matter

Outline

B. Finite density quantum matter

1. Graphene

   Fermi surfaces and Fermi liquids

2. Quantum phase transitions of Fermi liquids

   Pomeranchuk instability and spin density waves;
   Fermi surfaces and "non-Fermi liquids"

3. AdS_2 theory

4. Cuprate superconductivity

Outline

B. Finite density quantum matter

1. Graphene

   Fermi surfaces and Fermi liquids

2. Quantum phase transitions of Fermi liquids

   Pomeranchuk instability and spin density waves;
   Fermi surfaces and "non-Fermi liquids"

3. AdS_2 theory

4. Cuprate superconductivity

Quantum phase transition in graphene

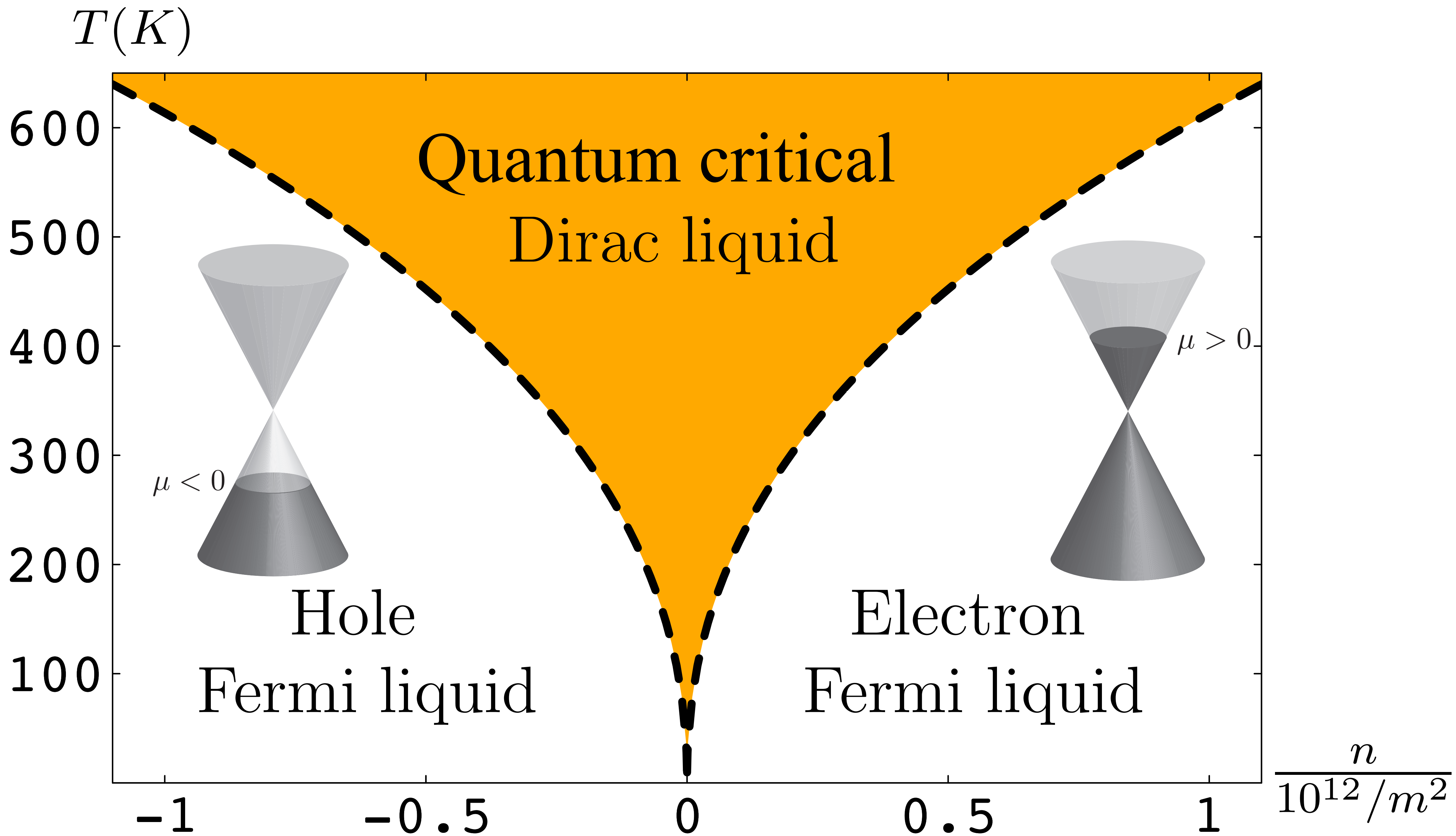

Electron Green's function in Fermi liquid (T=0)

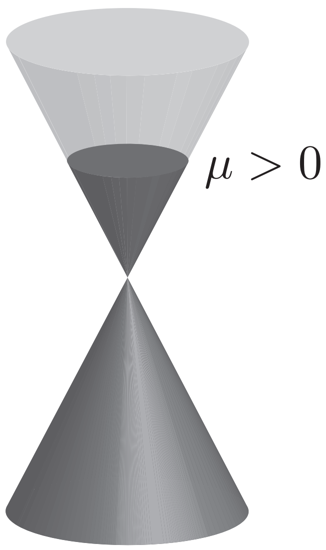

$$G(k,\omega) = \frac{Z}{\omega - v_F(k-k_F) - i\omega^2 \mathcal{F}\left(\frac{k-k_F}{\omega}\right)} + \ldots$$

Electron Green's function in Fermi liquid (T=0)

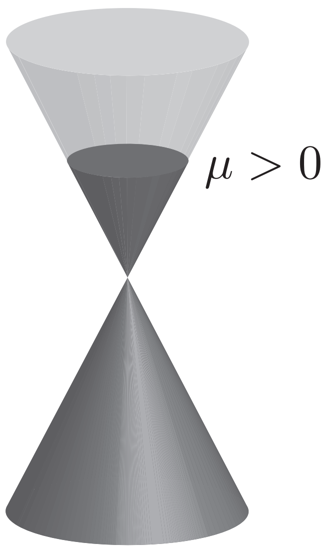

$$G(k,\omega) = \frac{Z}{\omega - v_F(k-k_F) - i\omega^2 \mathcal{F}\left(\frac{k-k_F}{\omega}\right)} + \ldots$$

Green's function has a pole in the LHP at

$$\omega = v_F(k-k_F) - i\alpha(k-k_F)^2 + \ldots$$

Pole is at $\omega = 0$ precisely at $k = k_F$ *i.e.* on a sphere of radius k_F in momentum space. This is the *Fermi surface.*

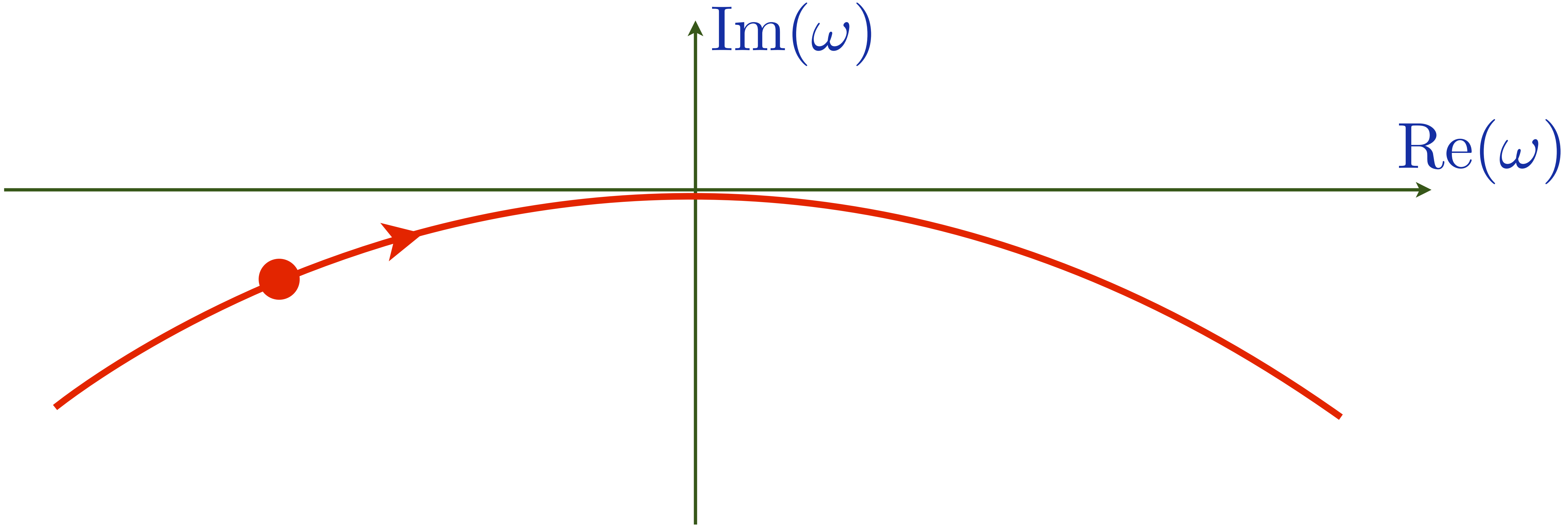

Outline

B. Finite density quantum matter

1. Graphene

   Fermi surfaces and Fermi liquids

2. Quantum phase transitions of Fermi liquids

   Pomeranchuk instability and spin density waves;
   Fermi surfaces and "non-Fermi liquids"

3. AdS_2 theory

4. Cuprate superconductivity

Outline

B. Finite density quantum matter

1. Graphene
   Fermi surfaces and Fermi liquids

2. Quantum phase transitions of Fermi liquids
   Pomeranchuk instability and spin density waves;
   Fermi surfaces and "non-Fermi liquids"

3. AdS_2 theory

4. Cuprate superconductivity

Quantum criticality of Pomeranchuk instability

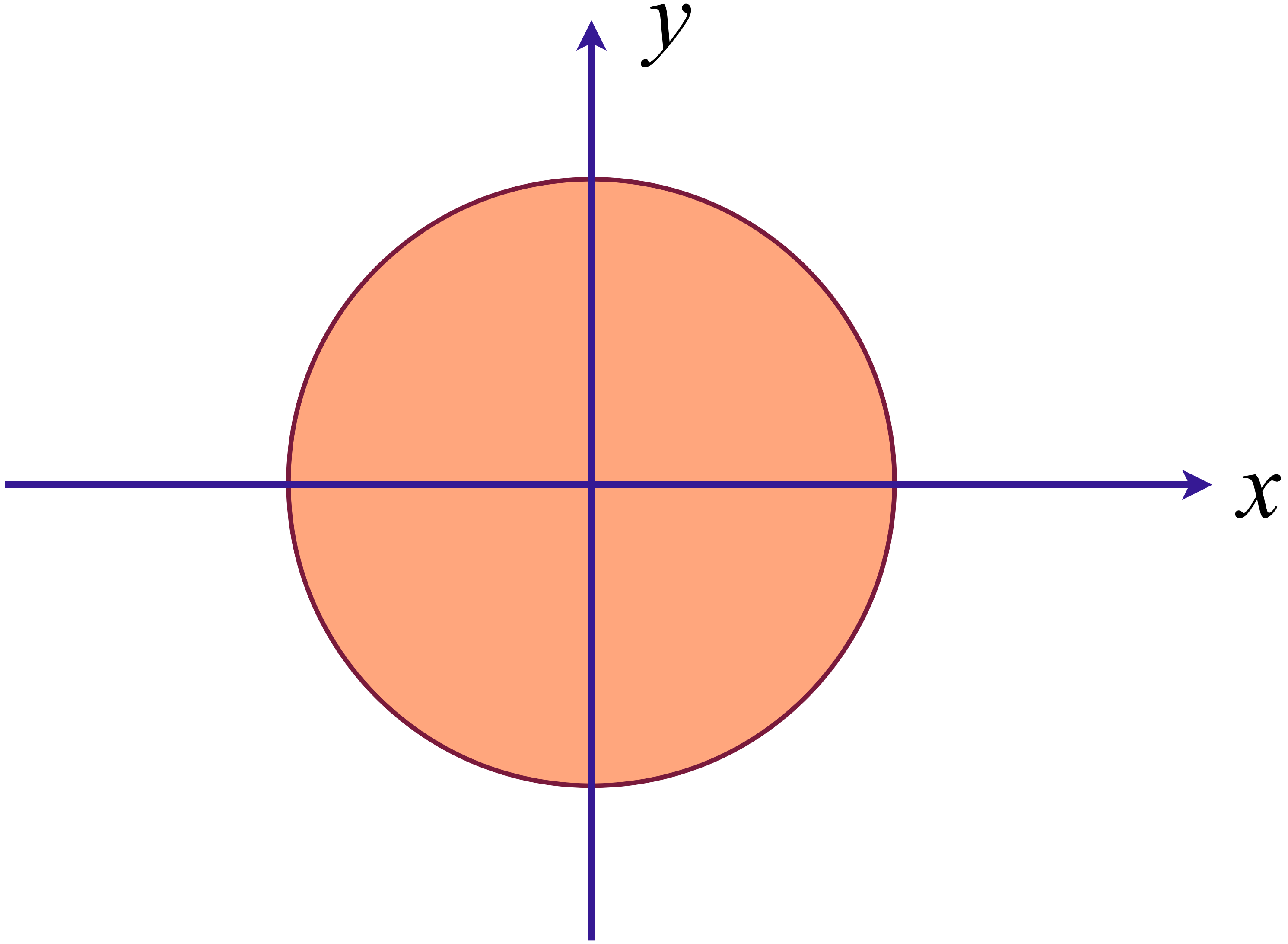

Fermi surface with full square lattice symmetry

Quantum criticality of Pomeranchuk instability

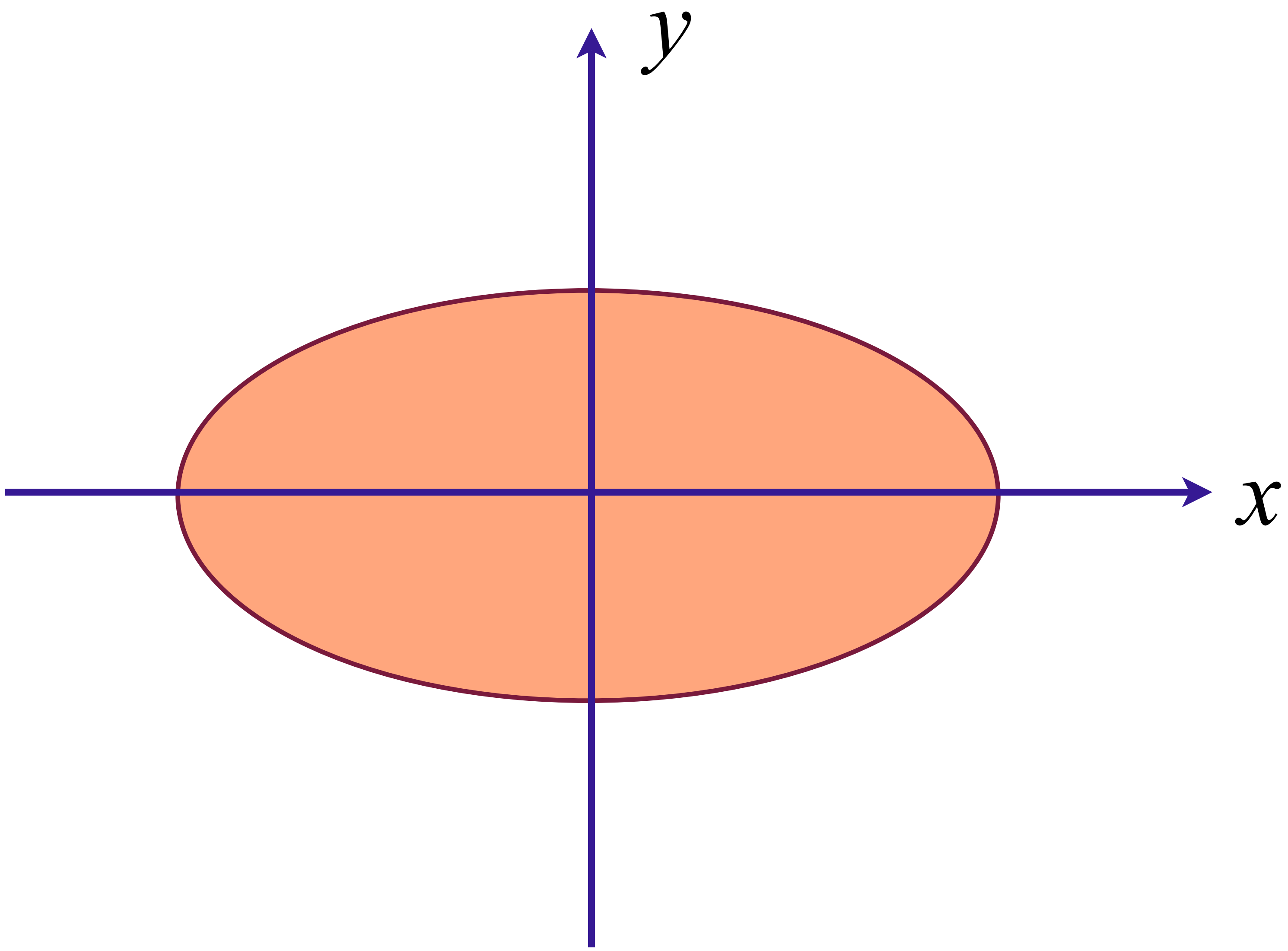

Spontaneous elongation along x direction:
Ising order parameter $\phi > 0$.

Quantum criticality of Pomeranchuk instability

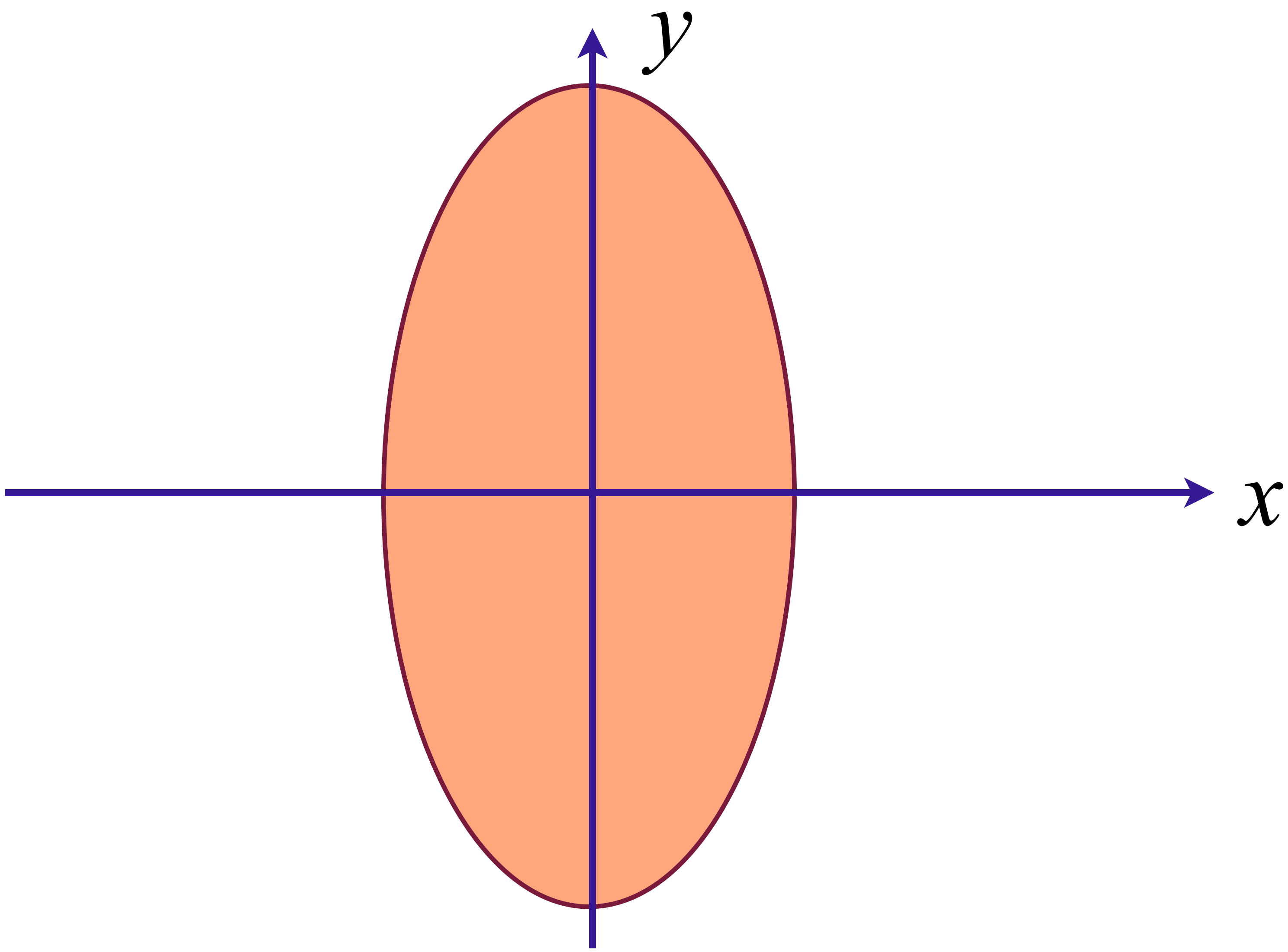

Spontaneous elongation along y direction:
Ising order parameter $\phi < 0$.

Quantum criticality of Pomeranchuk instability

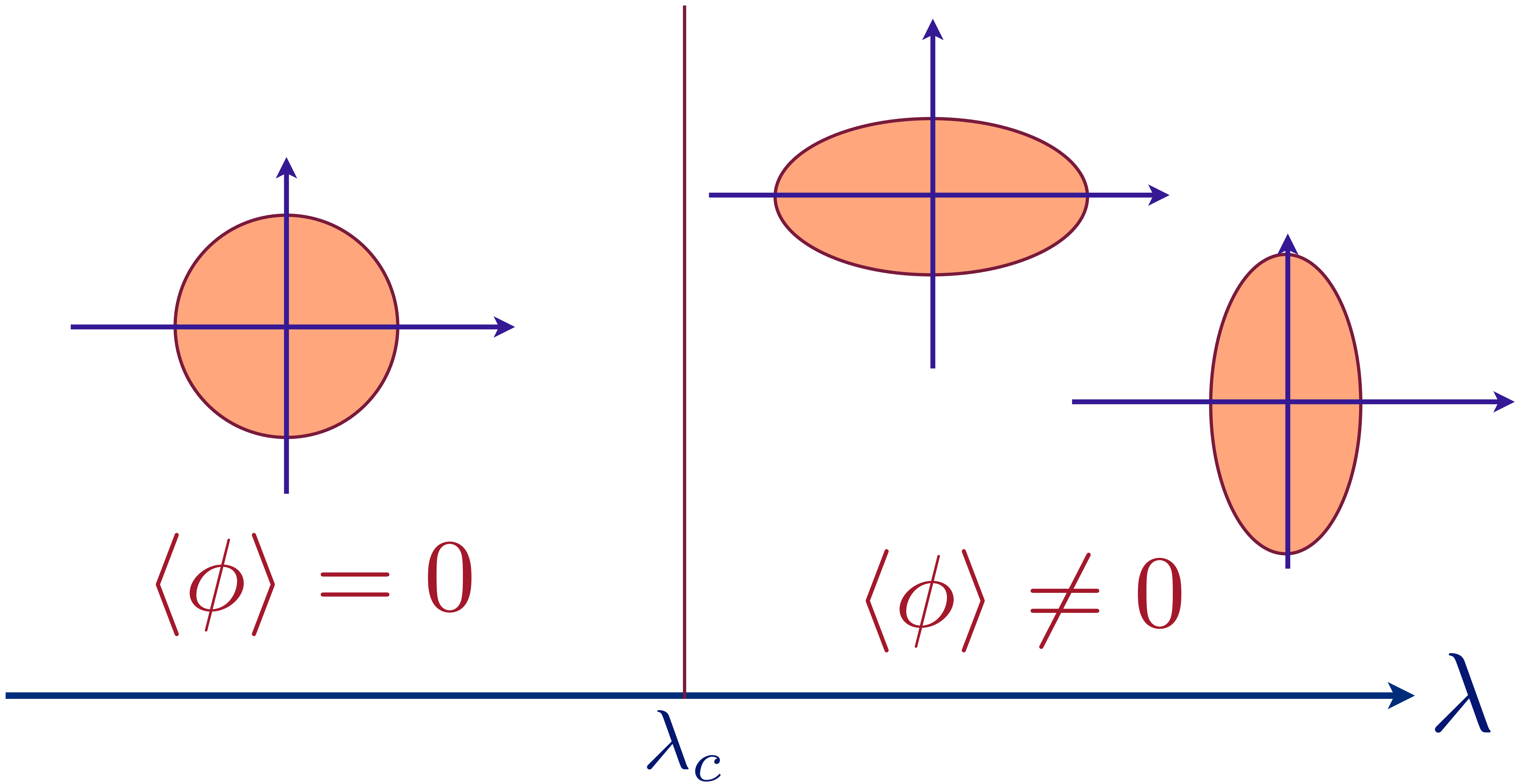

Pomeranchuk instability as a function of coupling λ

Quantum criticality of Pomeranchuk instability

Effective action for Ising order parameter

$$\mathcal{S}_\phi = \int d^2 r d\tau \left[(\partial_\tau \phi)^2 + c^2 (\nabla \phi)^2 + (\lambda - \lambda_c) \phi^2 + u \phi^4 \right]$$

Quantum criticality of Pomeranchuk instability

Effective action for Ising order parameter

$$\mathcal{S}_\phi = \int d^2 r d\tau \left[(\partial_\tau \phi)^2 + c^2 (\nabla \phi)^2 + (\lambda - \lambda_c)\phi^2 + u\phi^4 \right]$$

Effective action for electrons:

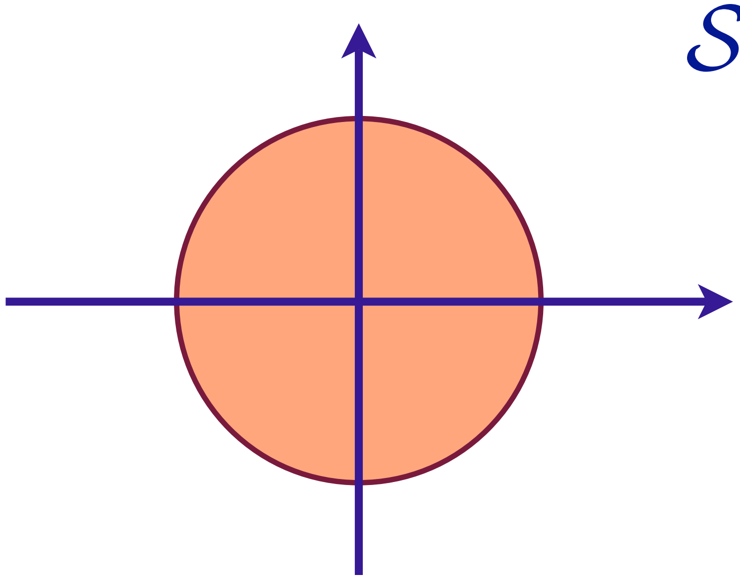

$$\begin{aligned} \mathcal{S}_c &= \int d\tau \sum_{\alpha=1}^{N_f} \left[\sum_i c_{i\alpha}^\dagger \partial_\tau c_{i\alpha} - \sum_{i<j} t_{ij} c_{i\alpha}^\dagger c_{i\alpha} \right] \\ &\equiv \sum_{\alpha=1}^{N_f} \sum_{\mathbf{k}} \int d\tau c_{\mathbf{k}\alpha}^\dagger \left(\partial_\tau + \varepsilon_{\mathbf{k}} \right) c_{\mathbf{k}\alpha} \end{aligned}$$

Quantum criticality of Pomeranchuk instability

Coupling between Ising order and electrons

$$\mathcal{S}_{\phi c} = -\gamma \int d\tau\, \phi \sum_{\alpha=1}^{N_f} \sum_{\mathbf{k}} (\cos k_x - \cos k_y) c_{\mathbf{k}\alpha}^{\dagger} c_{\mathbf{k}\alpha}$$

for spatially independent ϕ

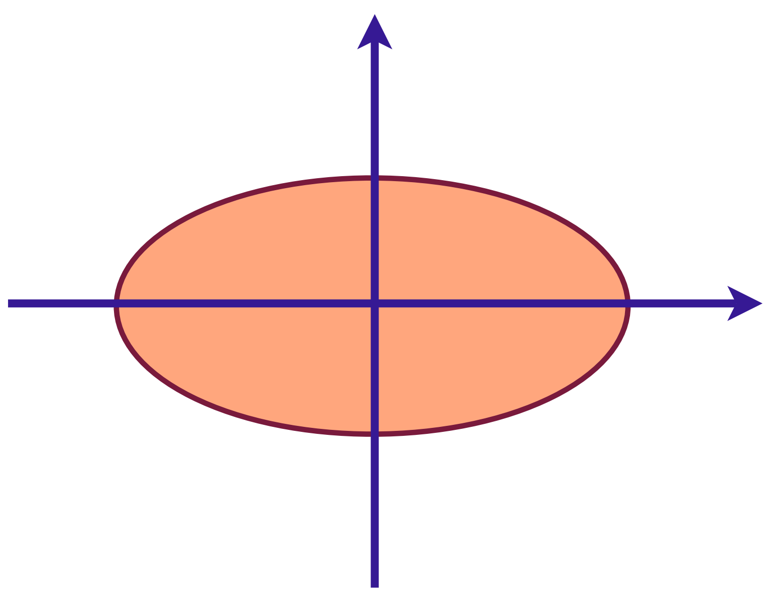

$$\langle \phi \rangle > 0$$

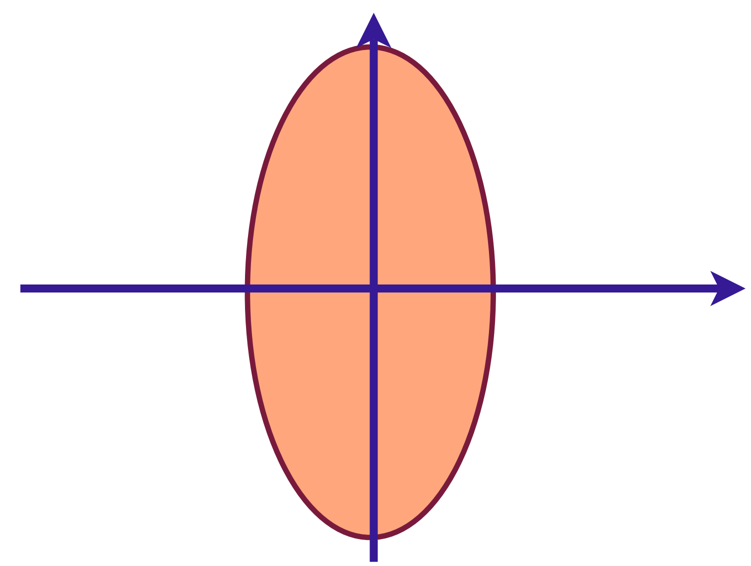

$$\langle \phi \rangle < 0$$

Quantum criticality of Pomeranchuk instability

Coupling between Ising order and electrons

$$\mathcal{S}_{\phi c} = -\gamma \int d\tau \sum_{\alpha=1}^{N_f} \sum_{\mathbf{k},\mathbf{q}} \phi_{\mathbf{q}} \left(\cos k_x - \cos k_y\right) c^\dagger_{\mathbf{k}+\mathbf{q}/2,\alpha} c_{\mathbf{k}-\mathbf{q}/2,\alpha}$$

for spatially dependent ϕ

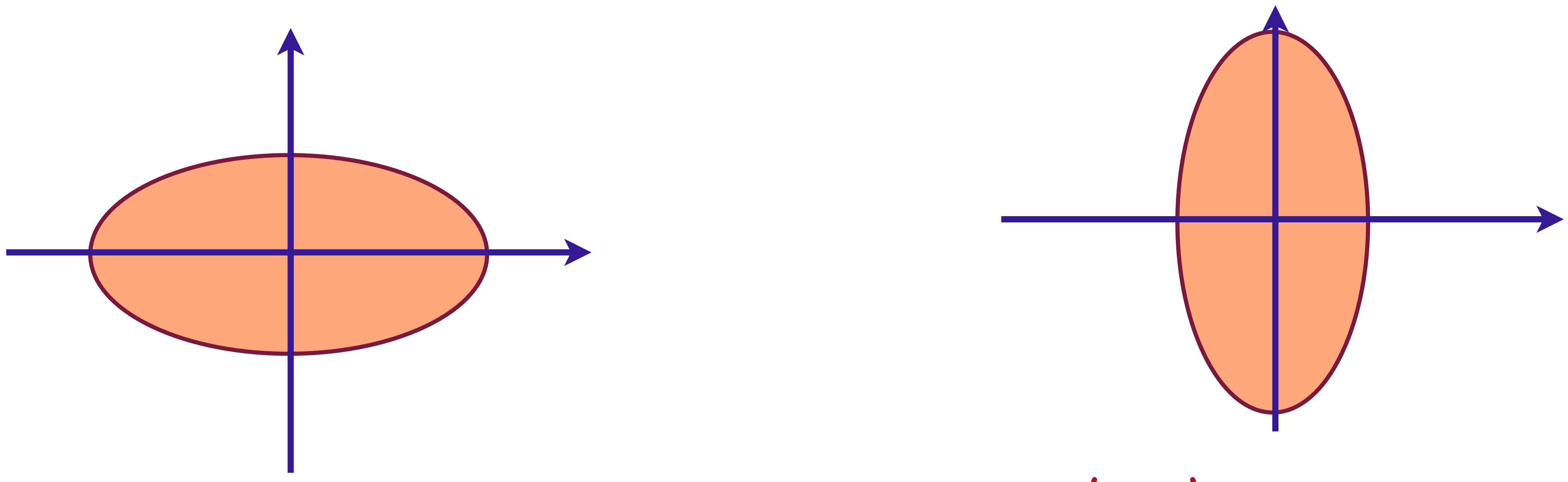

$\langle \phi \rangle > 0$ $\qquad\qquad$ $\langle \phi \rangle < 0$

Quantum criticality of Pomeranchuk instability

$$\mathcal{S}_\phi = \int d^2r d\tau \left[(\partial_\tau \phi)^2 + c^2 (\nabla \phi)^2 + (\lambda - \lambda_c)\phi^2 + u\phi^4 \right]$$

$$\mathcal{S}_c = \sum_{\alpha=1}^{N_f} \sum_{\mathbf{k}} \int d\tau c_{\mathbf{k}\alpha}^\dagger \left(\partial_\tau + \varepsilon_{\mathbf{k}} \right) c_{\mathbf{k}\alpha}$$

$$\mathcal{S}_{\phi c} = -\gamma \int d\tau \sum_{\alpha=1}^{N_f} \sum_{\mathbf{k},\mathbf{q}} \phi_{\mathbf{q}} \left(\cos k_x - \cos k_y \right) c_{\mathbf{k}+\mathbf{q}/2,\alpha}^\dagger c_{\mathbf{k}-\mathbf{q}/2,\alpha}$$

Quantum critical field theory

$$\mathcal{Z} = \int \mathcal{D}\phi \mathcal{D}c_{i\alpha} \exp\left(-\mathcal{S}_\phi - \mathcal{S}_c - \mathcal{S}_{\phi c} \right)$$

Quantum criticality of Pomeranchuk instability

$\boxed{\text{Hertz theory}}$

Integrate out c_α fermions and obtain non-local corrections to ϕ action

$$\delta \mathcal{S}_\phi \sim N_f \gamma^2 \int \frac{d^2 q}{4\pi^2} \int \frac{d\omega}{2\pi} |\phi(\mathbf{q}, \omega)|^2 \left[\frac{|\omega|}{q} + q^2 \right] + \ldots$$

This leads to a critical point with dynamic critical exponent $z = 3$ and quantum criticality controlled by the Gaussian fixed point.

Quantum criticality of Pomeranchuk instability

Hertz theory

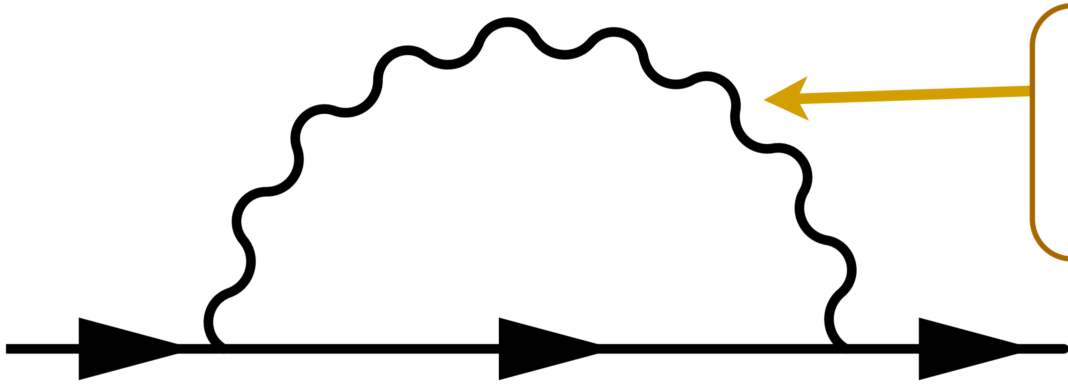

$$\frac{1}{N_f(q^2 + |\omega|/q)}$$

Self energy of c_α fermions to order $1/N_f$

$$\Sigma_c(k,\omega) \sim \frac{i}{N_f}\omega^{2/3}$$

This leads to the Green's function

$$G(k,\omega) \approx \frac{1}{\omega - v_F(k - k_F) - \frac{i}{N_f}\omega^{2/3}}$$

Note that the order $1/N_f$ term is more singular in the infrared than the bare term; this leads to problems in the bare $1/N_f$ expansion in terms that are dominated by low frequency fermions.

Quantum criticality of Pomeranchuk instability

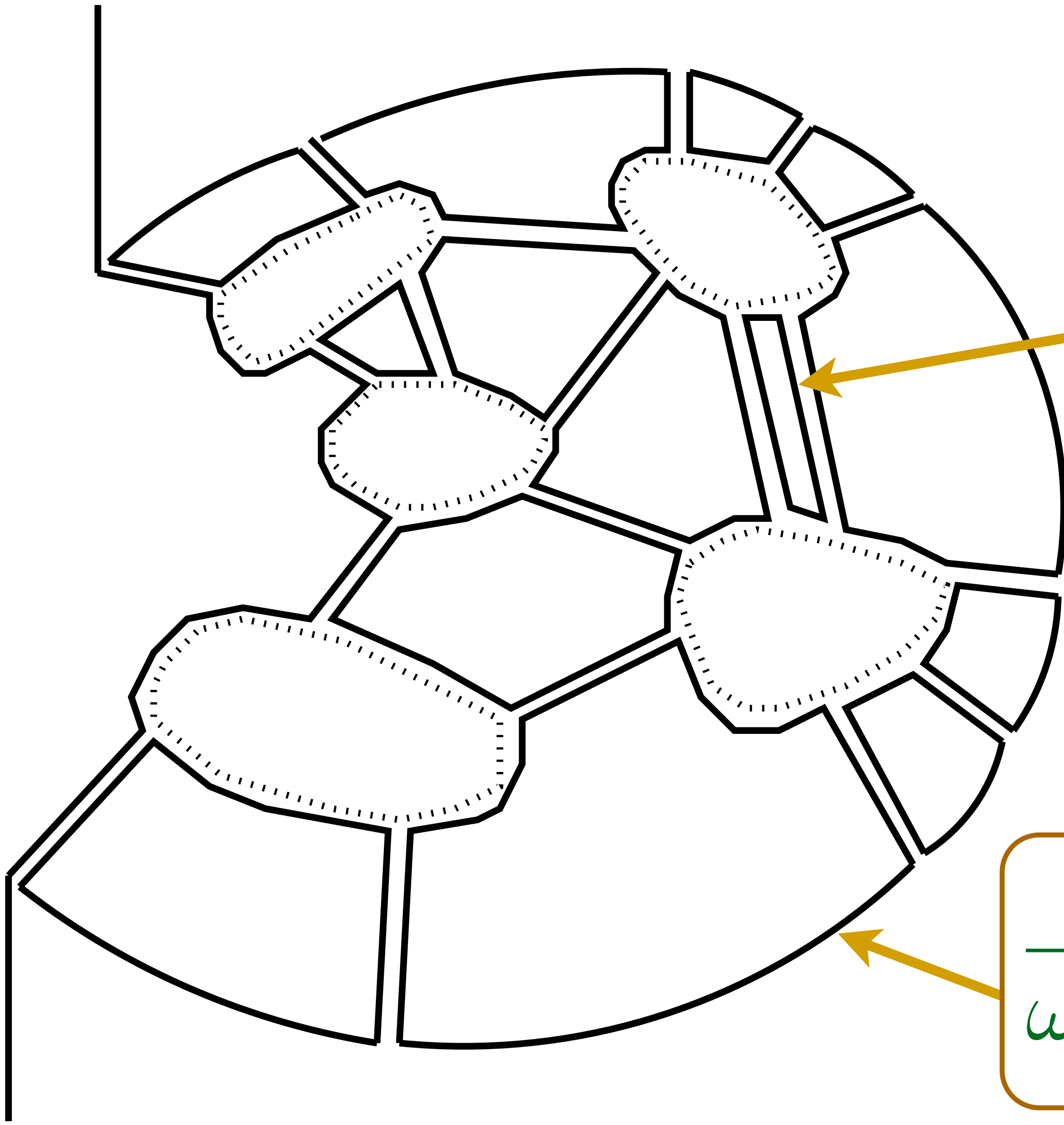

$$\frac{1}{N_f(q^2 + |\omega|/q)}$$

$$\frac{1}{\omega - v_F(k - k_F) - \frac{i}{N_f}\omega^{2/3}}$$

The infrared singularities of fermion particle-hole pairs are most severe on planar graphs: these all contribute at leading order in $1/N_f$.

Sung-Sik Lee, arXiv:0905.4532

Evolution of the (ARPES) Fermi surface on the cuprate phase diagram

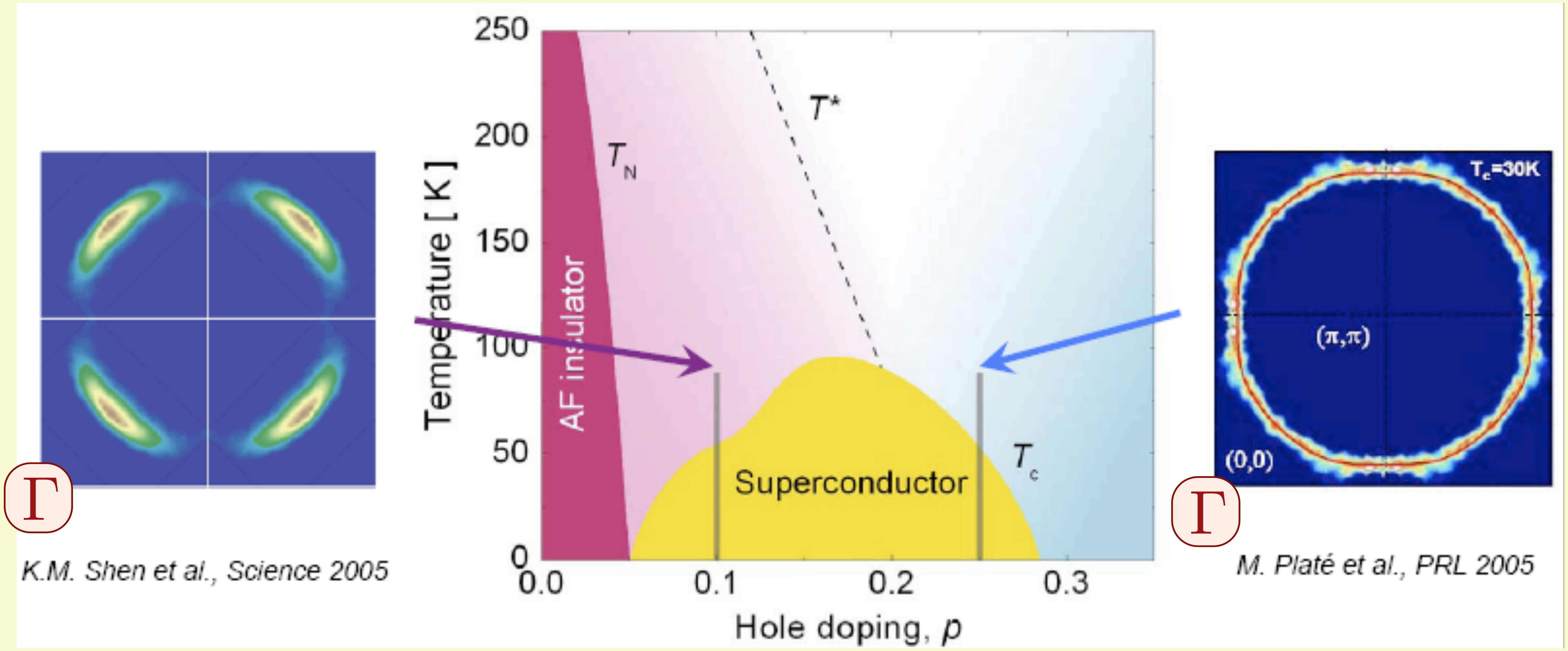

Smaller hole Fermi-pockets

Large hole Fermi surface

Fermi surfaces in electron- and hole-doped cuprates

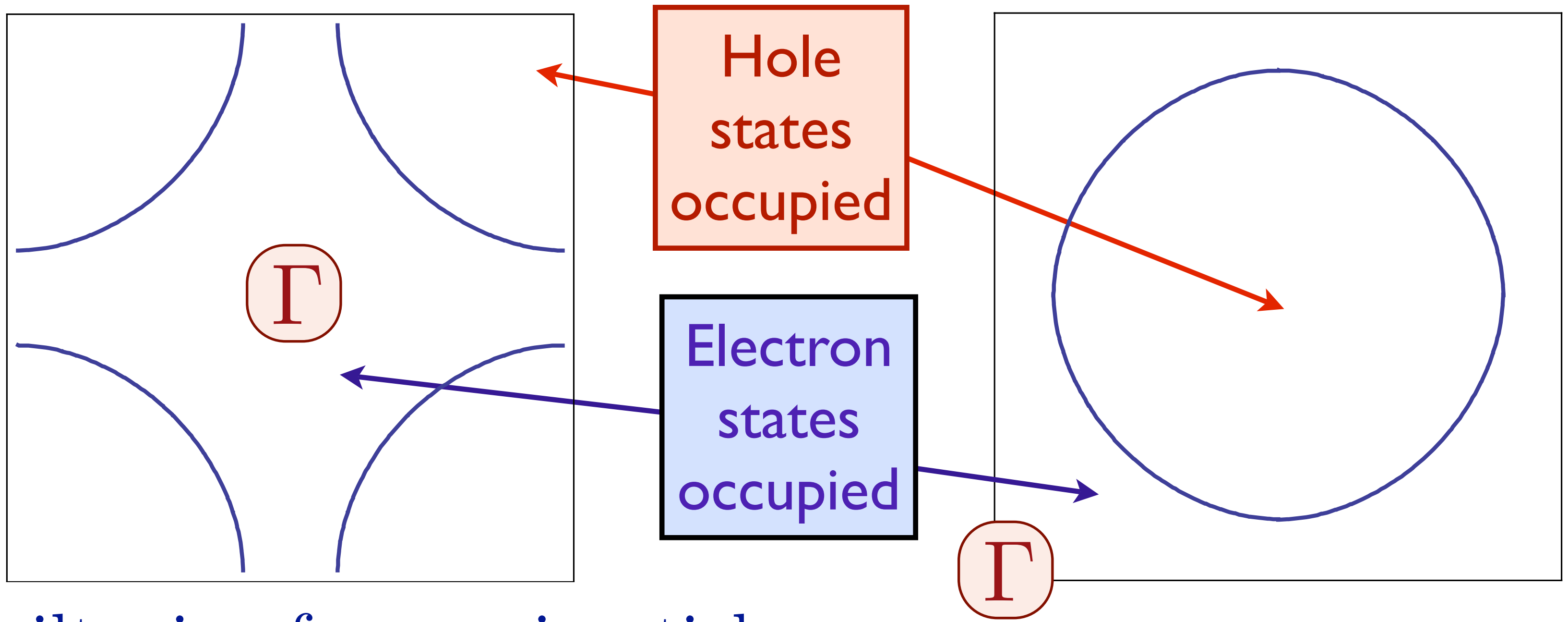

Effective Hamiltonian for quasiparticles:

$$H_0 = -\sum_{i<j} t_{ij} c^\dagger_{i\alpha} c_{i\alpha} \equiv \sum_{\mathbf{k}} \varepsilon_{\mathbf{k}} c^\dagger_{\mathbf{k}\alpha} c_{\mathbf{k}\alpha}$$

with t_{ij} non-zero for first, second and third neighbor, leads to satisfactory agreement with experiments. The area of the occupied electron states, $\mathcal{A}_e$, from Luttinger's theory is

$$\mathcal{A}_e = \begin{cases} 2\pi^2(1-p) & \text{for hole-doping } p \\ 2\pi^2(1+x) & \text{for electron-doping } x \end{cases}$$

The area of the occupied hole states, $\mathcal{A}_h$, which form a closed Fermi surface and so appear in quantum oscillation experiments is $\mathcal{A}_h = 4\pi^2 - \mathcal{A}_e$.

Spin density wave theory

A spin density wave (SDW) is the spontaneous appearance of an oscillatory spin polarization. The electron spin polarization is written as

$$\vec{S}(\mathbf{r},\tau) = \vec{\varphi}(\mathbf{r},\tau)e^{i\mathbf{K}\cdot\mathbf{r}}$$

where $\vec{\varphi}$ is the SDW order parameter, and $\mathbf{K}$ is a fixed ordering wavevector. For simplicity we will consider the case of $\mathbf{K} = (\pi,\pi)$, but our treatment applies to general $\mathbf{K}$.

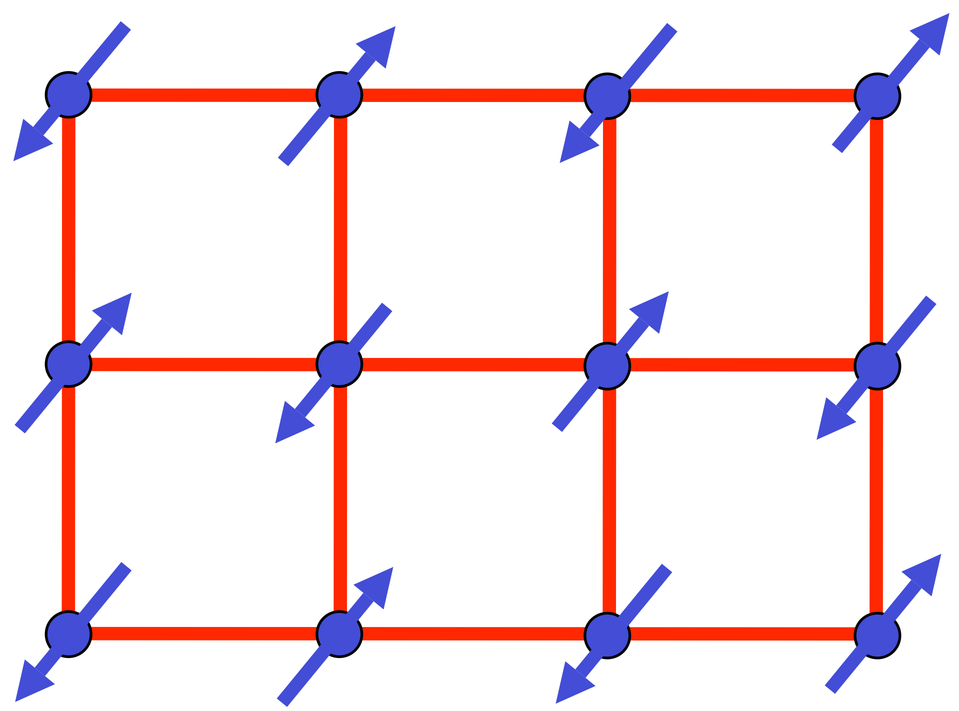

Spin density wave theory

In the presence of spin density wave order, $\vec{\varphi}$ at wavevector $\mathbf{K} = (\pi, \pi)$, we have an additional term which mixes electron states with momentum separated by $\mathbf{K}$

$$H_{\rm sdw} = \vec{\varphi} \cdot \sum_{\mathbf{k},\alpha,\beta} c^\dagger_{\mathbf{k},\alpha} \vec{\sigma}_{\alpha\beta} c_{\mathbf{k}+\mathbf{K},\beta}$$

where $\vec{\sigma}$ are the Pauli matrices. The electron dispersions obtained by diagonalizing $H_0 + H_{\rm sdw}$ for $\vec{\varphi} \propto (0,0,1)$ are

$$E_{\mathbf{k}\pm} = \frac{\varepsilon_{\mathbf{k}} + \varepsilon_{\mathbf{k}+\mathbf{K}}}{2} \pm \sqrt{\left(\frac{\varepsilon_{\mathbf{k}} - \varepsilon_{\mathbf{k}+\mathbf{K}}}{2}\right) + \varphi^2}$$

This leads to the Fermi surfaces shown in the following slides for electron and hole doping.

Spin density wave theory in hole-doped cuprates

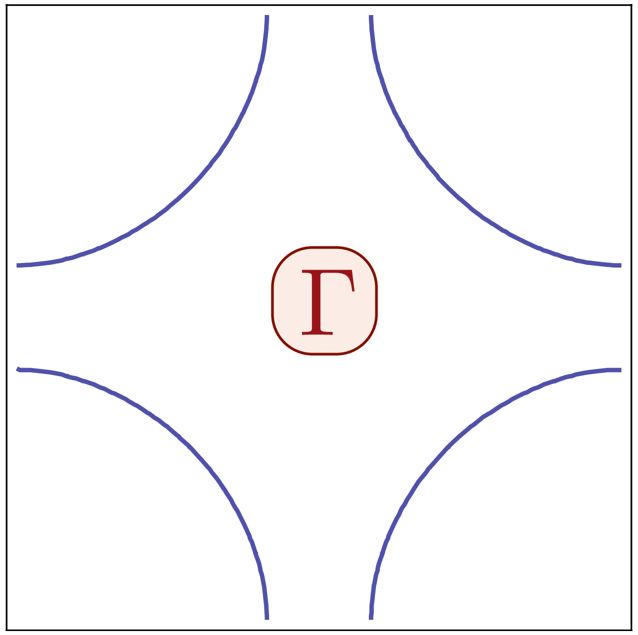

S. Sachdev, A. V. Chubukov, and A. Sokol, *Phys. Rev. B* **51**, 14874 (1995).
A. V. Chubukov and D. K. Morr, *Physics Reports* **288**, 355 (1997).

Spin density wave theory in hole-doped cuprates

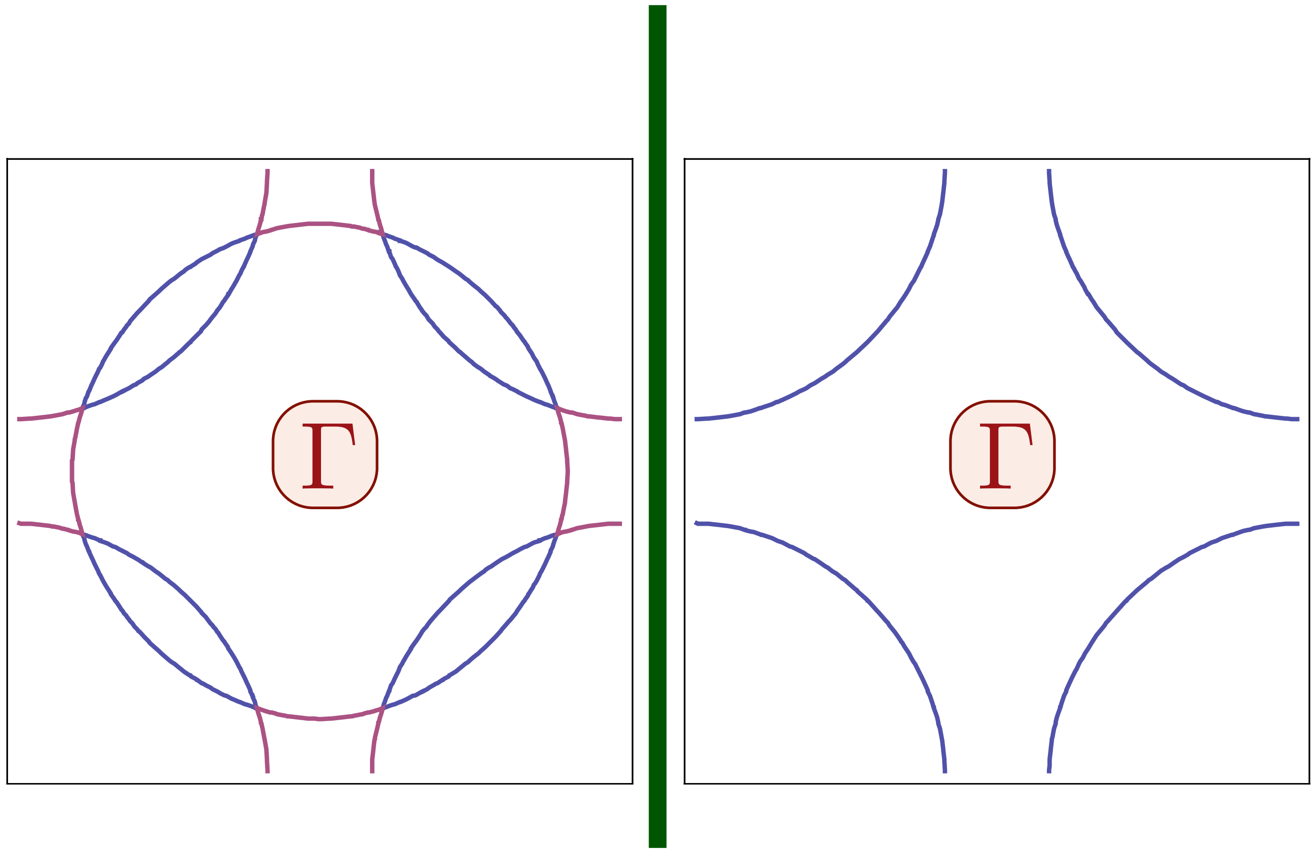

S. Sachdev, A. V. Chubukov, and A. Sokol, *Phys. Rev. B* **51**, 14874 (1995).
A. V. Chubukov and D. K. Morr, *Physics Reports* **288**, 355 (1997).

Spin density wave theory in hole-doped cuprates

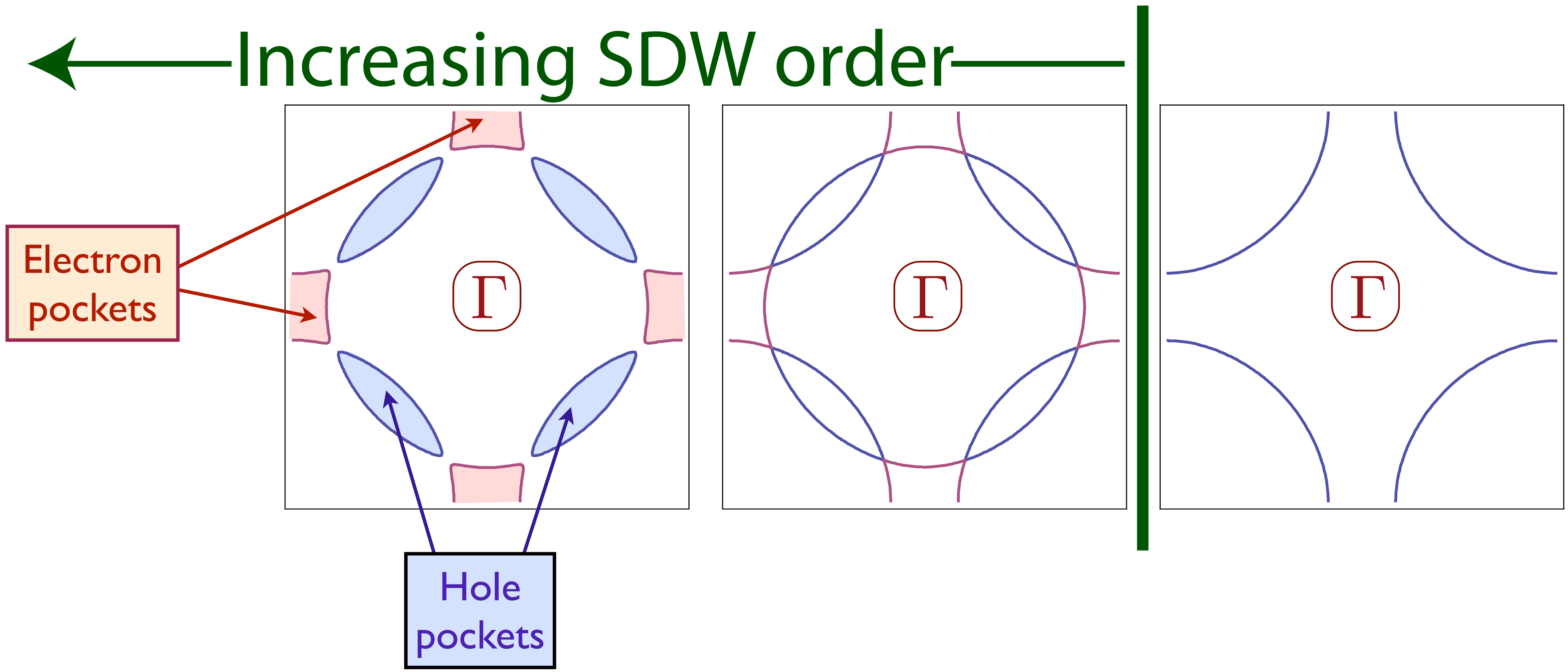

S. Sachdev, A. V. Chubukov, and A. Sokol, *Phys. Rev. B* **51**, 14874 (1995).
A. V. Chubukov and D. K. Morr, *Physics Reports* **288**, 355 (1997).

Spin density wave theory in hole-doped cuprates

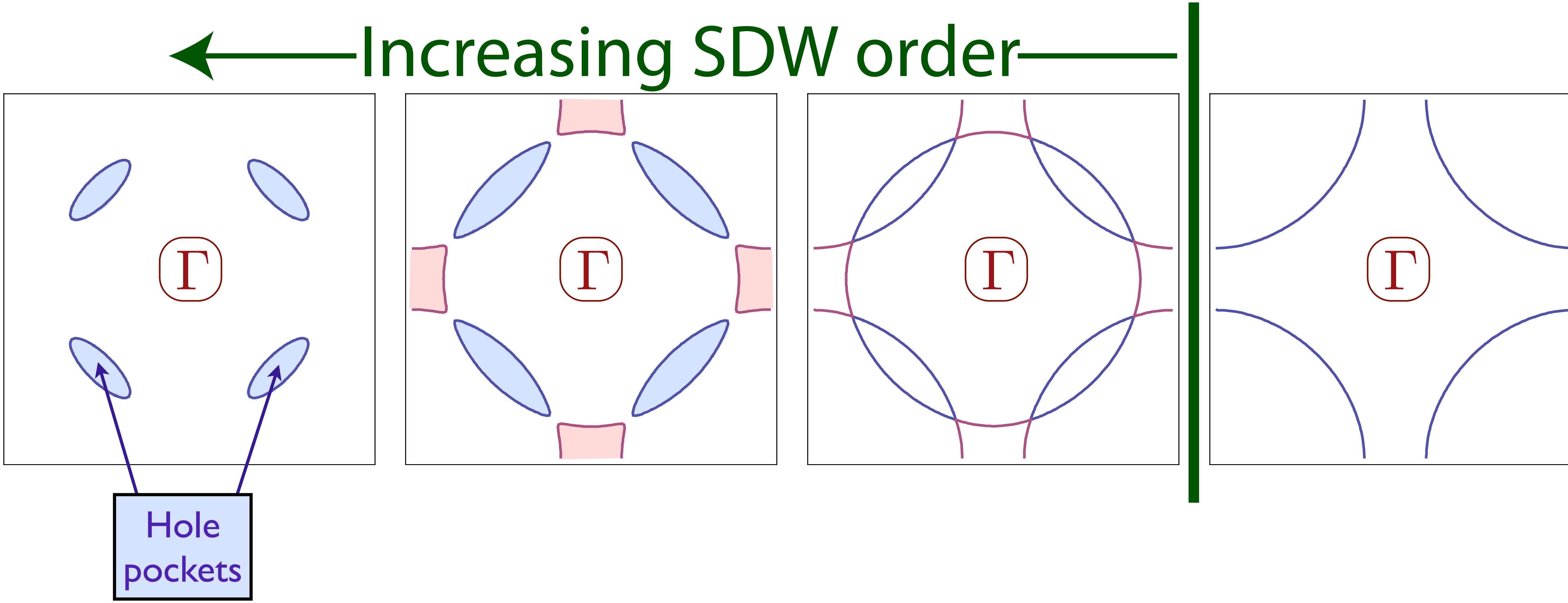

SDW order parameter is a vector, $\vec{\varphi}$, whose amplitude vanishes at the transition to the Fermi liquid.

S. Sachdev, A.V. Chubukov, and A. Sokol, *Phys. Rev. B* **51**, 14874 (1995).
A.V. Chubukov and D. K. Morr, *Physics Reports* **288**, 355 (1997).

Spin density wave theory

In the presence of spin density wave order, $\vec{\varphi}$ at wavevector $\mathbf{K} = (\pi, \pi)$, we have an additional term which mixes electron states with momentum separated by $\mathbf{K}$

$$H_{\rm sdw} = \vec{\varphi} \cdot \sum_{\mathbf{k},\alpha,\beta} c^{\dagger}_{\mathbf{k},\alpha} \vec{\sigma}_{\alpha\beta} c_{\mathbf{k}+\mathbf{K},\beta}$$

where $\vec{\sigma}$ are the Pauli matrices. At the quantum critical point for the onset of SDW order, we integrate out the fermions and derive an effective action functional for $\vec{\varphi}$.

Spin density wave theory

This functional has the form

$$\mathcal{S} = \int \frac{d^2 q}{4\pi^2} \int \frac{d\omega}{2\pi} |\vec{\varphi}(\mathbf{q},\omega)|^2 \Big[r + q^2 + \chi(\mathbf{K},\omega) \Big] + u \int d^2 x d\tau (\vec{\varphi}^2(x,\tau))^2 + \ldots$$

The susceptibility, χ, has a non-analytic dependence on ω because of Landau damping:

$$\chi(\mathbf{K},\omega) = \chi_0 + \chi_1 |\omega| + \ldots$$

This leads to a critical point with dynamic critical exponent $z = 2$, and upper-critical dimension $d = 2$.

Spin density wave theory

This functional has the form

$$
\begin{aligned}
\mathcal{S} &= \int \frac{d^2q}{4\pi^2} \int \frac{d\omega}{2\pi} |\vec{\varphi}(\mathbf{q},\omega)|^2 \Big[r + q^2 + \chi(\mathbf{K},\omega) \Big] \\
&\quad + u \int d^2x d\tau (\vec{\varphi}^2(x,\tau))^2 + \ldots
\end{aligned}
$$

However, the higher order corrections require summation of all planar graphs, as in the Pomeranchuk instability.

M. Metlitski

Outline

B. Finite density quantum matter

1. Graphene

   Fermi surfaces and Fermi liquids

2. Quantum phase transitions of Fermi liquids

   Pomeranchuk instability and spin density waves;
   Fermi surfaces and "non-Fermi liquids"

3. AdS_2 theory

4. Cuprate superconductivity

Outline

B. Finite density quantum matter

1. Graphene
   Fermi surfaces and Fermi liquids

2. Quantum phase transitions of Fermi liquids
   Pomeranchuk instability and spin density waves; Fermi surfaces and "non-Fermi liquids"

3. AdS_2 theory

4. Cuprate superconductivity

Conformal field theory in 2+1 dimensions at $T = 0$

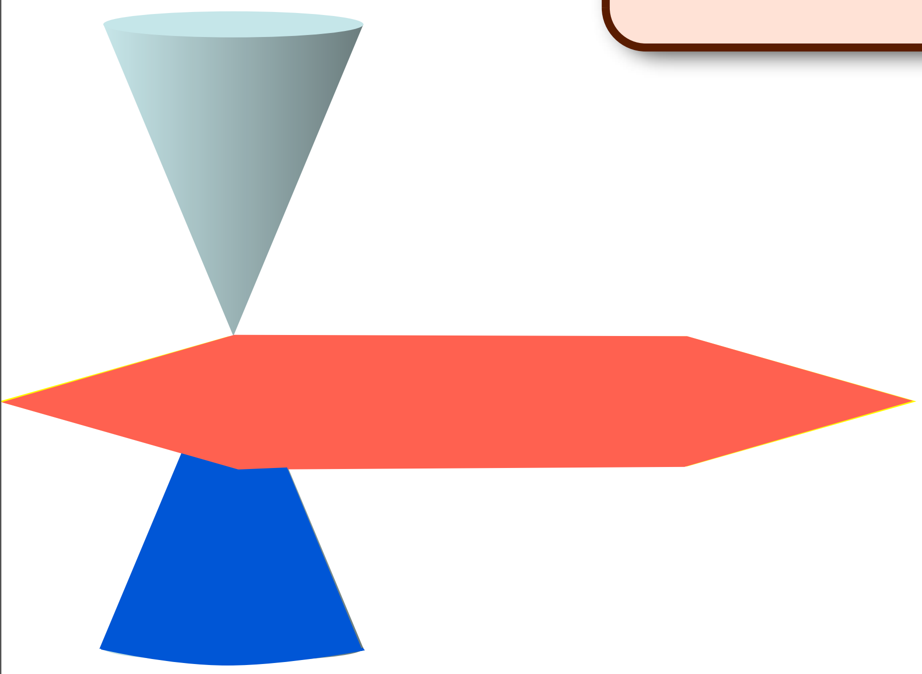

$\Updownarrow$

Einstein gravity on AdS_4

Conformal field theory
in 2+1 dimensions at $T > 0$

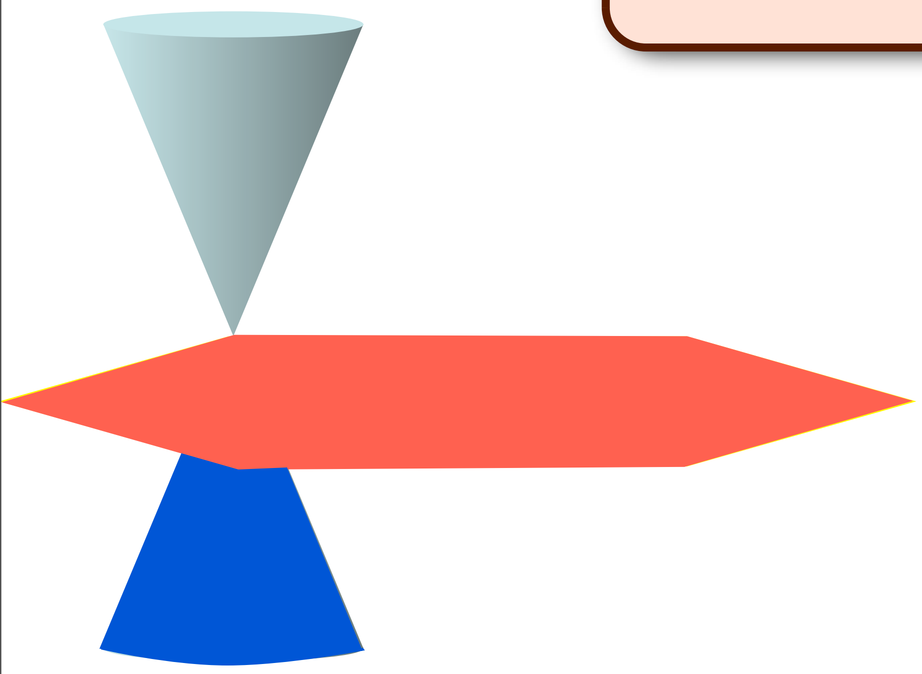

$\Updownarrow$

Einstein gravity on AdS_4
with a Schwarzschild
black hole

Conformal field theory
in 2+1 dimensions at $T > 0$,
with a non-zero chemical potential, μ
and applied magnetic field, B

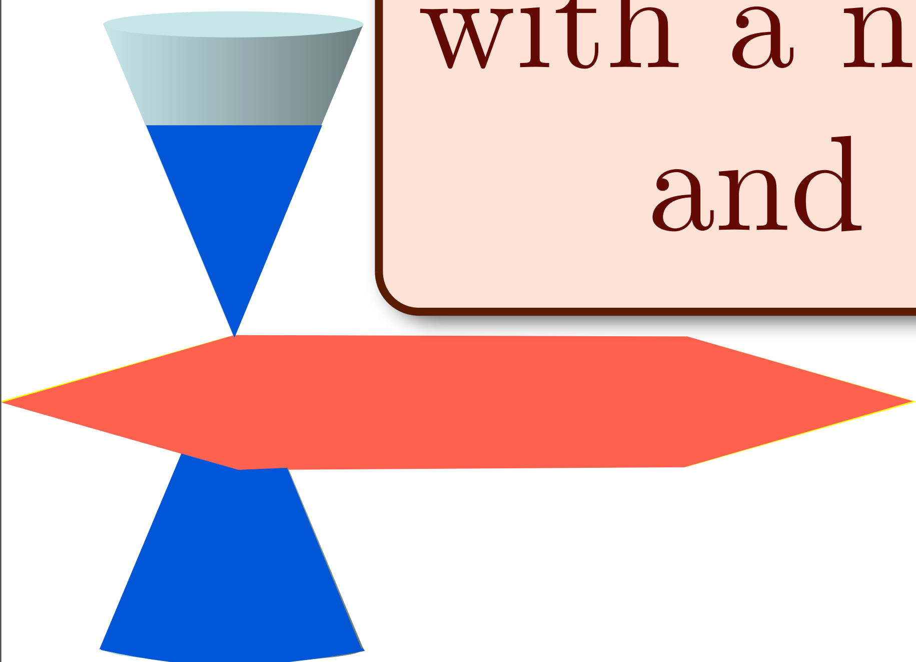

Einstein gravity on AdS_4
with a Reissner-Nordstrom
black hole carrying electric
and magnetic charges

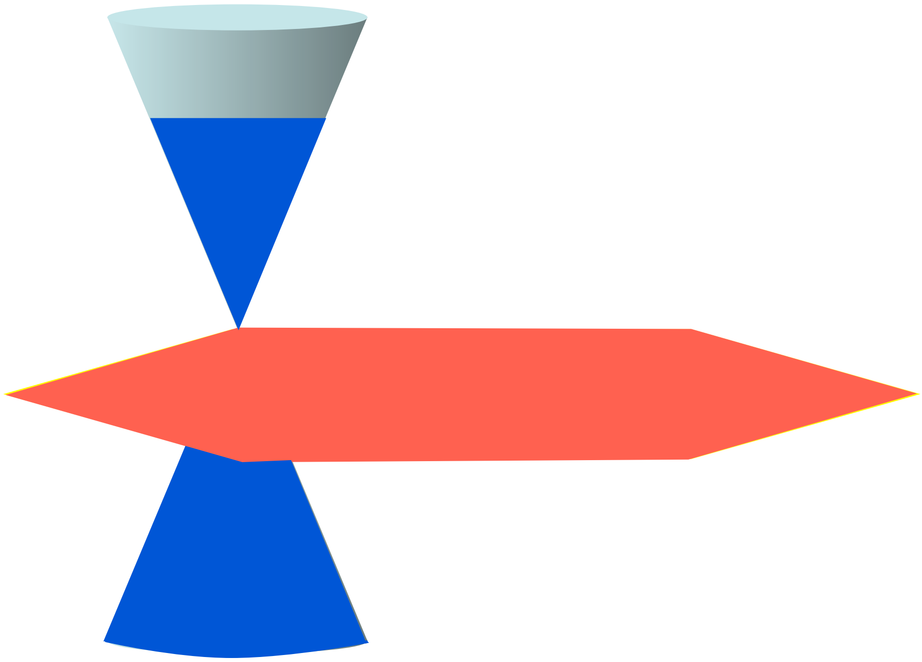

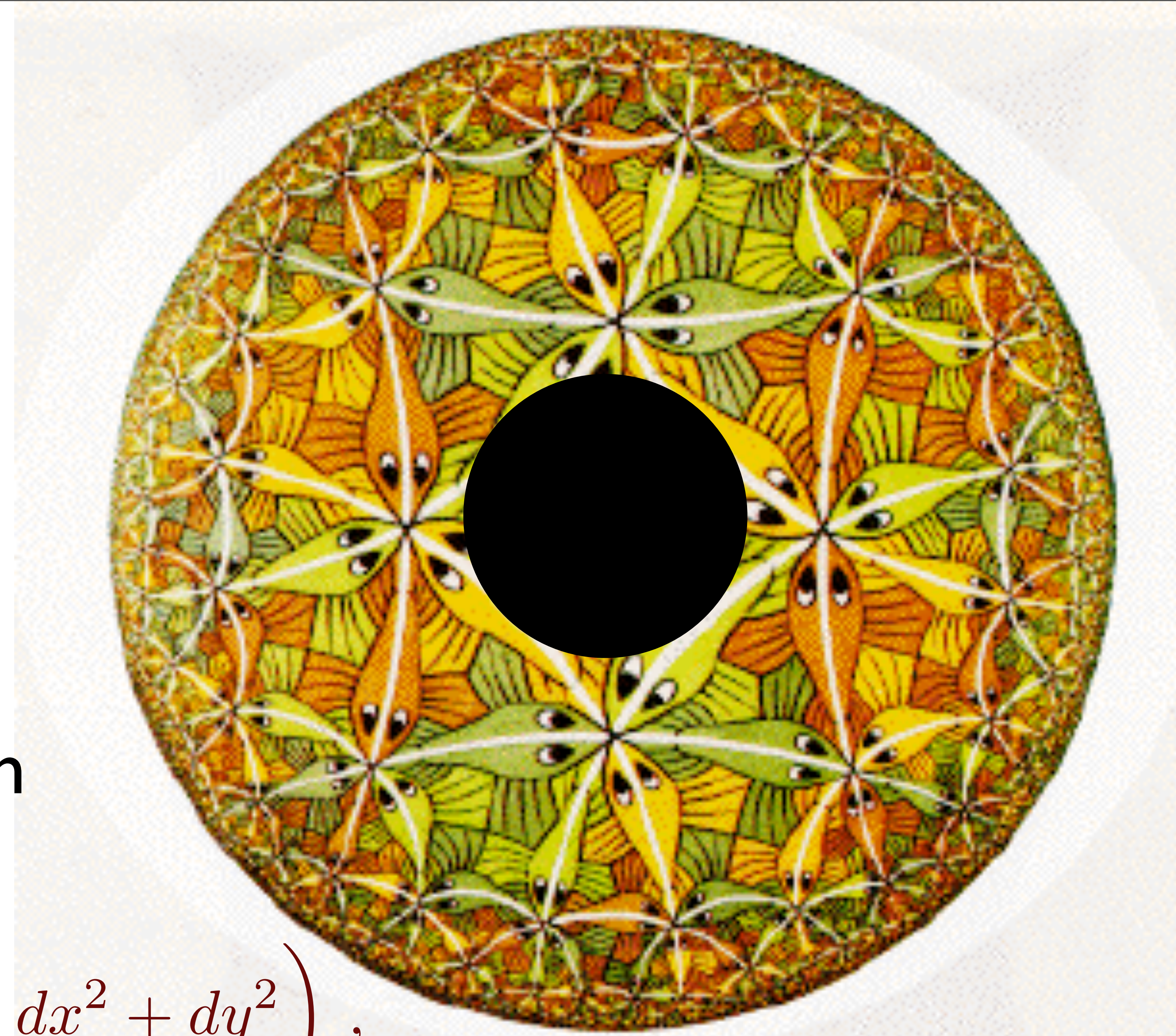

AdS$_4$-Reissner-Nordstrom
black hole

$$
\begin{aligned}
ds^2 &= \frac{L^2}{r^2}\left(f(r)d\tau^2 + \frac{dr^2}{f(r)} + dx^2 + dy^2\right) , \\
f(r) &= 1 - \left(1 + \frac{(r_+^2\mu^2 + r_+^4 B^2)}{\gamma^2}\right)\left(\frac{r}{r_+}\right)^3 + \frac{(r_+^2\mu^2 + r_+^4 B^2)}{\gamma^2}\left(\frac{r}{r_+}\right)^4 , \\
A &= i\mu\left[1 - \frac{r}{r_+}\right] d\tau + Bx\, dy \, . \\
T &= \frac{1}{4\pi r_+}\left(3 - \frac{r_+^2\mu^2}{\gamma^2} - \frac{r_+^4 B^2}{\gamma^2}\right) .
\end{aligned}
$$

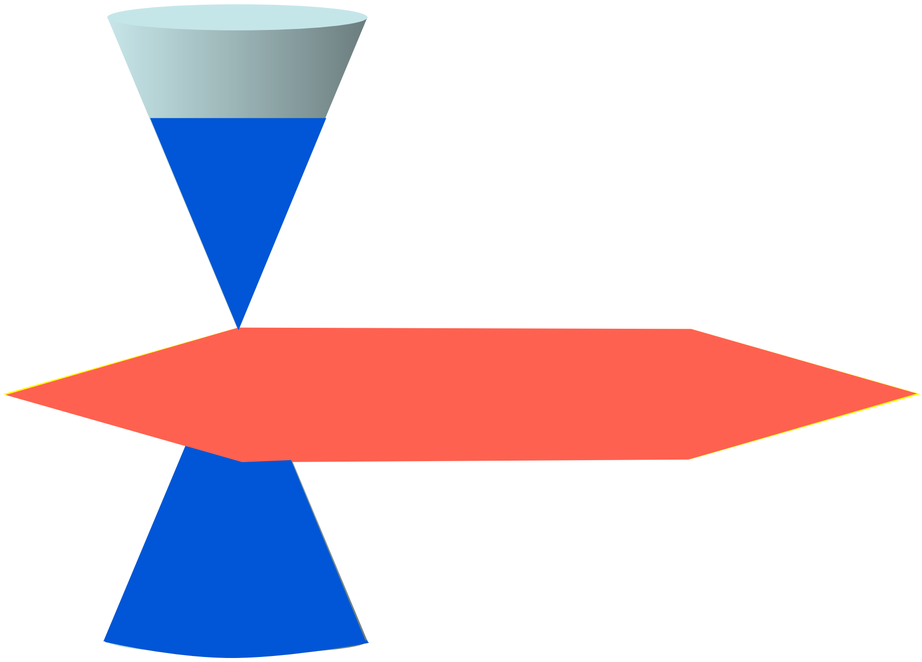

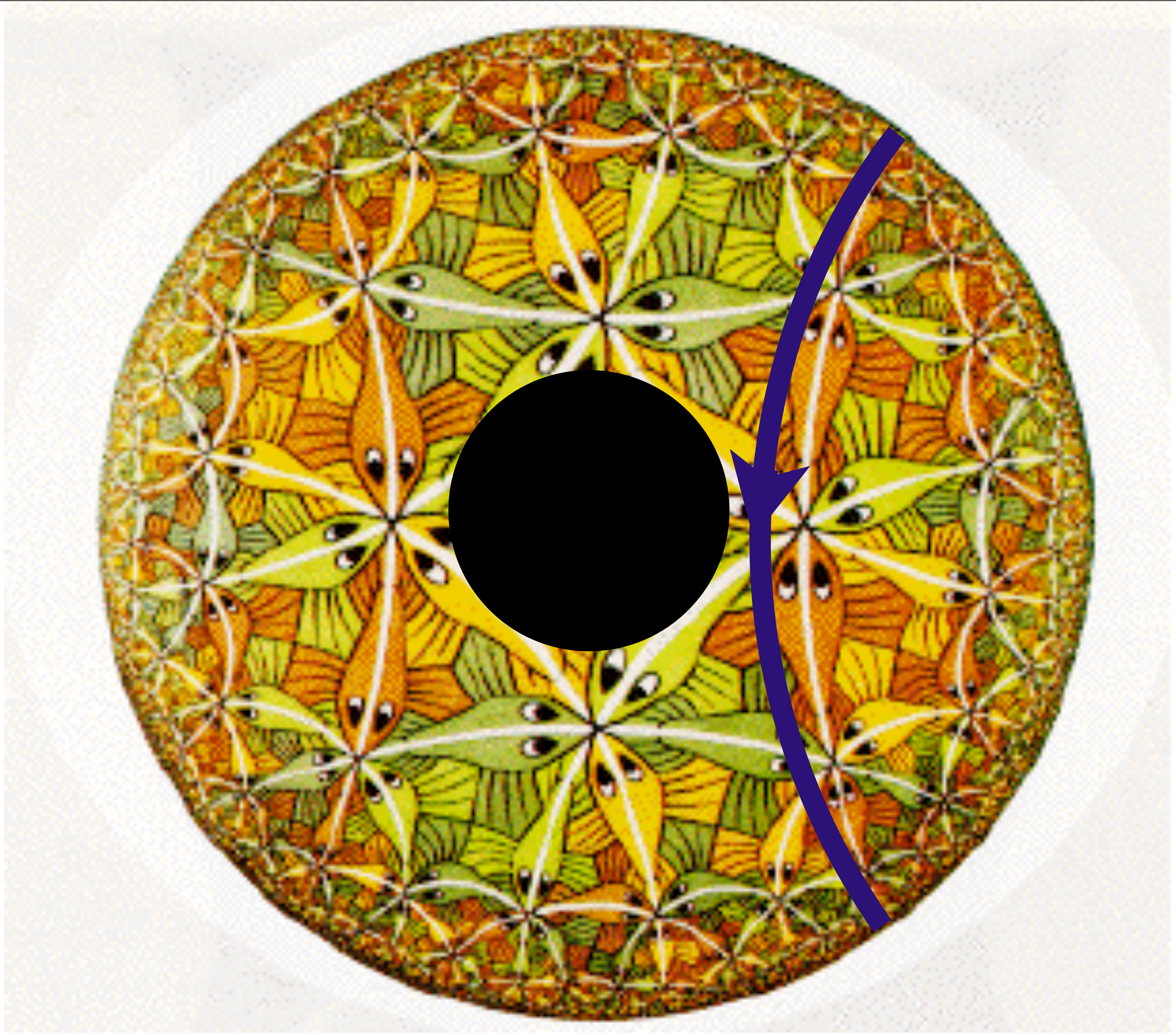

Examine free energy and Green's function of a probe particle

T. Faulkner, H. Liu, J. McGreevy, and D. Vegh, arXiv:0907.2694
F. Denef, S. Hartnoll, and S. Sachdev, arXiv:0908.1788

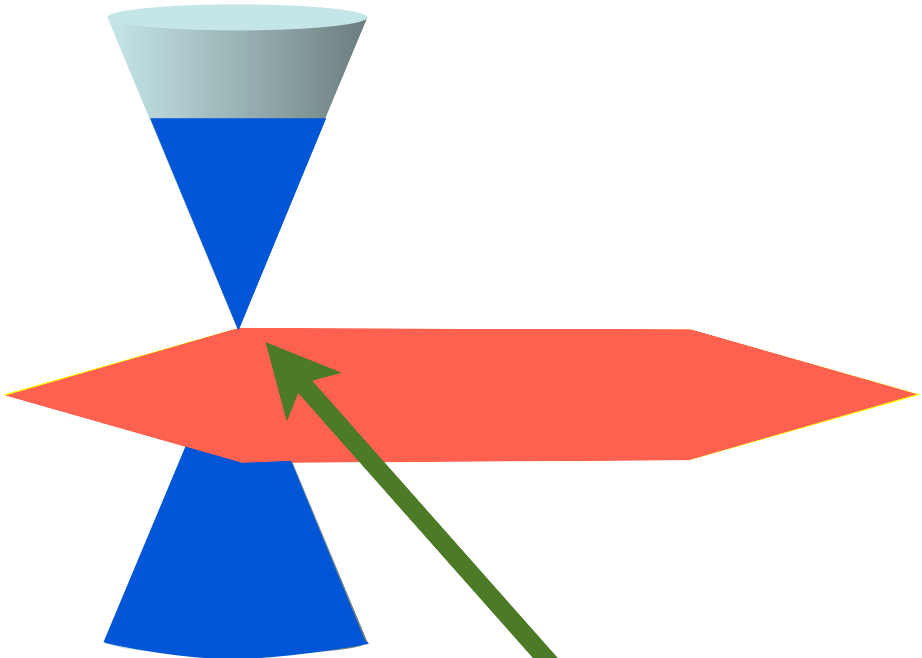

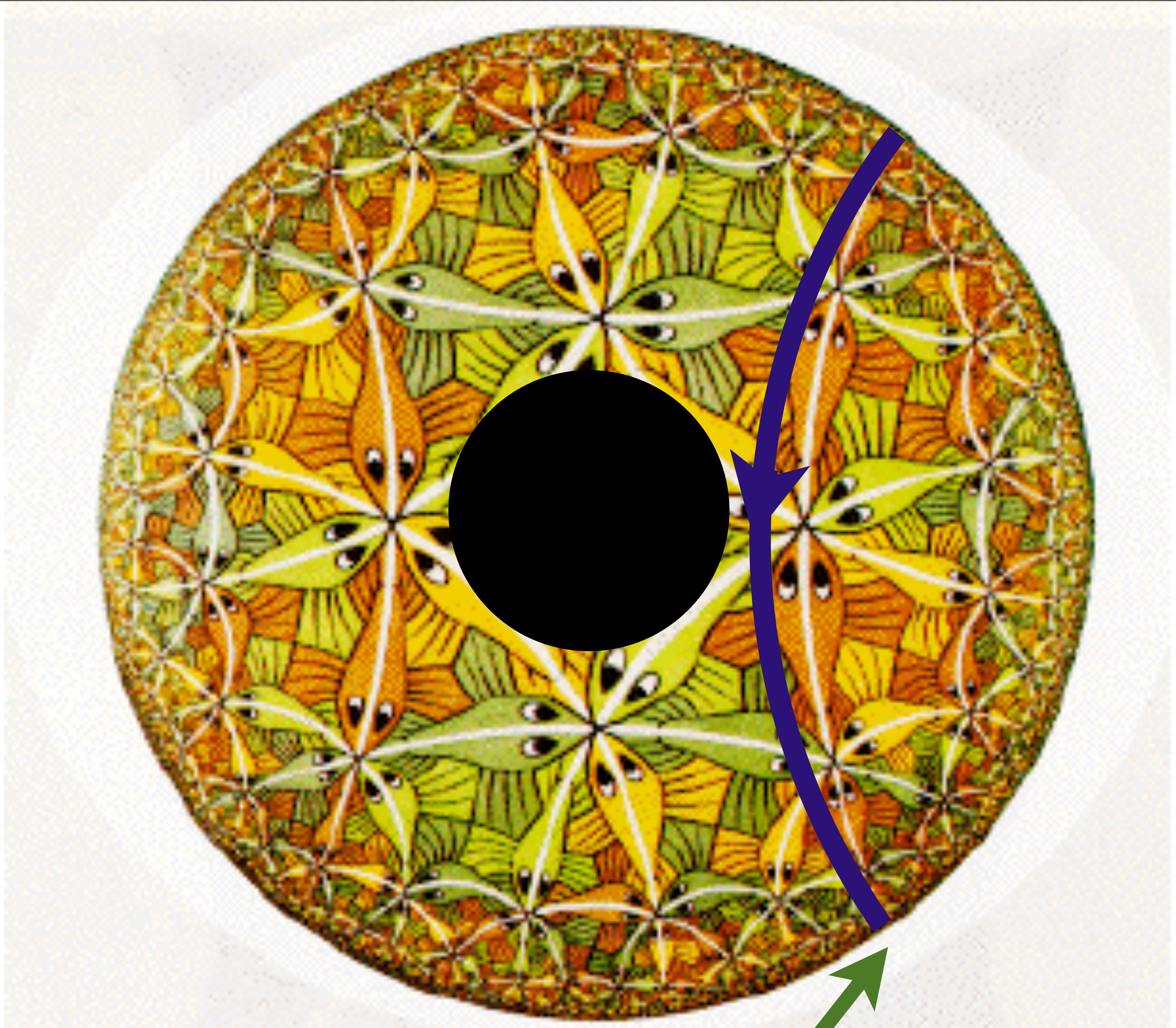

Short time behavior depends upon conformal AdS_4 geometry near boundary

T. Faulkner, H. Liu, J. McGreevy, and D. Vegh, arXiv:0907.2694
F. Denef, S. Hartnoll, and S. Sachdev, arXiv:0908.1788

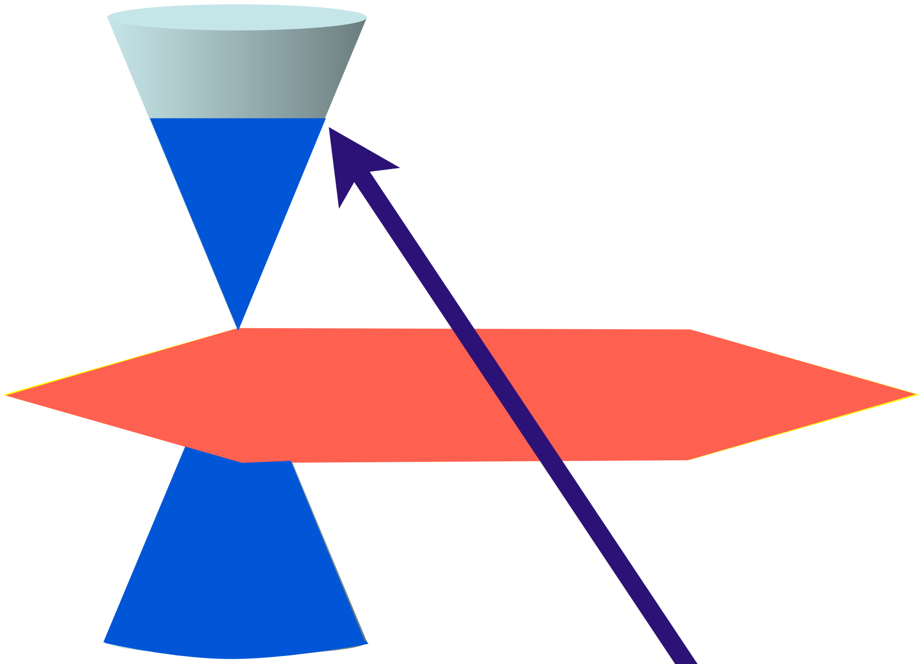

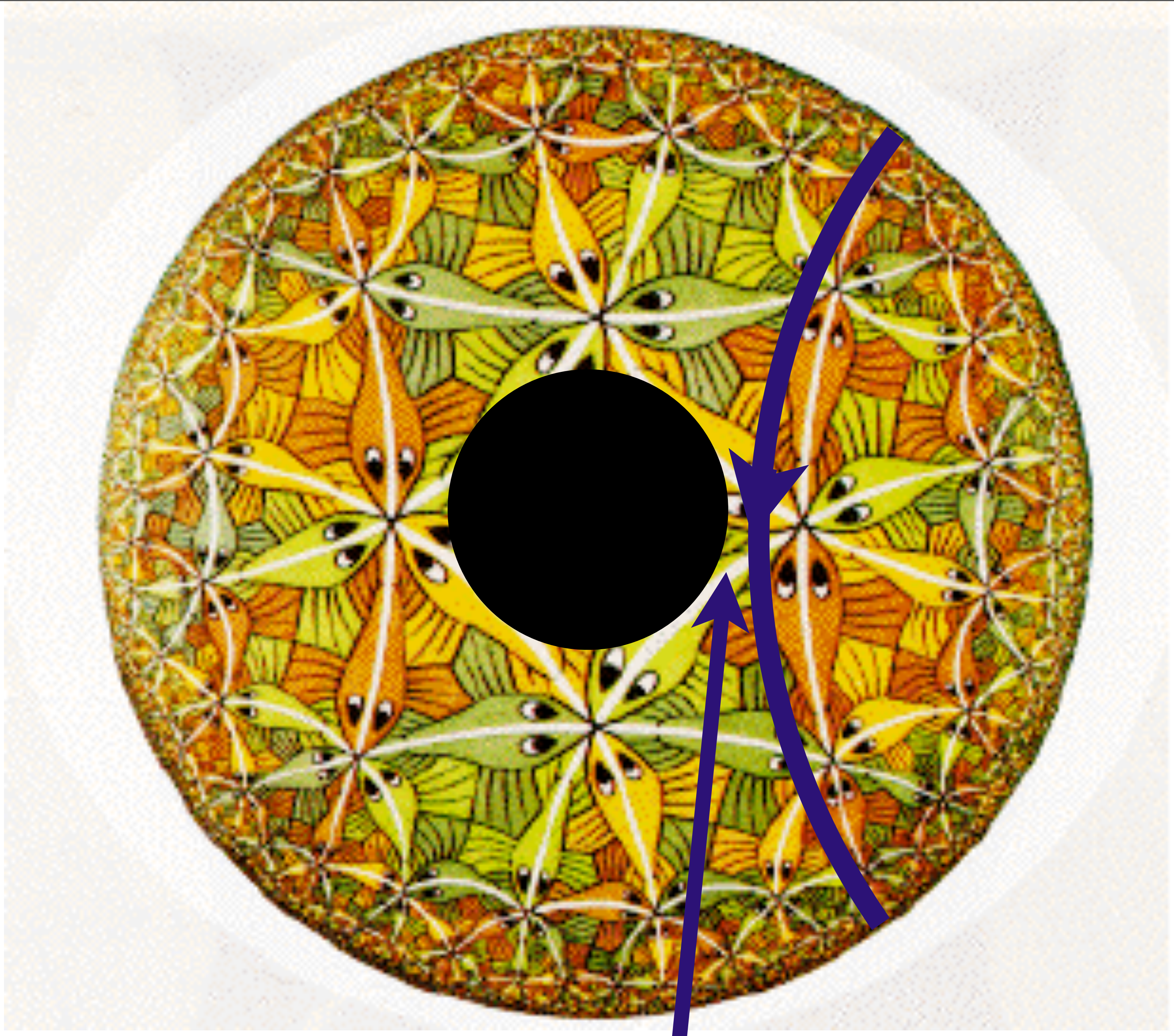

Long time behavior depends upon near-horizon geometry of black hole

T. Faulkner, H. Liu, J. McGreevy, and D. Vegh, arXiv:0907.2694
F. Denef, S. Hartnoll, and S. Sachdev, arXiv:0908.1788

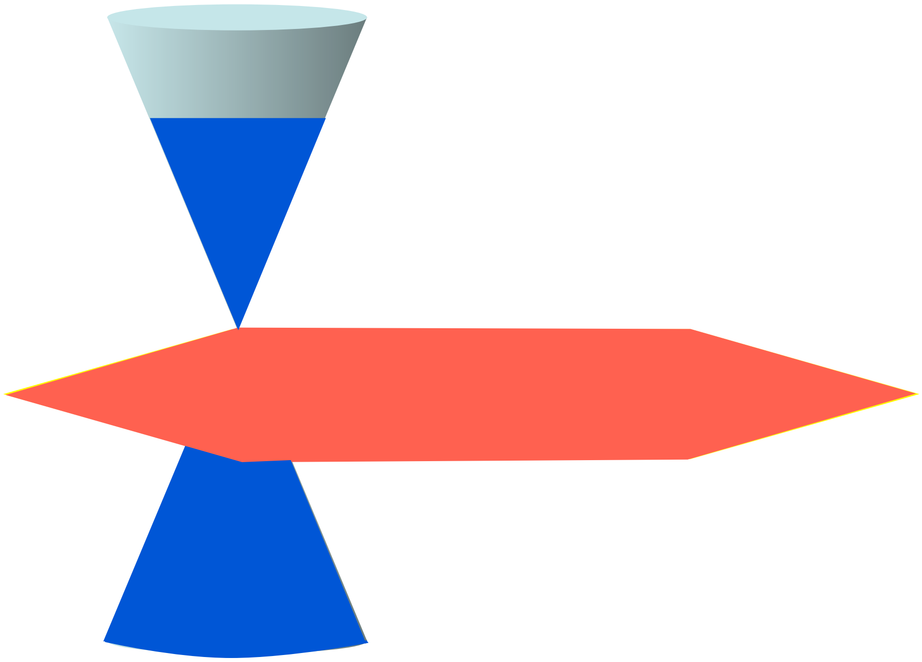

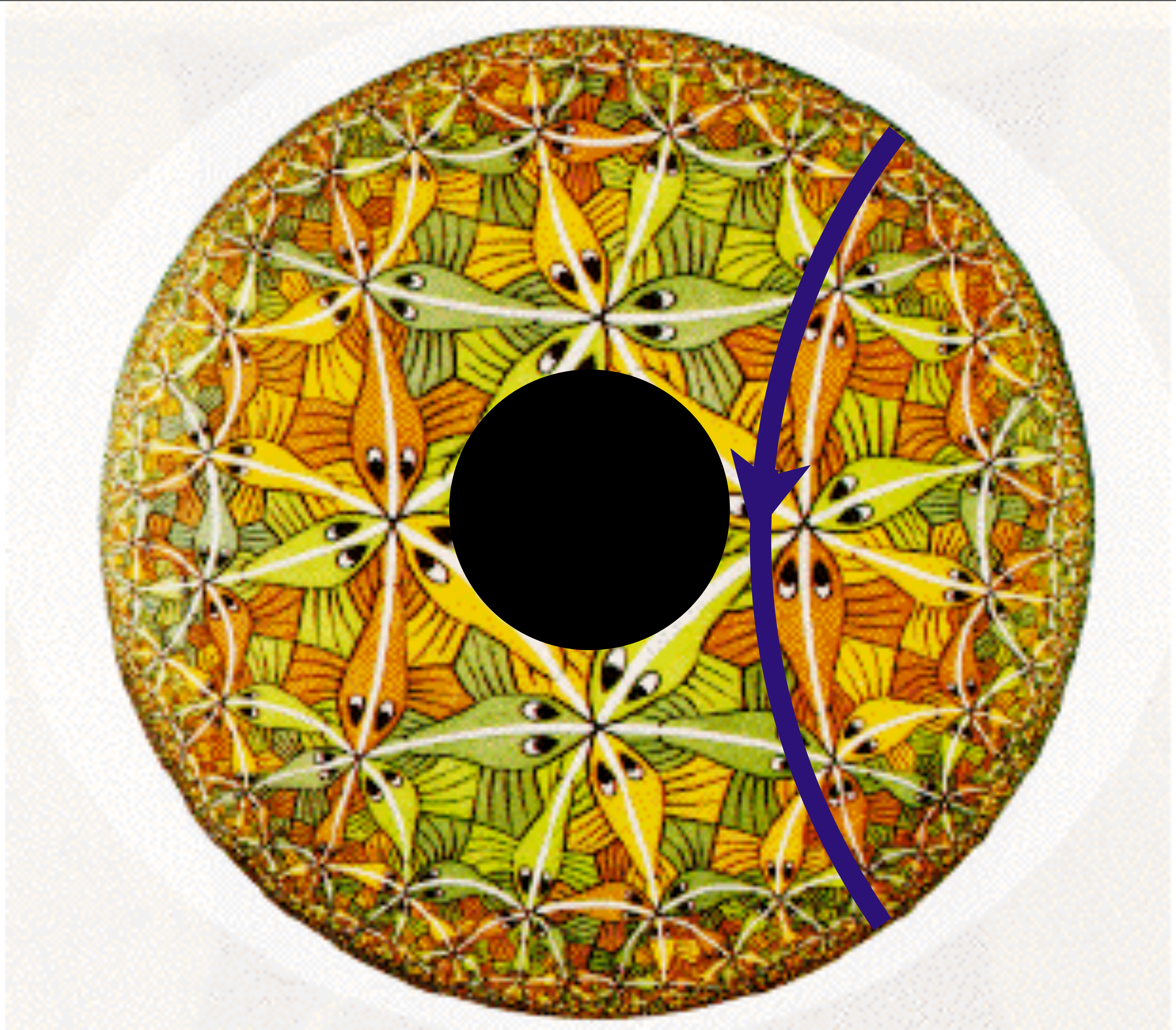

Radial direction of gravity theory is measure of energy scale in CFT

T. Faulkner, H. Liu, J. McGreevy, and D. Vegh, arXiv:0907.2694
F. Denef, S. Hartnoll, and S. Sachdev, arXiv:0908.1788

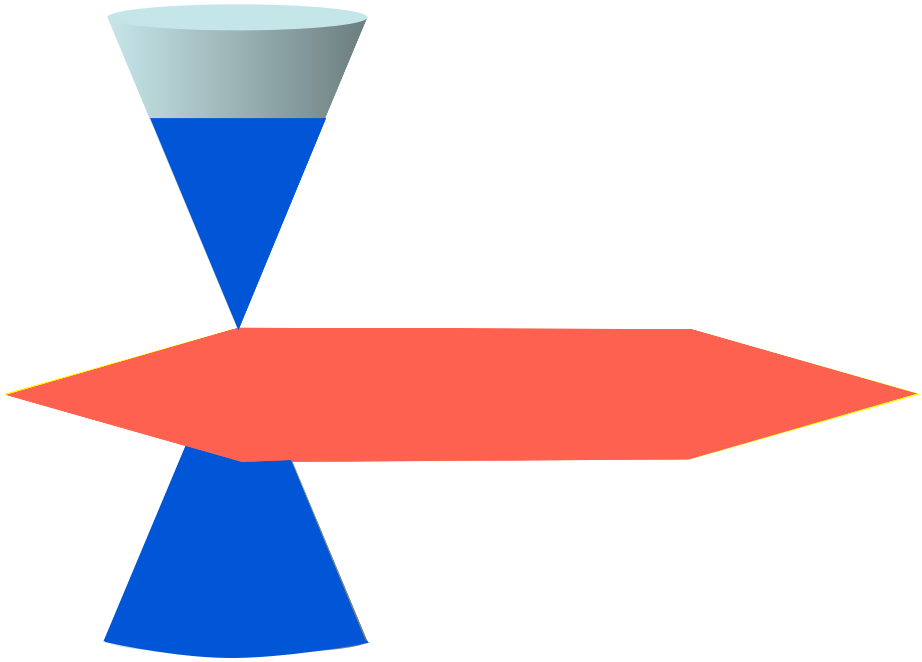

AdS$_4$-Reissner-Nordstrom black hole

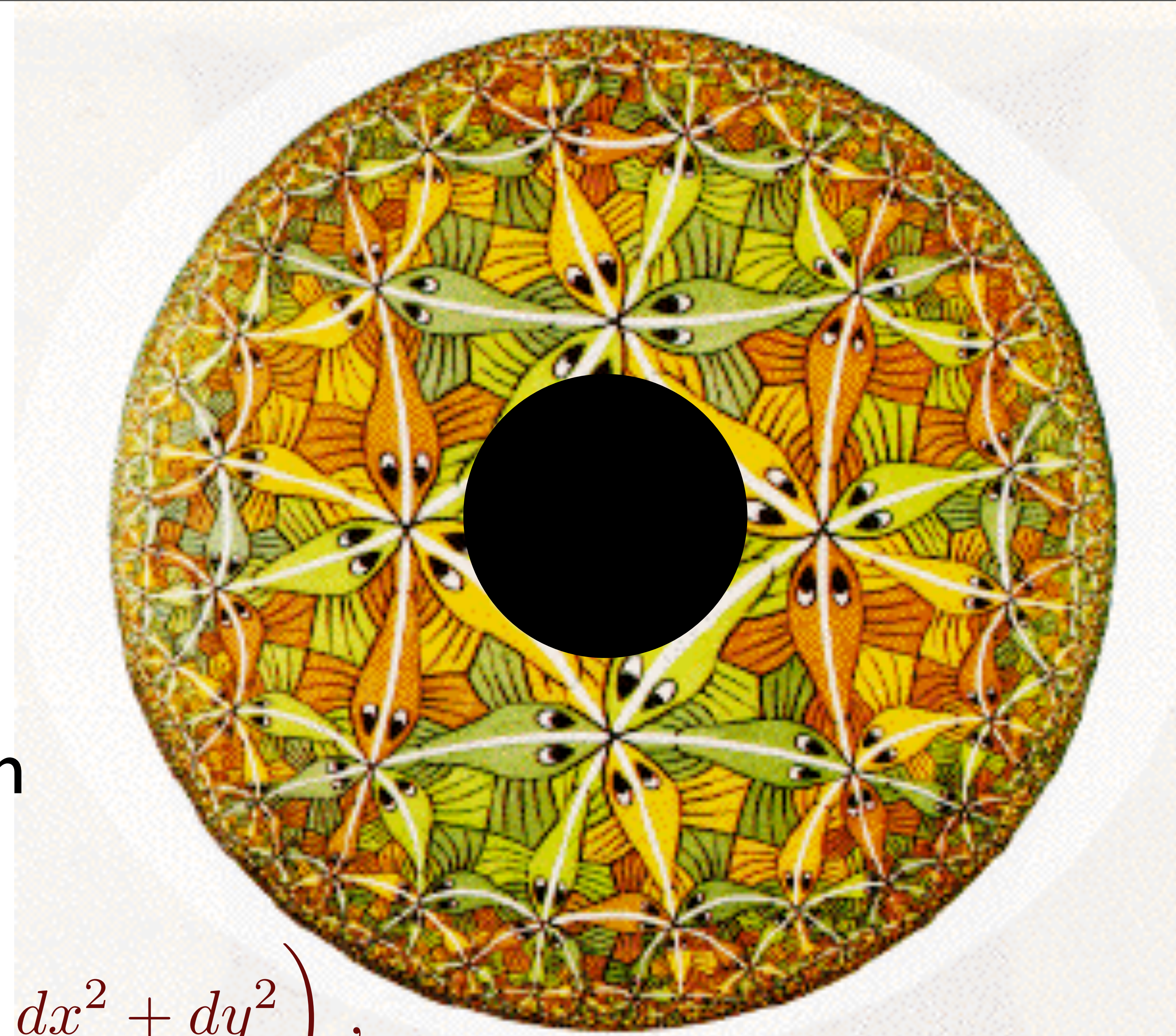

$$
\begin{aligned}
ds^2 &= \frac{L^2}{r^2}\left(f(r)d\tau^2 + \frac{dr^2}{f(r)} + dx^2 + dy^2\right), \\
f(r) &= 1 - \left(1 + \frac{(r_+^2\mu^2 + r_+^4 B^2)}{\gamma^2}\right)\left(\frac{r}{r_+}\right)^3 + \frac{(r_+^2\mu^2 + r_+^4 B^2)}{\gamma^2}\left(\frac{r}{r_+}\right)^4, \\
A &= i\mu\left[1 - \frac{r}{r_+}\right] d\tau + B x\, dy\,. \\
T &= \frac{1}{4\pi r_+}\left(3 - \frac{r_+^2\mu^2}{\gamma^2} - \frac{r_+^4 B^2}{\gamma^2}\right).
\end{aligned}
$$

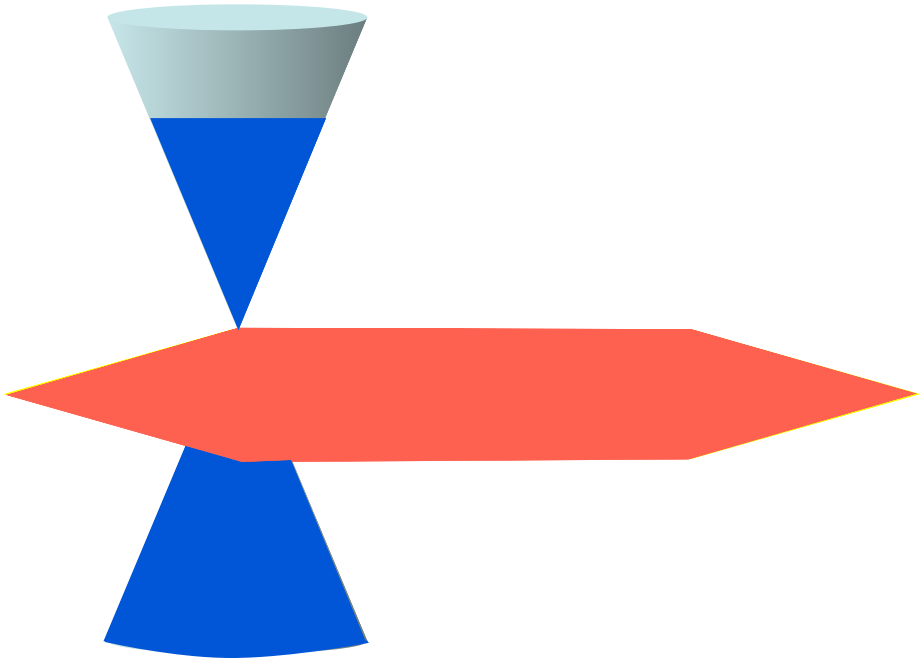

$AdS_2 \times R^2$ near-horizon geometry

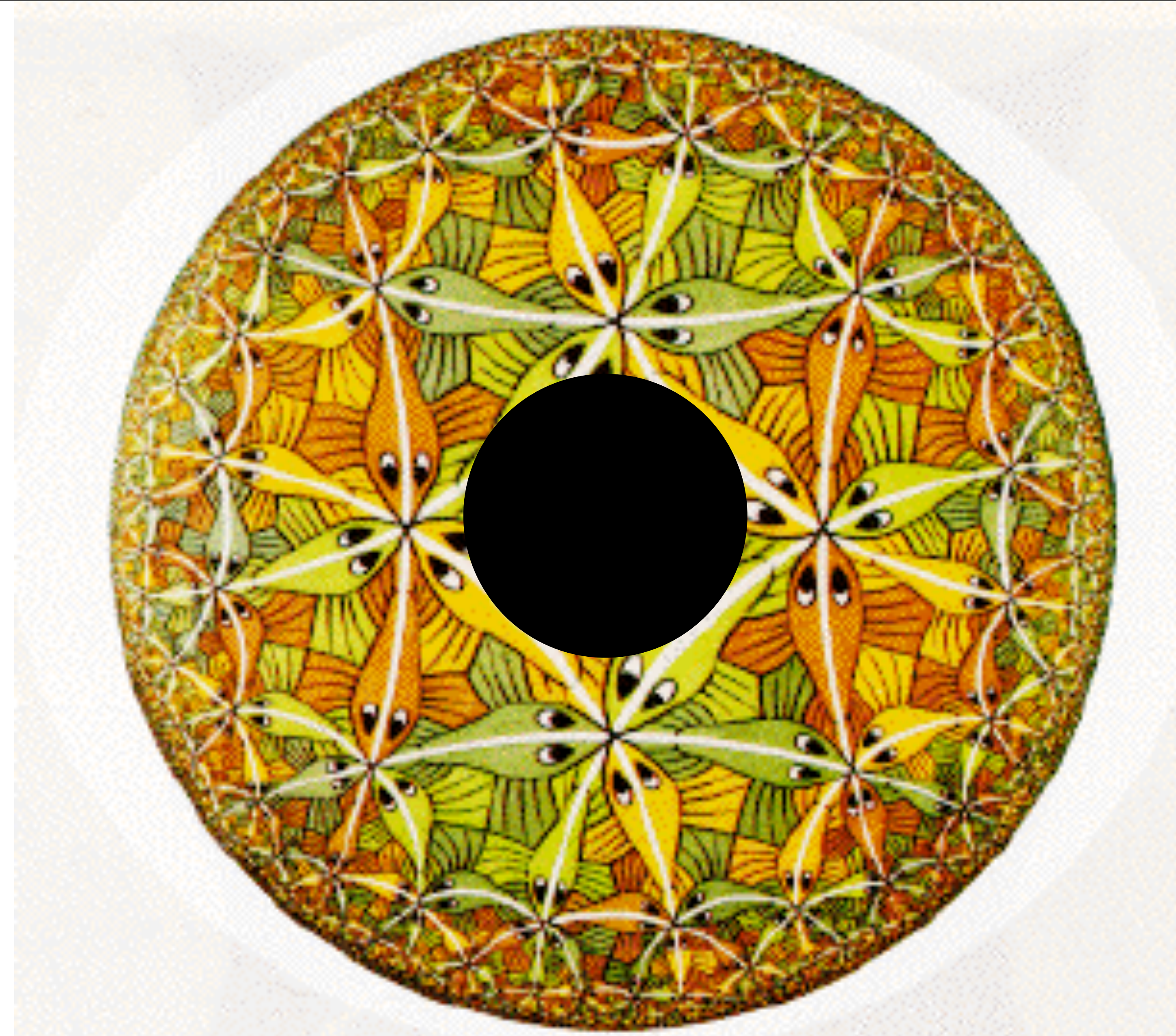

$$r - r_+ \sim \frac{1}{\zeta}$$

$$ds^2 = \frac{R^2}{\zeta^2}\left(-d\tau^2 + d\zeta^2\right) + \frac{r_+^2}{R^2}\left(dx^2 + dy^2\right)$$

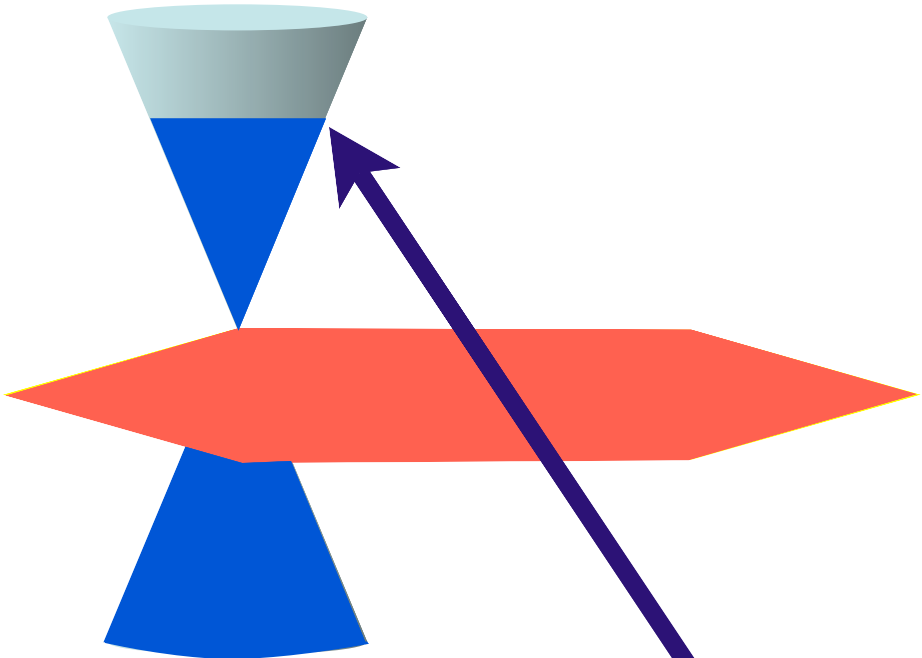

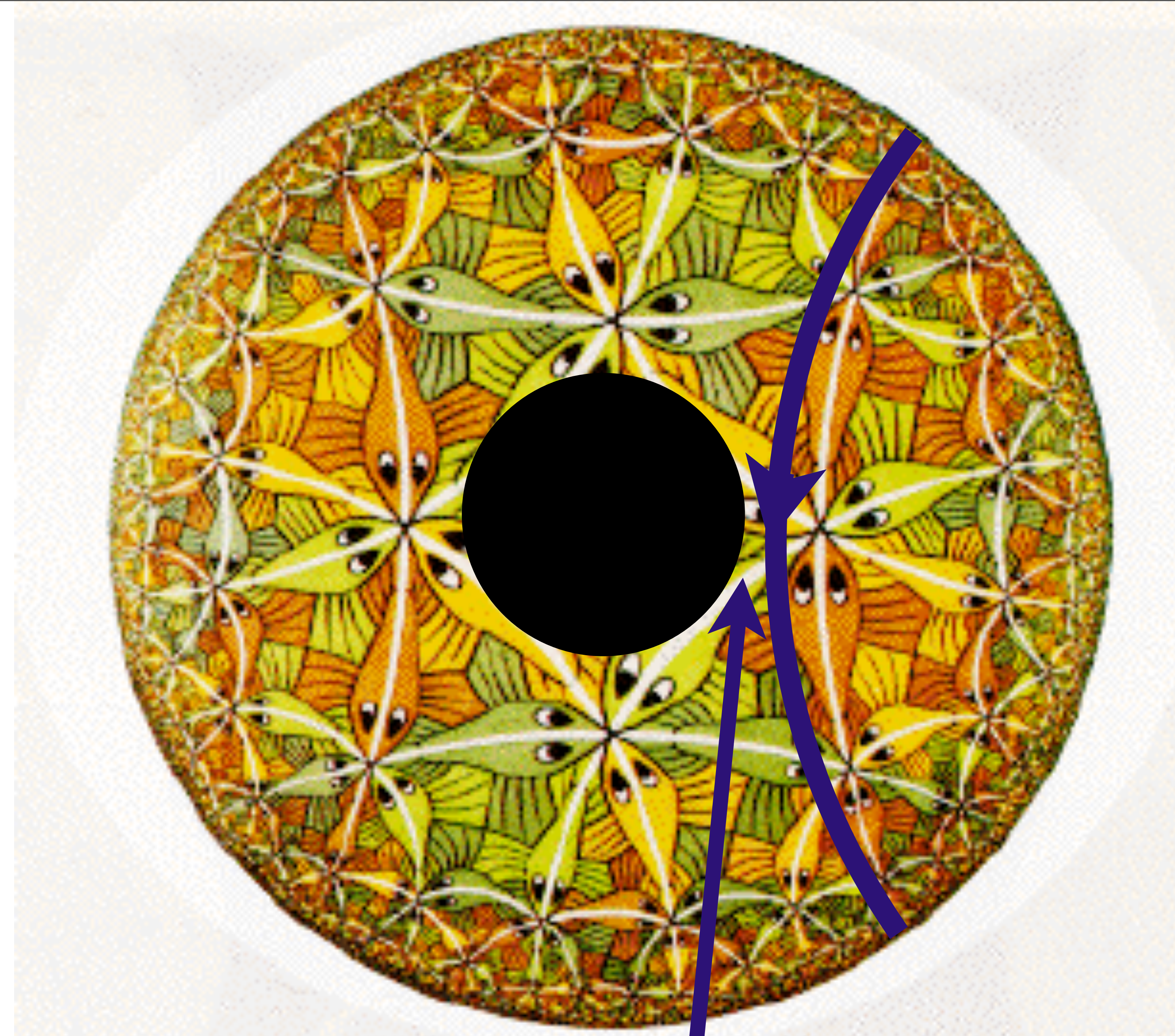

Infrared physics of Fermi surface is linked to the near horizon AdS_2 geometry of Reissner-Nordstrom black hole

T. Faulkner, H. Liu, J. McGreevy, and D. Vegh, arXiv:0907.2694

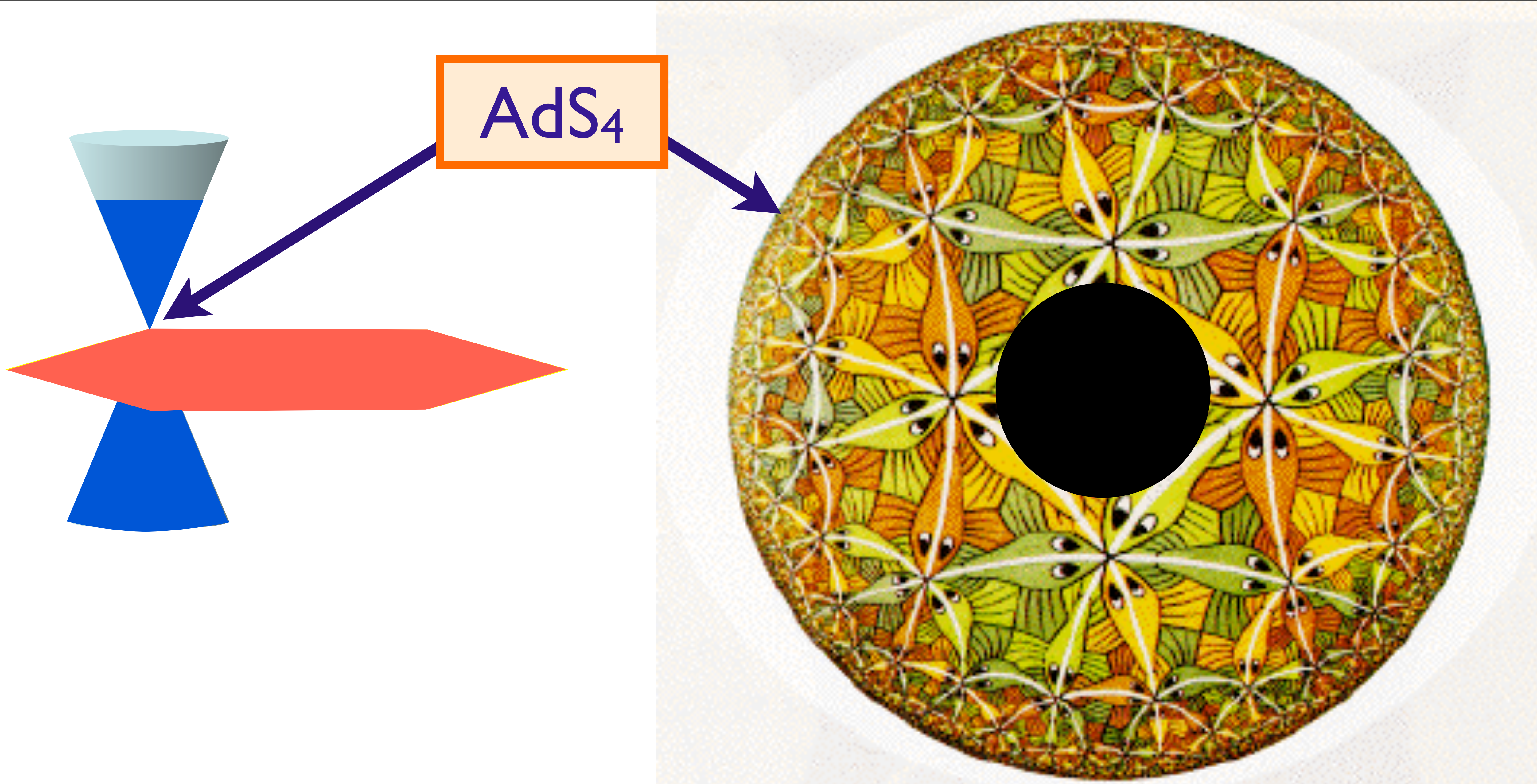

Geometric interpretation of RG flow

T. Faulkner, H. Liu, J. McGreevy, and D. Vegh, arXiv:0907.2694

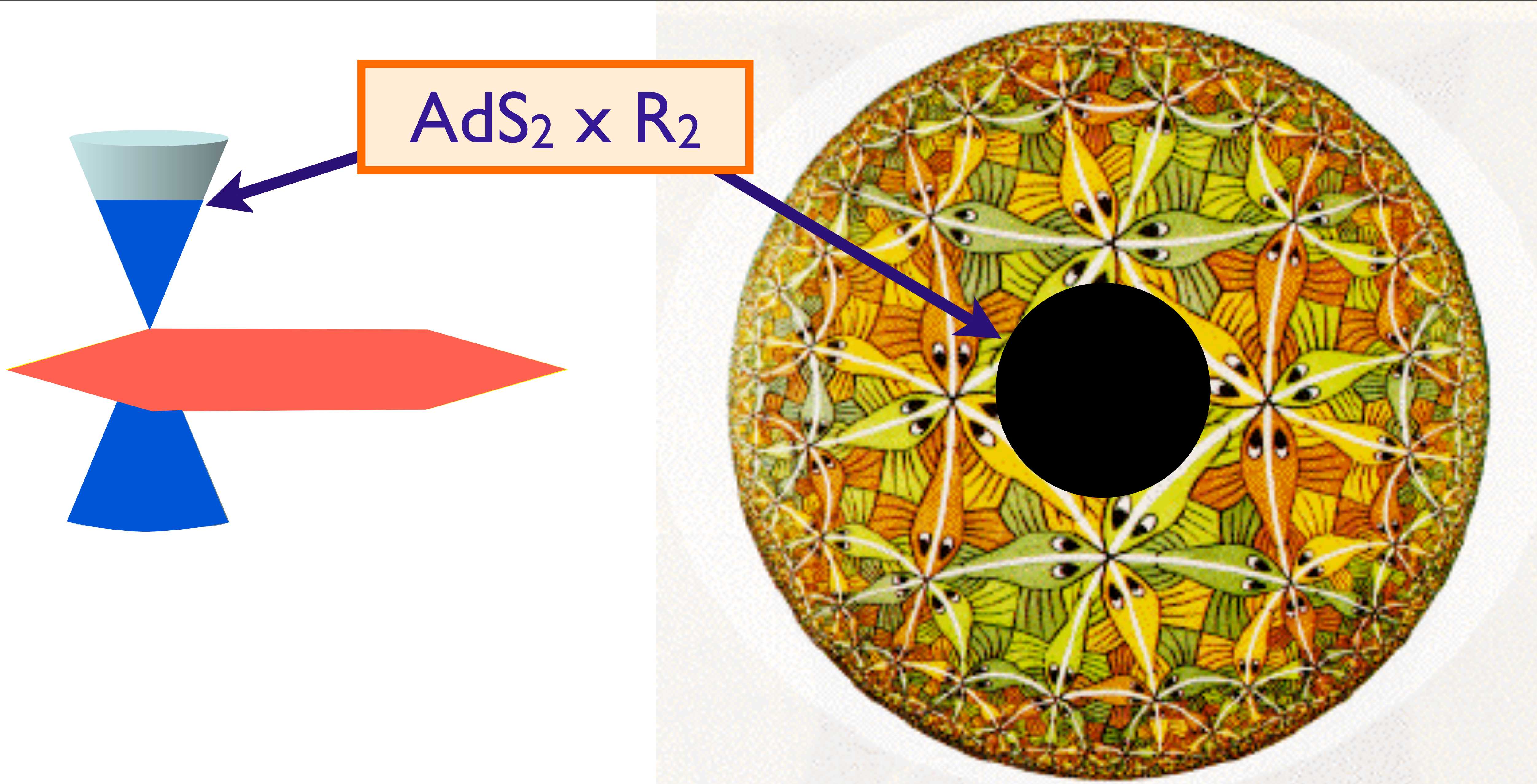

Geometric interpretation of RG flow

T. Faulkner, H. Liu, J. McGreevy, and D. Vegh, arXiv:0907.2694

Green's function of a fermion

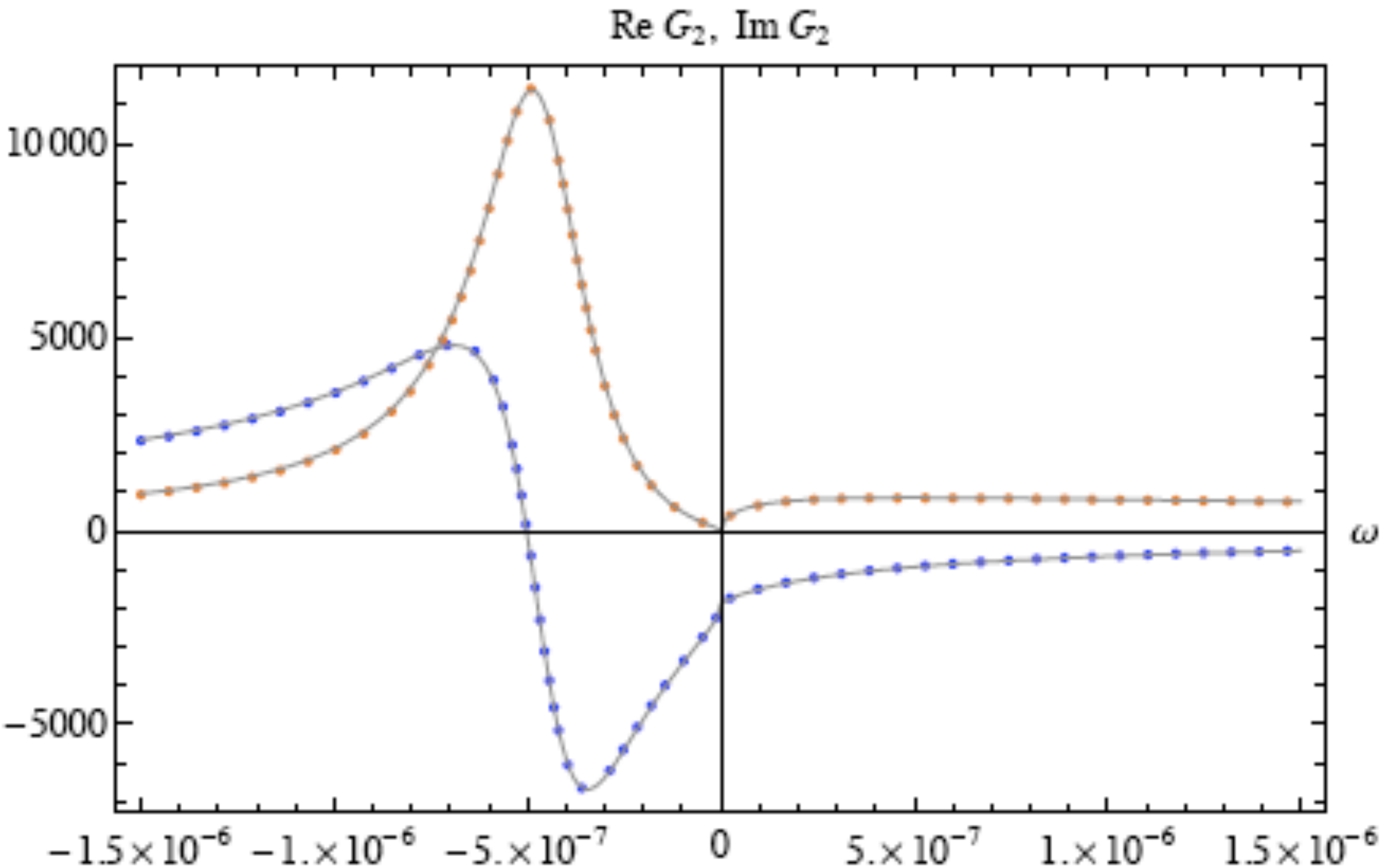

T. Faulkner, H. Liu, J. McGreevy, and D. Vegh, arXiv:0907.2694

$$G(k,\omega) \approx \frac{1}{\omega - v_F(k-k_F) - i\omega^{\theta(k)}}$$

See also M. Cubrovic, J Zaanen, and K. Schalm, arXiv:0904.1993

Green's function of a fermion

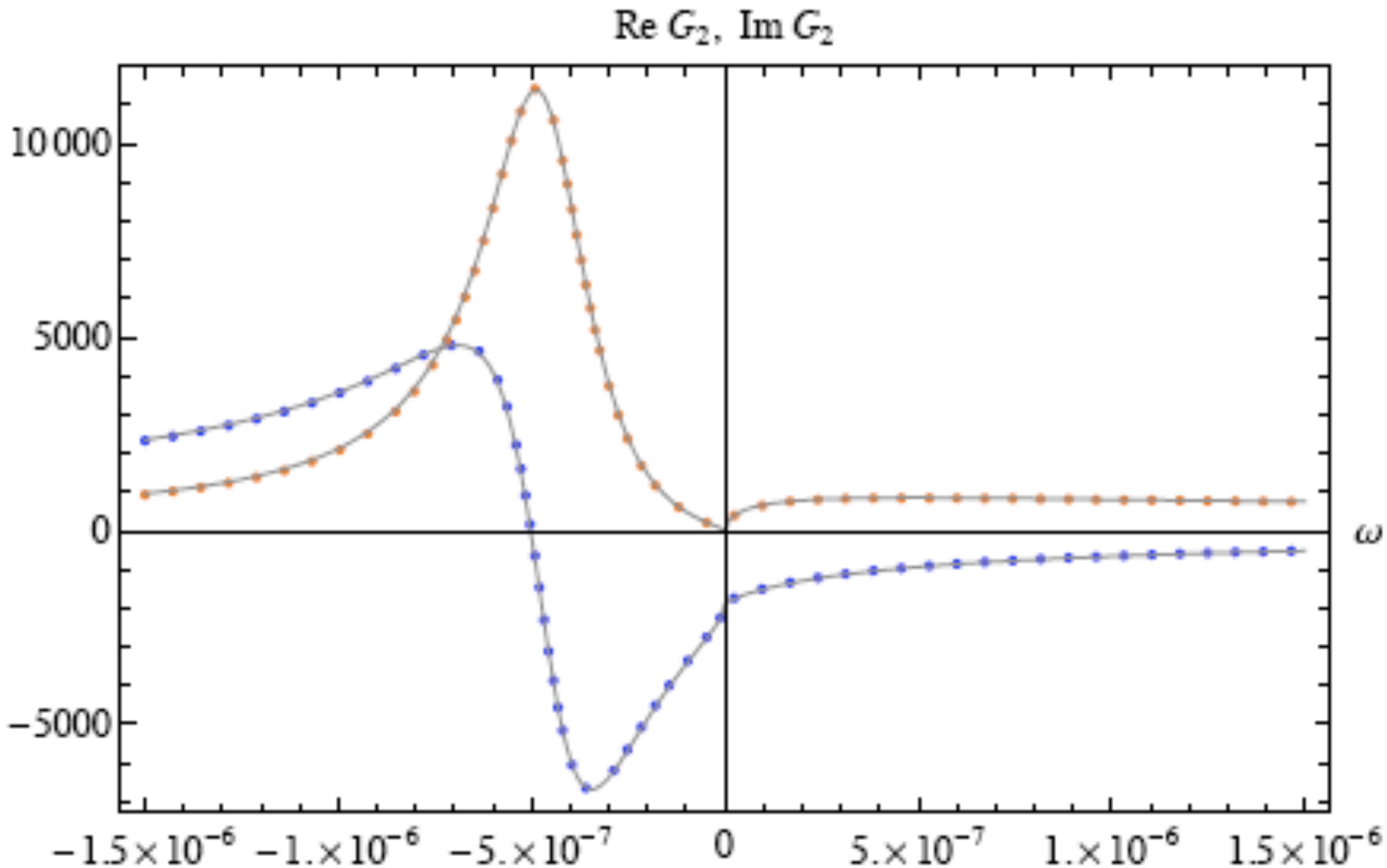

T. Faulkner, H. Liu, J. McGreevy, and D. Vegh, arXiv:0907.2694

$$G(k,\omega) \approx \frac{1}{\omega - v_F(k-k_F) - i\omega^{\theta(k)}}$$

Similar to non-Fermi liquid theories of Fermi surfaces coupled to gauge fields, and at quantum critical points

Free energy from gravity theory

The free energy is expressed as a sum over the "quasinormal frequencies", z_ℓ, of the black hole. Here ℓ represents any set of quantum numbers:

$$
\begin{aligned}
\mathcal{F}_{\text{boson}} &= -T \sum_\ell \ln \left(\frac{|z_\ell|}{2\pi T} \left| \Gamma \left(\frac{i z_\ell}{2\pi T} \right) \right|^2 \right) \\
\mathcal{F}_{\text{fermion}} &= T \sum_\ell \ln \left(\left| \Gamma \left(\frac{i z_\ell}{2\pi T} + \frac{1}{2} \right) \right|^2 \right)
\end{aligned}
$$

Application of this formula shows that the fermions exhibit the dHvA quantum oscillations with expected period ($2\pi/$(Fermi surface ares)) in $1/B$, but with an amplitude corrected from the Fermi liquid formula of Lifshitz-Kosevich.

F. Denef, S. Hartnoll, and S. Sachdev, arXiv:0908.1788

Outline

B. Finite density quantum matter

1. Graphene

   Fermi surfaces and Fermi liquids

2. Quantum phase transitions of Fermi liquids

   Pomeranchuk instability and spin density waves;
   Fermi surfaces and "non-Fermi liquids"

3. AdS_2 theory

4. Cuprate superconductivity

Outline

B. Finite density quantum matter

1. Graphene

   Fermi surfaces and Fermi liquids

2. Quantum phase transitions of Fermi liquids

   Pomeranchuk instability and spin density waves;
   Fermi surfaces and "non-Fermi liquids"

3. AdS_2 theory

4. Cuprate superconductivity

The cuprate superconductors

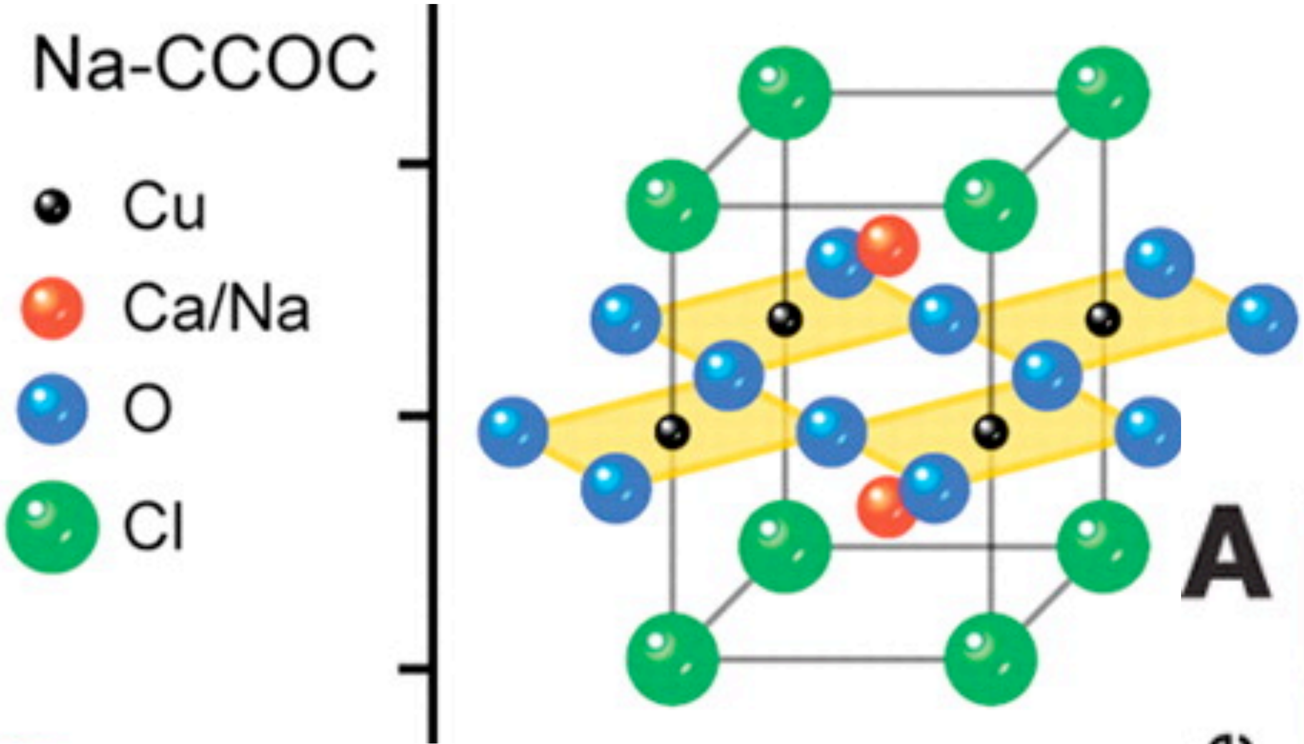

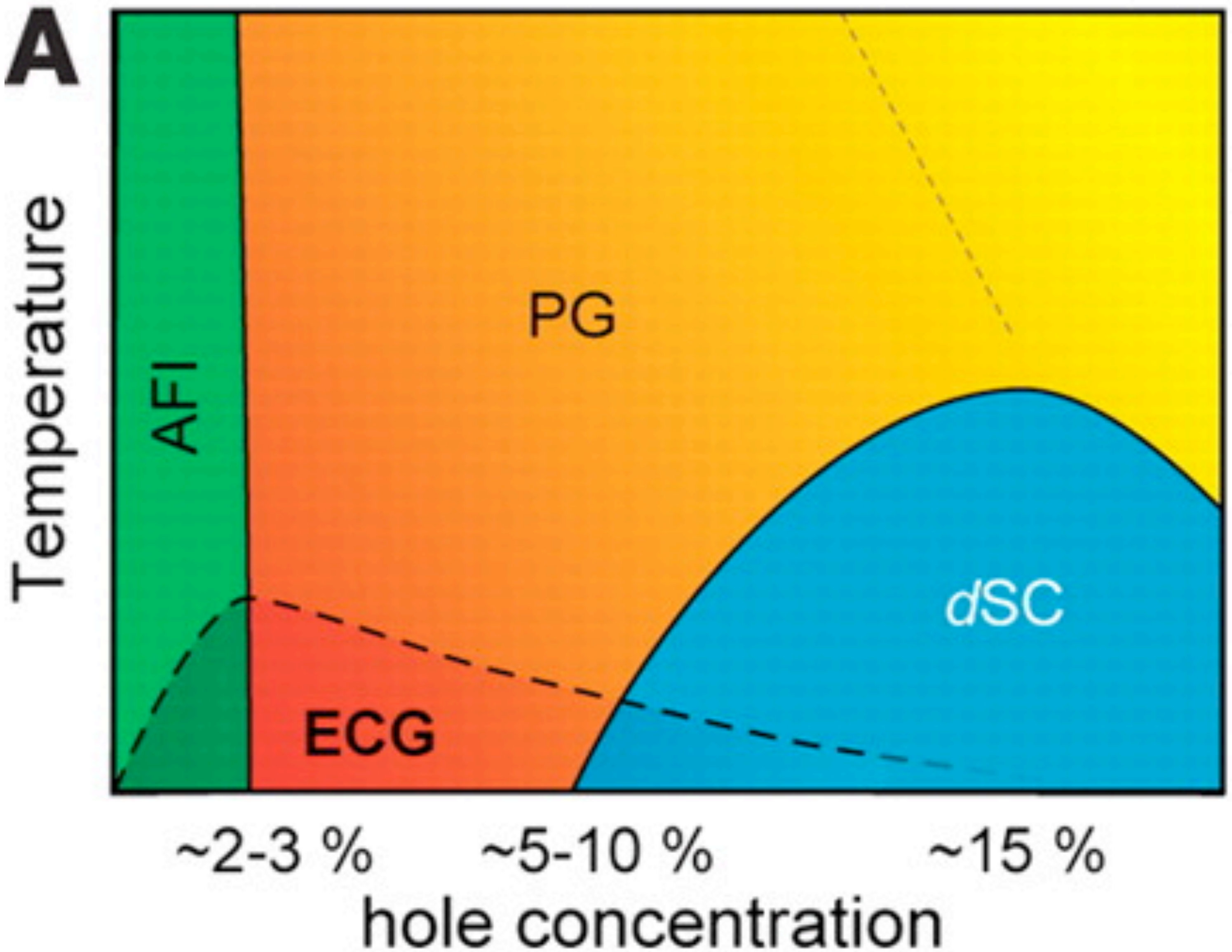

Evolution of the (ARPES) Fermi surface on the cuprate phase diagram

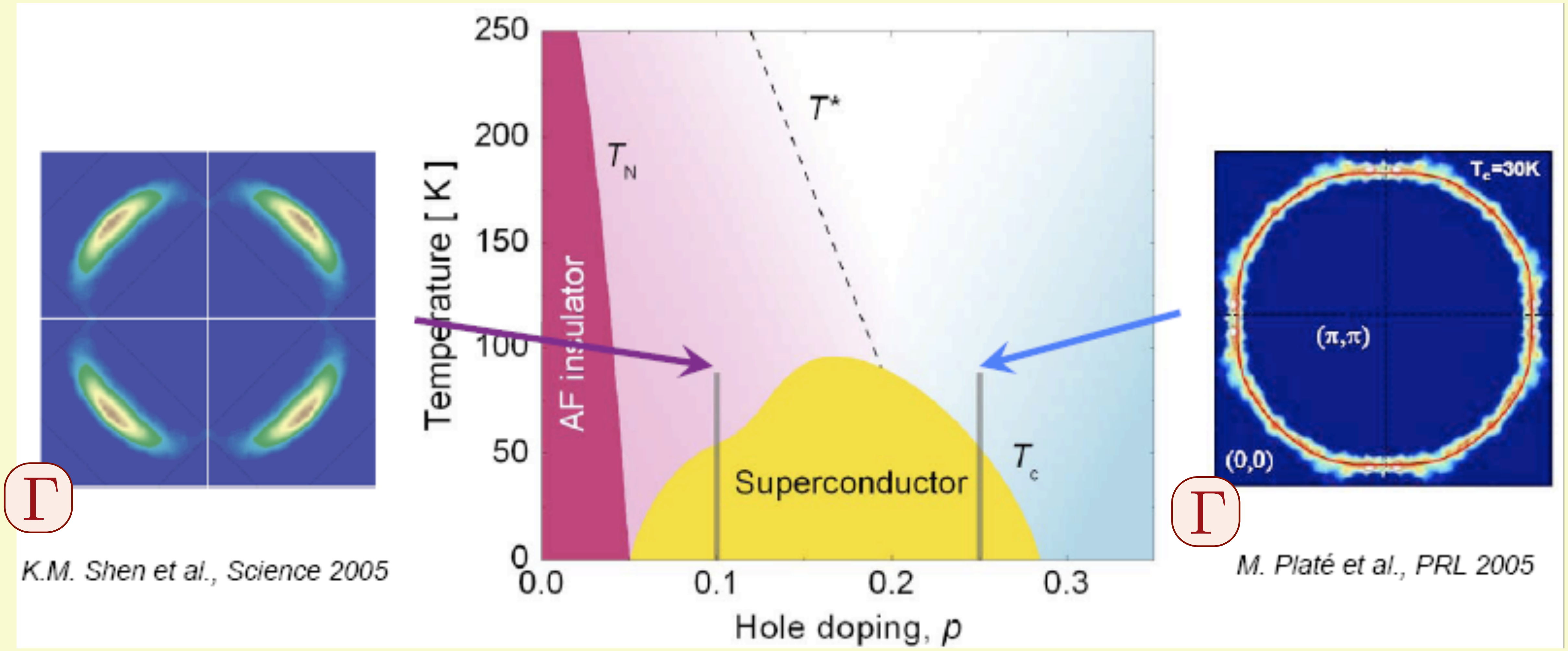

Smaller hole Fermi-pockets

Large hole Fermi surface

The cuprate superconductors

Multiple quantum phase transitions involving at least two order parameters (antiferromagnetism and superconductivity) and a topological change in the Fermi surface

Crossovers in transport properties of hole-doped cuprates

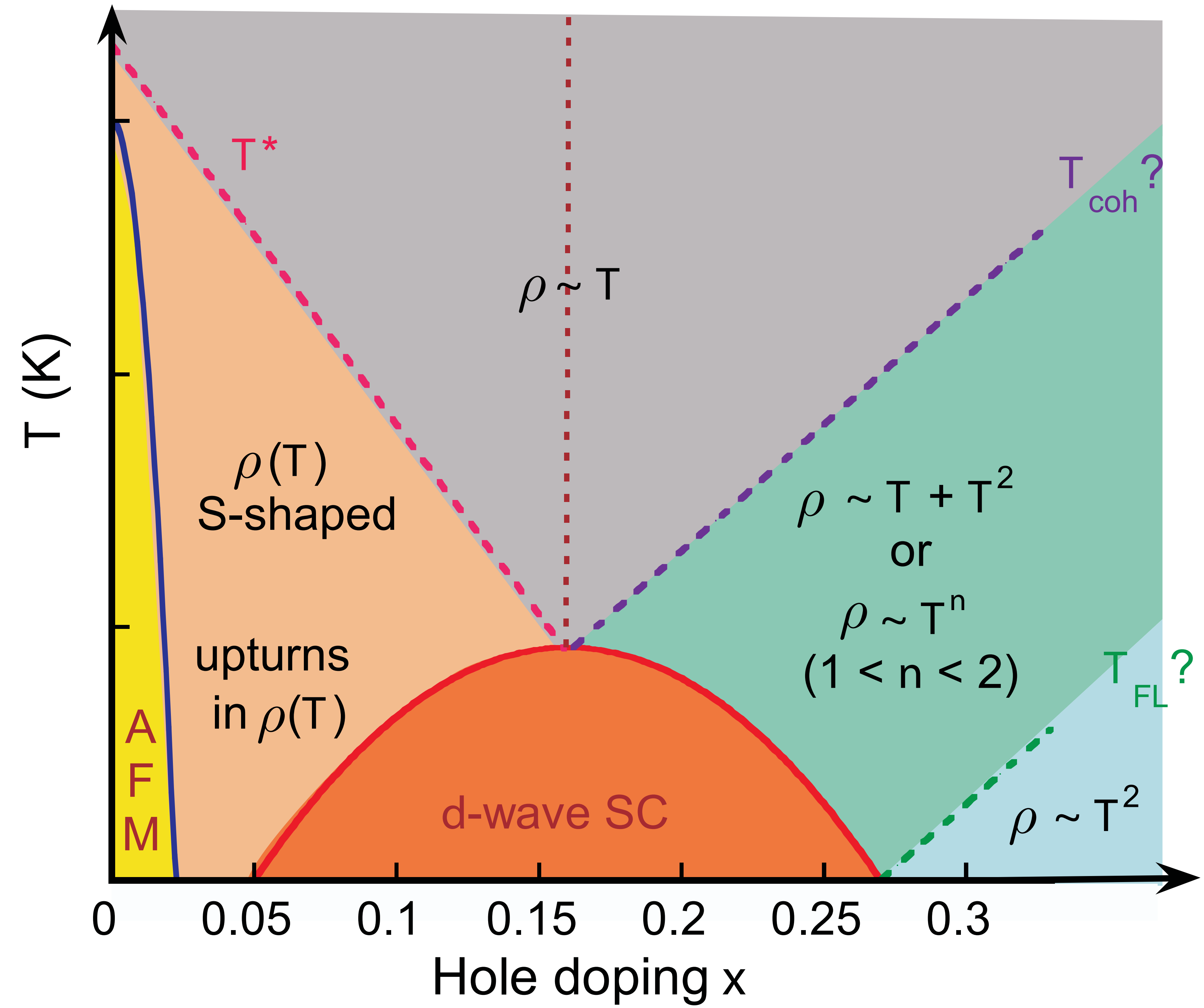

N. E. Hussey, *J. Phys: Condens. Matter* **20**, 123201 (2008)

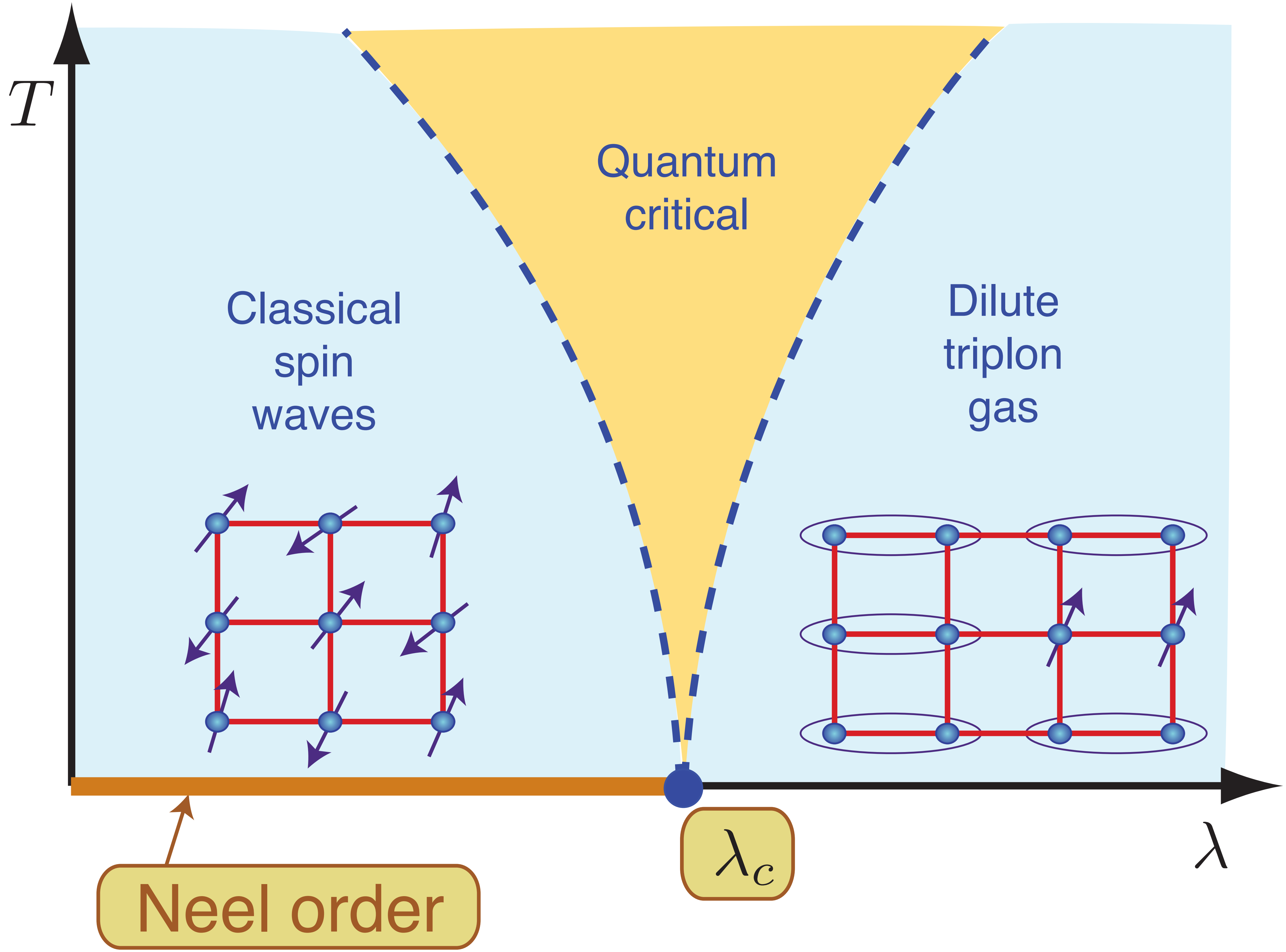

T
Quantum critical
Classical spin waves
Dilute triplon gas
λ
λ_c
Neel order

Crossovers in transport properties of hole-doped cuprates

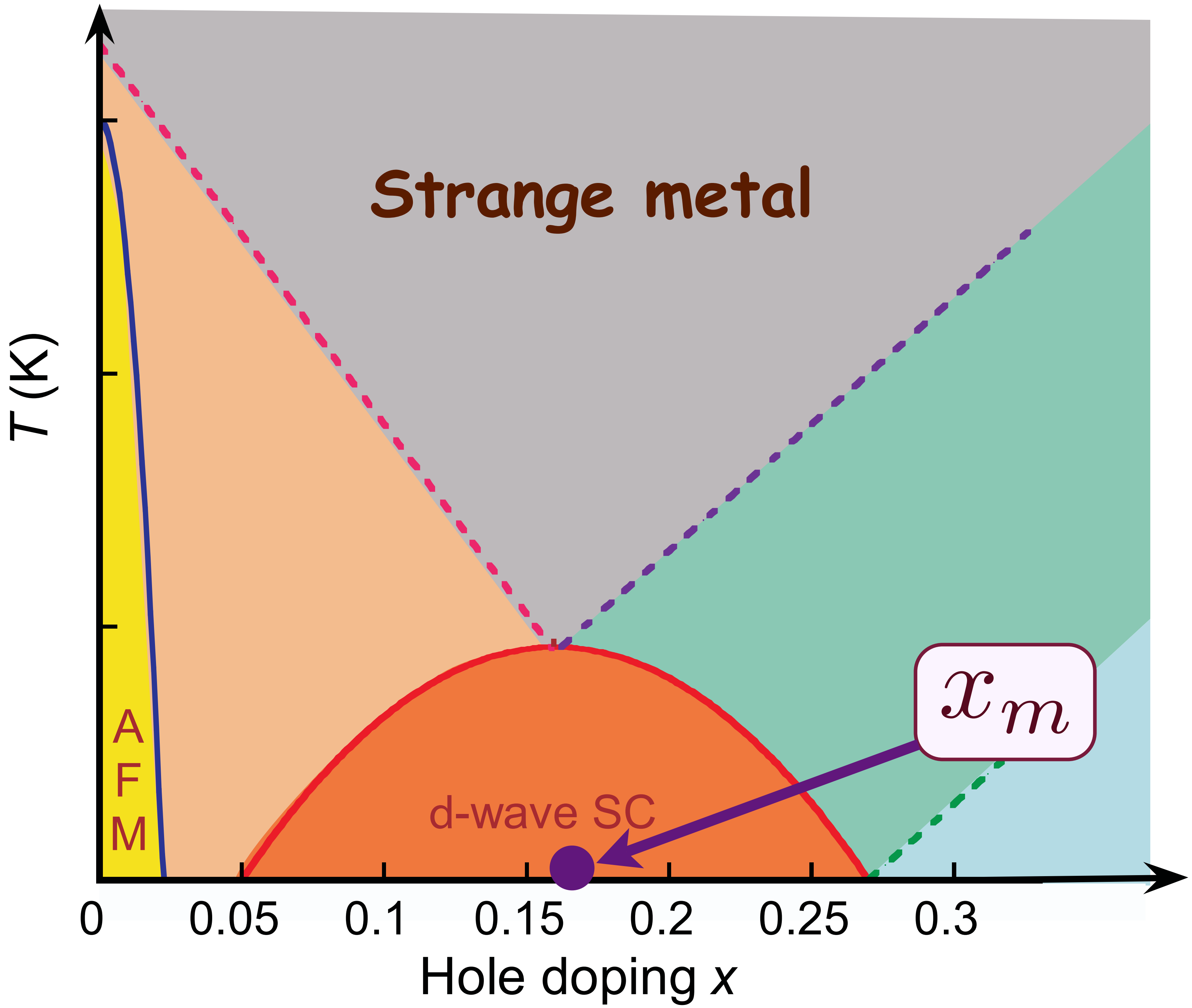

Strange metal: quantum criticality of optimal doping critical point at $x = x_m$?

Only candidate quantum critical point observed at low T

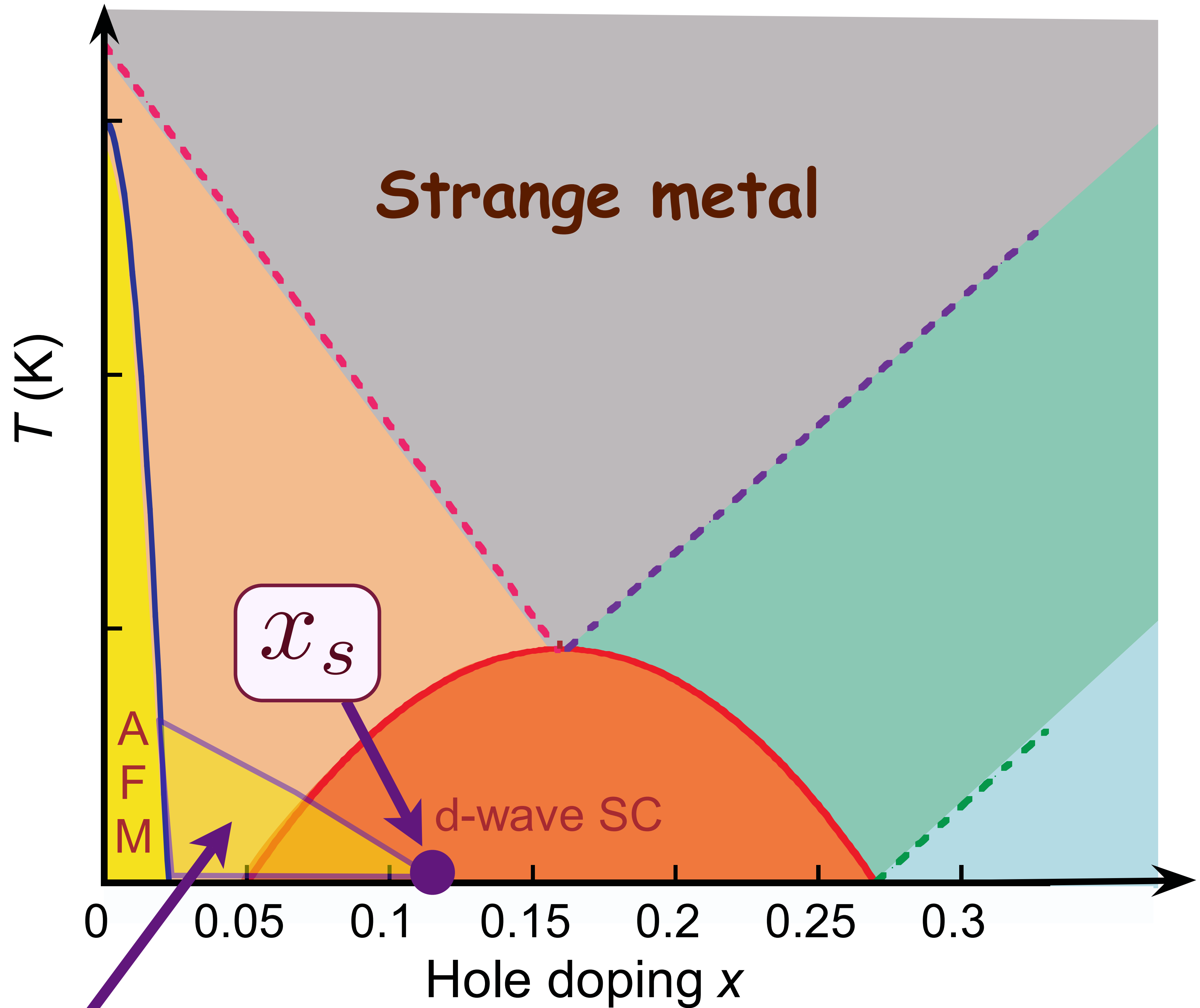

Spin density wave order present
below a quantum critical point at $x = x_s$
with $x_s \approx 0.12$ in the La series of cuprates

Evolution of the (ARPES) Fermi surface on the cuprate phase diagram

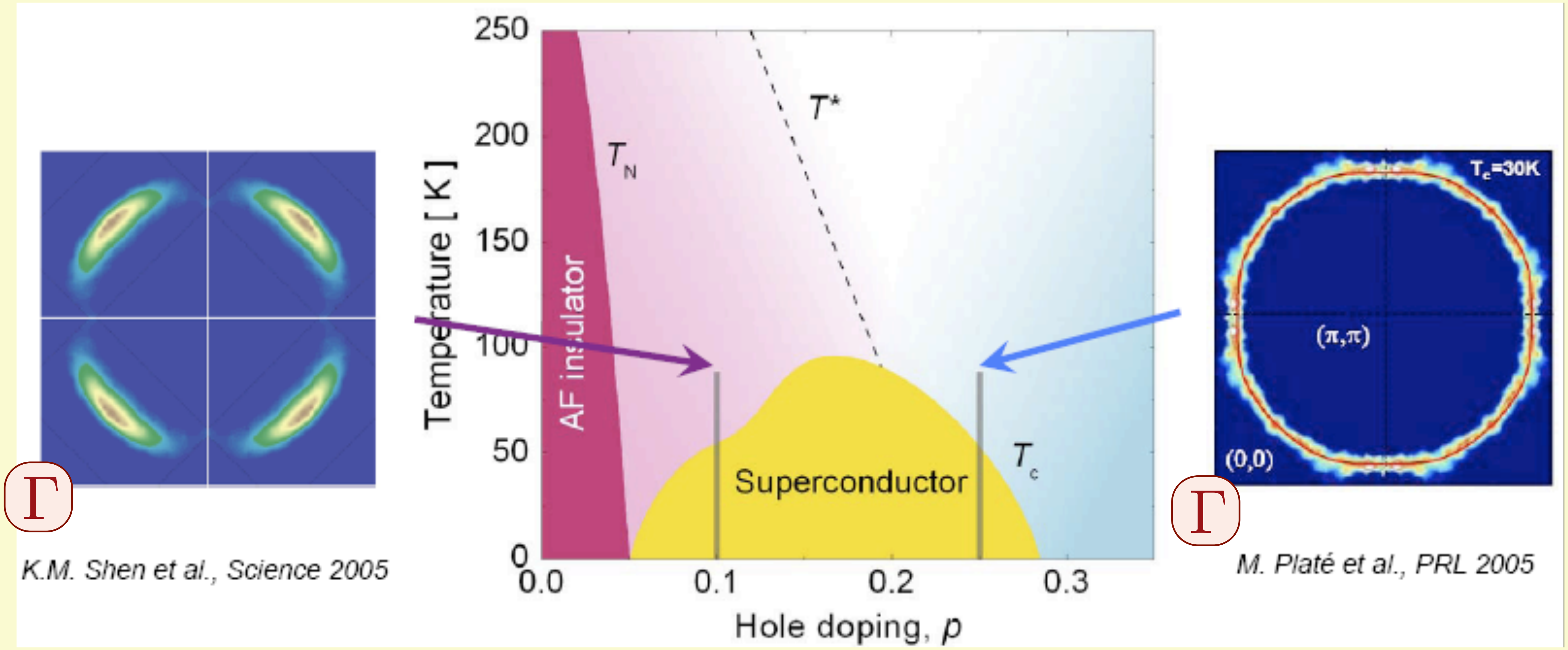

Smaller hole Fermi-pockets

Large hole Fermi surface

Theory of quantum criticality in the cuprates

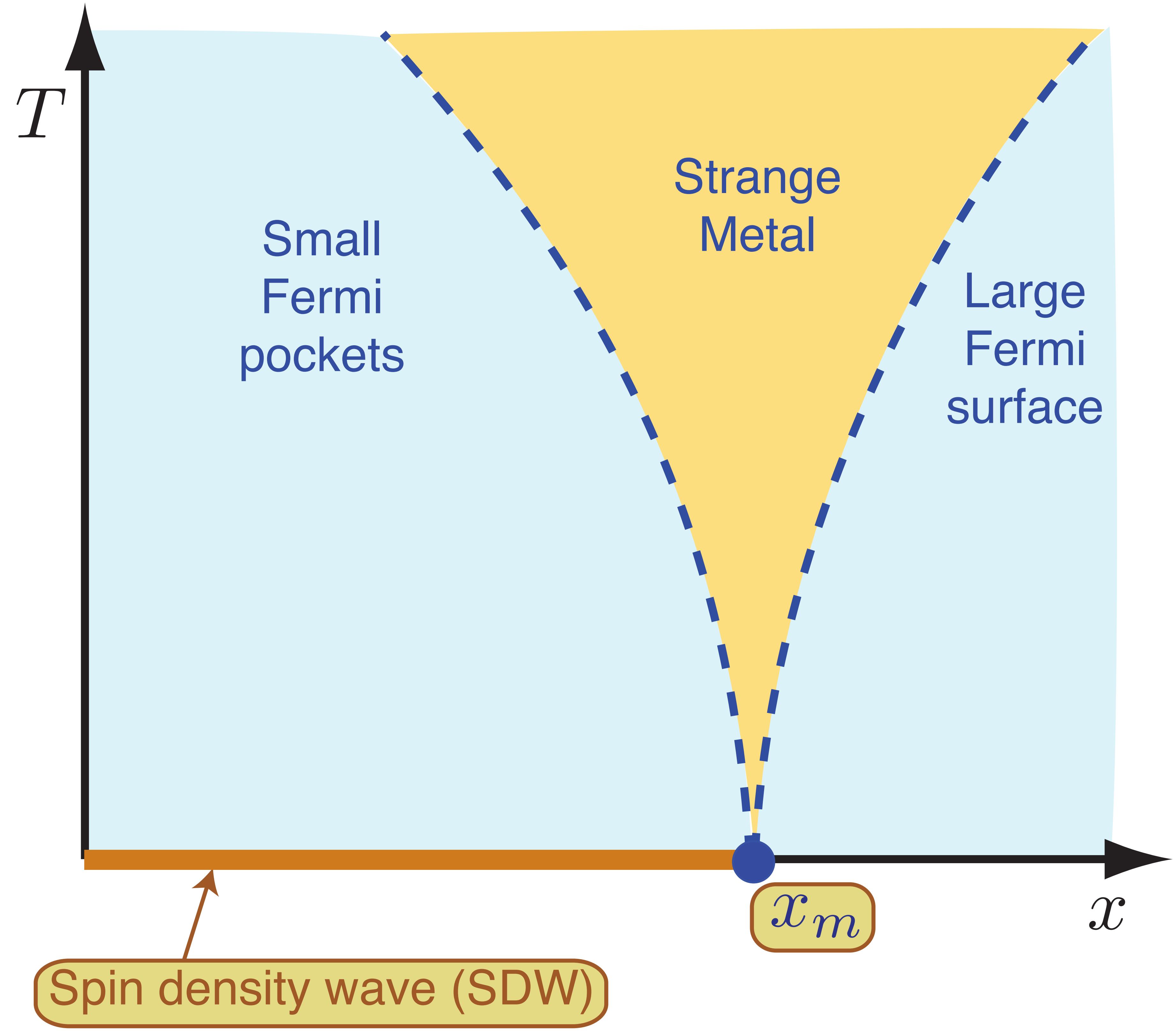

Underlying SDW ordering quantum critical point in **metal** at $x = x_m$

Evidence for connection between linear resistivity and stripe-ordering in a cuprate with a low T_c

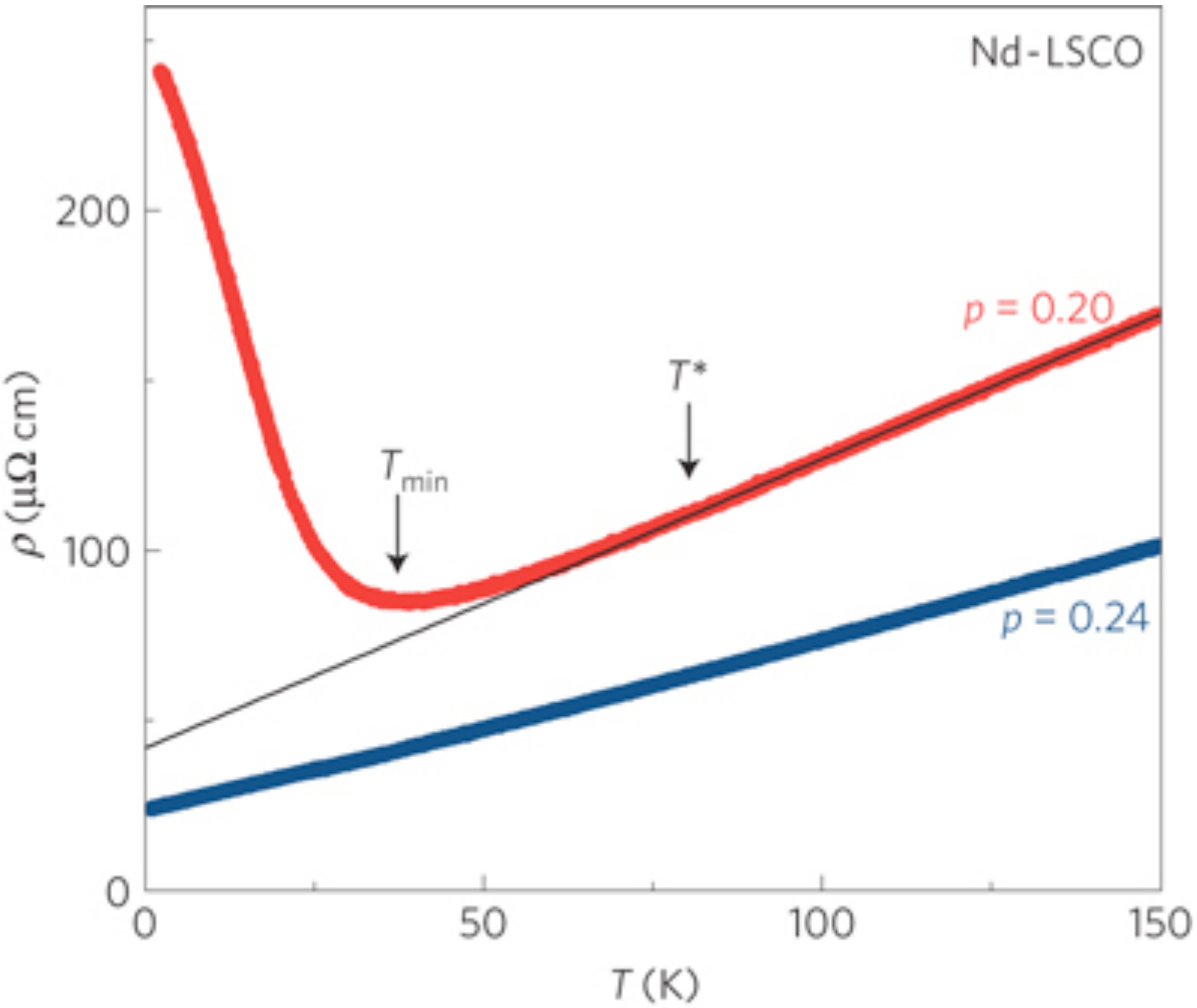

Magnetic field of upto 35 T used to suppress superconductivity

Linear temperature dependence of resistivity and change in the Fermi surface at the pseudogap critical point of a high-T_c superconductor

R. Daou, Nicolas Doiron-Leyraud, David LeBoeuf, S. Y. Li, Francis Laliberté, Olivier Cyr-Choinière, Y. J. Jo, L. Balicas, J.-Q. Yan, J.-S. Zhou, J. B. Goodenough & Louis Taillefer, *Nature Physics* **5**, 31 - 34 (2009)

Spin density wave theory in hole-doped cuprates

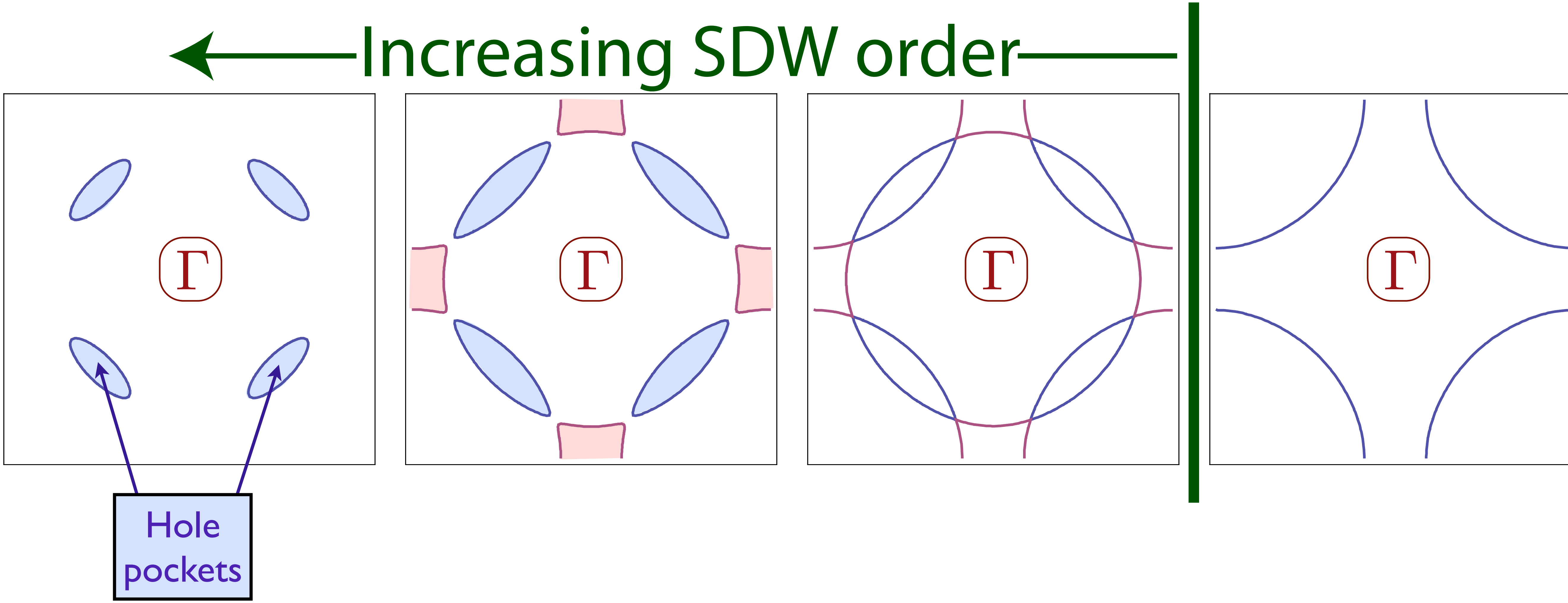

Quantum phase transition involves *both* a SDW order parameter $\vec{\varphi}$, and a topological change in the Fermi surface

S. Sachdev, A.V. Chubukov, and A. Sokol, *Phys. Rev. B* **51**, 14874 (1995).
A.V. Chubukov and D. K. Morr, *Physics Reports* **288**, 355 (1997).

Theory of quantum criticality in the cuprates

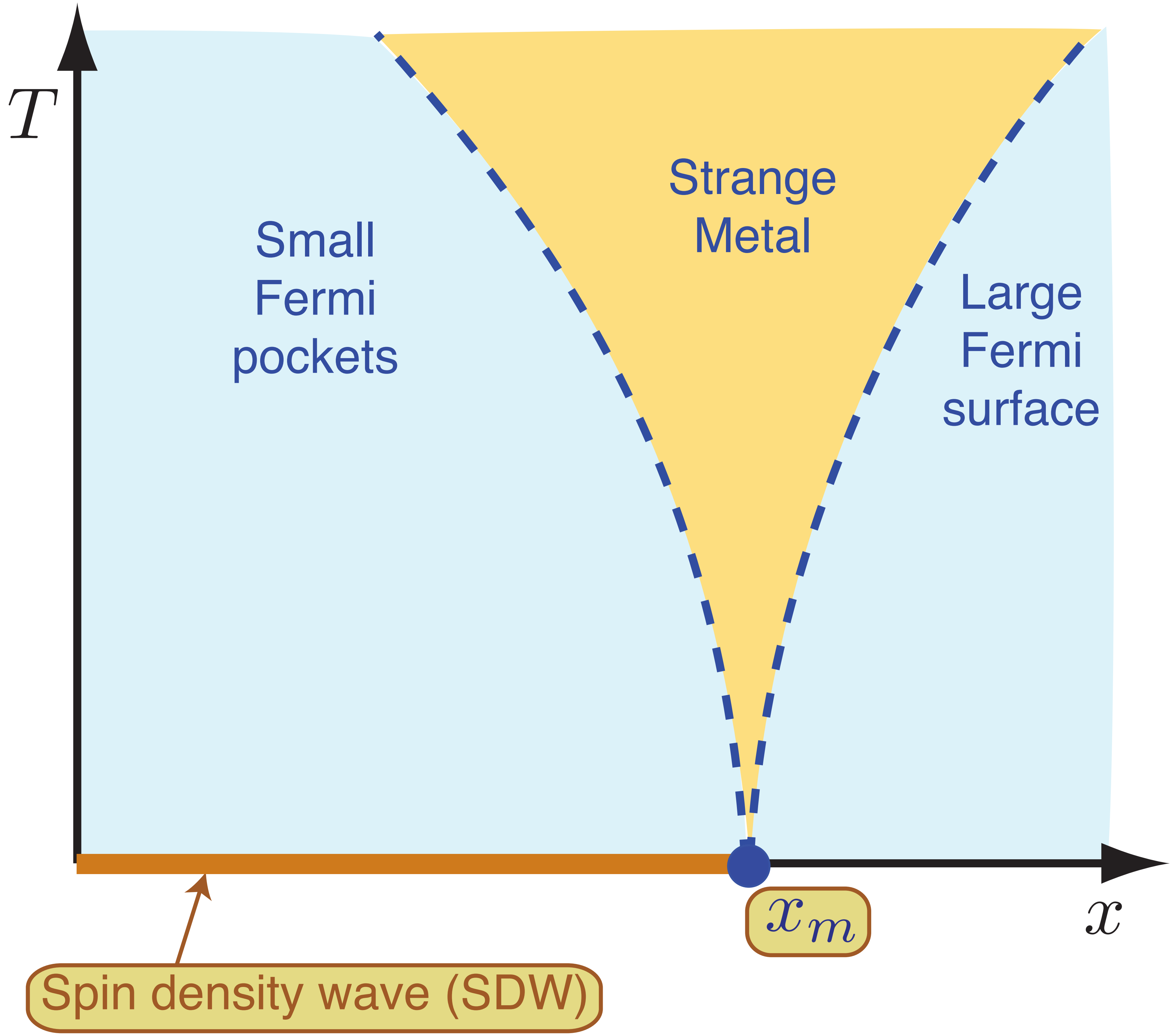

Underlying SDW ordering quantum critical point in **metal** at $x = x_m$

Theory of quantum criticality in the cuprates

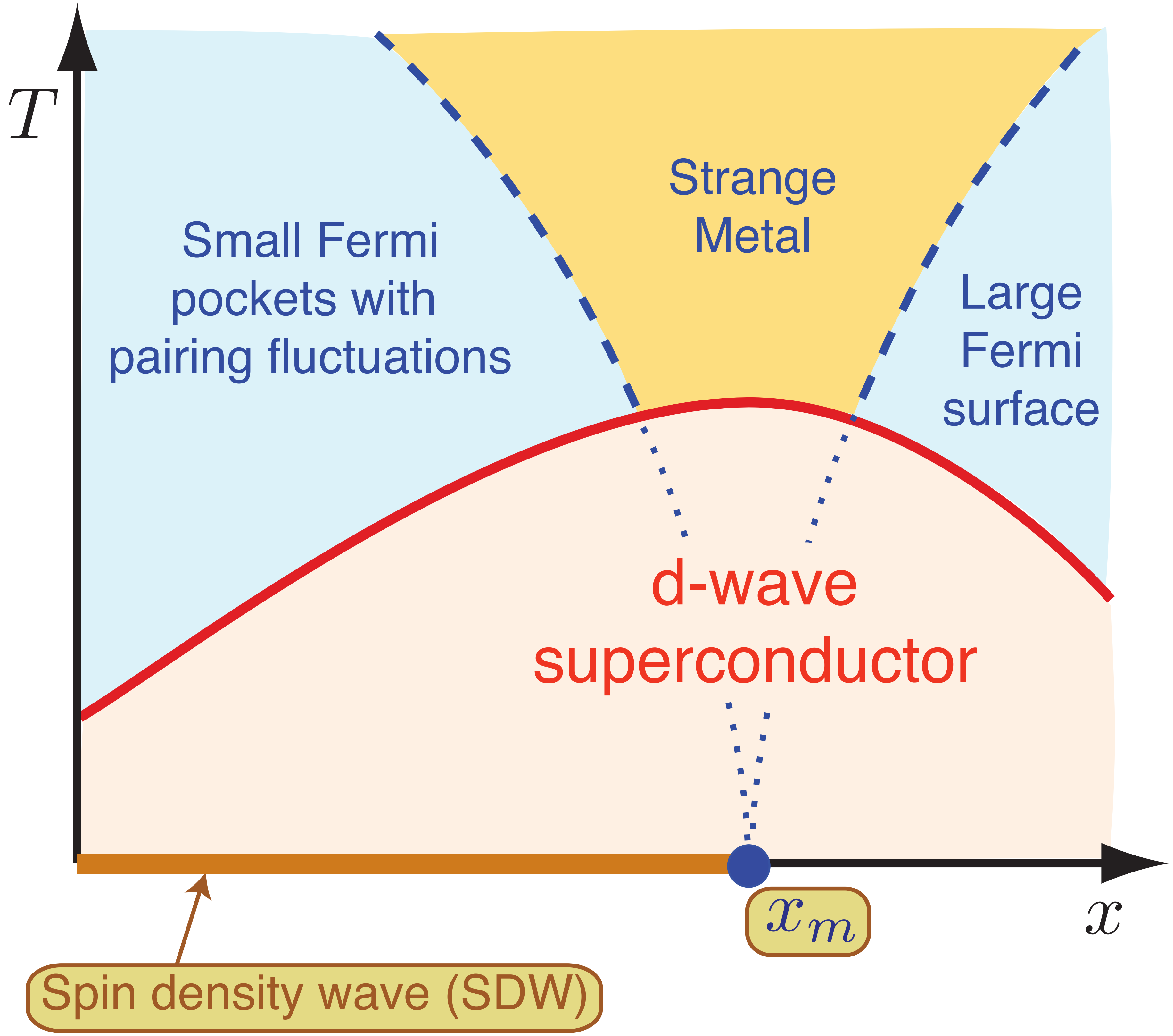

Onset of d-wave superconductivity hides the critical point $x = x_m$

Theory of quantum criticality in the cuprates

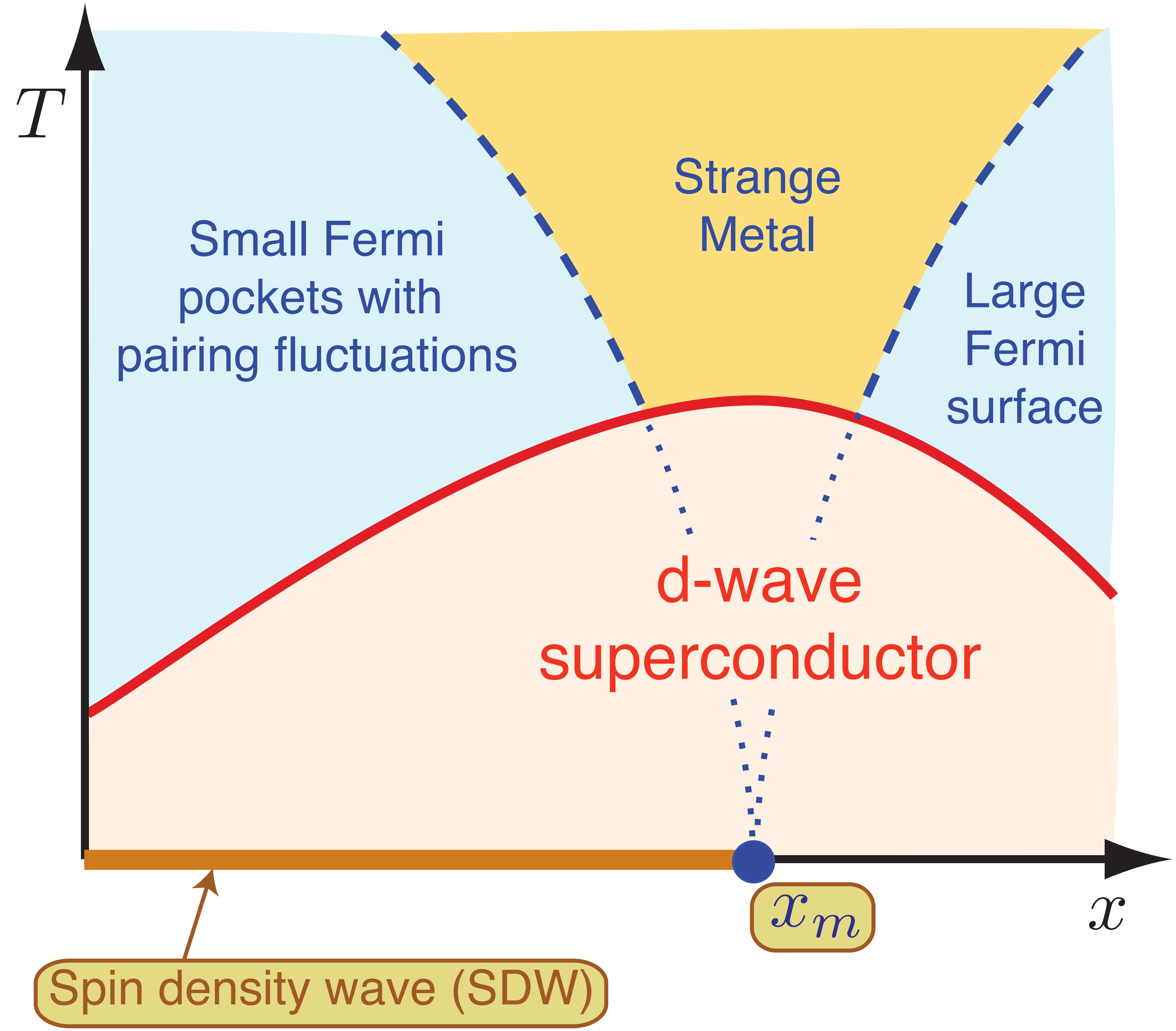

Competition between SDW order and superconductivity moves the actual quantum critical point to $x = x_s < x_m$.

Theory of quantum criticality in the cuprates

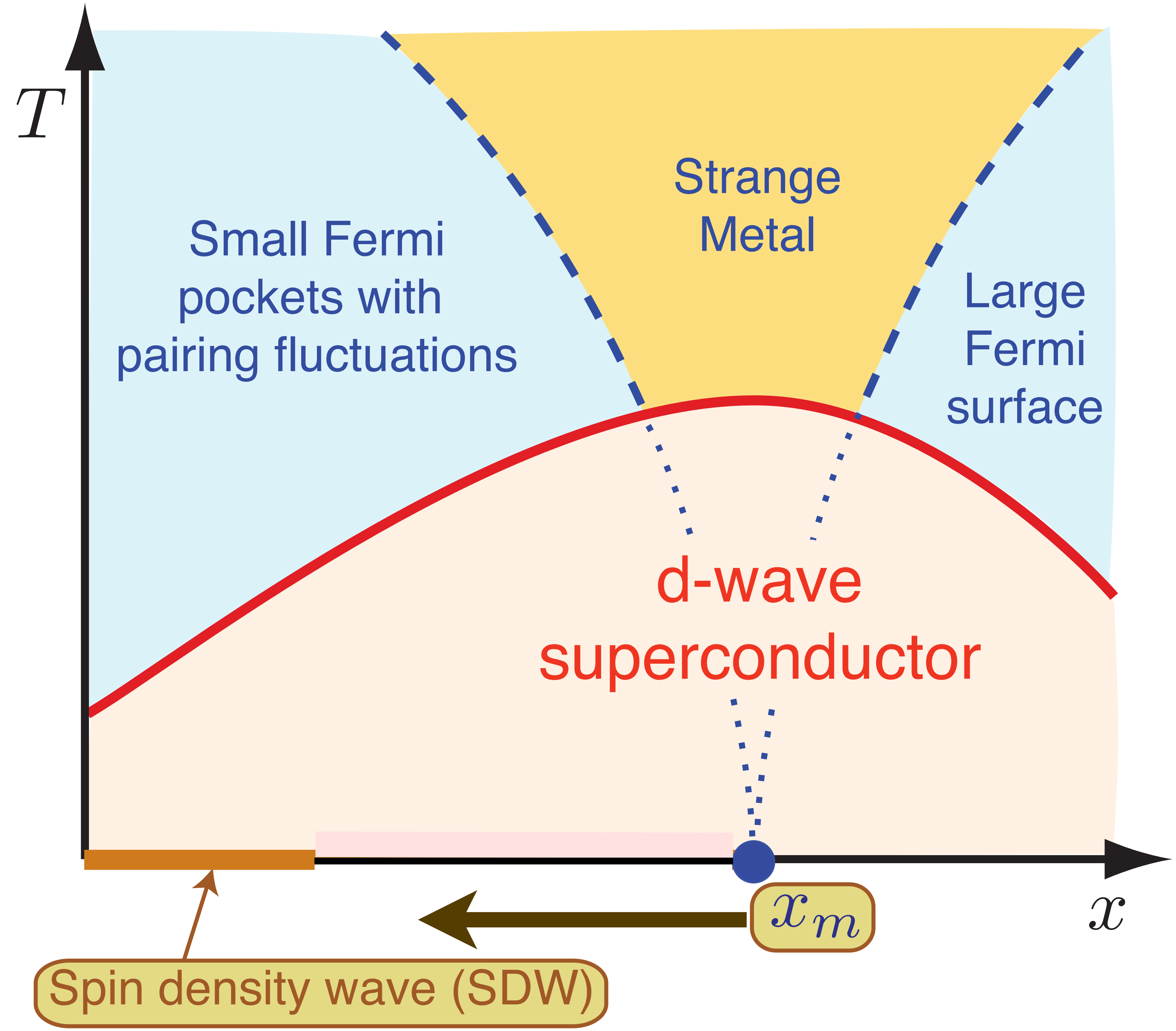

Competition between SDW order and superconductivity moves the actual quantum critical point to $x = x_s < x_m$.

Theory of quantum criticality in the cuprates

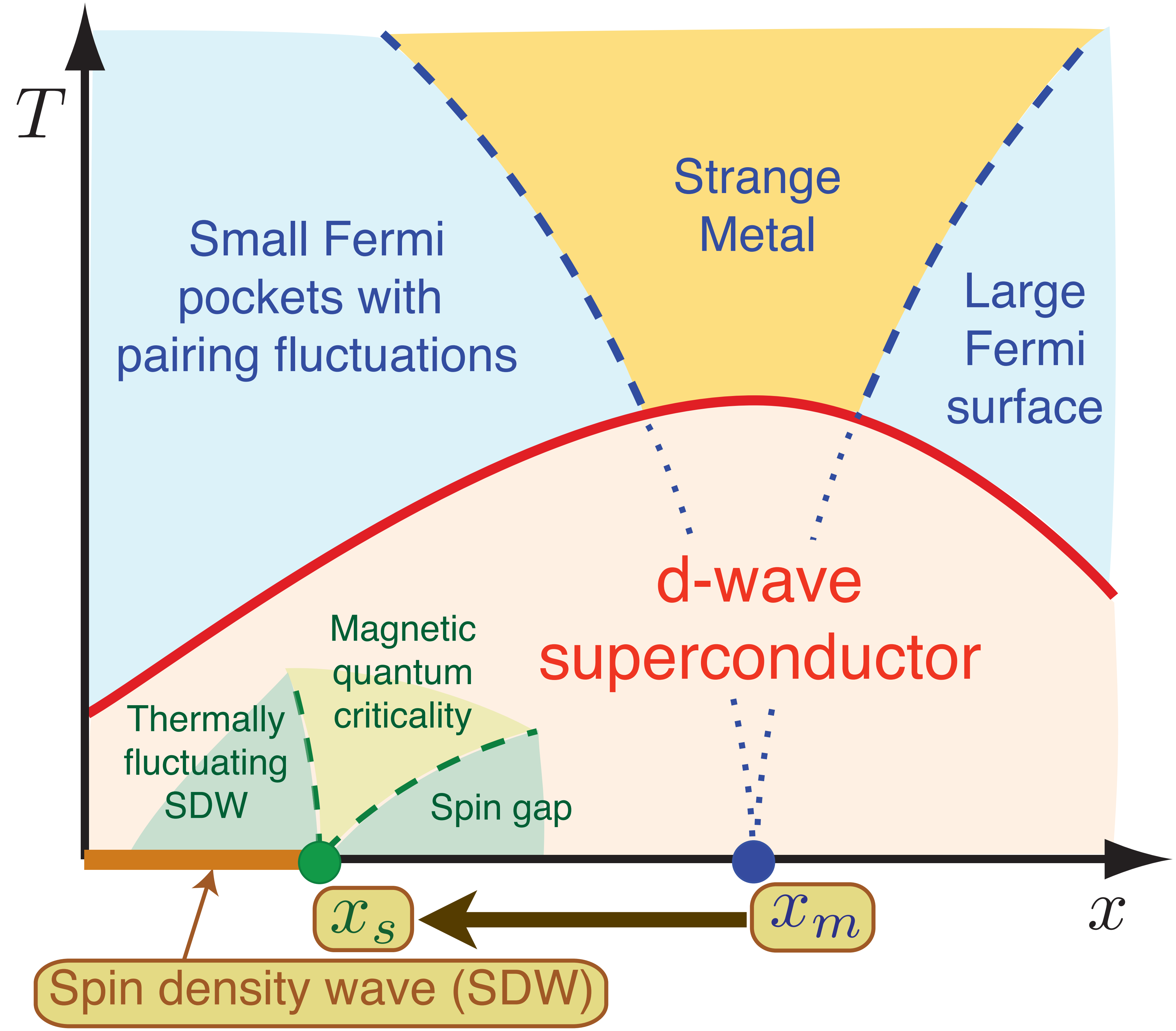

Competition between SDW order and superconductivity moves the actual quantum critical point to $x = x_s < x_m$.

Theory of quantum criticality in the cuprates

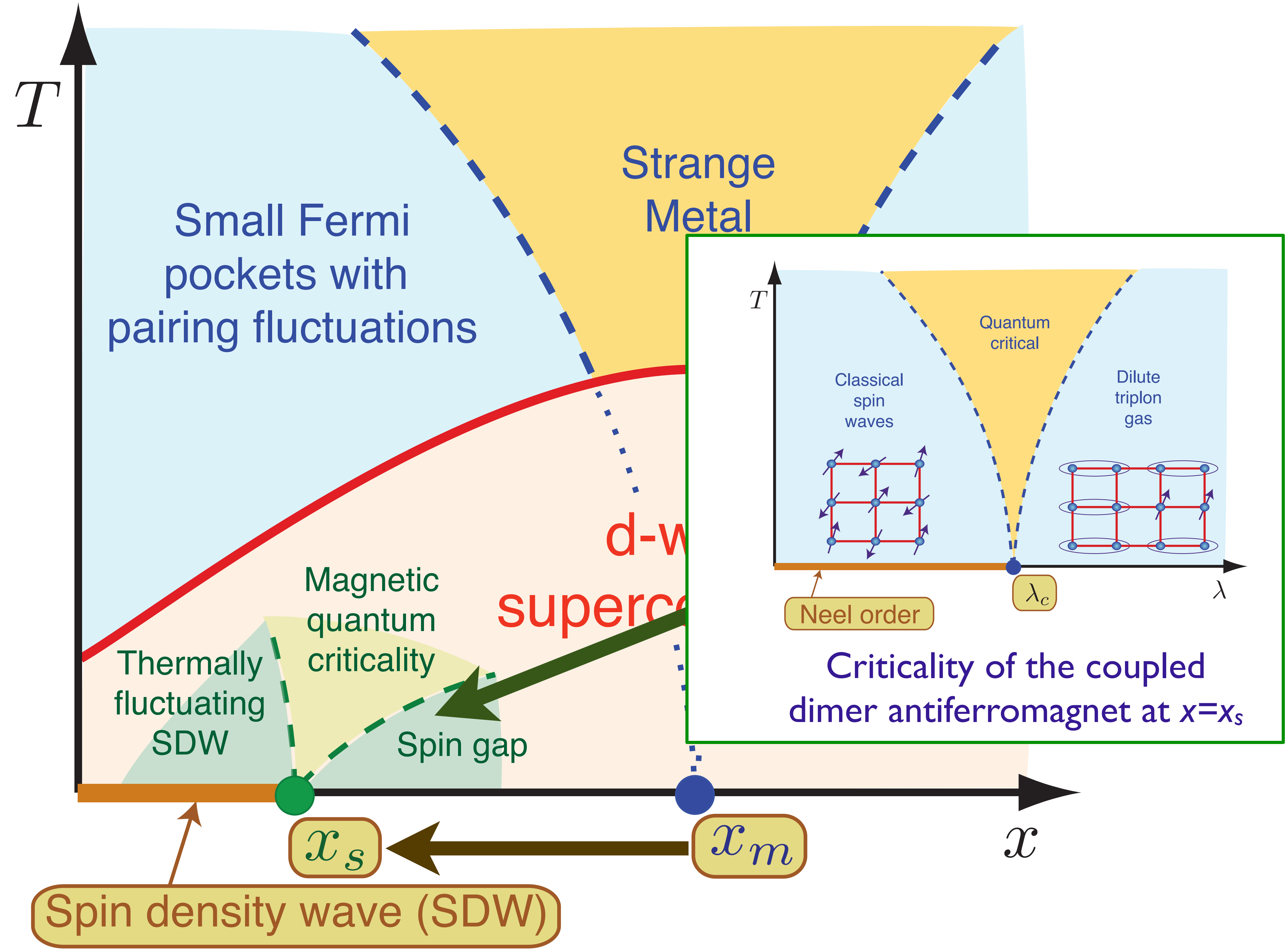

Competition between SDW order and superconductivity moves the actual quantum critical point to $x = x_s < x_m$.

Theory of quantum criticality in the cuprates

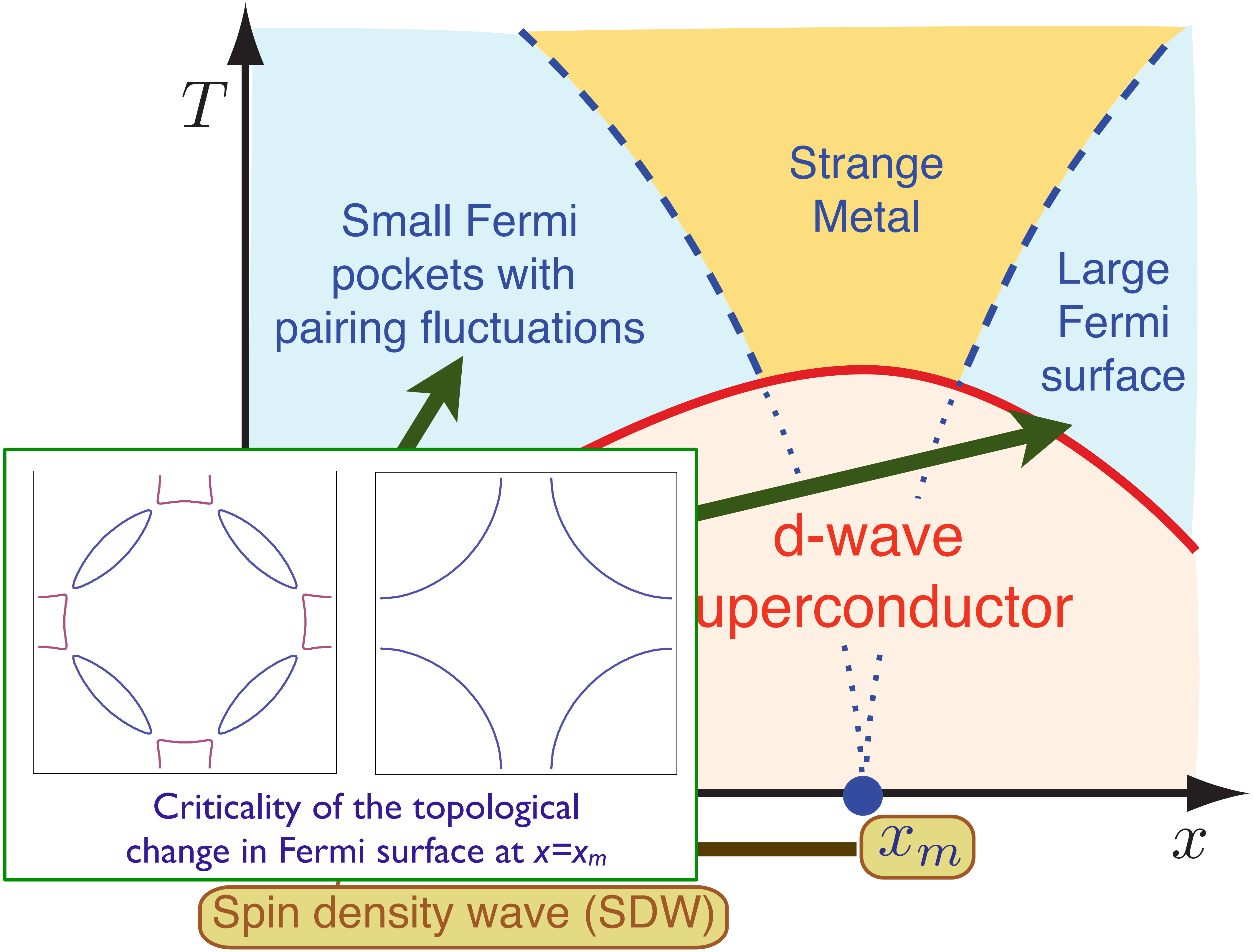

Competition between SDW order and superconductivity moves the actual quantum critical point to $x = x_s < x_m$.

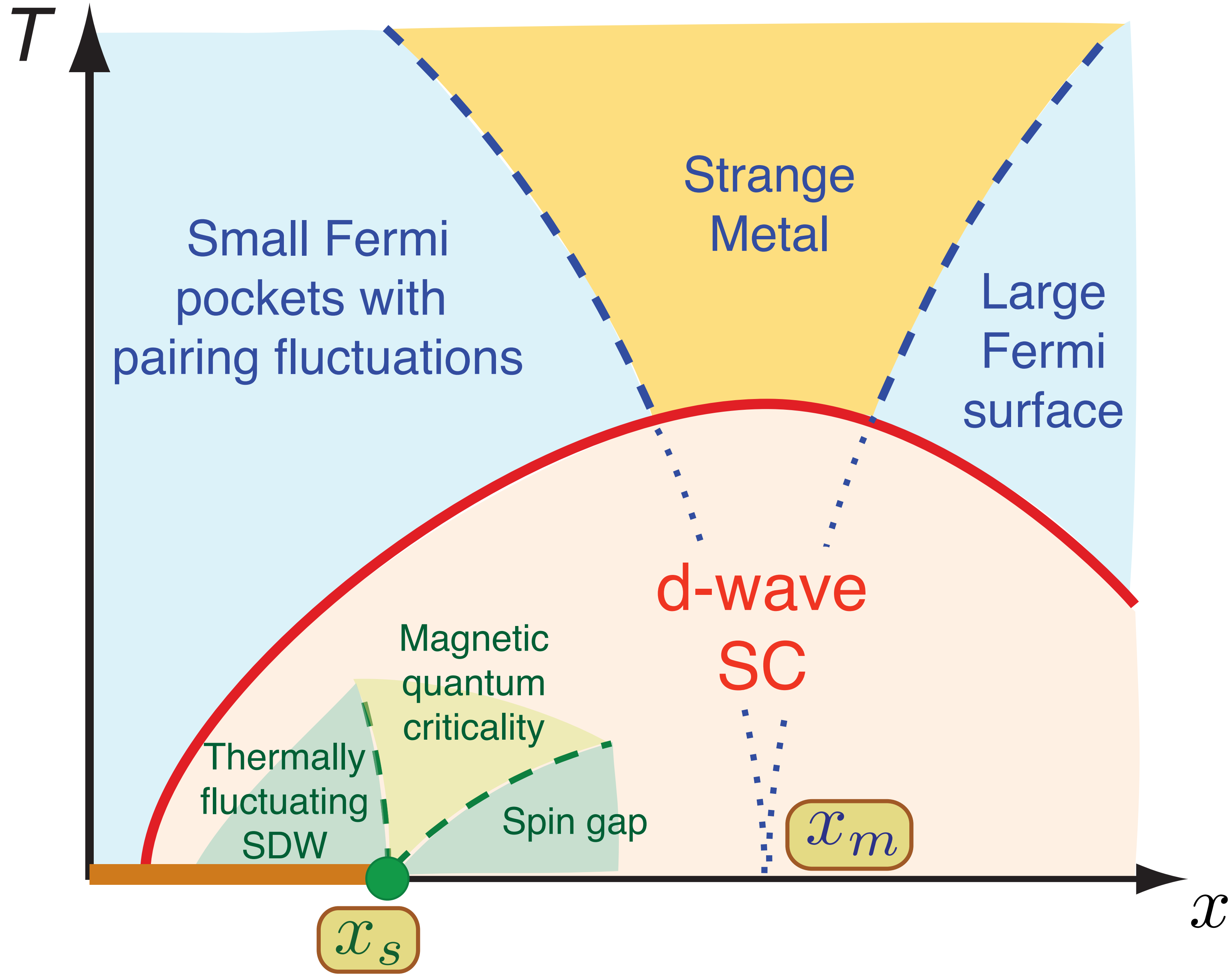

T
Small Fermi
pockets with
pairing fluctuations
Strange
Metal
Large
Fermi
surface
d-wave
SC
Magnetic
quantum
criticality
Thermally
fluctuating
SDW
Spin gap
x_m
x_s
x

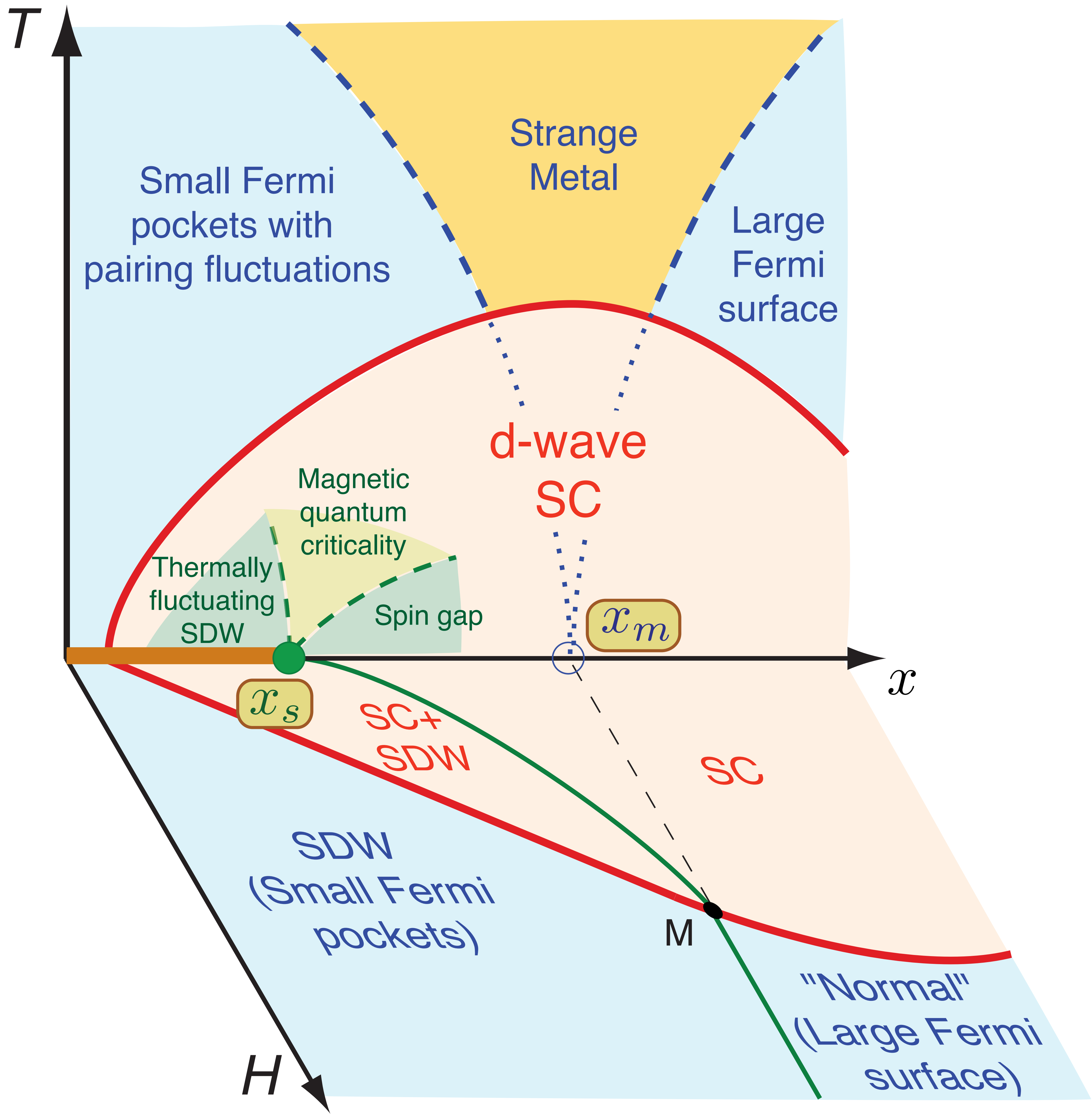

T
Small Fermi pockets with pairing fluctuations
Strange Metal
Large Fermi surface
d-wave SC
Magnetic quantum criticality
Thermally fluctuating SDW
Spin gap
x_m
x_s
x
SC+ SDW
SC
SDW (Small Fermi pockets)
M
"Normal" (Large Fermi surface)
H

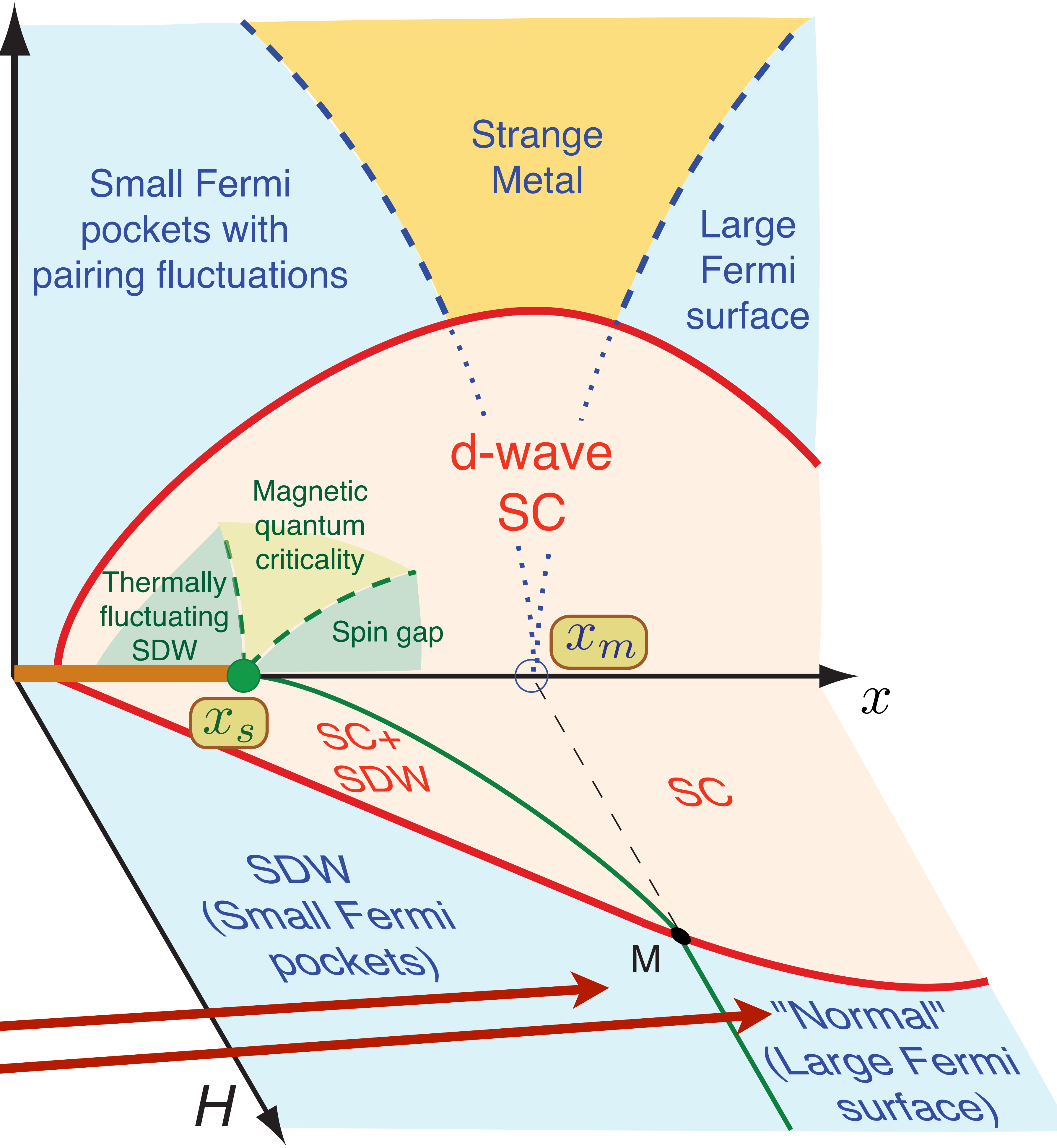

Change in frequency of quantum oscillations in electron-doped materials identifies $x_m = 0.165$

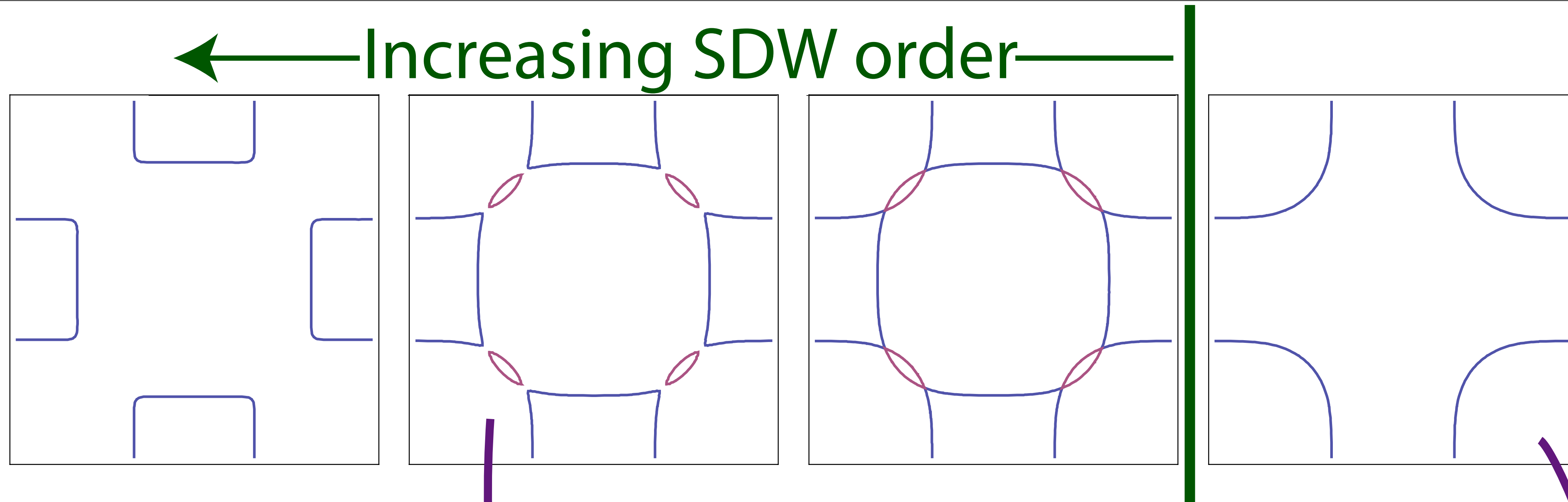

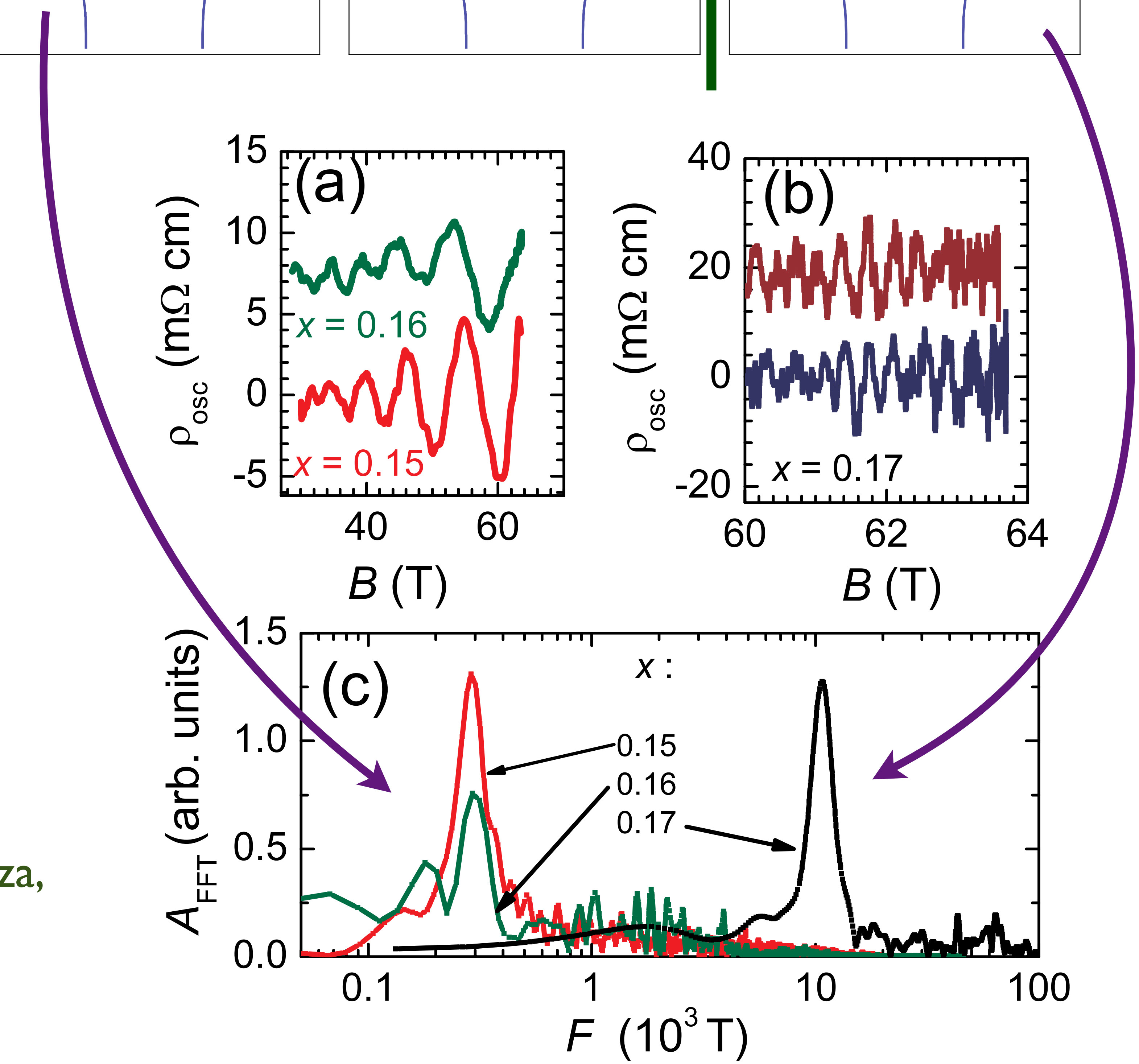

$Nd_{2-x}Ce_xCuO_4$

T. Helm, M.V. Kartsovni,
M. Bartkowiak, N. Bittner,
M. Lambacher, A. Erb, J. Wosnitza,
R. Gross, arXiv:0906.1431

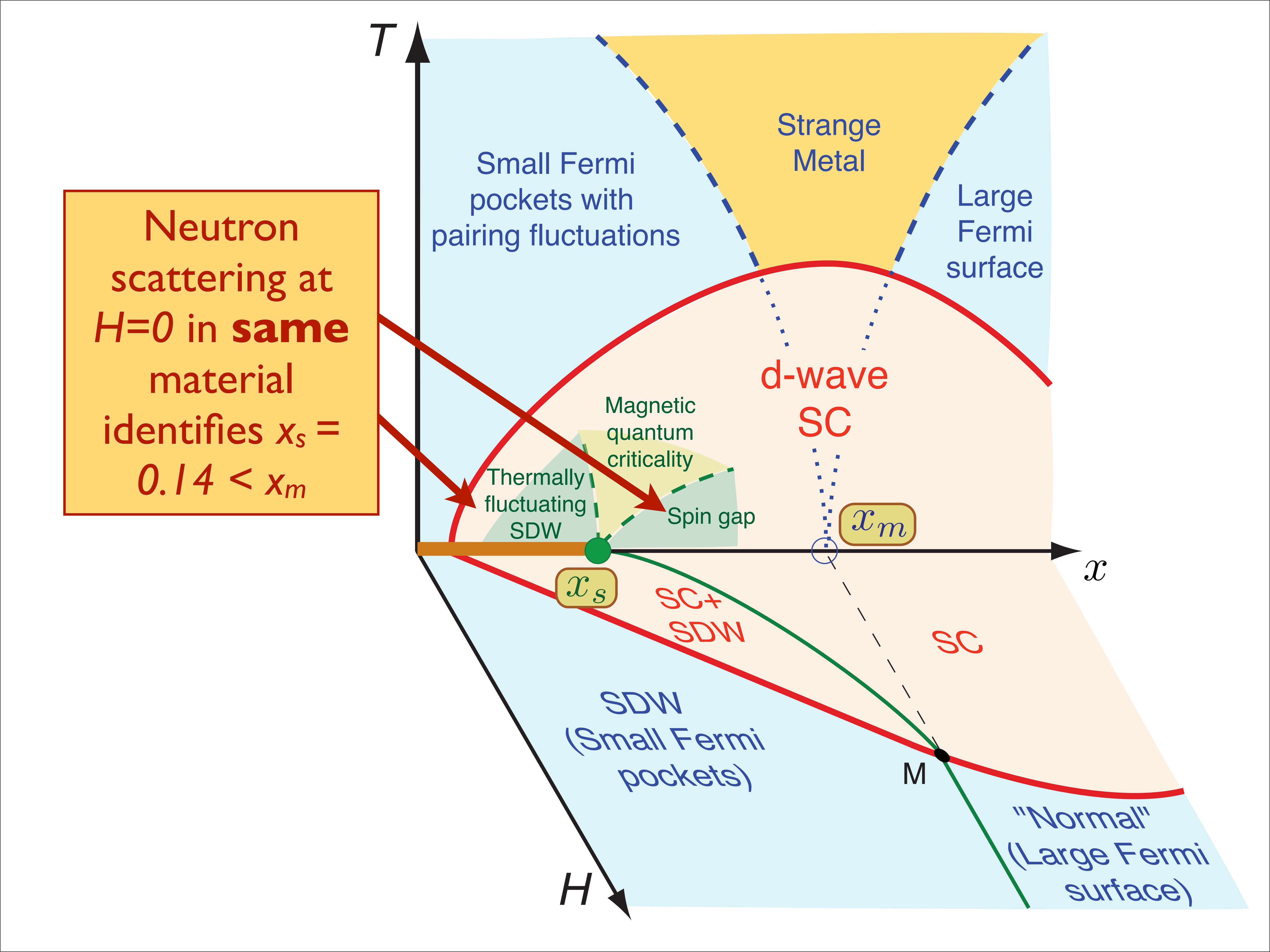
Neutron scattering at H=0 in **same** material identifies x_s = 0.14 < x_m
T
Small Fermi pockets with pairing fluctuations
Strange Metal
Large Fermi surface
d-wave SC
Magnetic quantum criticality
Thermally fluctuating SDW
Spin gap
x_m
x
x_s
SC+ SDW
SC
SDW (Small Fermi pockets)
M
"Normal" (Large Fermi surface)
H

$Nd_{2-x}Ce_xCuO_4$

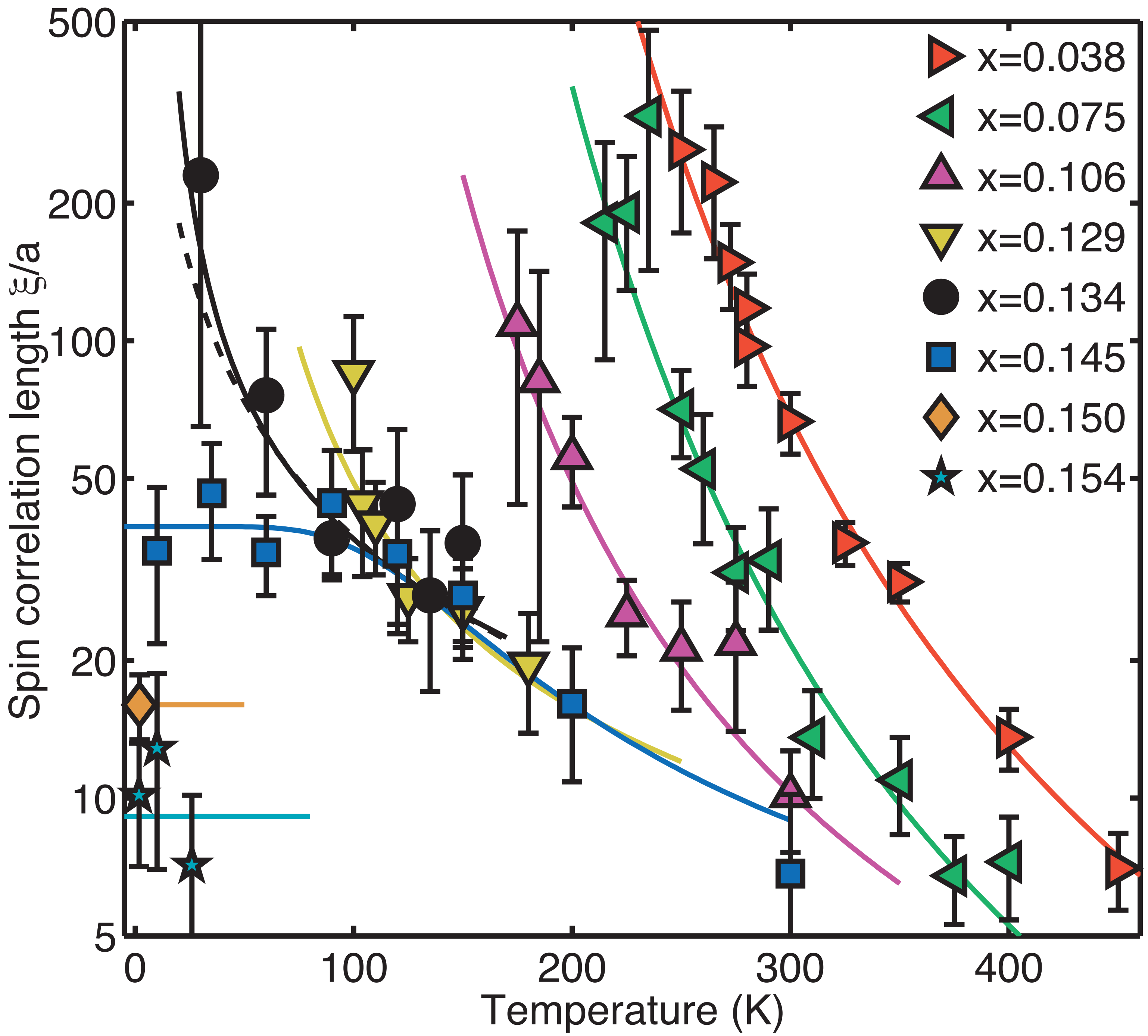

E. M. Motoyama, G. Yu, I. M. Vishik, O. P. Vajk, P. K. Mang, and M. Greven, *Nature* **445**, 186 (2007).

Experiments on $Nd_{2-x}Ce_xCuO_4$ show that at low fields $x_s = 0.14$, while at high fields $x_m = 0.165$.

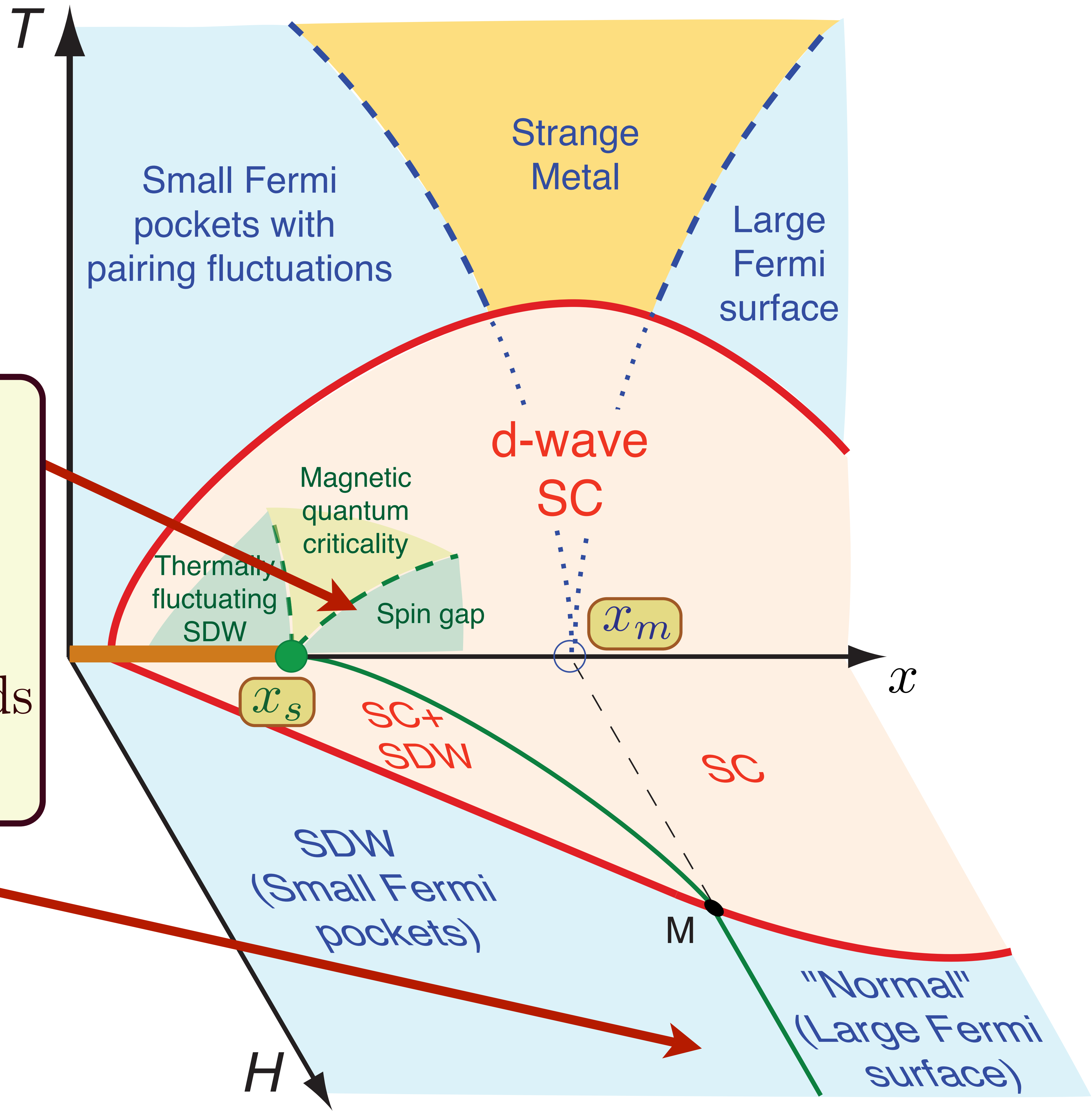

Conclusions

General theory of finite temperature dynamics and transport near quantum critical points, with applications to antiferromagnets, graphene, and superconductors

Conclusions

The AdS/CFT offers promise in providing a new understanding of strongly interacting quantum matter at non-zero density

Conclusions

Identified quantum criticality in cuprate superconductors with a critical point at optimal doping associated with onset of spin density wave order in a metal

Elusive optimal doping quantum critical point has been "hiding in plain sight".

It is shifted to lower doping by the onset of superconductivity